STRINGQFT

String-Theoretic Construction
of Quantum Field Theory

VOLUME VI

D-Branes at Orbifold Singularities

Xingyang Yu

StringQFT v1.0

Drafted with AI assistance under the supervision of the author.
Manuscript free to read. All rights reserved.

Contents

VI.1 The probe paradigm **1**
- VI.1.1 Open strings as the field theory . . . 1
- VI.1.2 The theory on the branes . . . 2
- VI.1.3 The decoupling limit . . . 5
- VI.1.4 Moduli space as target geometry . . . 9
- VI.1.5 Reading geometry with branes . . . 11
- VI.1.6 Conditions on the probe construction . . . 13

Status and sources . . . 14
References . . . 16

VI.2 Quivers from orbifold projections **17**
- VI.2.1 From flat space to a singularity . . . 17
- VI.2.2 The orbifold geometry and the Calabi–Yau condition . . . 18
- VI.2.3 The orbifold projection . . . 21
- VI.2.4 Nodes and arrows: solving the projection . . . 22
- VI.2.5 Regular and fractional branes . . . 25
- VI.2.6 The non-chiral example: the affine necklace . . . 27
- VI.2.7 The chiral example: the dP0 quiver . . . 30
- VI.2.8 The worldsheet origin . . . 32
- VI.2.9 What the construction does and does not give . . . 35

Status and sources . . . 36
References . . . 38

VI.3 $\mathbb{C}^2/\Gamma$: $\mathcal{N}=2$ ADE quivers and the McKay correspondence as gauge theory **39**
- VI.3.1 From the abelian warm-up to the McKay correspondence . . . 39
- VI.3.2 The setup, inherited: $\Gamma \subset SU(2)$ and its branes . . . 41
- VI.3.3 The McKay quiver and its smallest case . . . 42
- VI.3.4 The McKay correspondence in general . . . 45
- VI.3.5 The classification and the regular brane . . . 47
- VI.3.6 The D series: binary dihedral groups . . . 48
- VI.3.7 The E series: the binary tetrahedral group . . . 49
- VI.3.8 The worldsheet origin . . . 52
- VI.3.9 The Higgs branch is the ALE space . . . 54
- VI.3.10 What the construction does and does not give . . . 56

Status and sources . . . 57
References . . . 60

VI.4 Moduli spaces: Higgs branches as resolved orbifolds and hyperkähler quotients 61
VI.4.1 The moduli space of vacua . . . 61
VI.4.2 The moduli space is a hyperkähler quotient . . . 62
VI.4.3 The smallest case: $\mathbb{C}^2/\mathbb{Z}_2$ and the Eguchi–Hanson space . . . 64
VI.4.4 Kronheimer's construction in general . . . 67
VI.4.5 The A series in closed form: multi-centre metrics . . . 68
VI.4.6 Non-abelian examples: D_4 and E_6 . . . 70
VI.4.7 The geometric McKay correspondence . . . 72
VI.4.8 Resolution versus deformation . . . 74
VI.4.9 What the construction does and does not give . . . 77
Status and sources . . . 78
References . . . 80

VI.5 Fractional branes and the wrapped-brane interpretation 82
VI.5.1 What is left to say about the fractional brane . . . 82
VI.5.2 The first puzzle: $r{+}1$ fractional branes, r curves . . . 83
VI.5.3 The wrapped-brane identity . . . 85
VI.5.4 The charge lattice . . . 87
VI.5.5 Tension, and what "stuck" means . . . 89
VI.5.6 The worldsheet and geometric charge descriptions . . . 91
VI.5.7 Worked examples: A_1 and D_4 . . . 92
VI.5.8 D-brane charges and the derived category . . . 94
VI.5.9 What the construction does and does not give . . . 97
Status and sources . . . 98
References . . . 100

VI.6 $\mathbb{C}^3/\Gamma$: $\mathcal{N}{=}1$ quivers and superpotentials 101
VI.6.1 Out of the ADE miracle . . . 101
VI.6.2 The D3-brane projection, slowly . . . 103
VI.6.3 From Chan–Paton blocks to the directed McKay quiver . . . 105
VI.6.4 Chirality, reality of Q, anomaly . . . 107
VI.6.5 The cubic superpotential . . . 109
VI.6.6 Abelian examples: isolated vs non-isolated . . . 111
VI.6.7 Non-abelian examples: $\Delta(27)$, A_4, $\Sigma(168)$ . . . 116
VI.6.8 The Higgs branch and FI chambers . . . 120
VI.6.9 What the construction gives . . . 122
Status and sources . . . 123
References . . . 124

VI.7 Tadpoles, anomalies, and quiver consistency 125
VI.7.1 Why a drawable quiver still needs consistency checks . . . 125
VI.7.2 Non-abelian anomalies . . . 126

VI.7.3 Fractional ranks and the integer kernel . . . 128
VI.7.4 Twisted Ramond–Ramond tadpoles from the annulus . . . 131
VI.7.5 Localized tadpoles versus fixed-line sectors . . . 133
VI.7.6 The abelian sector . . . 134
VI.7.7 Worked example I: dP_0 in full . . . 139
VI.7.8 Worked example II: $\mathbb{C}^3/(\mathbb{Z}_2 \times \mathbb{Z}_2)$ in full . . . 142
VI.7.9 Worked example III: $\Delta(27)$ regular ranks . . . 144
VI.7.10 What the consistency analysis gives . . . 146
Status and sources . . . 147
References . . . 148

VI.8 Orientifolded probes: SO/Sp quivers 150
VI.8.1 Orientifolds of the probe quiver . . . 150
VI.8.2 The orientifold data . . . 151
VI.8.3 The Chan–Paton projection: SO versus USp . . . 154
VI.8.4 Folding the nodes, arrows, and superpotential . . . 156
VI.8.5 Charges and anomalies . . . 160
VI.8.6 Worked example I: flat $\mathbb{C}^3$ with an O3-plane . . . 164
VI.8.7 Worked example II: the $\mathbb{C}^2/\mathbb{Z}_2$ orientifold, two ways . . . 165
VI.8.8 Worked example III: the dP_0 orientifold in full . . . 167
VI.8.9 What orientifolds add, and what they do not solve . . . 171
Status and sources . . . 172
References . . . 174

VI.9 Discrete torsion probes 176
VI.9.1 Discrete torsion as a choice of orbifold CFT . . . 176
VI.9.2 Cocycles and projective representations . . . 178
VI.9.3 Twisted group algebras and projective characters . . . 180
VI.9.4 The projective McKay quiver . . . 181
VI.9.5 Torsion phases in W and q-commutator F-terms . . . 183
VI.9.6 Worked example: $\mathbb{C}^3/(\mathbb{Z}_2 \times \mathbb{Z}_2)$ with Pauli matrices . . . 185
VI.9.7 General $\mathbb{Z}_n \times \mathbb{Z}_n$: clock and shift . . . 190
VI.9.8 Charges, tadpoles, and projective traces . . . 192
VI.9.9 What discrete torsion does and does not do . . . 194
Status and sources . . . 195
References . . . 197

VI.10 Large-N inheritance from $\mathcal{N}$=4 SYM 198
VI.10.1 Orbifold daughters of $\mathcal{N}$=4: statement and scope . . . 198
VI.10.2 Projection and coupling matching . . . 199
VI.10.3 Planar inheritance and the neutral sector . . . 201
VI.10.4 Two consequences: degree count and beta coefficient . . . 206
VI.10.5 Worked abelian examples . . . 208
VI.10.6 Worked non-abelian example: $\Delta(27)$ . . . 211
VI.10.7 Boundaries and bridges . . . 212
Status and sources . . . 215

References 217

VI.11 Atlas: a low-rank orbifold catalog with calculation checks 218
VI.11.1 Reading the atlas 218
VI.11.2 The dP0 construction 219
VI.11.3 The ADE catalog 221
VI.11.4 The directed-quiver catalog 222
VI.11.5 Orientifold projections 225
VI.11.6 Discrete torsion 226
VI.11.7 Patterns and large N 227
VI.11.8 Extending the atlas 228
Status and sources 229

Chapter VI.1

The probe paradigm

VI.1.1 Open strings as the field theory

The position of a D3-brane in transverse space is visible to strings ending on it. A stack of such branes therefore offers a way to ask a geometric question using a gauge theory. Its light open strings become worldvolume fields, and the scalar vacuum values record where the branes can move. The relation becomes useful when the transverse space is singular: the resulting gauge theory can reveal a geometric branch that was not evident from the spectrum alone. We first establish this relation in flat space, where every step can be followed directly.

It pays to be precise about the object and the strings before quantizing anything. A Dp-brane is a $(p+1)$-dimensional hypersurface on which open strings end; the name records the Dirichlet boundary conditions,

$$\partial_n X^\mu\big|_\partial = 0 \quad (\mu = 0, \dots, p), \qquad X^m\big|_\partial = \text{const} \quad (m = p{+}1, \dots, 9), \tag{VI.1.1}$$

the $p{+}1$ Neumann directions along the brane and the $9{-}p$ Dirichlet directions transverse to it pinning the endpoints to the surface. It is not a rigid wall but a dynamical object, a BPS state of the closed string carrying Ramond–Ramond charge, and its shape fluctuations are themselves open-string modes. In the presence of a brane the string spectrum splits into two sectors: closed strings, which propagate in the ten-dimensional bulk and contain the graviton, and open strings, whose endpoints lie on the brane and whose massless modes are the worldvolume fields. The two sectors are distinct but not dynamically isolated: worldsheets with boundaries couple open strings to closed strings, so at finite α' the brane theory is not yet a closed system. The decoupling limit of §VI.1.3 is precisely the statement that, once the massive tower and gravity have been sent away with the closed-string bulk, the open-string degrees of freedom become an autonomous field theory, living entirely in the open sector.

The energy range in which the open-string fields suffice is controlled by the string and gravitational scales. We display the string coupling beside them because it also

sets the D3 gauge coupling:

$$\underbrace{M_s = \alpha'^{-1/2}}_{\text{string tower}}, \qquad \underbrace{g_s = e^{\Phi}}_{\text{string loops}}, \qquad \underbrace{M_{\rm P} \sim g_s^{-1/4} M_s}_{\text{gravity}}. \tag{VI.1.2}$$

An open string carries a tower of excitations spaced by the string scale M_s, with the massless modes at the bottom and the first massive states a gap M_s above; at energies $E \ll M_s$ only the massless modes are excited, and integrating out the tower leaves a local field theory of them. That is what the brane carries. The string coupling g_s controls loop corrections, and the ten-dimensional Planck scale $M_{\rm P}$ controls gravity. Holding E below M_s isolates the massless dynamics; the decoupling limit of §VI.1.3 will in addition send M_s and $M_{\rm P}$ to infinity, so the field theory becomes exact and gravity switches off.

Take N coincident D3-branes in flat ten-dimensional type IIB string theory. We identify their light fields, take the limit that isolates those fields, and then compute their scalar vacua. The result is $\mathrm{Sym}^N(\mathbb{C}^3)$: the positions of N identical branes in the transverse space. This flat-space calculation fixes the physical meaning of the dictionary used for singular backgrounds in Chapter 2.

It is worth naming the ambition this fixes, since the whole volume runs on it. A brane placed in a chosen background is a probe: it barely disturbs the background, but its worldvolume theory is acutely sensitive to it, so reading that theory off is a way of turning geometry into field theory. In flat space the dictionary returns the chosen flat geometry. Its power appears when the background carries a singularity, where the same construction produces gauge theories that no Lagrangian guess would have written down, with matter content and interactions fixed by the shape of the singularity. The chapters that follow are a catalogue of what the probe sees as the geometry is made progressively richer; this chapter fixes the dictionary's flat-space entry and the discipline for reading it.

We work in the mostly-plus signature throughout, with the brane-action normalizations fixed once and for all. The four-dimensional case carries the development for two reasons. The gauge theories we care about live in four dimensions; and the D3-brane is the four-dimensional member of a family. Type IIB string theory contains Dp-branes of odd p, and a Dp-brane has $9-p$ transverse dimensions, an even number for odd p, so once a complex structure is chosen the transverse space is a complex space $\mathbb{C}^{(9-p)/2}$ and, in later chapters, a Calabi–Yau cone over a singularity. For the D3-brane this is the transverse $\mathbb{R}^6$ with its chosen complex structure,

$$\mathbb{R}^6 \cong \mathbb{C}^3, \tag{VI.1.3}$$

the home of the threefold singularities this volume probes. The other odd-p branes give gauge theories in other dimensions, collected as a dimensional axis in §VI.1.5; the D3 is the case developed here.

VI.1.2 The theory on the branes

Put N D3-branes on top of one another in flat space and ask the only question that matters at low energy: what are the lightest excitations that live on them? They are

carried by the open strings that end on the stack, so we quantize one.

An open superstring carries worldsheet fields $X^M(\sigma,\tau)$ and their fermionic partners $\psi^M(\sigma,\tau)$, $M=0,\ldots,9$. A D3-brane fixes the boundary conditions: Neumann along the four worldvolume directions $M=0,\ldots,3$ and Dirichlet along the six transverse directions $M=4,\ldots,9$, so the endpoints move freely along the brane but are pinned in the transverse space. In the NS sector the mass of a state is set by its total oscillator level N,

$$\alpha' M^2 = N - \tfrac{1}{2}. \tag{VI.1.4}$$

The ground state $|0;k\rangle$ has $\alpha' M^2 = -\frac{1}{2}$ and is a tachyon; the GSO projection, keeping odd worldsheet-fermion number, removes it, and the lightest surviving state is the single half-integer oscillator

$$\psi^M_{-1/2}\,|0;k\rangle, \qquad \alpha' M^2 = 0, \tag{VI.1.5}$$

massless and carrying one spacetime vector index M. This index labels a covariant state before the massless gauge constraint: on shell the NS sector has two physical vector helicities and six transverse scalar states, eight bosonic states in all.

The fermions come from the Ramond sector, where the ψ^M are integer-moded and carry zero modes ψ_0^M obeying a ten-dimensional Clifford algebra,

$$\{\psi_0^M, \psi_0^N\} = \eta^{MN}, \tag{VI.1.6}$$

so the ground state is a spacetime spinor rather than a scalar. Its normal-ordering constant vanishes, $a_{\rm R}=0$, so it is already massless, $\alpha' M^2 = 0$, with no tachyon to project away; the GSO projection keeps a single chirality, cutting the **32** of $\mathrm{Spin}(9,1)$ down to one Majorana–Weyl spinor **16** of covariant real components. The massless Dirac constraint leaves eight physical fermionic states, matching the NS count. The NS and R sectors together are the massless open-string content on the brane: a vector and a Majorana–Weyl spinor, the ten-dimensional gauge multiplet.

This is where the brane does its work. The boundary conditions split the index M into the four Neumann directions $\mu=0,\ldots,3$ and the six Dirichlet directions $m=4,\ldots,9$, and with it the massless state (VI.1.5). The four Neumann components assemble into a four-dimensional gauge field A_μ; the six Dirichlet ones carry no worldvolume index and are six scalars X^m. Said invariantly, the brane breaks the ten-dimensional Lorentz group $SO(9,1)$ to $SO(3,1)\times SO(6)$ (or their spin covers when acting on fermions), the worldvolume Lorentz group times the rotations of the transverse $\mathbb{R}^6$, under which the massless vector decomposes as $(A_\mu,\, X^m)$. The Majorana–Weyl spinor splits in step,

$$\mathbf{16} \to (\mathbf{2},\mathbf{4}) \oplus (\bar{\mathbf{2}},\bar{\mathbf{4}}), \tag{VI.1.7}$$

four four-dimensional Weyl fermions in the spinor **4** of $\mathrm{Spin}(6)\simeq SU(4)$: the gauginos. The conjugate summand is related by the ten-dimensional Majorana condition; it does not double the independent fermions.

Now restore the labels. With N branes each endpoint records which brane it ends on, so a string runs from brane a to brane b and wears a pair of indices; the massless fields become $N\times N$ matrices, the adjoint (and trace) of $U(N)$. The gauge group records which branes a string connects. Everything sits in the adjoint of $U(N)$, which is the adjoint of $SU(N)$ together with the trace; the trace is an overall $U(1)$ under

which nothing is charged, and its scalar is the centre-of-mass position $\frac{1}{N}\operatorname{Tr} X^m$ of the stack. We carry the full $U(N)$ because the brane construction outputs it, and return in §VI.1.3 to the precise sense in which the interacting four-dimensional theory is $SU(N)$.

Keep the picture that comes with the scalars. The value of X^m records where the string endpoint, and so the brane, sits in the transverse $\mathbb{R}^6$,

$$y^m = 2\pi\alpha'\, X^m, \tag{VI.1.8}$$

the physical position. The diagonal entry X^m_{aa} is the position of brane a; the off-diagonal entry X^m_{ab} is a string stretched from a to b, and we will find in §VI.1.4 that it is heavy precisely when the two branes are far apart. The fields on the branes are already a dictionary for the geometry around them.

A word on the notation, since the same letter recurs in related roles. The worldsheet embedding coordinate is $X^M(\sigma,\tau)$; the four-dimensional adjoint scalar is the matrix X^m; its eigenvalues, once it is diagonalized in §VI.1.4, are x^m_a; and the physical transverse positions are $y^m_a = 2\pi\alpha'\, x^m_a$. So X^m is a matrix field, x^m_a an eigenvalue, and y^m_a a spacetime length.

This theory is one the reader may recognize, and the identification is worth deriving field by field rather than asserting. Ten-dimensional $U(N)$ super-Yang–Mills, used here as the local reduction parent of an oriented D9 open-string sector, has minimal $\mathcal{N}=1$ supersymmetry, a single Majorana–Weyl supercharge of positive chirality, written $(1,0)$ in the convention in which type IIB itself is $(2,0)$. An isolated flat type IIB D9 stack is not by itself a tadpole-consistent background; in type I the orientifold projection changes the Chan–Paton group, while Ramond–Ramond charge cancellation also fixes the required brane number. The local $U(N)$ reduction below does not impose that global completion. Its action is

$$S_{10} = \frac{1}{g_{10}^2}\int d^{10}x\ \operatorname{Tr}\Big(-\tfrac{1}{4}F_{MN}F^{MN} - \tfrac{i}{2}\,\bar\lambda\,\Gamma^M D_M\lambda\Big), \qquad M=0,\dots,9, \tag{VI.1.9}$$

with the gauge field A_M and the gaugino λ, a single ten-dimensional Majorana–Weyl spinor of sixteen real components, both in the adjoint of $U(N)$. Reduce to the D3 worldvolume by dropping all dependence on the six transverse coordinates, $\partial_m(\cdot)=0$. The gauge field splits $A_M \to (A_\mu, A_m)$ with the six internal components becoming adjoint scalars $X^m \equiv A_m$, and the field strength splits in step,

$$F_{\mu\nu}\ \text{(the 4d field strength)}, \qquad F_{\mu m} = D_\mu X^m, \qquad F_{mn} = i\,[X^m, X^n], \tag{VI.1.10}$$

so the bosonic Lagrangian splits along the components of $F_{MN}F^{MN}$,

$$\begin{aligned}\operatorname{Tr}\big(-\tfrac{1}{4}F_{MN}F^{MN}\big) &= \operatorname{Tr}\Big(-\tfrac{1}{4}F_{\mu\nu}F^{\mu\nu} - \tfrac{1}{2}F_{\mu m}F^{\mu m} - \tfrac{1}{4}F_{mn}F^{mn}\Big)\\ &= \operatorname{Tr}\Big(-\tfrac{1}{4}F_{\mu\nu}F^{\mu\nu} - \tfrac{1}{2}D_\mu X^m D^\mu X_m + \tfrac{1}{4}[X^m,X^n]^2\Big),\end{aligned} \tag{VI.1.11}$$

the first line the index split $F_{MN}F^{MN} = F_{\mu\nu}F^{\mu\nu} + 2F_{\mu m}F^{\mu m} + F_{mn}F^{mn}$, the second the substitution of the scalar and commutator pieces of (VI.1.10): a four-dimensional gauge field, six adjoint scalars with covariant kinetic term, and a commutator-square term.

With the Hermitian X^m the commutator $[X^m, X^n]$ is anti-Hermitian, so $\mathrm{Tr}[X^m, X^n]^2 = -\mathrm{Tr}[X^m, X^n]^\dagger[X^m, X^n]$, and the term is minus the manifestly non-negative scalar potential

$$V = \frac{1}{4g^2} \sum_{m,n} \mathrm{Tr}\,[X^m, X^n]^\dagger [X^m, X^n] \;\geq\; 0$$

that drives §VI.1.4 and reappears as (VI.1.25) there. The gaugino reduces to the same four four-dimensional Weyl fermions found in the Ramond sector above, sitting in the **4** of $SU(4)_R$. The reduction thus reproduces the open-string massless content field for field. Reduction changes neither the field content nor the sixteen supercharges, so the worldvolume theory carries sixteen supercharges, which in four dimensions is $\mathcal{N} = 4$:

massless open-string mode	10d field	4d field	$SU(4)_R$
NS $\psi^\mu_{-1/2}\lvert 0;k\rangle$	A_μ	gauge field A_μ	**1**
NS $\psi^m_{-1/2}\lvert 0;k\rangle$	A_m	six scalars X^m	**6**
R ground-state spinor	λ	four Weyl fermions λ	**4**

all in the adjoint of $U(N)$. The group rotating the six scalars is the $SO(6)$ of rotations of the transverse $\mathbb{R}^6$, with double cover $\mathrm{Spin}(6) \cong SU(4)_R$: the scalars in the vector **6**, the fermions in the spinor **4**. The internal R-symmetry of the gauge theory is the rotation group of the space the branes inhabit: the first entry of a dictionary the rest of the volume only extends.

What we have not yet found is the dynamics of these fields: their action, their coupling, and the precise sense in which they make a decoupled field theory at all. All three come from the brane's effective action, to which we turn next.

VI.1.3 The decoupling limit

We have been calling the worldvolume theory a field theory, but a stack of D3-branes is part of a full string theory, with gravity and an infinite tower of massive modes. In what sense, and in what limit, is the gauge theory a closed system of its own? Answering this both derives the field theory from the brane and names the single assumption the whole construction rests on.

The low-energy dynamics of a D-brane is governed by the Dirac–Born–Infeld action, written here at the constant dilaton of flat space,

$$S_{\mathrm{DBI}} = -\tau_p \int d^{p+1}\xi \, \sqrt{-\det\bigl(g_{ab} + 2\pi\alpha' F_{ab}\bigr)}, \tag{VI.1.12}$$

with the Dp-brane tension $\tau_p = 1/\bigl((2\pi)^p \alpha'^{(p+1)/2} g_s\bigr)$ (the string coupling $g_s = e^\Phi$ is already carried in τ_p, so at constant Φ no separate dilaton factor appears), induced worldvolume metric g_{ab}, which carries the transverse scalars through the brane's embedding, and worldvolume field strength F_{ab}. This is only the Dirac–Born–Infeld part of the D-brane action; the full action also carries the Wess–Zumino coupling to the Ramond–Ramond potentials, essential for the brane charges, anomalies, and fractional branes met later in the volume, but it does not affect the flat-background quadratic

Yang–Mills kinetic term derived here, so we suppress it in this subsection. The action is nonlinear, resumming the slowly varying powers of $2\pi\alpha' F$ (it is not the full derivative-corrected open-string effective action), but we want only its low-energy part, so expand the determinant for weak, slowly varying fields:

$$\sqrt{-\det\bigl(\eta + 2\pi\alpha' F + (2\pi\alpha')^2\,\partial X\,\partial X\bigr)} = 1 + \frac{(2\pi\alpha')^2}{4}\,F_{ab}F^{ab} + \frac{(2\pi\alpha')^2}{2}\,\partial_a X^m\,\partial^a X_m + O(\alpha'^4). \tag{VI.1.13}$$

The leading 1 integrates to the brane tension, a constant. The next two terms are precisely a Yang–Mills plus scalar action. The quadratic term fixes the coupling,

$$g^2_{\mathrm{D}p} = \frac{1}{\tau_p\,(2\pi\alpha')^2} = (2\pi)^{p-2} g_s\,\alpha'^{(p-3)/2}, \tag{VI.1.14}$$

which sits in the fundamental-trace action $\frac{1}{4g^2}\,\mathrm{Tr}_f\,F^2$. With $\mathrm{Tr}_f(T^a T^b) = \delta^{ab}/2$, the Yang–Mills term in adjoint components is $-\frac{1}{4g^2}F^a_{\mu\nu}F^{a\mu\nu} = -\frac{1}{2g^2}\,\mathrm{Tr}_f\,F^2$, a factor of two above the fundamental-trace form, so

$$g^2_{\mathrm{D}p,\mathrm{YM}} = 2(2\pi)^{p-2} g_s\,\alpha'^{(p-3)/2}, \qquad g^2_{\mathrm{D3,YM}} = 4\pi g_s, \tag{VI.1.15}$$

the second its four-dimensional ($p = 3$) value. The remaining $O(\alpha'^4) \sim \alpha'^2 F^4$ terms carry extra powers of α'. That $g^2_{\mathrm{D3,YM}}$ comes out dimensionless says four is the critical worldvolume dimension for this brane; the general mass dimension $3 - p$ is the dimensional axis of §VI.1.5.

Now the limit that turns this into a closed quantum field theory. Hold g_{YM} of (VI.1.15) and the worldvolume energies fixed, and send $\alpha' \to 0$,

$$g_{\mathrm{YM}},\ E \ \text{ fixed}, \qquad \alpha' \to 0. \tag{VI.1.16}$$

The massive open-string modes, of mass $\sim \alpha'^{-1/2}$, run to infinity and leave the spectrum. The higher DBI terms in (VI.1.13), weighted by α'^2, vanish, so the nonlinear action collapses to its Yang–Mills leading term: for N branes, its non-abelian $U(N)$ completion, the $\mathcal{N} = 4$ theory of §VI.1.2. The ten-dimensional Newton constant $G_N \sim g_s^2\alpha'^4$ runs to zero, so gravity, whose dimensionless strength at energy E is $G_N E^8 = (E/M_{\mathrm{P}})^8$, switches off and the closed-string sector decouples. What survives is exactly the gauge theory, standing alone. This is why the brane becomes a quantum field theory: the field-theory limit keeps only the leading term of the DBI expansion.

The same limit settles what the gauge group really is. Split the $U(N)$ field strength into its trace and traceless parts,

$$F_{ab} = f_{ab}\,\mathbb{1} + \hat{F}_{ab}, \qquad f_{ab} = \partial_a a_b - \partial_b a_a, \qquad \mathrm{Tr}_f\,\hat{F}_{ab} = 0, \tag{VI.1.17}$$

the trace part f_{ab} abelian because $\mathbf{1}$ is central and receives no commutator, the traceless part $\hat{F}_{ab}$ the $SU(N)$ field strength. At the two-derivative order the mixed term drops by tracelessness,

$$\mathrm{Tr}_f\,F_{ab}F^{ab} = N\,f_{ab}f^{ab} + 2\,f_{ab}\underbrace{\mathrm{Tr}_f\,\hat{F}^{ab}}_{=0} + \mathrm{Tr}_f\,\hat{F}_{ab}\hat{F}^{ab}, \tag{VI.1.18}$$

so the leading Yang–Mills action is a free Maxwell term for a_a plus the interacting $SU(N)$ action, nothing joining them: at this order the trace $U(1)$ is already free, the centre of mass of the stack. The adjoint matter is neutral under the trace at every order, so the only open-string tie to the rest is the gauge self-interaction, and that first appears one order up, in the $O(\alpha'^4)$ term of (VI.1.13). Inserting $F = f\mathbf{1} + \hat{F}$ into the symmetrized-trace F^4 structure of the Born–Infeld action leaves a mixed piece,

$$\mathcal{L}^{(4)} \supset \frac{c\,(2\pi\alpha')^2}{g^2}\, f_{ab}f^{ab}\ \mathrm{Tr}_f\, \hat{F}_{cd}\hat{F}^{cd} + \cdots\,, \tag{VI.1.19}$$

with c a definite order-one coefficient fixed by the symmetrized trace, whose value we will not need. This is a genuine interaction between the trace $U(1)$ and the $SU(N)$: at finite α' the centre-of-mass photon is not free, it talks to the non-abelian fields through the higher Born–Infeld vertices. Its weight relative to the Yang–Mills term is the same $(2\pi\alpha')^2$ that suppresses every higher term in (VI.1.13),

$$\frac{\mathcal{L}^{(4)}_{\text{mix}}}{\mathcal{L}^{(2)}} \ \sim\ (2\pi\alpha')^2\, E^4 \ \xrightarrow[\alpha'\to 0]{}\ 0 \qquad (g_{\text{YM}},\, E \text{ fixed}), \tag{VI.1.20}$$

so in the field-theory limit (VI.1.16) this open-string coupling switches off. The one remaining tie is through closed strings: the trace scalar, the centre-of-mass position $\frac{1}{N}\,\mathrm{Tr}_f\, X^m$, sources the bulk graviton and Ramond–Ramond fields with strength $\kappa_{10} \sim g_s\alpha'^2$, and that vanishes in the same limit. With both channels closed, the trace $U(1)$ becomes exactly free and decouples in the very step that produces the field theory. The decoupling of the $U(1)$ is thus not a separate infrared limit ordered after the field-theory limit; it is one face of it, and the interacting four-dimensional Lie-algebra sector is $\mathfrak{su}(N)$. The full gauge group remains $U(N) = (SU(N) \times U(1))/\mathbb{Z}_N$; setting aside the free local trace multiplet does not identify global gauge groups or their line operators.

Free here means decoupled, not absent. The trace gauge field keeps its scalar partner, the centre-of-mass coordinate $\frac{1}{N}\,\mathrm{Tr}_f\, X^m$, and that scalar is exactly where the geometry is read. It is an unlifted flat direction precisely because nothing is charged under the trace $U(1)$: no D- or F-term potential can fix it, so its vacuum value is free to be the overall position of the stack in the transverse space. The moduli space of §VI.1.4 is built from these gauge-scalar vacuum values, and the gauge coupling never enters that vacuum structure, so a coupling sent weak, even a photon decoupled outright, costs the geometry nothing. This is the precise sense in which a free sector still carries physical information: it lives in the flat direction, not in the interaction. The same local adjoint trace split works in lower dimensions. The free abelian sector still carries dimension-dependent observables: a dual photon and monopole operators in three dimensions, or Fayet–Iliopoulos and theta data in two. Retaining these observables and the global gauge-group data is a separate choice from isolating the interacting local sector. Charged relative abelian factors in quiver theories are not covered by this trace argument. In four dimensions the local interacting $\mathfrak{su}(N)$ sector can likewise be studied separately; this does not erase the global $U(N)$ data.

The scales make this consistent. The limit holds $g^2_{\text{YM}} = 4\pi g_s$ fixed, hence g_s fixed,

and sends $\alpha' \to 0$. The scales then run as

$$\begin{aligned} M_s = \alpha'^{-1/2} \to \infty, \qquad & M_{\rm P} \sim g_s^{-1/4} \alpha'^{-1/2} \to \infty, \\ G_N \sim g_s^2 \alpha'^4 \to 0, \qquad & \kappa_{10} \sim \sqrt{G_N} \sim g_s \alpha'^2 \to 0, \end{aligned} \tag{VI.1.21}$$

so the string scale lifts the entire massive tower out of the spectrum, the Planck scale runs off in step (larger only by the fixed $g_s^{-1/4}$), the gravitational coupling at a fixed worldvolume energy E, the dimensionless $G_N E^8 = (E/M_{\rm P})^8$, vanishes, and closed strings decouple. What is left has a finite coupling $g_{\rm YM}$, a finite field content, and no gravity: a quantum field theory. The same counting shows why the limit is delicate. It requires the worldvolume energies to stay parametrically below M_s throughout, and it is the existence and smoothness of this scaling, not the algebra of the leading term, that §VI.1.6 states as an assumption.

One consequence will matter in §VI.1.4. The moduli of the gauge theory are the scalar eigenvalues,

$$x^m = \frac{y^m}{2\pi\alpha'} \ \text{ fixed} \qquad \Longrightarrow \qquad y^m = 2\pi\alpha' \, x^m \to 0, \tag{VI.1.22}$$

and it is these, not the physical separations y^m, that are held fixed as $\alpha' \to 0$: a finite separation in gauge-theory units is a physical length that shrinks with α'. The probe therefore reads the geometry in the field-theory coordinates x^m, restoring y^m only when a spacetime length is wanted.

The same decoupling limit also has a closed-string description when the D3-branes back-react appreciably. One then keeps the throat rather than the asymptotically flat bulk; at suitable large $g_s N$ the throat has a useful gravitational description. Here we use the open-string gauge theory as a probe of the prescribed transverse background. The near-horizon description is proposed as another description of the same interacting system in the common decoupling limit. Its useful gravitational regime is outside the small-back-reaction probe approximation used below.

The dimensionless coupling is the first sign of something stronger: the $\mathcal{N} = 4$ theory is not merely renormalizable but superconformal. Its beta function vanishes identically,

$$\beta(g_{\rm YM}) = 0 \quad \text{to all orders,} \tag{VI.1.23}$$

so $g_{\rm YM}$ is an exactly marginal parameter and the theory is scale invariant at every value of the coupling. Scale invariance is enhanced to the full conformal group, and with the sixteen Poincaré and sixteen conformal supercharges the symmetry closes into the superconformal group

$$\mathfrak{psu}(2,2|4)_{\bar{0}} \cong \mathfrak{so}(4,2) \oplus \mathfrak{su}(4)_R, \tag{VI.1.24}$$

whose even Lie algebra contains the conformal and transverse-rotation generators. The corresponding global groups can differ by central quotients. The transverse symmetry is the very R-symmetry we met as the transverse rotations $SO(6)$. The interacting $SU(N)$ part of the worldvolume theory is thus a four-dimensional superconformal field theory, the maximally supersymmetric one, with the decoupled diagonal $U(1)$ free. We note this as a property of the constructed theory and go no further: the exactly-marginal coupling as a conformal manifold, the central charges, and the exact results that the

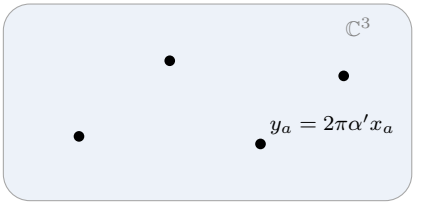


Figure VI.1.1: Moduli space as target geometry (schematic). Each of the N D-branes sits at a point $y_a = 2\pi\alpha' x_a$ of the transverse space, the joint eigenvalues of the commuting scalars X^m; the moduli space (VI.1.27) is N copies of the transverse $\mathbb{C}^3$ symmetrized, $\mathrm{Sym}^N(\mathbb{C}^3)$. The gauge theory hands back the geometry the branes live in.

superconformal symmetry controls are the synthesis of Part III, not the business of this construction chapter. This is also why the near-horizon scaling just set aside lands on $AdS_5 \times S^5$, whose isometry $SO(4,2) \times SO(6)$ reproduces the superconformal symmetry: the geometric face of the gauge/gravity duality we leave to its own program.

VI.1.4 Moduli space as target geometry

Where can the branes go? In a vacuum the fields are constant, so the only surviving piece of the ten-dimensional field strength is the purely transverse, derivative-free part $F_{mn} = i[X^m, X^n]$, and the energy is its norm,

$$V \;=\; \frac{1}{4g^2} \sum_{m,n} \mathrm{Tr}\,[X^m, X^n]^\dagger [X^m, X^n] \;\geq\; 0, \tag{VI.1.25}$$

manifestly non-negative with the Hermitian fundamental-trace convention, vanishing exactly when the six matrices commute,

$$[X^m, X^n] = 0, \tag{VI.1.26}$$

on which flat direction they are simultaneously diagonalizable, and their joint eigenvalues $\big(x_a^4, \ldots, x_a^9\big)$, $a = 1, \ldots, N$, fix the brane positions $y_a^m = 2\pi\alpha'\, x_a^m$ as N points of the transverse $\mathbb{R}^6 \cong \mathbb{C}^3$. The gauge rotations that survive permute the eigenvalues, the Weyl group S_N of $U(N)$, so the space of vacua is

$$\mathcal{M} \;=\; \mathrm{Sym}^N(\mathbb{C}^3) \;=\; (\mathbb{C}^3)^N / S_N, \qquad \dim_{\mathbb{R}} \mathcal{M} = 6N. \tag{VI.1.27}$$

The moduli space is the transverse geometry the branes probe: here, flatly, $\mathbb{C}^3$, N copies symmetrized.

That this is a reconstruction and not a formal identification is visible in the spectrum, and the cleanest way to see it is to separate two branes and quantize the string between them. Put brane a at transverse position y_a and brane b at y_b. The transverse worldsheet coordinates now satisfy Dirichlet conditions with *different* endpoints, pinning the two ends of the string to y_a and y_b; its classical profile stretches straight across the gap, of

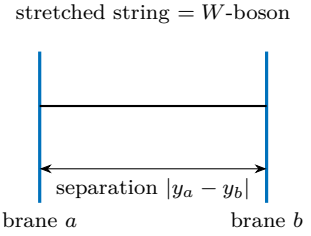


Figure VI.1.2: The stretched-string W-boson (schematic). When two branes separate, the off-diagonal open string stretched between them costs its tension times its length, giving mass $m_{ab} = |y_a - y_b|/2\pi\alpha'$ (VI.1.29): the W-boson of the Higgsing $U(2) \to U(1) \times U(1)$. An isolated coincident pair ($y_a = y_b$) restores its massless W and $U(2)$ factor. Full $U(N)$ requires all N branes to coincide.

length $|y_a - y_b|$, and this stretched configuration adds its tension-times-length energy to the mass. Quantitatively the Dirichlet zero mode shifts (VI.1.4) to

$$\alpha' M^2 = \alpha' \Big(\frac{|y_a - y_b|}{2\pi\alpha'} \Big)^2 + \big(N - \tfrac{1}{2}\big), \tag{VI.1.28}$$

so at the massless level $N = \frac{1}{2}$, where the zero-point term $(N - \frac{1}{2})$ cancels, the off-diagonal mode is the would-be W-boson of the broken $U(N)$, with mass

$$m_{ab}^2 = \Big(\frac{|y_a - y_b|}{2\pi\alpha'} \Big)^2 \quad \Longrightarrow \quad m_{ab} = \frac{|y_a - y_b|}{2\pi\alpha'} = |x_a - x_b|, \tag{VI.1.29}$$

the eigenvalue separation of the gauge scalars. The gauge theory measures distances in the geometry: an isolated coincident pair ($y_a = y_b$) restores its $U(2)$ factor. The full $U(N)$ is restored only when all N branes coincide; when all positions are distinct, the unbroken group is $U(1)^N$ and the massive vectors measure their pairwise separations. This is why "moduli space = geometry" is physics and not notation.

The breaking is a Higgs mechanism, and its counting is exact. At a generic point of $\mathcal{M}$ the N eigenvalues are distinct, and the gauge group is broken to its maximal torus,

$$U(N) \to U(1)^N, \qquad \#\{\text{broken generators}\} = N^2 - N = \#\{W\text{-bosons}\}, \tag{VI.1.30}$$

the $N^2 - N$ broken generators pairing with the $N^2 - N$ off-diagonal W-bosons (VI.1.29): each W-boson eats a would-be Goldstone scalar and becomes massive. The N diagonal vector multiplets stay massless and carry the $6N$ position moduli, matching $\dim_{\mathbb{R}} \mathcal{M} = 6N$. The metric on $\mathcal{M}$ is read from the scalar kinetic term $\mathrm{Tr}\, D_\mu X^m D^\mu X_m$ on the diagonal moduli: it is flat, the Euclidean metric on $(\mathbb{R}^6)^N$ descended to the quotient. Flatness is special to the maximally supersymmetric flat-space example; once the transverse space is replaced by a nontrivial quotient or singularity, in the orbifold chapters to come, the moduli-space geometry is no longer a trivial copy of $\mathbb{R}^6$, and its singular loci, quotient structure, and protected holomorphic data become the content of the construction rather than a restatement of the input.

The structure of $\mathcal{M}$ also encodes the spectrum at its singularities. Where two eigenvalues collide the corresponding W-bosons (VI.1.29) become massless and the gauge symmetry enhances, $U(1) \times U(1) \to U(2)$ for the colliding pair; the symmetric-product locus where branes coincide is exactly the locus of enhanced gauge symmetry. The geometry of the moduli space and the pattern of unbroken gauge symmetry are thus one set of data read two ways. These coincident-brane loci are the flat-space prototype of a general lesson: a singular locus of the moduli space signals extra light states and enhanced gauge symmetry. They should not be confused with the target-space singularity of the next chapter, the fixed locus of Γ acting on $\mathbb{C}^3$; it is that geometric fixed locus, not the symmetric-product collision, that carries the fractional branes and quiver nodes there.

Two cautions ride along, both load bearing later. First, $\mathcal{M}$ is the *symmetric* product: the S_N identification is physical, because the branes are identical. Second, the name "Coulomb branch" for $\mathcal{M}$ belongs to the maximally supersymmetric case, where the surviving $U(1)^N$ photons put the generic vacuum in a Coulomb phase. In $\mathcal{N} = 1$ language the X^m sit in adjoint chiral multiplets, and once the transverse space is orbifolded (next section, and Chapter 2 onward) the branch that reconstructs the geometry is a Higgs (mesonic) branch, not a Coulomb branch.

VI.1.5 Reading geometry with branes

The open-string spectrum supplies fields, the scaling limit isolates their dynamics, and their commuting scalar vacua supply positions. Together these steps give the following construction rule.

Principle VI.1.1 (The probe construction)**.** A quantum field theory is constructed as the field-theory limit of the worldvolume theory of branes probing a transverse geometry. The branch of its moduli space carrying the transverse-position moduli reconstructs an aspect of the probed geometry, exactly in the classical orbifold case and up to stated corrections otherwise.

In flat space the moduli space (VI.1.27) returns the $\mathbb{C}^3$ we started from. The construction rule depends on the decoupling assumption and the probe regime stated below. Its content appears the moment the transverse geometry becomes a nontrivial quotient. Replace $\mathbb{C}^3$ by an orbifold $\mathbb{C}^3/\Gamma$, $\Gamma \subset SU(3)$: the open-string spectrum is projected onto its Γ-invariant part, the single flat-space gauge group breaks into a product of nodes joined by bifundamentals, a quiver gauge theory, and the branch of its moduli space that moves a brane through the bulk recovers the orbifold geometry $\mathbb{C}^3/\Gamma$. At nonzero Fayet–Iliopoulos parameters the same quiver describes Kähler/GIT deformations of that branch, which in the basic examples are the familiar resolutions. The gauge theory is no longer free data; it is dictated by the singularity, and its protected quantities follow from the geometry. That projection is the content of Chapter 2; it is previewed here, not established.

The projection is worth stating in outline, since it is the mechanism the whole volume turns on. A finite group $\Gamma \subset SU(3)$ acts on the transverse $\mathbb{C}^3$, and consistency

forces it to act on the Chan–Paton space V, of dimension K, through a representation

$$\gamma : \Gamma \to U(K), \qquad U(K) \to \textstyle\prod_i U(N_i), \tag{VI.1.31}$$

the gauge field, inert on its transverse index, keeping the components commuting with $\gamma(\Gamma)$, so the upstairs $U(K)$ breaks into one factor for each irreducible representation appearing in γ; the scalars, rotated both by Γ on their transverse index and by γ on their labels, survive in the blocks paired by the geometric action and become bifundamental matter between nodes, with adjoint loops where a node pairs with itself. One mobile brane downstairs corresponds to $|\Gamma|$ Chan–Paton labels upstairs, so K counts labels, not physical branes. The outcome is a quiver gauge theory whose nodes and arrows are fixed by the representation theory of Γ, and whose geometric branch is the orbifold the branes probe. Once the singularity and the brane data are fixed, here the Chan–Paton representation γ and hence the rank vector, the nodes, arrows, and inherited interactions are no longer free choices: they are determined by the orbifold projection. That is the step where the construction gains content, and Chapter 2 carries it out in full.

Which branch reconstructs the geometry depends on how much supersymmetry survives, and it is not generically the Coulomb branch. The flat maximal case gives the $\mathcal{N} = 4$ Coulomb branch above. In the orbifold cases this volume develops, the geometry is a Higgs-type branch instead, and the embedding sets the surviving supersymmetry,

$$\mathcal{N} = \dim_{\mathbb{C}}(\mathbf{4}^{\Gamma}), \qquad \Gamma \subset SU(2) \;\Rightarrow\; \mathcal{N} \geq 2, \qquad \Gamma \subset SU(3) \;\Rightarrow\; \mathcal{N} \geq 1, \tag{VI.1.32}$$

a generic nontrivial $\mathbb{C}^2/\Gamma$ probe giving an $\mathcal{N} = 2$ quiver whose Higgs branch is the ALE space, a hyperkähler quotient (Chapters 3 and 4), a $\mathbb{C}^3/\Gamma$ probe with exactly one invariant spinor giving an $\mathcal{N} = 1$ quiver whose mesonic branch is the Calabi–Yau cone (Chapters 4 and 6). These are forward references, established there. A group contained in an $SU(2)$ subgroup is also contained in $SU(3)$, so subgroup inclusion alone cannot give the exact supersymmetry count; the identity group preserves all four components.

The D3 belongs to a family of odd-p branes. In flat space the same reduction preserves sixteen supercharges on any single Dp-brane, giving a $(p+1)$-dimensional maximally supersymmetric gauge theory; the coupling's mass dimension,

$$[\, g^2_{\mathrm{D}p,\mathrm{YM}} \,] = 3 - p, \tag{VI.1.33}$$

read from (VI.1.15), marks $p = 3$ as the unique classically scale-invariant case, with $p < 3$ super-renormalizable and $p > 3$ non-renormalizable as an effective theory.

This dimension count does not establish a gravity-free field-theory limit for every row. At fixed $g^2_{\mathrm{D}p,\mathrm{YM}}$ the DBI coupling gives $g_s \propto \alpha'^{(3-p)/2}$ and hence $G_{10} \propto g_s^2 \alpha'^4 \propto \alpha'^{7-p}$. For $p = 7$ this scaling alone supplies no suppression; higher-dimensional brane limits require their own decoupling analysis.

Type IIB supplies the odd-p branes, D(-1), D1, D3, D5, D7, D9, and a Dp-brane has $9 - p$ transverse dimensions, an even number for odd p, so once a complex structure is chosen the transverse space is packaged locally as

$$\mathbb{R}^{9-p} \cong \mathbb{C}^{(9-p)/2}, \tag{VI.1.34}$$

which can degenerate to a Calabi–Yau cone. The Calabi–Yau and orbifold examples used later come with such a choice. Probing such a cone the singularity reduces the

surviving supersymmetry, and $p+1$ sets the worldvolume dimension: an isolated D(-1)-brane gives a zero-dimensional matrix model while the D(-1)-D3 system realizes the ADHM data for instantons in the D3 gauge theory, a D1-brane at a CY_4 with generic $SU(4)$ holonomy gives a two-dimensional $(0,2)$ theory (Vol. VII), and the D3 at a CY_3 gives the four-dimensional theories developed in this volume. The full family, with the preserved supercharges and transverse cone of each brane, is collected in Table VI.1.1; here the D3 row carries the development and the others are named only to locate it.

p	$d=p+1$	transverse	cone	$[g^2_{\mathrm{YM}}]$	supercharges
-1	0	$\mathbb{C}^5$	CY_5	4	16
1	2	$\mathbb{C}^4$	CY_4	2	16
3	4	$\mathbb{C}^3$	CY_3	0	16
5	6	$\mathbb{C}^2$	CY_2	-2	16
7	8	$\mathbb{C}$	CY_1	-4	16
9	10	point	none	-6	16

Table VI.1.1: The Type IIB odd-p dimensional axis. Each single Dp-brane preserves sixteen supercharges and gives a $(p+1)$-dimensional maximally supersymmetric gauge theory; with a complex structure chosen, the transverse $\mathbb{R}^{9-p} \cong \mathbb{C}^{(9-p)/2}$ (VI.1.34) can degenerate to a Calabi–Yau cone $\mathrm{CY}_{(9-p)/2}$. The coupling mass dimension $[g^2_{\mathrm{YM}}] = 3-p$ (VI.1.33) marks the D3 (4d, in bold) as the unique classically scale-invariant case; $p=-1$ is the matrix-model/ADHM endpoint and $p=9$ the spacetime-filling case with no transverse space.

VI.1.6 Conditions on the probe construction

The position-moduli calculation gives an exact classical answer in flat space. Extending its interpretation to a decoupled theory on a probe of a singularity requires the following physical conditions.

The decoupling limit is the assumption. The field-theory limit of §VI.1.3 is taken both to exist and to remove gravity: we assume that holding g_{YM} and the worldvolume energies fixed while $\alpha' \to 0$ defines a smooth theory, and that the brane's full string dynamics flows to exactly the decoupled gauge theory, with no relic of the discarded massive tower or the bulk. For the pure field-theory limit this is on firm ground, since the $\mathcal{N}=4$ theory is a known, ultraviolet-complete quantum field theory in its own right; but the flow statement is an input, not a theorem, and it is the single load-bearing assumption every construction in this volume inherits. This is a distinct statement from the probe approximation below. The $\alpha' \to 0$ decoupling sends $G_{10} \sim g_s^2 \alpha'^4 \to 0$ and closes off gravity in the field-theory sense at any fixed g_s; what $g_s N$ controls is instead the back-reaction of the brane stack, and at large $g_s N$ that back-reaction is the province of holography, a separate program. The two are independent idealizations, and both are assumed here.

The reconstruction is of the protected, probe-visible geometry. The identification of the moduli space with a geometry rests on the supersymmetric branch, defined by the F-terms, the D-terms with their Fayet–Iliopoulos parameters, the gauge quotient, and the chiral ring. The higher-derivative DBI corrections, $\alpha'^2 F^4$ and beyond, correct the dynamics away from the strict two-derivative action; they do not by themselves change the constant-field vacuum variety. String loops and quantum effects can renormalize the non-protected metric data, in particular the Kähler metric on the moduli space. What is protected in the supersymmetric orbifold cases this volume treats is the holomorphic skeleton, the quiver, the superpotential, the chiral ring, and the complex structure of the geometric branch, and that holomorphic data is the geometry we extract. The metric corrections are real but belong to the non-protected Kähler data, flagged separately rather than folded into the statement that the moduli space equals the geometry.

The probe approximation neglects back-reaction. The branes are treated as probes of a fixed closed-string background, their own gravitational and Ramond–Ramond fields, which would curve the space they sit in, dropped. This is controlled at finite N and small $g_s N$, where the back-reaction $\sim g_s N$ is parametrically small and the brane reads off the geometry it was placed in. As $g_s N$ grows the dent deepens into a throat and the probe description crosses over to the supergravity solution and its near-horizon, holographic regime, named in §VI.1.3. The probe construction and holography are two ends of one system, valid in opposite regimes of $g_s N$.

The moduli space is a symmetric product, not the bare transverse space. Equation (VI.1.27) carries the physical S_N quotient: the N branes are identical, so configurations related by permuting them are one point, and $\mathrm{Sym}^N(\mathbb{C}^3)$ has orbifold singularities wherever branes coincide, exactly where the gauge symmetry enhances. The slogan moduli space = geometry is sharpest on the single-brane slice $N = 1$, where $\mathcal{M} = \mathbb{C}^3$ literally is the transverse space; for $N > 1$ the geometry is recovered one brane at a time, as the position of a single probe moving in the background set by the others. That single-probe reading is the one that survives the curving of the transverse space, and it is the sense in which the moduli space reconstructs the geometry throughout the volume.

Status and sources

The evidence tags ([WS] worldsheet, [DEC] decoupling-limit assumption), the convention pointers, and the source anchors are collected here, keyed by section. Conventions used: the mostly-plus signature, the spinor and supercharge counting, and the α' and brane-action normalizations τ_p and g^2_{YM} (brane-action and trace normalization).

§VI.1.1 Open strings as the field theory. The open-string origin of the worldvolume gauge theory is perturbative string data [WS] (Witten 1996, §3, pp. 7–8; Polchinski Vol. 2 §13.3–13.4; the boundary quantization is Vol. III, the DBI and Wess–Zumino action/ten-dimensional Yang–Mills reduction). The removal of gravity and massive modes is the decoupling assumption [DEC] made precise in §VI.1.3.

§VI.1.2 The theory on the branes. The open-string mode expansion, the NS mass formula (VI.1.4), and the GSO projection are the general quantization, cited to its home (Vol. III, ten-dimensional Yang–Mills reduction; Polchinski Vol. 2 ch. 10). The brane-specific results derived here: the $SO(9,1) \to SO(3,1) \times SO(6)$ split of the massless vector into (A_μ, X^m), $U(N)$ from Chan–Paton, and $X^m \leftrightarrow$ brane position [WS] (Witten 1996, §3, pp. 7–8, (3.1); Polchinski Vol. 2 §13.3–13.4). $\mathcal{N} = 4$ as the reduction of 10d SYM, sixteen supercharges, and R-symmetry = transverse $SO(6)$ [WS] (same; the supercharge

count and $16/4 = 4$ are evaluated, the finite calculation, against the spinor and supersymmetry counting reality conditions; the 10d SYM is $\mathcal{N} = (1, 0)$ and type IIB is $(2, 0)$, positive chirality in the first slot). The open-string-mode/field-component table is the worldsheet-to-field dictionary. The [WS] verdict holds for perturbative calculations in the untwisted string: the massless spectrum is fixed by quantizing the open string with the D3 boundary conditions (NS/R sectors, GSO, Chan–Paton), and the reduced super-Yang–Mills couplings by open-string disk amplitudes; no decoupling limit, duality, or geometric extrapolation enters, the decoupling step being the separate [DEC] of §VI.1.3. Gauge data recorded as the construction's output, with the diagonal $U(1)$ the decoupled center of mass. The coupling is derived in §VI.1.3.

§VI.1.3 The decoupling limit. The DBI action (VI.1.12) is cited to its home (Vol. III, the DBI and Wess–Zumino action; Polchinski Vol. 2 §13.3). Its leading-order expansion (VI.1.13), the coupling (VI.1.15) (this is Polchinski's (13.3.25) $g^2_{\mathrm{D}p}$, which sits in his $\frac{1}{4g^2}\,\mathrm{Tr}_f$ action (13.3.26); the factor of two raising it to $g^2_{\mathrm{D}p,\mathrm{YM}}$ is the brane-action and trace normalization adjoint-component versus fundamental-trace normalization, not an abelian/non-abelian effect; mass dimension $3-p$), and the collapse to Yang–Mills are derived here [WS] (brane-action and trace normalization). The [WS] verdict holds because the DBI action and the tension $\tau_p = 1/((2\pi)^p \alpha'^{(p+1)/2} g_s)$ (Polchinski (13.3.23)) are fixed by perturbative open-string disk data, with the $g_s = e^{\Phi}$ weight the disk Euler number; the coupling is the worldvolume coupling at any α' and does not invoke the decoupling step. The *existence* of the field-theory limit and the decoupling of gravity are assumed, not derived: the keystone assumption of the probe engine [DEC] (the field-theory limit and the decoupling of gravity are the standard ones, Polchinski Vol. 2 §13.3, and predate the holographic route; the scaling $G_N \sim g_s^2 \alpha'^4$ is Vol. II, gravity decoupling), recorded as such in §VI.1.6. The near-horizon limit is a roadmap engine, not used here. The $\mathcal{N} = 4$ theory's superconformal invariance ($\beta = 0$ to all orders; even Lie algebra $\mathfrak{so}(4,2) \oplus \mathfrak{su}(4)_R$ of $\mathfrak{psu}(2,2|4)$) is a standard property of the target field theory, not a string-construction claim of this engine; the match of that symmetry to the $AdS_5 \times S^5$ isometry is the holographic point (Maldacena 1998), set aside with the near-horizon limit. The SCFT-specific dynamics (the conformal manifold, central charges, exact results) are routed to Part III. The $U(N)$-vs-$SU(N)$ clarification, the trace $U(1)$ as the free centre of mass and its local decoupling as one face of the $\alpha' \to 0$ limit, while the global $U(N) = (SU(N) \times U(1))/\mathbb{Z}_N$ and lower-dimensional abelian observables remain distinct, is explained by (VI.1.17)–(VI.1.20): the F^4 Born–Infeld coupling of the trace to the $SU(N)$ and its $\alpha' \to 0$ removal, and the point that a free sector is not lost, its scalar VEV being the centre-of-mass modulus the moduli space reads. [WS].

§VI.1.4 Moduli space as target geometry. Scalar potential from the transverse field strength, flat directions = commuting X^m, eigenvalues = brane positions, and $\mathcal{M} = \mathrm{Sym}^N(\mathbb{C}^3)$ [WS] (Witten 1996, §3, pp. 7–8, (3.1); the per-brane factor $9 - p = 6$ and resulting $6N$ dimension are checked by the finite calculation, while that check does not derive the symmetric-product quotient). W-boson mass derived from the Dirichlet stretched string (VI.1.28)–(VI.1.29) [WS] (same; the DD zero-mode shift is the general quantization, Vol. III). The [WS] verdict: the potential descends from the reduced super-Yang–Mills action of §VI.1.2 (worldsheet-fixed couplings) and its flat directions are commuting X^m, while the reconstruction is confirmed independently by the stretched-string W-boson mass (VI.1.29), a direct DD open-string computation; both are perturbative, untwisted-string statements. The leading classical $\mathcal{M}$ is exact for the orbifold cases this volume treats, with α'/g_s corrections flagged in §VI.1.6. Symmetric product vs. bare space, Coulomb-vs-Higgs branch name, vacuum-branch nomenclature and the stated distinction.

§VI.1.5 Reading geometry with branes. The construction (Principle VI.1.1) is a physical principle with a stated domain [DEC], carried by the worldvolume identification [WS] (§VI.1.2), the decoupling assumption [DEC] (§VI.1.3), and the moduli-space reconstruction [WS] (§VI.1.4); its domain is §VI.1.6. Flat-space $(p+1)$-dim 16-supercharge reduction [WS]. The orbifold quiver, the Higgs/mesonic branches, and the lower-dimensional probes are forward references (VI.2; Chapters VI.3–VI.6; Vol. VII), with the conditions given in their chapters.

§VI.1.6 Conditions on the probe construction. The decoupling assumption [DEC] is specified in §VI.1.3. The probe approximation assumes finite N and small $g_s N$. The classical symmetric product has the stated α'/g_s qualifications, and the branch name depends on the preserved supersymmetry.

References

Maldacena, J. M. (1998). "The Large N limit of superconformal field theories and supergravity". In: *Adv. Theor. Math. Phys.* 2, pp. 231–252. DOI: 10.4310/ATMP.1998.v2.n2.a1. arXiv: hep-th/9711200.

Polchinski, J. (1998a). *String Theory. Vol. 1: An Introduction to the Bosonic String*. Cambridge Monographs on Mathematical Physics. Cambridge University Press. DOI: 10.1017/CBO9780511816079.

Polchinski, J. (1998b). *String Theory. Vol. 2: Superstring Theory and Beyond*. Cambridge Monographs on Mathematical Physics. Cambridge University Press. DOI: 10.1017/CBO9780511618123.

Witten, E. (1996). "Bound states of strings and p-branes". In: *Nucl. Phys. B* 460, pp. 335–350. DOI: 10.1016/0550-3213(95)00610-9. arXiv: hep-th/9510135.

Chapter VI.2

Quivers from orbifold projections

VI.2.1 From flat space to a singularity

In flat space, the scalar matrices on D3-branes describe their positions in $\mathbb{C}^3$. At an orbifold singularity the branes must also respect the identification of points under a finite group Γ. This geometric identification acts on the endpoints of their open strings. Requiring the combined action to leave a state invariant splits the flat-space gauge group into factors and places matter between them. The representation theory of Γ fixes both the factors and their connections.

The calculation has a second direction. Starting from the projected fields, we solve their vacuum equations and construct gauge-invariant coordinates. For a regular brane these coordinates recover the original quotient space. Thus the same group action first determines the quiver and then reappears as the geometry of its mesonic branch. The affine necklace and the chiral $\mathbb{C}^3/\mathbb{Z}_3$ quiver make the two steps explicit.

Two examples carry the chapter, chosen to bracket the two qualitatively different outcomes. When Γ acts on two of the transverse complex dimensions, $\mathbb{C}^2/\Gamma$ with $\Gamma \subset SU(2)$, eight supercharges survive and the gauge theory is non-chiral, a four-dimensional $\mathcal{N} = 2$ theory; the quiver is a closed necklace, the affine $\hat{A}_{n-1}$ diagram, and its moduli space reconstructs the A_{n-1} surface singularity. For the $\mathbb{Z}_3$ action on all three coordinates used here, $\Gamma \subset SU(3)$ leaves four supercharges and produces a chiral $\mathcal{N} = 1$ theory with a cubic superpotential. Its quiver describes the cone over $\mathbb{P}^2$, the local dP_0 geometry, three nodes cyclically joined, whose moduli space reconstructs $\mathbb{C}^3/\mathbb{Z}_3$. Both groups are abelian, so the character theory is one-dimensional and every step is explicit. The non-abelian $\mathbb{C}^2/\Gamma$ family and the McKay correspondence in its geometric depth are the next chapter, for which this one is the worked abelian warm-up. We keep the mostly-plus signature and the brane-action normalizations of Chapter 1 throughout, and we reuse, without re-deriving, the open-string spectrum, the reduced super-Yang–Mills theory, and the decoupling limit established there.

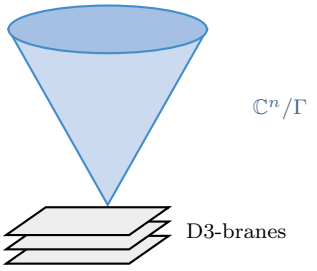


Figure VI.2.1: The setup (schematic). A stack of D3-branes sits at the tip of the singular cone $\mathbb{C}^n/\Gamma$ (here $\mathbb{C}^2/\mathbb{Z}_n$ and $\mathbb{C}^3/\mathbb{Z}_3$); the orbifold projection of their worldvolume $U(N)$ theory is the quiver gauge theory of this chapter, and a brane that leaves the tip into the bulk reconstructs the geometry. The D3-branes have six real transverse directions. The drawn cone represents the active $\mathbb{C}^2/\mathbb{Z}_n$ factor schematically, with its spectator $\mathbb{C}$ suppressed; the second example acts on all of $\mathbb{C}^3$.

Recipe: from orbifold data to the gauge theory.

The chapter is this one recipe, carried out twice. *Input:* a cyclic group $\Gamma = \mathbb{Z}_n$ with weights a_α on the transverse coordinates, and a Chan–Paton representation γ on the open-string labels. *Projection:* keep the gauge-field blocks that carry no net Γ phase, and the scalar blocks whose Chan–Paton phase cancels the geometric phase of z_α. *Output:* the nodes are the irreducible representations of Γ that appear in γ; the arrows are the surviving scalar blocks; and the superpotential is the projected $\mathcal{N} = 4$ cubic. For the regular branes of the worked examples, the mesonic branch, built from gauge-invariant closed loops, reproduces $\mathbb{C}^m/\Gamma$. In symbols, weights $a_\alpha \to$ representation $\gamma \to$ surviving blocks $\to$ quiver $\to$ mesonic branch.

VI.2.2 The orbifold geometry and the Calabi–Yau condition

Before any branes, fix the space they will probe. An orbifold $\mathbb{C}^m/\Gamma$ is the quotient of $\mathbb{C}^m$ by a finite group Γ of unitary rotations: points related by a group element are declared identical. The quotient is smooth at points where Γ acts freely, and it carries an orbifold singularity at any point with a nontrivial stabilizer, a point left fixed by some nontrivial group element. The branes will sit at such a singular point, and the gauge theory will be the probe's reading of the singularity.

We take Γ abelian and cyclic, $\Gamma = \mathbb{Z}_n$ of order n, generated by an element g acting on the m complex coordinates by phases,

$$g: \quad z_\alpha \longmapsto \omega^{a_\alpha} z_\alpha, \qquad \omega = e^{2\pi i/n}, \qquad \alpha = 1, \ldots, m, \tag{VI.2.1}$$

with integer weights a_α defined modulo n; the phase $\omega = e^{+2\pi i/n}$ is fixed once and globally. The dimension m and the order n are independent data: $\mathbb{C}^2/\mathbb{Z}_3$ has $m = 2$, $n = 3$.

The single most important property of the action is whether it preserves supersymmetry. The group element g multiplies the holomorphic volume form by the determinant of its action,

$$g: \quad dz_1 \wedge \cdots \wedge dz_m \;\longmapsto\; \omega^{a_1+\cdots+a_m}\, dz_1 \wedge \cdots \wedge dz_m, \tag{VI.2.2}$$

so the holomorphic volume form survives precisely when the exponent vanishes,

$$\sum_{\alpha=1}^{m} a_\alpha \;\equiv\; 0 \pmod{n}. \tag{VI.2.3}$$

The determinant-one condition puts the orbifold action in $SU(m)$ and preserves the holomorphic volume form. On the smooth locus of this flat quotient, the surviving spinors are precisely those invariant under the group action; this is the supersymmetry condition needed for the probe. The general relation between special holonomy and parallel spinors belongs to Part I. For the nontrivial embeddings used here, $\Gamma \subset SU(2)$ leaves eight four-dimensional supercharges, whereas an $SU(3)$ action with no invariant complex direction leaves four. The two examples of this chapter are the cyclic actions

$$\begin{aligned} &\mathbb{C}^2/\mathbb{Z}_n: \quad (a_\alpha) = (1,-1,0), \quad 1-1+0=0, \\ &\mathbb{C}^3/\mathbb{Z}_3: \quad (a_\alpha) = (1,1,1), \quad 1+1+1 \equiv 0 \pmod 3, \end{aligned} \tag{VI.2.4}$$

both Calabi–Yau, the first in $SU(2)$ with an inert third coordinate, the second in $SU(3)$.

The geometry of the quotient is read from its ring of invariant functions, and it is worth setting up the general recipe, since the gauge theory will hand this ring back. Under g a monomial picks up the product of its coordinate phases,

$$g: \quad z_1^{e_1} \cdots z_m^{e_m} \;\longmapsto\; \omega^{e_1 a_1+\cdots+e_m a_m}\, z_1^{e_1} \cdots z_m^{e_m}, \tag{VI.2.5}$$

so it is invariant exactly when its exponents satisfy

$$\sum_{\alpha=1}^{m} e_\alpha\, a_\alpha \;\equiv\; 0 \pmod{n}. \tag{VI.2.6}$$

The invariant monomials are closed under multiplication, so they form a ring, the coordinate ring of $\mathbb{C}^m/\Gamma$; choosing a finite set of generators and writing the relations among them presents the orbifold as an affine variety, the singular space whose conical tip is the image of the fixed point. For the weights used below we can find a small generating set explicitly. We carry it out for each example at the point where its gauge theory reconstructs the same ring, in §VI.2.6 and §VI.2.7, and the two we will meet are an A_{n-1} surface singularity from $\mathbb{C}^2/\mathbb{Z}_n$ and the cone over $\mathbb{P}^2$, the local dP_0 geometry, from $\mathbb{C}^3/\mathbb{Z}_3$.

One structural point about the embedding recurs and is general. A D3-brane has six transverse real dimensions, $\mathbb{R}^6 \cong \mathbb{C}^3$, so $m \le 3$. When Γ acts on only $m < 3$ of the complex directions, the remaining $3-m$ are inert spectators that the group fixes pointwise, and the transverse space factorizes,

$$(\mathbb{C}^m/\Gamma) \times \mathbb{C}^{\,3-m}, \tag{VI.2.7}$$

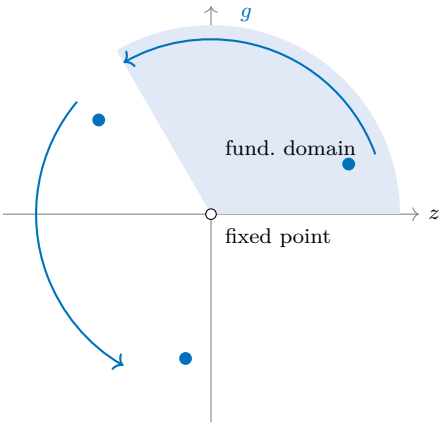


Figure VI.2.2: The orbifold quotient, drawn for one complex plane under $\mathbb{Z}_3$ (rotation by $g = \omega$). A generic point has $|\Gamma| = 3$ images, one Γ-orbit (blue), glued to a single point of the quotient; the shaded wedge is a fundamental domain, and the origin is fixed. This one-plane picture is only a cartoon of orbit identification and stabilizers: $\mathbb{C}/\mathbb{Z}_n$ is in fact smooth as an affine variety (its invariant ring is $\mathbb{C}[z^n]$), although the origin carries a nontrivial orbifold stabilizer. The algebraic singularities used below appear only in complex dimension two and three.

with singular locus, in the examples used here where the active factor has its fixed point at the origin, the fixed locus times the spectators,

$$\mathrm{Sing} = \{z_1 = \cdots = z_m = 0\} \times \mathbb{C}^{\,3-m}, \tag{VI.2.8}$$

a complex line $\{z_1 = z_2 = 0\} \times \mathbb{C}_{z_3}$ for $\mathbb{C}^2/\mathbb{Z}_n$ ($m = 2$) and the isolated origin for $\mathbb{C}^3/\mathbb{Z}_3$ ($m = 3$, no spectator). More general cyclic weights can produce additional stabilizer strata, but those do not enter the two worked examples. The spectator directions reappear in the gauge theory as adjoint moduli, which we meet in §VI.2.6.

It pays to hold the geometric picture in mind, because the branes will live inside it (Figure VI.2.2). Away from the fixed point every point of the quotient has exactly $|\Gamma|$ distinct preimages upstairs, a single Γ-orbit, which the quotient glues to one point. The fixed point is the lone exception: its geometric orbit has one point, since every group element leaves it fixed. A D-brane placed at a generic point of the quotient therefore lifts to $|\Gamma|$ image branes in the covering space, rotated into one another by Γ; a regular brane placed at the tip is the collapsed version of that full image-brane orbit, while a single elementary fractional brane has no orbit to move along. It is the Chan–Paton representation, not merely the geometric location, that tells regular from fractional, as the gauge theory will make precise.

VI.2.3 The orbifold projection

Three quotients not to confuse.

1. The geometric quotient: $\mathbb{C}^m/\Gamma$ is the orbifold of spacetime. *2. The open-string projection:* keep only the Γ-invariant open-string states, combining the geometric action on the transverse data with the Chan–Paton action γ on the labels. This produces the quiver. *3. The vacuum quotient:* in the resulting gauge theory, solve the F-term and D-term equations and divide by the gauge group to obtain the moduli space. The probe statement is that quotient 3 reproduces quotient 1, but only after quotient 2 has built the correct quiver. The rest of the chapter keeps these three operations apart.

Now place a stack of D-branes at the fixed point $z_\alpha = 0$ and ask what the orbifold does to their worldvolume theory. The flat-space theory of Chapter 1 is $U(K)$ super-Yang–Mills, where K is the number of Chan–Paton labels, but that theory is not yet the answer: it is the theory upstairs, on the covering space $\mathbb{C}^m$, and we keep only what is consistent with the identification that defines the quotient (the second of the three quotients above).

Consistency forces the group to act on the open strings. A symmetry of the brane configuration is a symmetry of its open-string Hilbert space, and an open string carries, besides its oscillators, a pair of Chan–Paton labels at its endpoints. For the configuration to be Γ-symmetric the group must therefore be represented on those labels, by a unitary representation on the K-dimensional Chan–Paton space V,

$$\gamma : \Gamma \longrightarrow U(K), \qquad K = \dim V. \tag{VI.2.9}$$

Orbifolding is then the instruction to keep only the open-string states left invariant by the *combined* action of Γ, geometric on the transverse oscillators and labels, and γ on the Chan–Paton factors.

Two features of γ are forced rather than chosen, and they are what make the construction rigid. First, γ must be a representation: acting by g_1 and then g_2 has to agree with acting by the single element $g_1 g_2$,

$$\gamma(g_1)\,\gamma(g_2) = \gamma(g_1 g_2), \tag{VI.2.10}$$

so the assignment is a homomorphism, not an arbitrary list of unitaries. Its one freedom is how many times each irreducible representation of Γ appears in V, and that multiplicity is exactly the brane content we fix in §VI.2.5. Second, orbifolding is literally a projection. Writing $\hat{\rho}(g)$ for the combined geometric and Chan–Paton action of g on a worldvolume field, the surviving fields are the image of the group average

$$P \;=\; \frac{1}{|\Gamma|}\sum_{g\in\Gamma}\hat{\rho}(g), \qquad P^2 = P, \tag{VI.2.11}$$

a genuine projector precisely because $\hat{\rho}$ is a representation. For a cyclic $\Gamma = \mathbb{Z}_n$ it is enough to impose invariance under the single generator g, which is what the two conditions below state. Relaxing γ from an ordinary to a projective representation is

permitted and is the extra choice of discrete torsion, taken up in Chapter 9; we do not need it here.

Apply this to the massless worldvolume fields, the gauge field A_μ and the six transverse scalars, the latter organized as three complex scalars Φ_α that rotate under the geometric action exactly as the coordinates z_α do, being the matrix-valued positions of the branes in those directions. Each such field is an open string carrying a Chan–Paton label at each end, so as a $K \times K$ matrix one index transforms in V, by $\gamma(g)$, and the other in the conjugate $\bar{V}$, by $\gamma(g)^{-1}$, hence in the adjoint,

$$M \;\longmapsto\; \gamma(g)\, M\, \gamma(g)^{-1}. \tag{VI.2.12}$$

The gauge field carries no transverse index, so the geometric action is trivial on it and invariance is the plain statement that it commutes with the group,

$$A_\mu \;=\; \gamma(g)\, A_\mu\, \gamma(g)^{-1}. \tag{VI.2.13}$$

The scalar Φ_α does carry a transverse index, so the geometric action multiplies it by the phase ω^{a_α} of (VI.2.1) in addition to the conjugation, and invariance is the twisted condition

$$\Phi_\alpha \;=\; \omega^{a_\alpha}\, \gamma(g)\, \Phi_\alpha\, \gamma(g)^{-1} \qquad \text{(no sum on } \alpha\text{)}. \tag{VI.2.14}$$

These two equations are the entire construction. Equation (VI.2.13) keeps the gauge field only in Chan–Paton blocks with zero net Γ phase, and we will see these become the quiver's nodes. Read without a basis the surviving gauge fields are the commutant of the image $\gamma(\Gamma)$,

$$\mathfrak{u}(K)^\Gamma = \{\, X : [\,X, \gamma(g)\,] = 0 \;\; \forall g \in \Gamma \,\} = \textstyle\bigoplus_i \mathfrak{u}(N_i), \tag{VI.2.15}$$

the matrices commuting with every $\gamma(g)$; by Schur's lemma this commutant breaks the single $U(K)$ into a product of factors, one per distinct irreducible, as the next section computes. Equation (VI.2.14) keeps a scalar in an off-diagonal block only when the Chan–Paton phase of that block cancels the geometric phase of z_α, and these become the arrows. Gauge fields produce nodes; scalars produce arrows. Solving the two equations is the work of the next section, and for abelian Γ it is a transparent exercise with matrices.

VI.2.4 Nodes and arrows: solving the projection

It is worth solving the projection once by hand, with matrices and no character theory, because the general formula at the end of the section only counts what the matrices already show. Take $\Gamma = \mathbb{Z}_3$ and the smallest brane content that uses all three labels, one Chan–Paton label in each of the three phases, so $K = 3$ and

$$\gamma(g) = \mathrm{diag}(1, \omega, \omega^2), \qquad \omega = e^{2\pi i/3}. \tag{VI.2.16}$$

For a general 3×3 matrix M the conjugation acts entry by entry,

$$\big(\gamma(g)\, M\, \gamma(g)^{-1}\big)_{ij} = \omega^{\,i-j} M_{ij}, \qquad \big(\omega^{\,i-j}\big) = \begin{pmatrix} \omega^0 & \omega^{-1} & \omega^{-2} \\ \omega^1 & \omega^0 & \omega^{-1} \\ \omega^2 & \omega^1 & \omega^0 \end{pmatrix}, \tag{VI.2.17}$$

constant along each diagonal. The gauge field has no transverse phase, so the condition (VI.2.13) keeps only the phase-one entries, the diagonal $i = j$,

$$A_\mu \;=\; \mathrm{diag}\,\big(A_\mu^{(0)}, A_\mu^{(1)}, A_\mu^{(2)}\big), \tag{VI.2.18}$$

and the single flat-space $U(3)$ gauge field has become three $U(1)$ gauge fields, one per diagonal entry. A transverse scalar of weight $a_\alpha = 1$ must instead satisfy $\Phi = \omega\,\gamma(g)\,\Phi\,\gamma(g)^{-1}$, that is $\omega^{\,1+i-j}\Phi_{ij} = \Phi_{ij}$, so the surviving entries are those with $j \equiv i+1$, the cyclic super-diagonal

$$\Phi \;=\; \begin{pmatrix} 0 & * & 0 \\ 0 & 0 & * \\ * & 0 & 0 \end{pmatrix}. \tag{VI.2.19}$$

Each star is a field linking label i to label $i+1$. For $\mathbb{C}^3/\mathbb{Z}_3$ there are three transverse scalars, all of weight one, so there are three such stars on every link: three fields from each label to the next. This is already the dP_0 quiver, obtained without any representation theory.

The general rule is visible in the example. Decompose the Chan–Paton space into the one-dimensional representations of $\mathbb{Z}_n$, labelled by $i \in \mathbb{Z}/n\mathbb{Z}$ with g acting as ω^i on the i-th and $i = 0$ the trivial one,

$$V \;=\; \bigoplus_i \mathbb{C}^{N_i} \otimes R_i, \qquad K \;=\; \sum_i N_i \dim R_i, \tag{VI.2.20}$$

on the i-th block of which $\gamma(g)$ acts as the scalar ω^i. The gauge-field condition keeps the block-diagonal matrices, and the surviving gauge symmetry is the product

$$\prod_i U(N_i), \tag{VI.2.21}$$

one factor per block. A scalar Φ_α restricted to the block from i to j is an $N_i \times N_j$ matrix on which the conjugation acts by $\omega^{\,i-j}$, and the twisted invariance (VI.2.14) keeps it only when $\omega^{a_\alpha}\omega^{\,i-j} = 1$, that is when

$$j \equiv i + a_\alpha \pmod{n}. \tag{VI.2.22}$$

This is the block rule, the single most useful statement in the chapter: gauge-field blocks survive on the diagonal and give nodes, while a scalar of weight a_α survives in the block shifted by a_α and gives matter.

The projection now has a graphical reading. Draw a *node* for each surviving gauge factor $U(N_i)$ and an *arrow* for each surviving scalar block. A node i stands for the group $U(N_i)$; an arrow from node i to node j stands for a matter field charged as a bifundamental of those two factors. The node label is the full $U(N_i)$ and stays so throughout the chapter, in the figures and in both worked examples; the infrared fate of the abelian factors, taken up in §VI.2.5, does not change it. In $\mathcal{N} = 1$ language each such field is a chiral multiplet in the bifundamental representation; in the $\mathbb{C}^2/\mathbb{Z}_n$ example below these chiral multiplets will pair into $\mathcal{N} = 2$ hypermultiplets. A labelled

directed graph of this kind is a *quiver*, and the gauge theory it encodes a quiver gauge theory. An arrow from a node to itself, allowed when $a_\alpha \equiv 0$, is an adjoint chiral multiplet, drawn as a small loop.

We owe one remark on the arrow convention, since it is the one place a sign of direction must be fixed. An arrow $i \to j$ denotes the chiral multiplet X_{ij} in $(\Box_i, \overline{\Box}_j)$, an $N_i \times N_j$ matrix transforming as $X_{ij} \to g_i\, X_{ij}\, g_j^\dagger$, and a gauge-invariant term is a cycle read left-to-right along the arrows, $\mathrm{Tr}\, X_{ij} X_{jk} X_{ki}$. This is the convention of the brane-probe and tiling literature; it is the reverse of the mathematicians' quiver-representation arrow, which sends $V_i \to V_j$, so any Hom or Ext data quoted from that literature transposes. We will not flag the transposition again.

Only now is the character formula worth stating, as a compact way to count the same surviving blocks for any group and any brane content. The number of arrows from node i to node j is the number of transverse directions whose weight carries i to j,

$$a_{ij} \;=\; \#\{\alpha : a_\alpha \equiv j - i \pmod n\} \;=\; \frac{1}{|\Gamma|} \sum_{g \in \Gamma} \chi_Q(g)\, \chi_i(g)\, \chi_j(g)^*, \tag{VI.2.23}$$

the multiplicity of R_j inside $Q \otimes R_i$, where Q is the transverse representation with character χ_Q. We write the orbifold weights with a single index, a_α, and the arrow multiplicities with two, a_{ij}: the former are the input data, the latter the output count. The character formula counts the same blocks as the matrix projection. For abelian Γ the group sum collapses to the block rule (VI.2.22) by the orthogonality $(1/n)\sum_k \omega^{\ell k} = \delta_{\ell \equiv 0}$. A worked character table makes this concrete: for $\mathbb{Z}_3$,

	e	g	g^2
R_0	1	1	1
R_1	1	ω	ω^2
R_2	1	ω^2	ω

$$\chi_i(g^k) = \omega^{ik}, \tag{VI.2.24}$$

each row an irreducible character, the rows orthonormal,

$$\frac{1}{n} \sum_{k=0}^{n-1} \chi_i(g^k)\, \chi_j(g^k)^* = \delta_{ij}. \tag{VI.2.25}$$

To run the count one supplies only the transverse character χ_Q and reads it against the rows; the two examples evaluate $\chi_Q(g^k) = \omega^k + \omega^{-k}$ for $\mathbb{C}^2/\mathbb{Z}_n$ and $\chi_Q(g^k) = 3\omega^k$ for $\mathbb{C}^3/\mathbb{Z}_3$, each a one-line sum.

For a threefold orbifold there is one more piece of data, the superpotential, and it too is inherited rather than chosen. A term in W survives only if its arrows compose into a closed path, so that the trace is gauge invariant; the parent $\mathcal{N} = 4$ theory carries the cubic coupling $W = \mathrm{Tr}\, X[Y, Z]$ of its three adjoint scalars, and the projection sends it to a sum of cubic words, one for each oriented closed triangle of the quiver,

$$W \;=\; \sum_{\triangle} \varepsilon_{\alpha\beta\gamma}\, \mathrm{Tr}\left(X^\alpha X^\beta X^\gamma\right), \tag{VI.2.26}$$

the relative signs inherited from the parent commutator, not chosen independently for each triangle. Gauge invariance alone would allow a general coefficient tensor on the

closed cubic words (for the dP_0 case below, the twenty-seven monomials $X_{01}^a X_{12}^b X_{20}^c$); the antisymmetric ε tensor is inherited from the parent $\mathcal{N}=4$ cubic. Only rotations commuting with the orbifold action survive as daughter flavor symmetries; the full $SU(3)$ survives in the equal-weight $\mathbb{C}^3/\mathbb{Z}_3$ example below.

VI.2.5 Regular branes, fractional branes, and the surviving supersymmetry

The quiver has its nodes and arrows fixed by Γ, but the ranks N_i are set by the choice of Chan–Paton representation γ, and two choices organize the physics. Before the choices, one point that puzzles every reader on first sight: a single mobile brane on the quotient does not correspond to a single Chan–Paton label upstairs. A brane at a generic point lifts to a full Γ-orbit of $|\Gamma|$ image branes in the covering space, so for $\Gamma=\mathbb{Z}_n$ it carries n Chan–Paton labels, one per image. Thus one mobile brane has $N_i=1$ at each node,

$$K=n, \qquad \prod_{i=0}^{n-1} U(N_i)=U(1)^n, \tag{VI.2.27}$$

and "one brane" and "n nodes" are not in conflict.

The symmetric choice is built from N regular branes, $\gamma = N\cdot(\text{regular})$, the representation in which every irreducible appears with multiplicity equal to its dimension. Then

$$N_i \;=\; N\,\dim R_i, \qquad K \;=\; N\,|\Gamma|, \tag{VI.2.28}$$

which for abelian Γ, where every $\dim R_i=1$, is simply $N_i=N$ at every node. A regular brane is mobile: its image is the full Γ-orbit of Figure VI.2.2, which can be lifted off the origin and carried into the bulk as a rigid whole, and this motion is the geometric branch we are after.

With the ranks chosen, the gauge group $\prod_i U(N_i)$ of §VI.2.4 is concrete, and for N regular branes it is $U(N)^n$. A word on its abelian part belongs here, because the diagram does not by itself fix the infrared fate of the $U(1)$ factors. The overall diagonal $U(1)$, the simultaneous trace of all the nodes, is the centre of mass of the whole brane system. An arrow X_{ij} carries charge $(+1,-1)$ under $U(1)_i\times U(1)_j$, so under that diagonal $U(1)_{\rm d}=\sum_i U(1)_i$ it is neutral,

$$q_{\rm d}(X_{ij})=(+1)+(-1)=0, \tag{VI.2.29}$$

and the same holds for the adjoints. By the Chapter 1 argument this diagonal $U(1)$ is a free Maxwell sector that decouples in the very $\alpha'\to 0$ limit that produced the gauge theory, not in a step ordered after it; it acts trivially on every bifundamental, so in the moduli computation of §VI.2.6 the brane moves into the bulk along the gauge-invariant bifundamental and adjoint vacuum expectation values, quotiented by the relative $U(1)$ factors, while this overall factor decouples.

The free diagonal gauge field does not remove the position moduli. Its charge vanishes on every arrow, so its gauge transformation imposes no additional identification on the mesonic vacuum values. The mesonic vacuum values carry the regular brane's position

in the quotient. At the dP_0 orbifold point these position scalars are bifundamental chirals, not scalars of the free diagonal $\mathcal{N} = 1$ vector. The relative $U(1)$'s behave differently: the bifundamentals carry net charge under them, so they are not free. In the chiral four-dimensional quivers they are often anomalous, the mixed anomalies cancelled by generalized Green–Schwarz couplings to twisted-sector closed-string axions, and the same couplings can give the $U(1)$ a Stuckelberg mass; in the non-chiral examples the ordinary four-dimensional gauge anomalies vanish and the fate is milder. Either way the interacting nonabelian content sits in the SU factors,

$$\prod_i U(N_i) \;\supset\; \prod_i SU(N_i), \tag{VI.2.30}$$

accompanied by r abelian factors that remain massless (anomaly-free and, beyond that, free of any Stuckelberg mass), with r a construction-dependent count whose systematic treatment is Chapter 7. This identifies where the interacting dynamics lives; it is not a relabeling of the nodes. We keep the full $U(N_i)$ as the gauge group throughout, because it is the brane Chan–Paton group the construction outputs and because the abelian factors carry physical data we do not bake into notation: the relative $U(1)$ Fayet–Iliopoulos terms are the resolution moduli of the geometry (Chapters 4 and 6), and the free overall diagonal $U(1)$ acts trivially, so it does not obstruct the mesonic flat directions of the reconstruction. As in Chapter 1, singling out the SU factors is special to four dimensions; in lower-dimensional brane theories the abelian sector carries physical content directly. This infrared fate of the abelian gauge bosons is separate from the classical vacuum quotient used below: the mesonic branch is the F- and D-term quotient of the ultraviolet quiver, modulo the trivially acting diagonal $U(1)$, and the Stuckelberg masses and anomaly cancellations act on the low-energy gauge bosons, not on that holomorphic quotient.

The complementary choice is a fractional brane, and the operational definition is representation-theoretic. An elementary fractional brane chooses γ supported on a single irreducible R_i,

$$\gamma = R_i : \qquad N_j = \delta_{ij}, \tag{VI.2.31}$$

so it occupies one node of the quiver rather than the full regular combination, and it cannot leave the singular locus (VI.2.8), since it has no Γ-orbit to ride out on. It may still slide along the spectators: for $(\mathbb{C}^2/\mathbb{Z}_n) \times \mathbb{C}$ the node adjoint Φ_i moves it along the line $\{z_1 = z_2 = 0\} \times \mathbb{C}_{z_3}$, while for $\mathbb{C}^3/\mathbb{Z}_3$ the locus is the isolated origin and the brane is fully pinned. A useful geometric picture, developed once the resolution geometry is in hand, is that fractional branes become branes wrapping the exceptional cycles of the resolution; at the orbifold point those cycles have collapsed, so the wrapped branes are pinned at the singular locus. For the present chapter, though, that picture is only a guide, and the definition we actually use is the Chan–Paton one: regular branes from the regular representation, fractional branes from a single irreducible. A general rank vector can be written, after choosing an integer N, as a regular contribution and a residual integer vector,

$$\vec{N} = N\,(\dim R_0, \ldots, \dim R_{n-1}) + \vec{N}_{\text{frac}}, \tag{VI.2.32}$$

where the decomposition depends on that choice of N. When the residual vector describes an allowed collection of fractional branes, it carries localized charge and

changes the theory at the singularity. An arbitrary residual vector need not define a consistent dynamical quiver; the rank constraints are treated in Chapters 5 and 7. The worked examples below use N regular branes.

The amount of supersymmetry is set, like the geometry, by the embedding. The orbifold breaks the transverse rotation group and with it the R-symmetry that rotates the supercharges; the survivors are the supercharges riding on the covariantly constant spinors of §VI.2.2. The sixteen supercharges of the Chapter 1 theory are projected by the embedding,

$$16 \xrightarrow{\Gamma\subset SU(2)} 8 \ \ (\mathcal{N}=2), \qquad 16 \xrightarrow{\Gamma\subset SU(3)} 4 \ \ (\mathcal{N}=1), \tag{VI.2.33}$$

eight survivors making a four-dimensional $\mathcal{N}=2$ theory, four an $\mathcal{N}=1$ one. The non-chiral and chiral characters of the two examples are the visible faces of these two counts.

One identification closes the section. At the regular rank vector the matter is exactly the orbifold projection of $\mathcal{N}=4$ super-Yang–Mills, and the $\mathcal{N}=2$ necklace one-loop beta coefficients of the $SU(N)$ factors vanish. Each node sees two bifundamental hypermultiplets, so

$$b_0 \ \propto \ 2N_c - N_f = 2N - 2N = 0, \tag{VI.2.34}$$

which for the necklace is already decisive, the $\mathcal{N}=2$ gauge beta function being one-loop exact. For the $\mathcal{N}=1$ dP_0 quiver the orbifold construction identifies a superconformal point, carrying the inherited cubic superpotential and the inherited relations among its couplings; whether and where the couplings are exactly marginal is the conformal-manifold question. We therefore record the regular orbifold quivers as landing on inherited superconformal field theories, the orbifold daughters of $\mathcal{N}=4$ (the necklace an $\mathcal{N}=2$ quiver, the dP_0 theory an $\mathcal{N}=1$ one), rather than proving the full conformal-manifold statement here. The further superconformal dynamics, the exactly marginal couplings and the conformal manifold, the central charges a and c, the superconformal index, and the dualities that relate these quivers to one another and to other constructions, are developed once and comparatively in Part III; here we record only that the regular-brane orbifolds land in that class.

VI.2.6 The non-chiral example: $\mathbb{C}^2/\mathbb{Z}_n$ and the affine necklace

Take $\Gamma=\mathbb{Z}_n$ acting on $\mathbb{C}^2\subset\mathbb{C}^3$ with the $SU(2)$ weights $(1,-1)$, the spectator z_3 inert. The transverse representation on the active $\mathbb{C}^2$ is $Q=R_1\oplus R_{-1}$, with character $\chi_Q(g^k)=\omega^k+\omega^{-k}$, and the character formula (VI.2.23) is a one-line sum,

$$a_{ij} \ = \ \frac{1}{n}\sum_{k=0}^{n-1}\left(\omega^k+\omega^{-k}\right)\omega^{(i-j)k} \ = \ \delta_{j,\,i+1}+\delta_{j,\,i-1}, \tag{VI.2.35}$$

one arrow $i\to i+1$ and one arrow $i\to i-1$ at every node, indices modulo n. The quiver is a closed necklace of n nodes, the affine $\hat{A}_{n-1}$ Dynkin diagram, with gauge

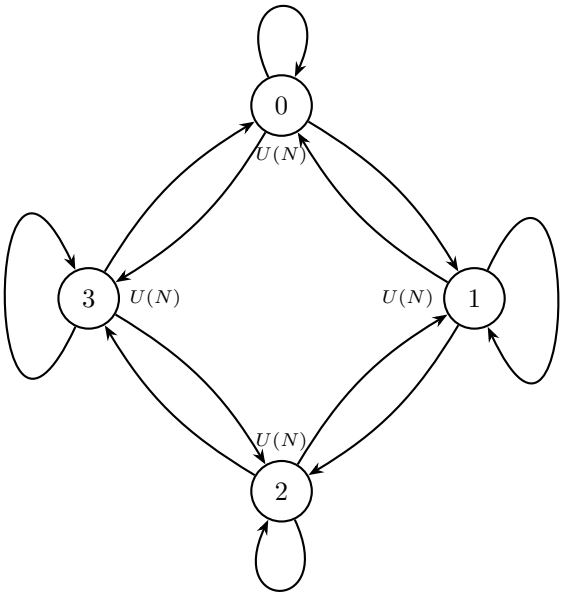


Figure VI.2.3: The affine $\hat{A}_{n-1}$ necklace quiver, shown for $n = 4$. Each of the n gauge nodes is a $U(N)$ factor; each neighbouring pair is joined by a pair of opposite bifundamental arrows, together one $\mathcal{N} = 2$ hypermultiplet; and each node carries an adjoint chiral Φ_i, the self-loop, from the inert spectator z_3. The quiver is drawn in $\mathcal{N} = 1$ language, every arrow a chiral multiplet, with the $\mathcal{N} = 2$ multiplets assembled from them.

group $U(N)^n$ from N regular branes (Figure VI.2.3). The symmetry of the adjacency is a consequence of the embedding: for $\Gamma \subset SU(2)$ the representation Q is pseudoreal, so $a_{ij} = a_{ji}$ and every arrow is matched by its reverse. The two opposite arrows $(i \to i+1,\ i+1 \to i)$ combine into one $\mathcal{N} = 2$ bifundamental hypermultiplet, as the eight preserved supercharges require.

Two pieces of $\mathcal{N} = 2$ vocabulary organize this matter, and since they recur throughout the volume it is worth pinning them down. With eight supercharges the fields fall into two kinds of multiplet. An $\mathcal{N} = 2$ *vector multiplet* holds a gauge field A_μ, one complex scalar in the adjoint, and their fermions; in $\mathcal{N} = 1$ language it is an $\mathcal{N} = 1$ vector multiplet, the gauge field and its gaugino, together with one adjoint chiral multiplet, the complex scalar. An $\mathcal{N} = 2$ *hypermultiplet* holds four real scalars and their fermions; in $\mathcal{N} = 1$ language it is two chiral multiplets in conjugate representations, one in $(\mathbf{N}_i, \overline{\mathbf{N}}_j)$ and one in $(\mathbf{N}_j, \overline{\mathbf{N}}_i)$. The projected necklace assembles precisely into these: at each node the gauge field A_μ and an adjoint scalar form a vector multiplet, and each opposite-arrow pair, the chiral A_i in $(\mathbf{N}_i, \overline{\mathbf{N}}_{i+1})$ with its reverse B_i, forms one hypermultiplet.

The adjoint scalar at each node is the spectator wearing a different hat, and it is

the cleanest place to see why "inert" does not mean "absent." Since z_3 has weight zero, the block rule (VI.2.22) keeps it in blocks with $j = i$, an adjoint loop Φ_i at every node. Physically these adjoints measure the brane's position along the spectator direction, the singular line $\{z_1 = z_2 = 0\} \times \mathbb{C}_{z_3}$ of §VI.2.2. The per-node matter is thus two $\mathcal{N} = 1$ bifundamental chirals pointing to neighboring nodes, their conjugate arrows completing the hypermultiplets, and the one adjoint Φ_i, the orbifold's distribution of the three transverse complex scalars over the quiver.

The superpotential is the $\mathcal{N} = 2$ daughter of the parent cubic, the projection of $W = \operatorname{Tr} X[Y, Z]$ with the spectator as the outer leg of the commutator. Writing A_i for the arrow $i \to i + 1$ and B_i for its reverse $i + 1 \to i$,

$$W \;=\; \sum_i \operatorname{Tr}\, \Phi_i\big(A_iB_i - B_{i-1}A_{i-1}\big), \tag{VI.2.36}$$

the adjoint Φ_i coupling to the difference of the two closed loops that leave node i, out to $i + 1$ and back through A_iB_i, and out to $i - 1$ and back through $B_{i-1}A_{i-1}$, each a genuine endomorphism of node i. The F-term of Φ_i sets that difference to zero,

$$\frac{\partial W}{\partial \Phi_i} \;=\; A_iB_i - B_{i-1}A_{i-1} \;=\; \mu_i \;=\; 0, \tag{VI.2.37}$$

which is the complex moment map of the affine $\hat{A}_{n-1}$ quiver. Together with the real D-term it builds the orbifold by a hyperkähler quotient: impose the complex moment-map equations $\mu_i = 0$, impose the real D-term equations, and divide by the gauge group. For the abelian single-regular-brane branch the moment maps obey the telescoping identity $\sum_i \mu_i = 0$, the trace part associated with the decoupled diagonal $U(1)$; for nonabelian ranks the μ_i are matrix-valued at different nodes and should not be added as matrices, but the same diagonal-$U(1)$ trace part is the decoupled one.

Now the payoff: the moduli space reconstructs the geometry, and we can compute it. Move a single regular brane into the bulk, so the gauge group is $U(1)^n$ and the fields are commuting numbers. The equations of motion for the adjoints, $\partial W/\partial A_i = (\Phi_i - \Phi_{i+1})B_i$ and $\partial W/\partial B_i = (\Phi_i - \Phi_{i+1})A_i$, force all the Φ_i to one common value Φ once the bifundamentals are switched on, the position along the spectator line, while the moment map (VI.2.37) sets every product A_iB_i equal to one common number w. The gauge invariants are the closed loops: the short loop $w = A_iB_i$ and the two long loops winding around the necklace,

$$u = A_0A_1 \cdots A_{n-1}, \qquad v = B_0B_1 \cdots B_{n-1}, \tag{VI.2.38}$$

clockwise and counter, which obey, using $A_iB_i = w$ at each node,

$$uv \;=\; \prod_i A_i \prod_i B_i \;=\; \prod_i (A_iB_i) \;=\; w^n. \tag{VI.2.39}$$

This reproduces the geometry the brane probes. By the general recipe (VI.2.6) the invariants of the active $\mathbb{C}^2/\mathbb{Z}_n$, $(z_1, z_2) \mapsto (\omega z_1, \omega^{-1} z_2)$, are the monomials with $a - b \equiv 0$ modulo n, generated by

$$u = z_1^{\,n}, \qquad v = z_2^{\,n}, \qquad w = z_1z_2, \qquad \text{subject to} \qquad uv = w^{\,n}, \tag{VI.2.40}$$

the A_{n-1} surface singularity, while the spectator z_3 supplies the extra $\mathbb{C}$ that the common adjoint Φ parametrizes. The long loops u, v and the short loop w of the gauge theory are exactly these invariants, with exactly their relation (VI.2.39), so the mesonic branch is $\{uv = w^n\} \times \mathbb{C} = (\mathbb{C}^2/\mathbb{Z}_n) \times \mathbb{C}$: the probe has reconstructed its own transverse space. This computation was done at vanishing Fayet–Iliopoulos parameter, a constant added to a $U(1)$ D-term equation; at zero FI the quotient yields the singular orbifold, while turning on the FI levels shifts the real moment maps and resolves the tip into the smooth ALE space, the subject of Chapters 3 and 4.

The smallest case is a useful check. For $n = 2$ the weights $(1, -1)$ coincide modulo 2, so the two arrows between the two nodes double up, $a_{01} = a_{10} = 2$, the affine $\hat{A}_1$ quiver with two hypermultiplets joining $U(N) \times U(N)$; the relation $uv = w^2$ is the A_1 surface singularity, the $\mathbb{Z}_2$ orbifold $\mathbb{C}^2/\mathbb{Z}_2$, an ordinary double point in two complex dimensions and not the threefold conifold.

VI.2.7 The chiral example: $\mathbb{C}^3/\mathbb{Z}_3$ and the dP_0 quiver

Now let $\Gamma = \mathbb{Z}_3$ act on all three transverse coordinates with equal weights $(1, 1, 1)$. The sum $1 + 1 + 1 = 3 \equiv 0$ modulo 3, so $\Gamma \subset SU(3)$ by (VI.2.3), the quotient is the Calabi–Yau threefold dP_0 of §VI.2.2, and four supercharges survive: a chiral $\mathcal{N} = 1$ theory. All three transverse scalars carry the same charge, the transverse representation is $Q = 3R_1$ with $\chi_Q(g^k) = 3\omega^k$, and the character formula gives

$$a_{ij} \;=\; \frac{1}{3}\sum_{k=0}^{2} 3\,\omega^k\,\omega^{(i-j)k} \;=\; 3\,\delta_{j,\,i+1}, \tag{VI.2.41}$$

three arrows from each node to the next and none returning. The adjacency is chiral, $a_{ij} \neq a_{ji}$. Its orientation $i \to i + 1$ is fixed once we choose the generator g and the convention that an arrow records a surviving block X_{ij} in $(\square_i, \overline{\square}_j)$; reversing the generator or the arrow convention would transpose the quiver, but once the convention is fixed the orientation is not a free dynamical choice. The quiver is three nodes $U(N)^3$ joined cyclically by three chiral arrows each (Figure VI.2.4), the gauge theory of the cone over $\mathbb{P}^2$. There is no adjoint and no reverse arrow, because no transverse direction is inert; in this example the chiral orientation records the equal nonzero weights, in contrast to the necklace, where opposite weights give symmetric pairs and the spectator gives adjoints.

Because the quiver is chiral, the ranks of a fully dynamical nonabelian theory are constrained. At a node with a nontrivial cubic $SU(N_i)$ gauge anomaly, the coefficient is proportional to the number of fundamentals minus antifundamentals, the arrows leaving minus the arrows entering,

$$3\,(N_{i+1} - N_{i-1}) \;=\; 0, \tag{VI.2.42}$$

With the fundamental cubic index normalized to $+1$ (and the antifundamental to -1), the three displayed node coefficients sum to zero, so only two rank equalities are independent. For $N_i \geq 3$ at all three nodes, their cancellation forces $N_0 = N_1 = N_2$, precisely the regular rank vector and the configuration of N regular branes. At low

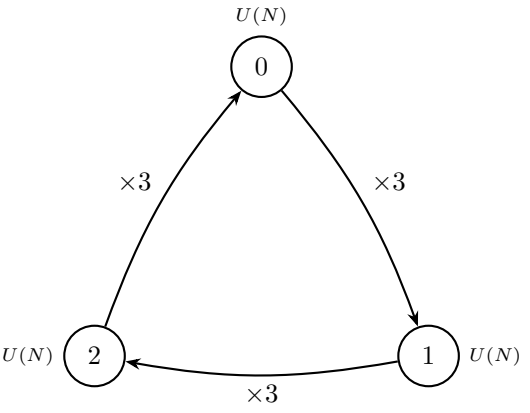


Figure VI.2.4: The dP_0 quiver. Three $U(N)$ gauge nodes are joined cyclically, $0 \to 1 \to 2 \to 0$, by three chiral bifundamental arrows on each edge ($a_{ij} = 3\delta_{j,i+1}$). Each edge labelled $\times 3$ denotes three distinct chiral bifundamental fields, not a charge-three field. There are no reverse arrows and no adjoint loops: the theory is chiral, $\mathcal{N} = 1$.

ranks the cubic $SU(N_i)$ test alone does not establish this necessity; abelian anomalies and string tadpoles require separate analysis. We use the equal-rank regular-brane example here. The systematic treatment of tadpoles and anomalies is Chapter 7.

The superpotential is the inherited cubic (VI.2.26) on the single oriented triangle $0 \to 1 \to 2 \to 0$. Writing $X^a_{01}, X^a_{12}, X^a_{20}$ for the three arrows on each edge, with $a = 1, 2, 3$ the flavor index of the transverse $\mathbb{C}^3$,

$$W \;=\; \varepsilon_{abc}\, \mathrm{Tr}\left(X^a_{01}\, X^b_{12}\, X^c_{20}\right), \tag{VI.2.43}$$

the unique cubic preserving the $SU(3)$ flavor symmetry the equal weights leave unbroken. Its F-terms set the antisymmetrized products of two consecutive arrows to zero, $\partial W/\partial X^a_{01} = \varepsilon_{abc} X^b_{12} X^c_{20} = 0$ and cyclically.

The superpotential now supplies the relations needed to recover the quotient. Take a single regular brane, so the gauge group is $U(1)^3$ and the arrow fields are complex numbers; each edge then carries a flavor vector in $\mathbb{C}^3$. The F-term $\varepsilon_{abc} X^b_{12} X^c_{20} = 0$ says the cross product of two neighbouring flavor vectors vanishes, so neighbouring vectors are parallel, and around the triangle all three become parallel. We may therefore write

$$X^a_{i,i+1} \;=\; p_i\, Z^a, \qquad p_i \in \mathbb{C}, \tag{VI.2.44}$$

for one common direction $Z = (Z^1, Z^2, Z^3)$, the position in the covering $\mathbb{C}^3$, with edge scales p_i. The closed-loop mesons are

$$M^{abc} \;=\; X^a_{01} X^b_{12} X^c_{20} \;=\; (p_0 p_1 p_2)\, Z^a Z^b Z^c. \tag{VI.2.45}$$

On the component where these vectors describe a mobile regular brane, the parametrization is redundant: the complexified gauge group $(\mathbb{C}^*)^3/\mathbb{C}^*_{\mathrm{diag}}$ rescales the three edges

independently while the overall diagonal acts trivially, and it removes two of the three scales p_i, leaving only their gauge-invariant product $P = p_0 p_1 p_2$. The covering coordinates Z^a are therefore not gauge-invariant coordinates on the moduli space; the closed loops give the degree-three combinations $P\, Z^a Z^b Z^c$. Their products generate higher-degree loops. This is exactly what the orbifold does to functions: under $Z^a \to \omega Z^a$ a monomial of degree d is invariant only when $d \equiv 0$ modulo 3, so the mesonic chiral ring is the degree-three invariant subring

$$\mathbb{C}[Z^1, Z^2, Z^3]^{\mathbb{Z}_3} \;=\; \bigoplus_{k\geq 0} \mathbb{C}[Z^1, Z^2, Z^3]_{3k}, \tag{VI.2.46}$$

generated by the ten cubic monomials $Z^a Z^b Z^c$: any monomial of degree $3k$ can be grouped into k cubic factors. It is the coordinate ring of $\mathbb{C}^3/\mathbb{Z}_3$. Its spectrum is the cone over $\mathbb{P}^2$,[1] the local dP_0 geometry, named for the zeroth del Pezzo surface $\mathbb{P}^2$ that appears as the exceptional divisor when its tip is resolved. The mesonic coordinate ring of the regular brane has reconstructed the orbifold with chiral matter fixed by the projection. As before this is the singular cone at zero FI. In the geometric chamber, an FI deformation blows the tip up to a $\mathbb{P}^2$, the crepant resolution, the total space of $\mathcal{O}_{\mathbb{P}^2}(-3)$, taken up in Chapter 6 and Volume VI.

*VI.2.8 The worldsheet origin: open-string sectors and boundary states

(Optional.) This section may be skipped on a first reading. Nothing in it is needed to construct the quiver or to compute the mesonic branch of the two examples just worked; it explains how the same projection looks from the worldsheet and in the closed-string channel.

The matrix projection gives the quiver, but its fields are massless open strings. Their oscillator polarizations explain why gauge fields occupy nodes and matter fields occupy arrows. The boundary-state channel then explains how the same group characters measure localized brane charge. We use the open superstring and its boundary states as inputs; their derivation belongs to the foundational orbifold conformal field theory cited at the chapter end.

One point of language must be fixed first, since it is the usual source of confusion. The matter fields are all open strings. What is "twisted" about a bifundamental is the relative orbifold image of the string's two endpoints, a grading of the Chan–Paton block, and not a closed-string twisted sector. The closed-string twisted sectors are a different object, the localized blow-up modes that enter §VI.2.9 as the Fayet–Iliopoulos data; they return below, but on the side of the brane charges, not the matter.

Recall the massless open-string content of Chapter 1, read on the covering space before projection. In the Neveu–Schwarz sector the massless states are $\psi^M_{-1/2}|0;\lambda\rangle$ with a Chan–Paton matrix λ: the longitudinal polarizations $M = \mu$ give the gauge field A_μ, and the six transverse polarizations give the scalars, organized as the three complex Φ^α.

[1] In the language of algebraic geometry this degree-three ring is the *third Veronese subring*, and the cone is the affine cone over the cubic Veronese embedding of $\mathbb{P}^2$.

The Ramond sector gives their fermionic partners. A worldvolume field is an open string with a Chan–Paton label at each end. The orbifold generator acts on the oscillator and the label together,

$$g: \quad \psi^\mu \to \psi^\mu, \qquad \psi^\alpha \to \omega^{a_\alpha}\,\psi^\alpha, \qquad \lambda \to \gamma(g)\,\lambda\,\gamma(g)^{-1}, \tag{VI.2.47}$$

the longitudinal ψ^μ inert and the transverse ψ^α, the worldsheet superpartner of z_α, carrying its phase. On the $i \to j$ block $\gamma(g)$ contributes $\omega^{\,i-j}$, so invariance keeps

$$A_\mu: \;\; \omega^{\,i-j} = 1 \;\Rightarrow\; j = i, \qquad \Phi^\alpha: \;\; \omega^{a_\alpha}\omega^{\,i-j} = 1 \;\Rightarrow\; j \equiv i + a_\alpha, \tag{VI.2.48}$$

the diagonal blocks of (VI.2.13) for the gauge field and the a_α-shifted block of (VI.2.22) for the scalar. This is the worldsheet content of "gauge fields make nodes, scalars make arrows": the gauge multiplet is the endpoint-untwisted (diagonal) open string, and a bifundamental is the endpoint-twisted (off-diagonal) one, with the endpoint shift fixed by its geometric weight. There is no separate open-string sector with shifted moding to introduce, unlike the closed string; the orbifold acts on the single open-string Hilbert space as the projection, and the Chan–Paton block is the only grading.

The amount of supersymmetry organizes these survivors into multiplets, and the worldsheet sees this directly. The Gliozzi–Scherk–Olive projection on the open superstring keeps the massless vector and scalars in Neveu–Schwarz and the gauginos in Ramond; the orbifold then projects the bosons and the supercharges by the same combined action. Of the sixteen supercharges of the Chapter 1 theory, the embedding keeps eight for $\Gamma \subset SU(2)$ and four for $\Gamma \subset SU(3)$, the count of §VI.2.2. Because the projection commutes with these survivors, the kept fields fill complete multiplets block by block, the fermionic partner of each surviving boson sitting in the same Chan–Paton block because it carries the same net phase. For $\Gamma \subset SU(2)$, with eight supercharges, the survivors assemble as

$$\underbrace{(A_\mu,\,\Phi^3)_{\,j=i}}_{\mathcal{N}=2 \text{ vector}} \qquad \text{and} \qquad \underbrace{(\Phi^1,\Phi^2)_{\,j=i\pm1}}_{\mathcal{N}=2 \text{ hyper}}, \tag{VI.2.49}$$

the gauge field with the invariant spectator scalar (weight $a_3 = 0$, hence diagonal) the vector multiplet, each opposite-arrow pair of weights ±1 a hypermultiplet. For $\Gamma \subset SU(3)$, with four, no scalar is invariant,

$$\underbrace{(A_\mu)_{\,j=i}}_{\mathcal{N}=1 \text{ vector}} \qquad \text{and} \qquad \underbrace{(\Phi^1,\Phi^2,\Phi^3)_{\,j=i+1}}_{\mathcal{N}=1 \text{ chirals}}, \tag{VI.2.50}$$

the diagonal block a bare $\mathcal{N} = 1$ vector and the three off-diagonal scalars chiral multiplets. This is why the non-chiral and chiral characters of the two examples track the surviving supersymmetry: the projection that selects the blocks also selects the supercharges that bind them into multiplets.

The branes themselves carry a second, complementary worldsheet label, and it is here that the closed-string twisted sectors enter. A D-brane couples to closed strings through a boundary state, and at the orbifold the state of the fractional brane on R_i decomposes, schematically, into untwisted and twisted closed-string sectors,

$$|B_i\rangle = c_e\,(\dim R_i)\,|B;e\rangle + \sum_{g\neq e} c_g\,\chi_i(g)\,|B;g\rangle, \tag{VI.2.51}$$

with sector-dependent normalizations c_g; what matters for us is the character dependence. The untwisted piece carries the ordinary bulk Ramond–Ramond charge; the twisted pieces carry charges localized on the fixed loci of the corresponding group elements, controlled by the character,

$$Q_g^{\mathrm{tw}}(R_i) \;\propto\; \chi_i(g). \tag{VI.2.52}$$

In the abelian cyclic examples of this chapter $\chi_i(g)$ is a nonzero phase for every g, so an elementary fractional brane carries twisted charge in every sector; more generally the twisted-charge vector is character-valued and individual components may vanish on some classes, and what marks a non-regular brane is simply that this vector is not zero. A brane with net twisted charge cannot leave the fixed locus that supports it: for the isolated $\mathbb{C}^3/\mathbb{Z}_3$ fixed point this pins it at the origin, while for $(\mathbb{C}^2/\mathbb{Z}_n)\times\mathbb{C}$ it pins it to the singular line of §VI.2.2, along which the spectator adjoint can still carry it. This is the worldsheet statement of §VI.2.5: the fractional brane is pinned, and "wraps a collapsed cycle" is the geometric name for carrying twisted charge. The regular brane is the combination $\sum_i(\dim R_i)\,R_i$, and its net twisted charge vanishes by the regular-representation identity

$$\sum_i (\dim R_i)\,\chi_i(g) = |\Gamma|\,\delta_{g,e}, \tag{VI.2.53}$$

which is zero for every $g \neq e$. Indeed a nonidentity element permutes the basis of the regular representation without fixed basis vectors, so its trace vanishes. Under the boundary-state charge relation, the regular combination carries only untwisted bulk charge. On the mesonic branch constructed above it can move, and that motion reconstructs the geometry. Regular versus fractional, the Chan–Paton choice of §VI.2.5, is thus the question of which twisted-sector charges the boundary state carries.

The two readings, the open-string matter and the closed-string charges, are one computation seen in two channels. The cylinder stretched between two fractional branes can be read as a trace over the open strings that connect them, which is the projected matter spectrum, or as the exchange of closed strings between the two boundary states, untwisted and twisted. Equating the channels expresses the matter multiplicity as a sum over the closed-string sectors, that is over the group elements. This is a closed-channel rewriting of the same open-string projection; it does not make the bifundamentals closed-string twisted states. For the massless transverse matter, the group-character coefficient in this channel relation is the McKay count (VI.2.23),

$$a_{ij} = \frac{1}{|\Gamma|}\sum_{g\in\Gamma}\chi_Q(g)\,\chi_i(g)\,\chi_j(g)^* = \underbrace{\frac{\dim Q}{|\Gamma|}}_{\text{untwisted},\,g=e} + \underbrace{\frac{1}{|\Gamma|}\sum_{g\neq e}\chi_Q(g)\,\chi_i(g)\,\chi_j(g)^*}_{\text{twisted}}, \tag{VI.2.54}$$

the $g = e$ term the universal untwisted (bulk) contribution and the $g \neq e$ terms the twisted-sector contributions. In this abelian chapter $\chi_i(e) = \chi_j(e) = 1$, so the $g = e$ term is simply $\dim Q/|\Gamma|$; for a nonabelian Γ that term carries an extra factor $\dim R_i\,\dim R_j$, postponed to the next chapter. Thus the matter is an open string, but its multiplicity is computed using the same twist insertions that label the closed-string sectors. The integer arrow count is the full sum; the twisted terms generically carry

its dependence on the nodes, except when Q is itself the regular representation, where they cancel and the count becomes $a_{ij} = \dim R_i \, \dim R_j$, uniform only for abelian Γ. The gauge multiplet is the same overlap with the trivial longitudinal character,

$$\frac{1}{|\Gamma|} \sum_{g \in \Gamma} \chi_i(g) \, \chi_j(g)^* = \delta_{ij}, \tag{VI.2.55}$$

one factor on each diagonal node; here "endpoint-untwisted" is the open-channel statement that the surviving block is diagonal, not the instruction to keep only the $g = e$ closed-channel term.

Read this way, the quiver is two faces of one orbifold computation. The open strings, projected block by block, give the gauge fields on the diagonal and the bifundamentals on the twist, in multiplets fixed by the surviving supercharges; the boundary states, decomposed into untwisted and twisted sectors, give the brane charges that say which branes move and which are stuck. The cylinder relates these open and closed descriptions through their common group characters. The foundational machinery used here, the orbifold conformal field theory, the open-string GSO projection, and the boundary-state construction, is developed in the foundational volumes and only used in this chapter.

VI.2.9 What the construction does and does not give

The construction delivers the gauge theory at the orbifold point, and it is worth marking the boundary of that statement. The quiver, its ranks, its bifundamentals, and its superpotential are produced at the singular quotient itself, with the Fayet–Iliopoulos parameters set to zero, and the two moduli-space computations above were done at zero FI for that reason. Turning on the FI parameters moves the quiver off the singular point, and in the two examples here it produces the familiar geometric resolutions, the ALE space for $\mathbb{C}^2/\mathbb{Z}_n$ (Chapter 4) and the $\mathbb{P}^2$ blow-up for $\mathbb{C}^3/\mathbb{Z}_3$ (Chapter 6 and Volume VII). In general, however, FI parameters are Kähler/stability data: depending on the chamber they may give a smooth resolution, a partial resolution, or a different phase, and the systematic discussion is split accordingly, the $\mathcal{N} = 2$ ALE story to Chapter 4 and the toric $\mathcal{N} = 1$ story to Chapter 6 and Volume VI.

The reconstruction is of the holomorphic, probe-visible geometry. The statements that the mesonic branches equal $\{uv = w^n\} \times \mathbb{C}$ and $\mathbb{C}^3/\mathbb{Z}_3$ are statements about the protected chiral ring and the complex structure cut out by the F-terms; they do not claim that the classical Kähler metric is exact, since higher-derivative α' corrections and string-loop effects can deform the non-protected metric data. The quiver, the inherited superpotential, the F-term relations, and the resulting holomorphic coordinate ring are the protected data the probe extracts. The closed-string twisted sectors, the blow-up modes localized on the fixed locus, are not seen directly by the mesonic branch; the probe meets them only through the FI parameters and, as §VI.2.8 showed, through the twisted charges carried by the fractional branes, and their geometry belongs to Volume III.

Two smaller cautions are load-bearing. The chiral quiver is consistent only when its rank vector is anomaly-free, the condition (VI.2.42) imposed by hand here and derived

systematically in Chapter 7. And, as set out in §VI.2.5, the quiver diagram is the ultraviolet gauge theory the projection produces, not by itself the infrared fate of every abelian factor: the overall diagonal $U(1)$ is the decoupled centre of mass, seen above in the $\sum_i \mu_i = 0$ relation, while the relative $U(1)$ factors generically become massive or anomalous, leaving the interacting $\prod_i SU(N_i)$ with whatever anomaly-free abelian factors survive. That fate is construction-dependent, and its systematic account is Chapter 7.

Status and sources

The evidence tags ([WS] worldsheet), the convention pointers, and the source anchors are collected here, keyed by section. The construction is the perturbative, untwisted-open-string orbifold projection of Douglas and Moore (1996). Conventions used: the orbifold action and weights (orbifold action), the McKay multiplicity (McKay 1980) and the $\mathbb{C}^3/\mathbb{Z}_3$ orientation fixture, the quiver arrow direction and the math-convention bridge (fundamental-at-tail arrows, first load-bearing use in this volume), the superpotential inheritance, and the gauge/rank data. The McKay adjacencies and selected superpotential and moduli identities are follow from the projection, cyclic derivatives and invariant-ring calculations. The section-level [WS] labels name the open-string construction. Mathematical identities and the imported infrared/conformal assertions are distinct from the sourced infrared and conformal assertions.

§VI.2.1 From flat space to a singularity. Framing, strategy, and the recipe box; the flat-space inputs (the $\mathcal{N} = 4$ worldvolume theory, the decoupling limit, the moduli space) are Chapter 1 results, reused.

§VI.2.2 The orbifold geometry and the Calabi–Yau condition. The orbifold action (VI.2.1) and the $\mathbb{C}^2$-in-$\mathbb{C}^3$ spectator are the stated orbifold action and supersymmetry conventions. The Calabi–Yau condition (VI.2.3) is the determinant-one condition for the flat orbifold action. Its relation to invariant spinors and the $SU(2) \to 8$, $SU(3) \to 4$ supercharge count uses the standard spinor projection cited to Part I (holonomy and invariant spinors; Vol. IV ch. 2). the finite calculation compares stored supercharge labels; it is not an independent spinor derivation. The general invariant-monomial condition (VI.2.6) and the spectator factorization (VI.2.7) are stated here; the two specific rings, the A_{n-1} relation (VI.2.40) and the third Veronese subring (VI.2.46), are computed in §VI.2.6 and §VI.2.7 where the gauge theory reconstructs them (elementary invariant theory; the ADE and McKay depth is Vol. IV ch. 3). The singular line of $(\mathbb{C}^2/\mathbb{Z}_n) \times \mathbb{C}$ and the orbit picture are geometry; Figure VI.2.2 is a cartoon (the disclaimer is in its caption).

§VI.2.3 The orbifold projection. The three-quotients box separates the geometric quotient, the open-string projection, and the vacuum quotient. The Chan–Paton representation (VI.2.9) and the projection conditions (VI.2.13)–(VI.2.14) are the Douglas–Moore orbifold projection [WS] (Douglas and Moore 1996, §3, Eqs. (3.2)–(3.3), §4.1; the action on Chan–Paton factors): a controlled perturbative computation on the untwisted open string, which gives the worldsheet construction. The homomorphism property of γ and the orbifold projector (VI.2.11) are standard; the open-string endpoints carry conjugate Chan–Paton representations, hence the adjoint conjugation, and the commutant reading of (VI.2.13) anticipates the gauge group of §VI.2.4. The projective-representation refinement is discrete torsion, deferred to VI.9. The reduction of the flat scalars to the three Φ_α is Chapter 1 (ten-dimensional Yang–Mills reduction); the orbifold open-string projection is the boundary-state/twisted-sector machinery of orbifold CFT and boundary states.

§VI.2.4 Nodes and arrows. The worked 3×3 projection, the isotypic decomposition (VI.2.20), the gauge group (VI.2.21), the block rule (VI.2.22), and the character formula (VI.2.23) with the table (VI.2.24) are the projection solved [WS] (Douglas and Moore 1996, §3 and §4; the projected open-string spectrum, McKay multiplicities, quiver gauge groups and ranks; the multiplicity formula and its abelian collapse evaluated, the finite calculation, and re-derived by exact representation theory, the symbolic calculation). The character theory used here, orthogonality and the regular representation, is cited to its home (finite-group character theory). The arrow convention and the math-convention bridge are fundamental-at-tail arrows, here at its first load-bearing use in the volume. The inherited cubic

superpotential (VI.2.26) and the flavor-symmetry selection of the ε contraction are superpotential normalization (full $\mathbb{C}^3/\Gamma$ technology, VI.6).

§VI.2.5 Regular and fractional branes; surviving supersymmetry. The one-brane/n-labels clarification, the regular rank vector $N_i = N \dim R_i$, $K = N|\Gamma|$ (VI.2.28), and the operational fractional-brane definition are quiver gauge groups and ranks (Q2/Q3; fractional-brane and wrapped-cycle deep dive, VI.5; the stated distinction, only the irreducibles present in γ are nodes). Preserved supersymmetry from the embedding, $SU(2) \to 8$ and $SU(3) \to 4$, is the stated action on spinors and spinor and supersymmetry counting, compared with the invariant spinor of §VI.2.2 (holonomy and invariant spinors). The abelian-factor discussion (overall diagonal $U(1)$ = free centre of mass, its neutral gauge action imposing no further mesonic quotient (the position moduli instead arise from the bifundamental and, for the necklace, spectator chiral vacuum values; the stated distinction); the relative $U(1)$'s anomalous or massive via twisted-sector axions, leaving the interacting $\prod_i SU(N_i)$) is quiver gauge groups and ranks with the Chapter 1 $U(N) \to SU(N)$ lesson made quiver-specific (the free sector carries the geometry as in VI.1; VI.7 analyzes the relative $U(1)$ factors and anomalies). The superconformal identification of the regular-rank quivers as orbifold daughters of $\mathcal{N} = 4$ is the engine-chapter statement of what the theory is; the SCFT dynamics (conformal manifold, central charges, superconformal index, dualities) route to Part III (Vol XIV).

§VI.2.8 The worldsheet origin. The open-string-sector reading of the spectrum (the gauge field in the diagonal/endpoint-untwisted blocks, the bifundamental in the off-diagonal/endpoint-twisted blocks, the ψ^α geometric phase equal to the weight a_α) is claim-atom [WS] (Douglas and Moore 1996, §3, Eqs. (3.2)–(3.3), §4.1; the open-string GSO and the orbifold projection of the open-string Hilbert space, orbifold CFT and boundary states); it refines the block rule (VI.2.22). The multiplet assembly from the GSO and the supercharge projection ($SU(2) \to \mathcal{N} = 2$ vector+hyper, $SU(3) \to \mathcal{N} = 1$ vector+chiral) is [WS] (spinor and supersymmetry counting; the SUSY count of §VI.2.2, holonomy and invariant spinors). The boundary-state decomposition (VI.2.51), the fractional brane as a twisted-charge boundary state (pinned) and the regular brane's vanishing twisted charge (VI.2.53) (mobile), is [WS] (Diaconescu and Gomis 2000, fractional branes as twisted boundary states, with the $\mathbb{C}^3/\mathbb{Z}_3$ case worked there in full). The open-closed channel duality giving the McKay count (VI.2.54) as a twisted-sector-graded overlap is [WS] (Cardy/boundary-state open-closed duality, Billo et al. 2001; orbifold CFT and boundary states). The two-meanings-of-"twist" distinction separates open-string endpoint-twist matter from closed-string twisted-sector blow-up and FI data; the GSO, boundary-state, and orbifold-CFT machinery is not re-derived (orbifold CFT and boundary states, home Vol. II ch. 6 / Vol. III).

§VI.2.6 The non-chiral example. The $\hat{A}_{n-1}$ adjacency (VI.2.35), the symmetric necklace, the $\mathcal{N} = 2$ vector/hyper organization, and the spectator adjoint Φ_i as motion along the singular line are [WS] (Douglas and Moore 1996, §4.1; the spectator direction, McKay multiplicities). The $\mathcal{N} = 2$ daughter superpotential (VI.2.36) and the moment map (VI.2.37) are superpotential normalization. The projected parent trace can be evaluated in the chapter convention $X = \omega\gamma X\gamma^{-1}$ at rectangular ranks $(2, 3, 4)$. With $\gamma X\gamma^{-1} = \omega X$, the field called X is instead the reverse arrow B and Y is A. Exchanging them reverses the commutator and translates the moment-map sign. The moduli computation (VI.2.39), $(\mathbb{C}^2/\mathbb{Z}_n) \times \mathbb{C}$, is the probe reconstruction of Chapter 1 made explicit [WS]. The ALE/hyperkähler reading and the Coulomb-vs-Higgs branch name are forward references to VI.3–VI.4.

§VI.2.7 The chiral example. The dP_0 adjacency (VI.2.41) with its orientation, the gauge group, and $\mathcal{N} = 1$ are [WS] (the projection method of Douglas and Moore 1996, whose worked case is $\mathbb{C}^2/\mathbb{Z}_n$, and the $\mathbb{C}^3/\Gamma$ construction of Douglas, Greene, et al. 1997; the stated McKay orientation). The cubic superpotential (VI.2.43), its F-terms, gauge invariance, and the parallel-flavor-vector branch are superpotential normalization, checked algebraically by the symbolic calculation ($W = \det$, the nine F-terms, the charge-neutral loop and F-flatness). The direct projection of the parent trace gives the coefficient-one ε cubic; both calculations retain the parent superpotential as a physical premise. The mesonic-branch reconstruction of $\mathbb{C}^3/\mathbb{Z}_3$ as the cubic invariant ring (VI.2.46), with the closed-loop mesons (VI.2.45), is [WS]; the full GIT identification is standard (Douglas, Greene, et al. 1997), the resolution VI.6 and Volume VI. The cubic $SU(N_i)$ anomaly condition (VI.2.42) constrains all three ranks when $N_i \geq 3$; low-rank abelian anomalies and tadpoles need separate analysis in VI.7. Moduli-space-equals-geometry caveats, the quiver is read off representation theory, not the geometry, the stated distinction.

§VI.2.9 What the construction does and does not give. FI parameters as Kähler/stability data, giving resolutions, partial resolutions, or different phases (resolution and discrete data; VI.4 for the ALE case, VI.6 and Volume VII for the toric case); the holomorphic, probe-visible reconstruction and its α'/g_s caveats (the stated distinction, inherited from Chapter 1); twisted sectors routed to Vol. IV; anomaly freedom of the chiral rank vector (VI.7); the per-$U(1)$ infrared fate not read off the diagram (quiver gauge groups and ranks; the line-operator machinery is a later chapter).

References

Billo, M., B. Craps, and F. Roose (2001). "Orbifold boundary states from Cardy's condition". In: *JHEP* 01, p. 038. DOI: 10.1088/1126-6708/2001/01/038. arXiv: hep-th/0011060.

Diaconescu, D.-E. and J. Gomis (2000). "Fractional branes and boundary states in orbifold theories". In: *JHEP* 10, p. 001. DOI: 10.1088/1126-6708/2000/10/001. arXiv: hep-th/9906242.

Douglas, M. R., B. R. Greene, and D. R. Morrison (1997). "Orbifold resolution by D-branes". In: *Nucl. Phys. B* 506, pp. 84–106. DOI: 10.1016/S0550-3213(97)00517-8. arXiv: hep-th/9704151.

Douglas, M. R. and G. W. Moore (1996). "D-branes, quivers, and ALE instantons". In: arXiv preprint; not published in a journal. arXiv: hep-th/9603167.

McKay, J. (1980). "Graphs, singularities, and finite groups". In: *Proc. Symp. Pure Math.* 37. American Mathematical Society, pp. 183–186.

Chapter VI.3

$\mathbb{C}^2/\Gamma$: $\mathcal{N}=2$ ADE quivers and the McKay correspondence as gauge theory

VI.3.1 From the abelian warm-up to the McKay correspondence

A brane at an orbifold singularity can carry several gauge factors even though it probes one transverse space. The orbifold projection explains how this happens: place N D-branes at the fixed point of a finite group Γ acting on the transverse space, let each group element act at once on the transverse coordinates and on the Chan–Paton labels, and keep the configurations invariant under the combined action. What survives is a product of gauge groups with matter strung between them, a quiver, and which factors and which matter survive is fixed by the representation theory of Γ. The two examples in the previous chapter were abelian: $\mathbb{C}^2/\mathbb{Z}_n$ with $\Gamma \subset SU(2)$, eight supercharges, the affine $\hat{A}_{n-1}$ necklace; and $\mathbb{C}^3/\mathbb{Z}_3$ with $\Gamma \subset SU(3)$, four supercharges, the dP_0 quiver. For an abelian Γ every irreducible representation is one dimensional, the character theory is a sum of phases, and each step is explicit.

Two axes organize the family these examples sample (Table VI.3.1). One axis is the embedding of the orbifold group: $\Gamma \subset SU(2)$ acting on two complex transverse directions, with the third an inert spectator, preserves eight supercharges and gives a four-dimensional $\mathcal{N}=2$ theory; $\Gamma \subset SU(3)$ acting on all three, with no further supersymmetry enhancement, preserves four and gives an $\mathcal{N}=1$ theory. The other axis is whether Γ is abelian or not. The last chapter filled the abelian column of this square, both rows, and introduced the general projection that applies to any $\mathbb{C}^m/\Gamma$. This chapter develops the upper-right cell, the non-abelian $\mathbb{C}^2/\Gamma$ with Γ a finite non-abelian subgroup of $SU(2)$. The bottom row, the $\mathbb{C}^3/\Gamma$ orbifolds with their $\mathcal{N}=1$ quivers and superpotentials, abelian and non-abelian alike, is the subject of Chapter 6; the abelian ones, being toric, also open the brane-tiling technology of Volume VI.

	abelian Γ	non-abelian Γ
$\mathbb{C}^2/\Gamma$, $\Gamma \subset SU(2)$ ($\mathcal{N}=2$)	$\mathbb{Z}_n \to \hat{A}_{n-1}$ (Ch. 2)	$2D_n, 2T, 2O, 2I \to \hat{D}, \hat{E}$ **(this ch.)**
$\mathbb{C}^3/\Gamma$, $\Gamma \subset SU(3)$ ($\mathcal{N}=1$)	$\mathbb{Z}_m \times \mathbb{Z}_n$ (Ch. 6)	$SU(3)$ McKay (Ch. 6)

Table VI.3.1: The two axes of the orbifold family: the dimension of the orbifold action ($\mathbb{C}^2$ or $\mathbb{C}^3$, fixing $\mathcal{N}=2$ or $\mathcal{N}=1$) against whether Γ is abelian. The $\mathbb{C}^2/\Gamma$ orbifolds split by the McKay correspondence into the abelian A series (Chapter 2) and the non-abelian D, E series (this chapter); the $\mathbb{C}^3/\Gamma$ orbifolds have no such ADE classification, so Chapter 6 takes the whole list, abelian and non-abelian alike. The diagonal abelian subgroups are cyclic $\mathbb{Z}_n$ in $SU(2)$ but products $\mathbb{Z}_m \times \mathbb{Z}_n$ in $SU(3)$, the rank-one against the rank-two maximal torus; $dP_0 = \mathbb{C}^3/\mathbb{Z}_3$ is the cyclic warm-up of Chapter 2, and the abelian $\mathbb{C}^3$ orbifolds, being toric, recur as the simplest brane tilings of Volume VI.

The new question is which non-abelian gauge factors and matter representations survive this projection. That $\Gamma \subset SU(2)$ gives $\mathcal{N}=2$ is a consequence, the same eight-supercharge count as the abelian necklace. The new structure is a theorem of representation theory special to two complex dimensions: the finite subgroups of $SU(2)$ are classified, and the quiver each one produces, read off its character table, is precisely an affine Dynkin diagram of type A, D, or E. This is the McKay correspondence. Stated as gauge theory it says that the diagram controlling a simply-laced Lie algebra, the same A–D–E list that classifies so much else, is the matter content of a brane probe of $\mathbb{C}^2/\Gamma$. The abelian necklaces of the last chapter were the A series of this list, the warm-up; the genuinely non-abelian content, the D and E series, is what we develop now.

We answer this question by decomposing the Chan–Paton space into irreducible representations. For non-abelian Γ these need not be one dimensional, so the representation dimensions now affect the gauge ranks. The quiver follows: the nodes are the irreducible representations, the arrows are counted by how the two-dimensional defining representation Q tensors them. Because Q is self-conjugate the quiver is undirected, the matter non-chiral; because $\Gamma \subset SU(2)$ preserves eight supercharges the theory is $\mathcal{N}=2$, and the two together make each undirected edge a hypermultiplet. The McKay correspondence identifies this quiver with the affine ADE diagram. We then organize the finite groups, work the smallest D and E examples in full, and close where the last chapter closed: the Higgs branch of the single regular brane reconstructs the active transverse surface, the orbifold $\mathbb{C}^2/\Gamma$ at the singular point and its ALE resolution once the Fayet–Iliopoulos parameters are turned on. Whenever we call the FI deformation a resolution, we hold the complex FI levels at zero in a chosen complex structure and vary the real levels away from their root walls. General FI triplets give the larger ALE family. We keep the inherited spectrum and the D3 field-theory limit of the previous two chapters: $\alpha' \to 0$ at fixed $g_{\rm YM}$ and fixed field-theory energies, with bulk gravity decoupled as assumed there.

Recipe: from a finite subgroup of $SU(2)$ to its ADE quiver.

Input: a finite subgroup $\Gamma \subset SU(2)$, with its character table. *Nodes:* one gauge node $U(N_i)$ for each irreducible representation R_i of Γ; the regular brane has ranks $N_i = N \dim R_i$. *Arrows:* between R_i and R_j put a_{ij} = the multiplicity of R_j in $Q \otimes R_i$, where Q is the defining two-dimensional representation; since Q is self-conjugate $a_{ij} = a_{ji}$, an undirected edge, which the eight supercharges of $\Gamma \subset SU(2)$ make one $\mathcal{N} = 2$ hypermultiplet. Each node also carries an adjoint chiral Φ_i from the spectator direction. *Output:* the resulting graph is the affine ADE Dynkin diagram matched to Γ; for one regular brane the active Higgs branch is $\mathbb{C}^2/\Gamma$, resolved to the ALE space at generic real Fayet–Iliopoulos parameter with vanishing complex level (the spectator direction and the N-brane symmetric product are §VI.3.9).

VI.3.2 The setup, inherited: $\Gamma \subset SU(2)$ and its branes

The geometry is the one from the last chapter with the group enlarged. A D3-brane has six transverse real dimensions, three complex, z_1, z_2, z_3. A finite group $\Gamma \subset SU(2)$ acts on the first two,

$$g: \quad (z_1, z_2) \;\longmapsto\; Q(g)\,(z_1, z_2)^{\mathsf{T}}, \qquad z_3 \;\longmapsto\; z_3, \qquad g \in \Gamma, \tag{VI.3.1}$$

through its defining two-dimensional representation Q, the inclusion $\Gamma \subset SU(2)$ itself, while z_3 is the inert spectator. The quotient $\mathbb{C}^2/\Gamma$ is a surface singularity at the origin, and the z_3-axis is a complex line of such singularities sitting inside the transverse $\mathbb{C}^3$. Because every $Q(g) \in SU(2)$ has unit determinant, the holomorphic two-form $dz_1 \wedge dz_2$ is preserved, the Calabi–Yau condition in two complex dimensions, and the probe keeps eight of its sixteen supercharges: a four-dimensional $\mathcal{N} = 2$ theory.

The novelty is entirely in Γ. The finite subgroups of $SU(2)$ fall into two families under the double cover

$$1 \;\to\; \mathbb{Z}_2 \;\to\; SU(2) \;\to\; SO(3) \;\to\; 1. \tag{VI.3.2}$$

The cyclic groups $\mathbb{Z}_n$ are listed separately: for odd n they miss $-\mathbb{1}$, while for even n they contain it and are the full preimage of a cyclic rotation group of half the order; either way they are abelian, the last chapter's A series. The genuinely new family is the *binary polyhedral groups*, the full preimages of the non-cyclic rotation subgroups $\bar{\Gamma} \subset SO(3)$, each containing $-\mathbb{1}$ and twice as large,

$$|\Gamma| = 2\,|\bar{\Gamma}|, \qquad -\mathbb{1} \in \Gamma, \qquad 2D_n\ (4n), \quad 2T\ (24), \quad 2O\ (48), \quad 2I\ (120), \tag{VI.3.3}$$

the binary dihedral or dicyclic groups $2D_n$ and the three exceptional binary groups, tetrahedral, octahedral, and icosahedral. The probe sees the binary group, not merely its $SO(3)$ quotient, and this is already true geometrically: the local coordinates (z_1, z_2) are the defining $SU(2)$ doublet Q, so the central element $-\mathbb{1}$ acts as

$$(z_1, z_2) \;\longmapsto\; -(z_1, z_2), \tag{VI.3.4}$$

not trivially as it would in $SO(3)$. The spin lift also acts on fermions and supercharges; only the invariant supercharge components survive the quotient. So the group relevant for the open-string Hilbert space and the Chan–Paton action is the finite subgroup $\Gamma \subset SU(2)$ itself, not its image $\bar{\Gamma} \subset SO(3)$, and the open strings carry the chosen representation γ of Γ on their Chan–Paton labels. *(Notation.)* We take $2D_n$ to be the binary dihedral, or dicyclic, group of order $4n$, nonabelian for $n \geq 2$ (the smallest being $Q_8 = 2D_2$); with this convention McKay sends $2D_n \to \hat{D}_{n+2}$. Some references shift the index and name the same group by its Dynkin label instead; the order-$4n$ convention is used throughout. The classification of these subgroups and their character tables is representation theory we use here and cite to its home; what we need is computed in each example.

The branes are projected as in the last chapter, but the non-abelian case parts from the abelian necklace exactly at the Chan–Paton structure, so it is worth doing carefully. To each $g \in \Gamma$ assign a Chan–Paton matrix $\gamma(g) \in U(K)$, a representation, $\gamma(g)\gamma(h) = \gamma(gh)$; the orbifold keeps the open-string fields invariant under the combined geometric and Chan–Paton action. For the gauge field, with no transverse index,

$$A_\mu \;=\; \gamma(g)\, A_\mu\, \gamma(g)^{-1} \qquad \text{for all } g \in \Gamma, \tag{VI.3.5}$$

so A_μ commutes with the whole image of γ. For an abelian Γ the irreducibles are one dimensional and γ is a list of phases, so commuting with it just selects diagonal blocks; for a non-abelian Γ the irreducibles R_i can be matrix blocks of dimension $d_i = \dim R_i > 1$, and the Chan–Paton space splits as multiplicity space tensored with irreducible,

$$\mathbb{C}^K \;\cong\; \bigoplus_i \mathbb{C}^{N_i} \otimes R_i, \qquad K = \sum_i N_i\, d_i, \tag{VI.3.6}$$

with N_i the multiplicity of R_i. By Schur's lemma an endomorphism commuting with every $\gamma(g)$ acts as the identity on each irreducible block and is free on the multiplicity factors,

$$\mathrm{End}_\Gamma\big(\mathbb{C}^K\big) \;=\; \bigoplus_i \mathrm{Mat}_{N_i}(\mathbb{C}) \otimes \mathbb{1}_{R_i}, \qquad \text{gauge group} \quad \prod_i U(N_i), \tag{VI.3.7}$$

one unitary factor per irreducible appearing in γ, each acting on its multiplicity space $\mathbb{C}^{N_i}$ while the orbifold fixes its action on the factor R_i. Thus a representation of dimension d_i contributes a gauge factor of rank N_i, not $N_i d_i$: the gauge field acts only on the copies of that representation. The nodes of the quiver are these representations. The matter, the surviving transverse scalars, is the content of the next section; the spectator z_3, carrying no Γ phase, survives in the same blocks as the gauge field and supplies an adjoint chiral Φ_i at each node, the brane's position along the singular line.

VI.3.3 The McKay quiver and its smallest case

The matter comes from the transverse scalars that do carry a Γ phase. The two active coordinates (z_1, z_2) transform in the defining representation Q, so a transverse scalar Z survives only if its geometric Q-rotation is undone by the Chan–Paton conjugation,

$$Z \;=\; Q(g)\, \gamma(g)\, Z\, \gamma(g)^{-1} \qquad \text{for all } g \in \Gamma. \tag{VI.3.8}$$

The surviving scalars joining node i to node j are the intertwiners realizing R_j inside $Q \otimes R_i$; their number is the multiplicity of R_j in that tensor product,

$$a_{ij} \;=\; \dim \mathrm{Hom}_\Gamma\big(R_j,\, Q\otimes R_i\big) \;=\; \big[\, Q\otimes R_i : R_j \,\big], \qquad Q\otimes R_i \;=\; \bigoplus_j a_{ij}\, R_j, \tag{VI.3.9}$$

the number of times R_j appears when $Q \otimes R_i$ is decomposed into irreducibles. This is the only computation the quiver needs, and by character orthogonality it is an integral over the group,

$$a_{ij} \;=\; \frac{1}{|\Gamma|}\sum_{g\in\Gamma} \chi_Q(g)\,\chi_i(g)\,\chi_j(g)^*, \tag{VI.3.10}$$

with χ_Q, χ_i, χ_j the characters of Q and of the two representations. For an abelian Γ this reduces to the phase-counting of the last chapter; for a non-abelian Γ it is a genuine representation- theoretic multiplicity, and the resulting graph, with a_{ij} edges between nodes i and j, is the *McKay quiver* of Γ.

The smallest non-abelian example makes the character average concrete. Take the quaternion subgroup of $SU(2)$, Q_8 of order eight.

How to read an edge from a character table.

The character inner product determines every edge of the quiver. To count the arrows from node i to node j, multiply the three rows χ_Q, χ_i, and χ_j^* entry by entry, average over the group with each conjugacy class weighted by its size, and read off the resulting integer,

$$a_{ij} = [\, Q\otimes R_i : R_j \,] = \frac{1}{|\Gamma|}\sum_{[g]} |[g]|\, \chi_Q([g])\,\chi_i([g])\,\chi_j([g])^*.$$

The worked examples are this one recipe carried out; an inner product is shown explicitly in each.

The group Q_8 is generated by $a = \mathrm{diag}(i,-i)$ and $b = \left(\begin{smallmatrix} 0 & 1 \\ -1 & 0 \end{smallmatrix}\right)$, the eight unit quaternions $\pm\mathbb{1}$, $\pm i\sigma_a$. It has five conjugacy classes, $\{\mathbb{1}\}$, $\{-\mathbb{1}\}$, and $\{\pm i\sigma_a\}$ for $a = 1,2,3$, hence five irreducibles, four one-dimensional and one two-dimensional (the defining Q). The character table is

	$\{\mathbb{1}\}$	$\{-\mathbb{1}\}$	$\{\pm i\sigma_1\}$	$\{\pm i\sigma_2\}$	$\{\pm i\sigma_3\}$
$\mathbf{1}$	1	1	1	1	1
$\mathbf{1}'$	1	1	1	-1	-1
$\mathbf{1}''$	1	1	-1	1	-1
$\mathbf{1}'''$	1	1	-1	-1	1
$\mathbf{2} = Q$	2	-2	0	0	0

(VI.3.11)

with $\chi_Q(\pm i\sigma_a) = 0$ and $\chi_Q(-\mathbb{1}) = -2$. To see the table do real work, compute one multiplicity explicitly, the number of $\mathbf{1}'$ inside $Q \otimes Q$, weighting each class by its size,

$$[\, Q\otimes Q : \mathbf{1}' \,] = \frac{1}{|Q_8|}\sum_{[g]} |[g]|\, \chi_Q\chi_Q\,\chi_{\mathbf{1}'}^* = \frac{1}{8}\big(1\cdot 2\cdot 2\cdot 1 + 1\cdot(-2)(-2)\cdot 1\big) = 1, \tag{VI.3.12}$$

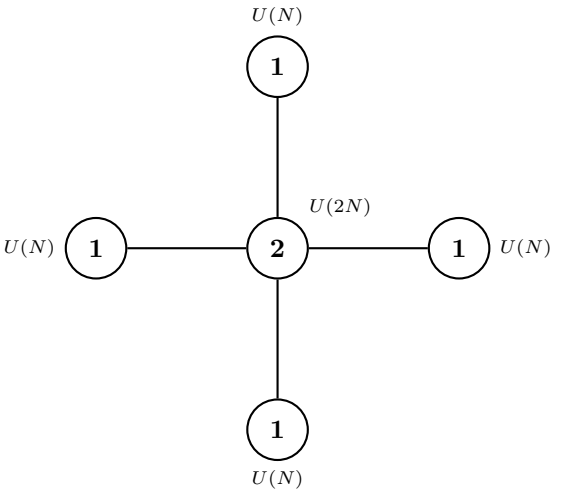


Figure VI.3.1: The affine $\hat{D}_4$ quiver of $Q_8 = 2D_2$, the four-pointed star. The central node $U(2N)$ is the two-dimensional representation; the four horns $U(N)$ are the one-dimensional representations. Each edge is one $\mathcal{N} = 2$ hypermultiplet (adjoint self-loops suppressed). This is the smallest non-abelian ADE quiver.

the three classes $\{\pm i\sigma_a\}$ dropping out because χ_Q vanishes on them. The same computation gives multiplicity one for $\mathbf{1}$, $\mathbf{1}''$, and $\mathbf{1}'''$, so

$$Q \otimes Q \;=\; \mathbf{1} \oplus \mathbf{1}' \oplus \mathbf{1}'' \oplus \mathbf{1}''', \tag{VI.3.13}$$

the two-dimensional node connecting to all four one-dimensional nodes, while conversely $Q \otimes \mathbf{1}^{(s)} = \mathbf{2}$ attaches each one-dimensional node to it by a single edge. The McKay quiver is the four-pointed star (Figure VI.3.1), which is the affine $\hat{D}_4$ Dynkin diagram, the two-dimensional representation at the centre. Its node labels are the dimensions $(1, 1, 1, 1; 2)$, the Dynkin marks of §VI.3.5; with N regular branes, of rank N times the dimension at each node, the gauge theory is

$$U(N)^4 \times U(2N), \qquad \text{ranks } (N, N, N, N; 2N), \tag{VI.3.14}$$

a central $U(2N)$ joined by one $\mathcal{N} = 2$ hypermultiplet to each of four $U(N)$ horns, every node carrying an adjoint Φ_i.

The McKay quiver of Q_8 came out an affine ADE diagram, undirected, with $\mathcal{N} = 2$ matter and an adjoint at every node. None of this was special to Q_8: that the McKay quiver is always an affine ADE diagram, why the matter is non-chiral and $\mathcal{N} = 2$, and how the gauge theory and its superpotential follow, are the general facts we now establish.

VI.3.4 The McKay correspondence in general

The Q_8 quiver came out undirected, its matter $\mathcal{N} = 2$; both are general, and two features of Q control them. First, Q is the defining two-dimensional representation of $SU(2)$, and every representation of $SU(2)$ is self-conjugate, $Q \cong Q^*$; more sharply, Q is *pseudoreal*, carrying an antisymmetric Γ-invariant form, the $SU(2)$ epsilon tensor $\varepsilon_{\alpha\beta}$,

$$\varepsilon\, Q\, \varepsilon^{-1} = Q^*, \qquad \chi_Q(g) = \chi_Q(g)^* \in \mathbb{R}. \tag{VI.3.15}$$

Its character is therefore real, so (VI.3.10) is symmetric,

$$a_{ij} \;=\; a_{ji}, \tag{VI.3.16}$$

so the McKay quiver is *undirected*: the scalar from i to j comes paired with one from j to i. The antisymmetric ε is the data of that pairing, the Γ-invariant form on Q that ties the two opposite bifundamentals together. Second, the supersymmetry is $\mathcal{N} = 2$, because $\Gamma \subset SU(2)$ preserves eight of the sixteen supercharges, and with eight supercharges the paired chirals are forced into single multiplets. The two opposite bifundamentals, $X_{ij} \in (\mathbf{N}_i, \overline{\mathbf{N}}_j)$ and its partner $X_{ji} \in (\mathbf{N}_j, \overline{\mathbf{N}}_i)$, the two chiral halves joined by ε, fill out one $\mathcal{N} = 2$ hypermultiplet; the gauge field, the gaugino, and the spectator adjoint Φ_i (from the phaseless z_3, in the diagonal blocks) fill out one $\mathcal{N} = 2$ vector. The two properties play distinct roles: pseudoreality makes the matter non-chiral (the undirected edge), while the eight supercharges make it $\mathcal{N} = 2$ (each edge a hyper, each node a vector with its adjoint). The worldsheet derivation of this assembly, where both come from the Ramond sector, is §VI.3.8.

A word on how we draw these quivers. We use the undirected affine Dynkin form: each edge a single line for one hypermultiplet, the opposite-arrow pair X_{ij}, X_{ji} left implicit, and the adjoint Φ_i at each node left off the diagram. The previous chapter drew the same affine $\hat{A}$ necklace in $\mathcal{N} = 1$ language, each hypermultiplet a pair of opposite chiral arrows and each adjoint an explicit self-loop; the two pictures are the same $\mathcal{N} = 2$ theory, and we use the undirected form here because it is the McKay diagram itself, the object the correspondence is about.

The character calculation also identifies the Lie-algebra diagram. For a nontrivial finite $\Gamma \subset SU(2)$, McKay's theorem states that the undirected graph (VI.3.9) is always an affine (extended) Dynkin diagram of type A, D, or E,

$$a_{ij} \;=\; 2\,\delta_{ij} - \hat{C}_{ij}, \qquad a_{ii} = 0, \qquad a_{ij} \in \{0, 1\} \;\; (i \neq j,\; \Gamma \neq \mathbb{Z}_2), \tag{VI.3.17}$$

where $\hat{C}$ is the affine Cartan matrix of the matched diagram. The McKay quiver and the affine Dynkin diagram are the same graph. The vanishing diagonal $a_{ii} = 0$ (the diagram has no node joined to itself) and the simply-laced off-diagonal $a_{ij} \in \{0, 1\}$ are read off the matched ADE diagram, not self-evident from Q alone; they are part of the McKay statement, and for each worked group they fall out of the character-table computation of the next sections. The one exception, a double edge $a_{ij} = 2$, is the affine $\hat{A}_1$ of $\mathbb{Z}_2$, an abelian A-series case of the last chapter; all the non-abelian D and E quivers here are simply-laced. The matched type is dictated by which binary group Γ is, the correspondence we run in the next section.

Two ADE graphs, not to confuse.

Two ADE graphs appear in the story, and they are not the same object. The *McKay quiver* of this chapter is *affine*: one node for every irreducible representation of Γ, the trivial representation included. The *exceptional-curve intersection graph* of the minimal resolution of $\mathbb{C}^2/\Gamma$ (Chapter 4) is *finite*: one node for each compact exceptional $\mathbb{P}^1$, the affine node absent. They share the ADE type, but the affine node is the representation-theoretic extra, present in the quiver and absent in the geometry. The full statement is in §VI.3.10.

The gauge theory is then read off the diagram. Its nodes carry the factors $U(N_i)$; its edges carry $\mathcal{N} = 2$ hypermultiplets in the bifundamentals; each node carries the adjoint Φ_i. The $\mathcal{N} = 2$ superpotential is the daughter of the parent $\mathcal{N} = 4$ cubic, the spectator playing the outer leg of the commutator,

$$W \;=\; \sum_i \mathrm{Tr}\;\Phi_i\,\mu_i, \qquad \mu_i \;=\; \sum_{a:\,h(a)=i} X_a X_{\bar a} \;-\; \sum_{a:\,t(a)=i} X_{\bar a} X_a, \tag{VI.3.18}$$

Here we choose one orientation a per undirected edge, with $\bar a$ its opposite. In this formula $X_a : \mathbb{C}^{N_{t(a)}} \to \mathbb{C}^{N_{h(a)}}$ is a linear map, an $N_{h(a)} \times N_{t(a)}$ matrix. Thus a follows the mathematical map direction, opposite to the drawn chiral arrow convention $X_{ij} \in (\mathbf{N}_i, \overline{\mathbf{N}}_j)$. This translation makes both products in μ_i square matrices at node i. The quantity μ_i is the complex moment map at node i, the oriented sum of the hypermultiplet bilinears entering and leaving the node, valued in the adjoint of $U(N_i)$, an endomorphism of the multiplicity space $\mathbb{C}^{N_i}$. Matrix derivatives below use the trace pairing, $\delta W = \mathrm{Tr}((\partial W/\partial\Phi_i)\delta\Phi_i)$, so the entrywise gradient is transposed when written as a matrix. The F-term of the adjoint sets the moment map to zero,

$$\frac{\partial W}{\partial \Phi_i} \;=\; \mu_i \;=\; 0, \tag{VI.3.19}$$

the complex moment-map equations whose solution, divided by the gauge group, is the Higgs branch of §VI.3.9. Varying the hypermultiplet fields instead gives the companion F-terms; for an oriented arrow $a : t(a) \to h(a)$, varying the conjugate arrow $X_{\bar a}$ gives the relation for X_a,

$$\frac{\partial W}{\partial X_{\bar a}} \;=\; \Phi_{h(a)}\,X_a - X_a\,\Phi_{t(a)} \;=\; 0, \tag{VI.3.20}$$

the adjoints at the two ends of a acting on it, with the conjugate equation from $\partial W/\partial X_a$. On the pure Higgs branch the Φ_i are set to zero and these are trivially solved; on the regular-brane geometric branch, where the bifundamentals take values, the nonzero maps identify a common value of the Φ_i along each connected stable component, the position along the spectator z_3 line (for N branes, N such common values). These equations connect the matter spectrum to the brane positions. We next determine the ranks and edges for each ADE family, before using the moment maps to count the Higgs-branch directions.

Γ	$\lvert\Gamma\rvert$	irreducible dimensions = marks	affine type
$\mathbb{Z}_n$	n	$(1,1,\ldots,1)$	$\hat{A}_{n-1}$
$2D_n$	$4n$	$(1,1,1,1,2,\ldots,2)$	$\hat{D}_{n+2}$
$2T$	24	$(1,1,1,2,2,2,3)$	$\hat{E}_6$
$2O$	48	$(1,1,2,2,2,3,3,4)$	$\hat{E}_7$
$2I$	120	$(1,2,2,3,3,4,4,5,6)$	$\hat{E}_8$

Table VI.3.2: The McKay correspondence as a classification. For each finite $\Gamma \subset SU(2)$: its order, the multiset of irreducible-representation dimensions, and the affine Dynkin type. The entries of the third column are at once the representation dimensions, the regular-brane rank units δ_i, and the affine Dynkin marks. Only $\hat{A}$ (Chapter 2), $\hat{D}_{n+2}$, and $\hat{E}_6$ are worked here; the $\hat{E}_7$ and $\hat{E}_8$ character tables are deferred to Chapter 11, but their marks and affine diagrams are already fixed by McKay.

VI.3.5 The classification and the regular brane

McKay's correspondence is a dictionary between two lists that, a priori, have nothing to do with each other: the finite subgroups of $SU(2)$ and the affine ADE Dynkin diagrams. The dictionary is

$$\mathbb{Z}_n \;\to\; \hat{A}_{n-1}, \qquad 2D_n \;\to\; \hat{D}_{n+2}, \qquad 2T \;\to\; \hat{E}_6, \quad 2O \;\to\; \hat{E}_7, \quad 2I \;\to\; \hat{E}_8, \tag{VI.3.21}$$

the cyclic groups to the A series, the binary dihedral to the D series, the three exceptional binary groups to $\hat{E}_6, \hat{E}_7, \hat{E}_8$. The number of nodes is the number of irreducible representations of Γ, which for an affine diagram of finite type X_r is $r+1$, the rank plus the extra affine node. The cyclic case was the warm-up; the rest of the chapter works the first non-abelian entries of the D and E columns. It is worth keeping the whole list in view (Table VI.3.2).

The ranks are fixed by the regular representation. A single regular D-brane, obtained by bringing a mobile bulk brane to the orbifold point, carries not one Chan–Paton label but a copy of the *regular representation* of Γ, the representation on the $|\Gamma|$-dimensional group algebra, in which every irreducible R_i appears with multiplicity equal to its own dimension,

$$\gamma_{\mathrm{reg}} \;=\; \bigoplus_i (\dim R_i)\, R_i, \qquad N_i \;=\; N \dim R_i, \qquad K \;=\; N \sum_i (\dim R_i)^2 \;=\; N|\Gamma|, \tag{VI.3.22}$$

for N such regular branes, using $\sum_i (\dim R_i)^2 = |\Gamma|$. These ranks are not an extra input: $\dim R_i$ is exactly the i-th *mark* (or Dynkin label) of the affine diagram, the component of its primitive positive integer null vector, normalized to $\delta_0 = 1$ at the trivial representation. Writing δ for the vector of marks,

$$\hat{C}\,\delta \;=\; 0, \qquad \delta_i \;=\; \dim R_i, \qquad \sum_i \delta_i^2 \;=\; |\Gamma|, \tag{VI.3.23}$$

the statement that the affine Cartan matrix is degenerate with null vector the representation dimensions. This is not a coincidence to be checked diagram by diagram but a

direct consequence of (VI.3.17): contracting $a_{ij} = 2\delta_{ij} - \hat{C}_{ij}$ with the dimensions and using $Q \otimes R_i = \bigoplus_j a_{ij} R_j$,

$$\sum_j a_{ij} \dim R_j \;=\; \dim\bigl(Q \otimes R_i\bigr) \;=\; 2 \dim R_i, \qquad \Longleftrightarrow \qquad \hat{C}\,\delta = 0, \tag{VI.3.24}$$

because Q is two dimensional, so tensoring any representation with Q doubles its dimension. The marks being the dimensions is the statement that each node's neighbours carry, with multiplicity, twice its own rank. The regular-brane ranks are this null vector, and δ is the primitive positive imaginary root of the affine algebra, the marker that the diagram is affine and not finite: a finite Dynkin diagram has a positive-definite Cartan matrix and no null vector at all, while the affine extension adds exactly one node, in McKay labelling the trivial representation, and with it the imaginary root δ. The next two sections compute $\dim R_i$, the marks, for the binary dihedral and binary tetrahedral groups, and watch the McKay quiver assemble into $\hat{D}_{n+2}$ and $\hat{E}_6$.

VI.3.6 The D series: $2D_n \to \hat{D}_{n+2}$

The binary dihedral group $2D_n$, of order $4n$, is the double cover of the dihedral group of order $2n$. It is generated by two elements, a rotation a of order $2n$ and a flip b, with

$$a^{2n} = \mathbb{1}, \qquad b^2 = a^n, \qquad bab^{-1} = a^{-1}, \tag{VI.3.25}$$

realized inside $SU(2)$ by

$$a \;=\; \begin{pmatrix} \zeta & 0 \\ 0 & \zeta^{-1} \end{pmatrix}, \qquad b \;=\; \begin{pmatrix} 0 & 1 \\ -1 & 0 \end{pmatrix}, \qquad \zeta = e^{i\pi/n}. \tag{VI.3.26}$$

Here $b^2 = -\mathbb{1} = a^n$ is the nontrivial element of the kernel of $SU(2) \to SO(3)$, the signature of the double cover. Its irreducible representations are four one-dimensional and $n-1$ two-dimensional, and the Burnside sum checks the count,

$$4 \cdot 1^2 + (n-1) \cdot 2^2 \;=\; 4n \;=\; |2D_n|. \tag{VI.3.27}$$

The four one-dimensional representations factor through the abelianization: a maps to ± 1 (forced by $bab^{-1} = a^{-1}$, so a and a^{-1} have the same image) and b to a square root of a^n's image. The $n-1$ two-dimensional representations ρ_h, $h = 1, \ldots, n-1$, are

$$\begin{aligned} \rho_h(a) &= \left(\begin{smallmatrix} \zeta^h & 0 \\ 0 & \zeta^{-h} \end{smallmatrix}\right), \qquad \rho_h(b) = \left(\begin{smallmatrix} 0 & 1 \\ (-1)^h & 0 \end{smallmatrix}\right), \\ \chi_{\rho_h}(a^k) &= 2\cos\frac{\pi h k}{n}, \qquad \chi_{\rho_h}(b\,a^k) = 0, \end{aligned} \tag{VI.3.28}$$

and the defining representation is $Q = \rho_1$, with $\chi_Q(a^k) = 2\cos(\pi k/n)$, real as promised.

The McKay quiver follows by tensoring with $Q = \rho_1$. The chain arises from the elementary product

$$2\cos\theta\, 2\cos(h\theta) = 2\cos((h-1)\theta) + 2\cos((h+1)\theta), \qquad \theta = \pi k/n.$$

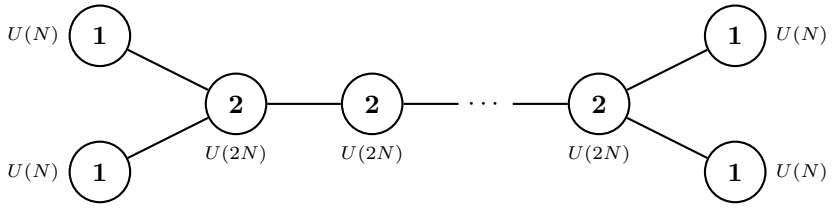


Figure VI.3.2: The affine $\hat{D}_{n+2}$ quiver of $2D_n$, drawn for the generic $n \geq 3$ case. A chain of $n-1$ mark-two nodes $U(2N)$, the two-dimensional representations, is capped at each end by a fork of two mark-one nodes $U(N)$, the four one-dimensional representations. Each edge is one $\mathcal{N}=2$ hypermultiplet; each node also carries an adjoint Φ_i (suppressed). Ranks shown are those of N regular branes, $N_i = N \dim R_i$. For $n=2$ the chain has only one mark-two node and the two forks meet: this degenerate smallest case is the $\hat{D}_4$ star of Figure VI.3.1.

This is the character identity on a^k; both sides vanish on ba^k for the interior representations. Thus the neighboring labels $h-1$ and $h+1$ are fixed by tensoring, rather than inferred from a drawing. On a one-dimensional representation ϵ, $Q \otimes \epsilon$ is again two dimensional and equals one of the ρ_h, so each of the four one-dimensional nodes attaches by a single edge to a two-dimensional node. On the two-dimensional representations the interior is a chain,

$$Q \otimes \rho_h \;=\; \rho_{h-1} \oplus \rho_{h+1}, \qquad 2 \leq h \leq n-2, \tag{VI.3.29}$$

while at the two ends the formal symbols ρ_0 and ρ_n are replaced by pairs of one-dimensional representations. For $n \geq 3$ this gives

$$Q \otimes \rho_1 = \rho_2 \oplus \chi_+ \oplus \chi_-, \qquad Q \otimes \rho_{n-1} = \rho_{n-2} \oplus \chi'_+ \oplus \chi'_-, \tag{VI.3.30}$$

the four χ's being the four one-dimensional representations, so the chain grows a two-pronged fork at each end. The result is the affine $\hat{D}_{n+2}$ diagram: a chain of $n-1$ two-dimensional nodes, each of mark 2, capped at both ends by a fork of two one-dimensional nodes, each of mark 1, four such mark-one "horns" in all. The marks are the dimensions $(1,1,\ldots,2,2,\ldots,1,1)$, their null-vector property $\hat{C}\,\delta = 0$ the statement that every node, the forks included, sees twice its own mark among its neighbours.

The smallest case, $n=2$, is the quaternion group $Q_8 = 2D_2$, worked in §VI.3.3 as the chapter's first example: its McKay quiver came out the four-pointed star $\hat{D}_4$ (Figure VI.3.1), the degenerate end of this family with the chain shrunk to a single mark-two node and the two forks meeting. The next case, $2D_3$ of order 12, has the two two-dimensional representations ρ_1, ρ_2 forming a two-node chain with a fork at each end, the affine $\hat{D}_5$ diagram.

VI.3.7 The E series: $2T \to \hat{E}_6$

The exceptional series is reached by the binary tetrahedral group $2T$, of order 24, the double cover of the tetrahedral rotation group A_4. It is generated by the quaternion

subgroup Q_8 together with an order-three element, the quaternion $\omega = \frac{1}{2}(-1 + i\sigma_1 + i\sigma_2 + i\sigma_3)$ that cyclically permutes $i\sigma_1 \to i\sigma_2 \to i\sigma_3$ (we reserve ω for this quaternion and write $\eta = e^{2\pi i/3}$ for the cube root of unity below); equivalently $2T \cong SL(2,3)$. The element $-\mathbb{1}$ again generates the kernel of the double cover, with quotient $2T/\{\pm\mathbb{1}\} \cong A_4$. The group has seven conjugacy classes and so seven irreducible representations, of dimensions

$$\{1,1,1,2,2,2,3\}, \qquad 1^2+1^2+1^2+2^2+2^2+2^2+3^2 \;=\; 24 \;=\; |2T|, \tag{VI.3.31}$$

the Burnside sum again checking the list. The three one-dimensional representations factor through the abelianization $2T \to 2T/Q_8 \cong \mathbb{Z}_3$, taking values $1, \eta, \eta^2$ on the three cosets of Q_8, with $\eta = e^{2\pi i/3}$. The defining representation Q is the two-dimensional $\mathbf{2}$, with $\chi_Q(g) = \operatorname{tr} g$ taking the values $2, -2, 0, -1, 1$ on the elements of order $1, 2, 4, 3, 6$.

The remaining representations are built from Q and the one-dimensional representations, and this is the cleanest way to see the McKay quiver assemble. The two other two-dimensional representations are Q twisted by the nontrivial one-dimensional characters,

$$\mathbf{2}' = Q \otimes \mathbf{1}', \qquad \mathbf{2}'' = Q \otimes \mathbf{1}'', \tag{VI.3.32}$$

and the three-dimensional representation is the symmetric square of Q, the spin-one representation $\mathbf{3} = \operatorname{Sym}^2 Q$, the pullback of the standard three-dimensional representation of A_4, with character

$$\chi_{\mathbf{3}}(g) \;=\; \tfrac{1}{2}\big(\chi_Q(g)^2 + \chi_Q(g^2)\big) \;=\; (3,3,-1,0,0) \tag{VI.3.33}$$

on the orders $1, 2, 4, 3, 6$. Collecting the one-, two-, and three-dimensional characters over the seven conjugacy classes gives the character table, with $\eta = e^{2\pi i/3}$,

	$\{\mathbb{1}\}$	$\{-\mathbb{1}\}$	$6C_4$	$4C_3$	$4C_3'$	$4C_6$	$4C_6'$
$\mathbf{1}$	1	1	1	1	1	1	1
$\mathbf{1}'$	1	1	1	η	η^2	η	η^2
$\mathbf{1}''$	1	1	1	η^2	η	η^2	η
$\mathbf{2} = Q$	2	-2	0	-1	-1	1	1
$\mathbf{2}'$	2	-2	0	$-\eta$	$-\eta^2$	η	η^2
$\mathbf{2}''$	2	-2	0	$-\eta^2$	$-\eta$	η^2	η
$\mathbf{3}$	3	3	-1	0	0	0	0

(VI.3.34)

the three two-dimensional rows being Q and its two one-dimensional twists, the three-dimensional row the symmetric square. Tensoring with Q now reads off the edges directly, again by character inner products. As a sample, the multiplicity of $\mathbf{3}$ inside $Q \otimes \mathbf{2}$ is

$$[\,Q \otimes \mathbf{2} : \mathbf{3}\,] = \frac{1}{24}\sum_{[g]} |[g]|\,\chi_Q\,\chi_{\mathbf{2}}\,\chi_{\mathbf{3}}^* = \frac{1}{24}\big(1\cdot 2\cdot 2\cdot 3 + 1\cdot(-2)(-2)\cdot 3\big) = 1, \tag{VI.3.35}$$

the order-4 class dropping out because $\chi_Q = 0$, and the order-3 and order-6 classes because $\chi_{\mathbf{3}} = 0$; likewise $[\,Q \otimes \mathbf{2} : \mathbf{1}\,] = 1$ and the rest vanish. Carried out on every row, the decompositions are each one-dimensional representation tensoring Q into one two-dimensional representation; each two-dimensional representation into

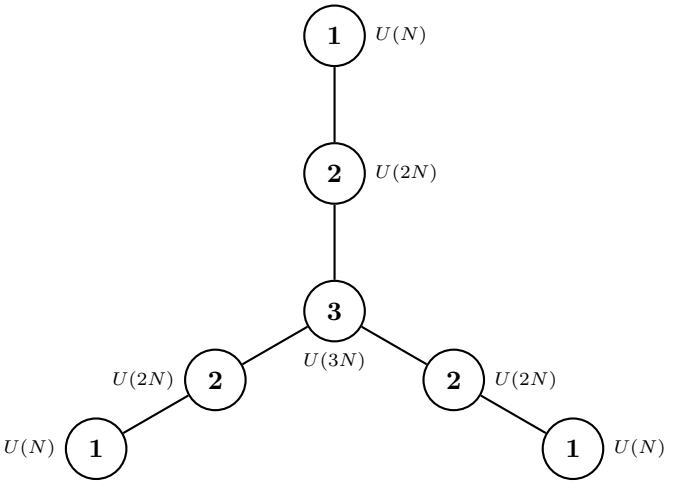


Figure VI.3.3: The affine $\hat{E}_6$ quiver of $2T$. The trivalent centre $U(3N)$ is the three-dimensional representation; three arms of length two run out through the two-dimensional nodes $U(2N)$ to the one-dimensional nodes $U(N)$. Each edge is one $\mathcal{N}=2$ hypermultiplet (adjoint self-loops suppressed). The marks $(1,1,1,2,2,2,3)$ are the representation dimensions.

its one-dimensional partner plus the three-dimensional representation; and the three-dimensional representation into all three two-dimensional representations,

$$Q\otimes\mathbf{1}^{(s)}=\mathbf{2}^{(s)},\qquad Q\otimes\mathbf{2}^{(s)}=\mathbf{1}^{(s)}\oplus\mathbf{3},\qquad Q\otimes\mathbf{3}=\mathbf{2}\oplus\mathbf{2}'\oplus\mathbf{2}'',\tag{VI.3.36}$$

with $s=0,1,2$ labelling the trivial and the two nontrivial one-dimensional representations. These decompositions are the McKay quiver: a central three-dimensional node joined to the three two-dimensional nodes, each of which is joined on to its one-dimensional node, three arms of length two emanating from a trivalent centre. This is the affine $\hat{E}_6$ diagram. Its marks, the dimensions, are

$$(1,1,1,2,2,2,3),\qquad \text{centre mark } 3,\ \text{three arms } 2,1,\tag{VI.3.37}$$

and the regular-brane gauge theory is

$$U(3N)\times U(2N)^3\times U(N)^3,\qquad \text{ranks } (3N;\,2N,2N,2N;\,N,N,N),\tag{VI.3.38}$$

a central $U(3N)$ joined by one $\mathcal{N}=2$ hypermultiplet to each of three $U(2N)$ arm nodes, each of those joined on to a $U(N)$ tip, every node carrying its adjoint Φ_i. The central $U(3N)$'s neighbours are the three $U(2N)$'s, $\sum 2N=6N=2\cdot 3N$, twice its rank, the marginal balance again.

The remaining two exceptional groups complete the E column the same way and we only name them. The binary octahedral group $2O$ of order 48, with irreducible dimensions $\{1,1,2,2,2,3,3,4\}$ summing in squares to 48, gives the affine $\hat{E}_7$ diagram; the binary icosahedral group $2I$ of order 120, with dimensions $\{1,2,2,3,3,4,4,5,6\}$,

gives $\hat{E}_8$. Their character tables and quivers are collected in Chapter 11; with $\hat{E}_6$ in hand the pattern, a trivalent ADE diagram with marks the representation dimensions, is already clear.

*VI.3.8 The worldsheet origin: open-string sectors and boundary states

(Optional.) This section may be skipped on a first reading. It re-derives the matter content from the open string, where two facts the rep-theory account took as given become visible: why the count is the McKay multiplicity (VI.3.9), and why the undirected edge is a hypermultiplet. The open-string-sector and boundary-state machinery itself is the one set up for the abelian case in the previous chapter; what is new here is the non-abelian refinement, where the multiplicity is a true representation-theoretic number and the twisted sectors are labelled by conjugacy classes.

The open strings on the projected brane carry two Chan–Paton labels, in K and $\bar{K}$, and a transverse oscillator. The massless states before projection sit in $K \otimes \bar{K}$ for the gauge field, with no geometric phase, and in $K \otimes \bar{K} \otimes Q$ for the transverse scalars, which carry the Q-phase of (z_1, z_2). The orbifold keeps the states fixed by the group averaging that acts geometrically and on both Chan–Paton labels at once,

$$P \;=\; \frac{1}{|\Gamma|}\sum_{g\in\Gamma} \mathcal{R}(g)\otimes\gamma(g)\,(\,\cdot\,)\,\gamma(g)^{-1}, \qquad \mathcal{R}(g)=\begin{cases}\mathbb{1}, & \text{gauge field},\\ Q(g), & \text{active scalars},\end{cases} \tag{VI.3.39}$$

with $\mathcal{R}(g)$ the geometric action on the transverse index. The surviving states are the image of P; with $K = \bigoplus_i N_i R_i$ they are

$$\big(K\otimes\bar{K}\big)^{\Gamma} = \bigoplus_i \mathrm{End}(\mathbb{C}^{N_i}), \qquad \big(K\otimes\bar{K}\otimes Q\big)^{\Gamma} = \bigoplus_{i,j} a_{ij}\ \mathrm{Hom}(\mathbb{C}^{N_i},\mathbb{C}^{N_j}), \tag{VI.3.40}$$

The $\mathrm{Hom}(\mathbb{C}^{N_i},\mathbb{C}^{N_j})$ factors here use mathematical map directions $i \to j$: their matrices have size $N_j \times N_i$ and correspond to the drawn chiral arrows $j \to i$. Since $a_{ij} = a_{ji}$, transposing both labels gives the same ADE spectrum. The first invariant space gives the gauge group $\prod_i U(N_i)$, the second the bifundamentals with multiplicity $a_{ij} = [\,Q \otimes R_i : R_j\,]$, exactly (VI.3.9). For the abelian groups of the last chapter this counting was a shift of phases; for a non-abelian Γ it is the genuine intertwiner count, and (VI.3.40) is its worldsheet statement. The spectator z_3 carries no phase, so its invariants are the $i = j$ blocks, the adjoints Φ_i.

The multiplet structure comes from the same projection acting on the worldsheet fermions, while the global supercharge count is set by the geometric action alone, not by γ: the supercharges carry no Chan–Paton labels, and the orbifold keeps the spinor components invariant under Γ acting geometrically. The transverse $SO(6)$ rotation group splits into the four active and the two spectator directions, and $\Gamma \subset SU(2)$ sits in just one factor of the active $SO(4)$,

$$\mathfrak{so}(6) \supset \mathfrak{so}(4)\oplus\mathfrak{so}(2) \cong \mathfrak{su}(2)_L \oplus \mathfrak{su}(2)_R \oplus \mathfrak{u}(1)_r, \quad \Gamma\subset SU(2)_L, \quad 16 \to 8, \tag{VI.3.41}$$

where the equality is at the level of Lie algebras; the spinor action uses the spin cover. The chiral spinor of Spin(6) splits as $(\mathbf{2},\mathbf{1})\oplus(\mathbf{1},\mathbf{2})$ under the two $SU(2)$ factors, with opposite spectator charges. A nontrivial finite subgroup acting in the first factor leaves the second doublet invariant. Thus eight of the sixteen D3 supercharges survive, the $\mathcal{N}=2$ count, and the surviving R-symmetry is

$$SU(2)_R \times U(1)_r, \tag{VI.3.42}$$

the untouched $SU(2)_R$ of the active $SO(4)$ together with the $U(1)_r$ that rotates the spectator complex line $\mathbb{C}_{z_3}$; $SU(2)_R$ organizes the hypermultiplet scalars, $U(1)_r$ the spectator scalar in the vector multiplet. The antisymmetric invariant of the pseudoreal Q is the singlet in $Q\otimes Q$,

$$\varepsilon_{\alpha\beta} \in \big(Q\otimes Q\big)^{\Gamma}, \qquad \big(X_{ij},\, X^{\dagger}_{ji}\big) \;\longmapsto\; SU(2)_R \text{ doublet}, \tag{VI.3.43}$$

and it is what pairs the two opposite bifundamentals; the two $\mathcal{N}=1$ chiral halves X_{ij} and X_{ji} furnish one hypermultiplet, their scalars arranged (with one conjugated, $X^{\dagger}_{ji}$, so both sit in the same bifundamental) into an $SU(2)_R$ doublet, while the gauge field, the gaugino, and the spectator adjoint Φ_i make the $\mathcal{N}=2$ vector. So the two inputs are the eight surviving supercharges, which set $\mathcal{N}=2$, and the pseudoreal pairing ε, which makes the matter non-chiral, both read on the Ramond sector. In the chiral $\mathbb{C}^3/\Gamma$ orbifolds of Chapter 6 the active representation is instead the three-dimensional defining representation of $SU(3)$, generically complex, the edges then directed and the count $\mathcal{N}=1$.

The branes themselves are boundary states, and here the non-abelian structure is sharpest. A fractional brane stuck at the fixed point is the boundary state associated with a single irreducible representation R_i. Schematically it decomposes over the closed-string conjugacy-class sectors as

$$|B_i\rangle \;=\; \sum_{[g]} c_{[g]}\,\chi_i([g])^*\;|B;[g]\rangle\!\rangle, \tag{VI.3.44}$$

a sum over conjugacy classes $[g]$ of Γ rather than over group elements, with $c_{[g]}$ a sector-dependent normalization. The exact normalization is convention-dependent (closed-sector conventions, the incoming-versus-outgoing boundary-state choice that fixes the conjugation); nothing below uses it. What matters is the character dependence: the twisted charges are read from the character table. For an abelian group every element is its own class and this is the last chapter's phase sum. The regular brane is the combination $\sum_i(\dim R_i)\,|B_i\rangle$, and by the column orthogonality of the character table its weighted charge vanishes in every twisted ($[g]\neq[\mathbb{1}]$) sector,

$$\sum_i (\dim R_i)\,\chi_i([g]) \;=\; |\Gamma|\,\delta_{[g],[\mathbb{1}]}, \tag{VI.3.45}$$

so the regular brane carries only untwisted (bulk) charge and is free to move off the fixed point. A fractional brane $|B_i\rangle$, by contrast, has a nonzero twisted-charge *vector* and is pinned; individual components may still vanish on some conjugacy classes, since a

non-abelian character can, and what distinguishes the regular brane is that the weighted sum (VI.3.45) vanishes on every nontrivial class at once. This is the boundary-state reading of which brane has a geometric branch. Finally, the cylinder stretched between two fractional branes is computed two ways, as a closed string propagating between the boundary states and as an open-string trace, the two related by the modular transform $\ell \to 1/\ell$ of the cylinder modulus,

$$Z^{ij}_{\rm cyl} \;=\; \langle B_i|\, e^{-\ell H_{\rm cl}}\, |B_j\rangle \;=\; {\rm Tr}_{\mathcal{H}_{ij}}\; e^{-(1/\ell)H_{\rm op}}, \tag{VI.3.46}$$

the Cardy consistency condition. Reading off the massless open-string content on the right, graded by the transverse Q-rotation, reproduces the matter count: the McKay multiplicity is the closed-string overlap of the two boundary states, graded by Q,

$$a_{ij} \;=\; \frac{1}{|\Gamma|}\sum_g \chi_Q(g)\,\chi_i(g)\,\chi_j(g)^* \;\sim\; \langle B_i|\,\big(\textstyle\sum_g \chi_Q(g)\,g\big)\,|B_j\rangle, \tag{VI.3.47}$$

the right-hand side schematic for the class-graded boundary-state insertion. This is the open-closed channel duality: the bifundamental between i and j, an open-string state, is counted by the boundary-state overlap graded by the closed twisted sectors, the precise sense in which the matter is organized by, rather than literally sourced from, the twisted sectors.

VI.3.9 The Higgs branch is the ALE space

The hypermultiplets describe motion away from the singular line, while the adjoint scalars describe motion along it. Their vacuum equations must therefore recover two different factors of the transverse geometry. The D3 transverse space is a product, the active orbifold surface times the spectator line,

$$\big(\mathbb{C}^2/\Gamma\big)\times\mathbb{C}_{z_3}, \tag{VI.3.48}$$

and the two factors are reconstructed by different fields. The active $\mathbb{C}^2/\Gamma$ is reconstructed by the *hypermultiplets*, the Higgs branch; the spectator $\mathbb{C}_{z_3}$ is carried by the vector-multiplet adjoints Φ_i, whose common value on the regular brane is the position along z_3, forced equal by the hypermultiplet F-terms (VI.3.20) once the bifundamentals switch on. The full geometric branch is therefore *mixed*,

$$\mathcal{M}_{\rm geom} \;=\; \mathcal{M}_{\rm Higgs}\big(\mathbb{C}^2/\Gamma\big)\times\mathbb{C}_{z_3}, \tag{VI.3.49}$$

and "the Higgs branch" below means the active $\mathbb{C}^2/\Gamma$ factor; the adjoints Φ_i, being vector-multiplet scalars and not hypermultiplets, do not enter the hyperkähler quotient that reconstructs it.

Which branch reconstructs which part of $(\mathbb{C}^2/\Gamma)\times\mathbb{C}_{z_3}$.

Hypermultiplets on the ADE edges reconstruct the active surface $\mathbb{C}^2/\Gamma$ as the hyperkähler Higgs branch (the ALE space at generic FI). *Vector-multiplet adjoints* Φ_i supply the spectator $\mathbb{C}_{z_3}$ direction through their common value, and do not enter the Higgs quotient. The *full geometric branch* of one regular brane is the mixed product Higgs(ALE) $\times\,\mathbb{C}_{z_3}$; of N regular branes, its symmetric-product version.

With eight supercharges the Higgs branch is a hyperkähler quotient, possibly singular. At zero FI level it is cut out by the vanishing of the moment maps μ_i of (VI.3.18) and divided by the gauge group with its trivially-acting overall diagonal $U(1)$ removed,

$$\mathcal{M}_{\text{Higgs}}(\zeta) \;=\; \big\{\, \vec{\mu}_i = \vec{\zeta}_i\, \mathbb{1}_{N_i} \,\big\} \,/\, G, \qquad G = \Big(\textstyle\prod_i U(N_i)\Big)/U(1)_{\text{diag}}, \tag{VI.3.50}$$

the adjoint-valued moment maps set equal to the central, $\mathcal{N} = 2$-triplet Fayet–Iliopoulos levels $\vec{\zeta}_i$ times the identity (a complex and a real moment map once a complex structure is chosen, $\mu_i^{\mathbb{C}} = \zeta_i^{\mathbb{C}}\mathbb{1}$, $\mu_i^{\mathbb{R}} = \zeta_i^{\mathbb{R}}\mathbb{1}$). The diagonal $U(1)$ acts trivially, so its moment map vanishes identically; taking the trace of the level equations, $\sum_i \operatorname{Tr}\mu_i = 0$ forces the constraint

$$\sum_i N_i\, \vec{\zeta}_i \;=\; 0, \tag{VI.3.51}$$

leaving r independent FI triplets, one for each compact exceptional curve of the finite ADE resolution.

The dimension count is the cleanest check, and we do it for *one* regular brane, $N_i = \delta_i = \dim R_i$. At a generic point of this branch the only unbroken gauge symmetry is the trivially-acting diagonal $U(1)$, so the hyperkähler quotient subtracts $\sum_i \delta_i^2 - 1$, while the hypermultiplets on the edges contribute $\sum_{\text{edges}} \delta_i\delta_j$ quaternionic dimensions,

$$\dim_{\mathbb{H}} \mathcal{M}_{\text{Higgs}} \;=\; \sum_{\text{edges}} \delta_i\delta_j \;-\; \Big(\sum_i \delta_i^2 - 1\Big). \tag{VI.3.52}$$

The edge sum is fixed by the null-vector identity $\sum_j a_{ij}\delta_j = 2\delta_i$ from (VI.3.23),

$$\sum_{\text{edges}} \delta_i\delta_j \;=\; \tfrac{1}{2}\sum_{i,j} a_{ij}\,\delta_i\delta_j \;=\; \tfrac{1}{2}\sum_i \delta_i(2\delta_i) \;=\; \sum_i \delta_i^2, \tag{VI.3.53}$$

so the two large sums in (VI.3.52) cancel and

$$\dim_{\mathbb{H}} \mathcal{M}_{\text{Higgs}} \;=\; \sum_i \delta_i^2 - \Big(\sum_i \delta_i^2 - 1\Big) \;=\; 1, \tag{VI.3.54}$$

quaternionic dimension one, real dimension four, for every ADE type. One regular brane sees a single copy of the active surface $\mathbb{C}^2/\Gamma$: the probe has reconstructed it. The same null-vector identity that makes the diagram affine makes the Higgs branch four dimensional.

The count is for one brane, and the restriction matters. For N regular branes, $N_i = N\delta_i$, the geometric branch is the symmetric product, $\operatorname{Sym}^N(\mathbb{C}^2/\Gamma)$ at $\zeta = 0$ and $\operatorname{Sym}^N(X_\zeta)$ at generic FI, of quaternionic dimension N; the naive -1 above would wrongly give 1, because at a generic separated configuration the unbroken symmetry is the larger $U(1)^N$, one per brane, not the single diagonal $U(1)$. The single-brane count is the probe's reading of the local transverse geometry; the N-brane symmetric-product structure, with the α' and g_s caveats on the moduli-space metric, is the reconstruction refinement inherited from Chapter 1.

To distinguish resolution from complex deformation, fix a complex structure and restrict here to $\zeta^{\mathbb{C}} = 0$, writing ζ for the real FI levels obeying (VI.3.51). A generic level avoids the root walls. Writing X_ζ for the resolved space,

$$\begin{aligned} \zeta = 0: &\quad \mathcal{M}_{\text{Higgs}} = \mathbb{C}^2/\Gamma \ \text{ (singular)}, \\ \zeta \text{ generic}: &\quad \mathcal{M}_{\text{Higgs}} = X_\zeta \ \text{ (the ALE resolution)}. \end{aligned} \tag{VI.3.55}$$

At vanishing Fayet–Iliopoulos parameter the moment-map equations cut out the singular orbifold $\mathbb{C}^2/\Gamma$ itself; turning on generic ζ resolves the singularity into the smooth ALE space X_ζ, while non-generic values on the walls of the parameter space leave partial resolutions. Kronheimer's theorem makes the generic statement exact: the hyperkähler quotient of the affine ADE quiver, as the FI triplet varies, gives the ALE hyperkähler four-manifolds with asymptotic group Γ, including the minimal resolution of $\mathbb{C}^2/\Gamma$ at generic real stability parameter and zero complex level. Nonzero complex FI levels instead change the complex surface within the ALE family. We have identified the Higgs branch using this theorem and checked its dimension; the hyperkähler-quotient construction, the resolution geometry, the chamber structure, and Kronheimer's theorem are the dedicated content of Chapter 4.

It bears emphasis that this is the *Higgs* branch, not a Coulomb branch. In the flat-space $\mathcal{N} = 4$ chapter the transverse geometry was the Coulomb branch, the maximal-supersymmetry case where the position scalars sit in the vector multiplet. Here the position along the active $\mathbb{C}^2/\Gamma$ is set by the hypermultiplet bifundamentals, so the surface is the hyperkähler Higgs branch; the flat-space "Coulomb" name does not carry over, and the one vector-multiplet direction that does survive is the spectator $\mathbb{C}_{z_3}$ of the mixed branch above. The same regular-rank quivers are, at their conformal point, four-dimensional $\mathcal{N} = 2$ superconformal theories, the orbifold daughters of $\mathcal{N} = 4$: the one-loop beta function at node i, an $\mathcal{N} = 2$ vector against its bifundamental hypers, is

$$b_i \ \propto \ 2N_i - \sum_j a_{ij} N_j \ = \ 0 \qquad \text{at} \qquad N_i = N\delta_i, \tag{VI.3.56}$$

vanishing at the regular ranks by the same null-vector identity $\sum_j a_{ij}\delta_j = 2\delta_i$ that gave the dimension. The marginality of every non-abelian node is the McKay relation once more. This coefficient applies to the nontrivial $SU(N_i)$ factors, in the normalization $T(\mathbf{N_i}) = 1/2$. A full bifundamental hyper contributes N_j fundamental flavors at node i. The diagonal $U(1)$ acts trivially on all hypers, but removing it still leaves relative $U(1)$ factors. Those abelian couplings are not certified conformal by (VI.3.56); the conformal statement concerns the non-abelian quiver theory with the same matter. Their superconformal dynamics, the conformal manifold and the exactly-marginal couplings, belong to Part III.

VI.3.10 What the construction does and does not give

The construction delivers the $\mathcal{N} = 2$ quiver gauge theory at the $\mathbb{C}^2/\Gamma$ orbifold point, with its gauge group, its ADE matter content, its superpotential, and the identification

of the regular-brane Higgs branch as the ALE space. The character calculation fixes the spectrum; identifying its vacuum geometry uses additional results about hyperkähler quotients.

The Higgs branch was *named*, not constructed. That it is the resolved $\mathbb{C}^2/\Gamma$ rests here on the dimension count, a consistency check, and on Kronheimer's theorem cited, not derived; the hyperkähler quotient, the exceptional cycles, the Fayet–Iliopoulos resolution, and the explicit metric are the next chapter. Two metric statements should be kept apart. The hyperkähler metric of the field-theory Higgs branch is itself a protected $\mathcal{N} = 2$ quantity, fixed by the quiver data and computed exactly by the quotient of Chapter 4; this is not where the corrections live. The caveat is the probe identification of that branch with the geometry the closed strings see: as at every orbifold point the probe extracts the holomorphic data, the complex structure and chiral ring, while the match of the full metric to the target geometry is the leading classical statement, corrected at finite α' and g_s.

The McKay correspondence we used is its representation-theory half. The McKay quiver was computed from the character table of Γ, pure representation theory, and the matched affine Dynkin diagram read off. The correspondence has a geometric half as well, the statement that the same ADE diagram is the dual graph of the exceptional curves in the resolution of $\mathbb{C}^2/\Gamma$, and this we cite rather than prove; it belongs to the mathematics of ADE singularities in Part I. The two graphs coincide as the ADE type but are computed on opposite sides and are not literally the same object: the McKay quiver, with a node for every irreducible representation including the trivial one, is the *affine* diagram, with one more node than the rank; the exceptional-curve intersection graph of the minimal resolution, with a node for every compact curve, is the *finite* diagram, the trivial representation corresponding to the affine node that has no exceptional curve. The McKay quiver is the intersection graph plus that affine node. Conflating the representation-theory input with the resolution-geometry output inverts the logic of the whole construction, in which the characters of Γ build the quiver and the geometry is the output.

Two further limits are named here and worked elsewhere. The exceptional groups $2O$ and $2I$, giving $\hat{E}_7$ and $\hat{E}_8$, were stated and not worked; their tables are collected in Chapter 11. And the whole family treated here is the non-abelian $\mathbb{C}^2/\Gamma$, eight supercharges; the $\mathbb{C}^3/\Gamma$ orbifolds with $\Gamma \subset SU(3)$, four supercharges, their directed quivers and cubic superpotentials, abelian $\mathbb{Z}_m \times \mathbb{Z}_n$ and non-abelian alike, are Chapter 6.

Status and sources

The evidence-code tags ([WS] worldsheet), the convention pointers, and the source anchors are collected here, keyed by section. The construction is the perturbative orbifold projection of Douglas and Moore (1996) with the correspondence of McKay (1980); it reuses the projection machine, the inherited spectrum, and the decoupling limit of Chapters 1–2 and applies them to a non-abelian $\Gamma \subset SU(2)$. The finite group calculations apply under the stated physical projection. Conventions used: the orbifold action and the $\mathbb{C}^2$-in-$\mathbb{C}^3$ spectator; the McKay multiplicity and the affine-node labelling (McKay multiplicities, here at its load-bearing non-abelian first use, the affine ADE diagrams); the gauge/rank data $\prod_i U(N_i)$, $N_i = N \dim R_i$; the superpotential inheritance (superpotential normalization, with the mathematical-map translation stated before the moment maps); the FI resolution slice; the supercharge count $\Gamma \subset SU(2) \to 8$; the quiver-arrow and math-convention bridge. The McKay adjacencies, the

character tables of Q_8 and $2T$, the affine-Cartan match, and the null-vector and Higgs-dimension identities follow from the finite character and representation calculations.

§VI.3.1 From the abelian warm-up to the McKay correspondence. Framing, the two-axis map (abelian/non-abelian × $\mathbb{C}^2/\mathbb{C}^3$), and the recipe box. The abelian column and the general projection are VI.2; the $\mathbb{C}^3/\Gamma$ row (abelian $\mathbb{Z}_m \times \mathbb{Z}_n$ and non-abelian alike) is VI.6, the toric abelian cases recurring as brane tilings in Vol. VI.

§VI.3.2 The setup, inherited. The action (VI.3.1), spectator and supercharge count use orbifold action and spinor and supersymmetry counting, inherited from VI.2. the finite calculation pins the supercharge label; it does not derive the invariant spinors. The finite-subgroup classification and double cover are mathematical inputs [MATH], cited via the finite-group and geometric McKay correspondence, not proved by the spectrum calculation. The isotypic decomposition and commutant (VI.3.6)–(VI.3.7) follow from Schur's lemma for ordinary finite-group representations over $\mathbb{C}$ [MATH]. Their identification with open-string gauge fields is the projection claim [WS]. Douglas–Moore develops the cyclic case (Douglas and Moore 1996, §4.2); the non-abelian character projection is supported directly by Billo et al. 2001, §4.3, Eqs. (4.25)–(4.26). That source conjugates the first endpoint character; transposing its endpoint labels gives our second-slot conjugation convention. Self-duality of Q makes the ADE adjacency symmetric, so this translation leaves the spectrum unchanged.

§VI.3.3 The McKay quiver and its smallest case. The character inner product (VI.3.10), the Q_8 table and tensor products (VI.3.11)–(VI.3.13), and the $\hat{D}_4$ graph are finite-group calculations [MATH], derived here from the explicit representations. McKay's general identification is a cited theorem ((McKay 1980)); a finite example is not its proof. The use of these multiplicities as the open-string matter spectrum, and of the multiplicity spaces as gauge ranks in (VI.3.14), is Q1/The physical atom [WS] (Billo et al. 2001, §4.3.1, Eqs. (4.59)–(4.62)). For Q_8 the adjacency and regular character are finite representation calculations. The brane interpretation is the physical premise cited above.

§VI.3.4 The McKay correspondence in general. The invariant epsilon form and symmetric adjacency are representation theory [MATH], with finite examples in the finite calculation. The assembly into $\mathcal{N} = 2$ vectors and full hypers is The physical spectrum statement [WS], explained in §VI.3.8. McKay's relation (VI.3.17) is [MATH] for nontrivial finite subgroups of $SU(2)$, cited rather than proved ((McKay 1980)). The cyclic construction in Douglas and Moore 1996, §4.2 is extended here using the non-abelian character projection, not a non-abelian worked example in that section. The two affine/finite graphs are distinguished by the stated distinction. Inheritance of (VI.3.18) from the parent cubic is an inherited physical premise under superpotential normalization, with exact primary support unresolved here; its trace differentiation in (VI.3.19) and (VI.3.20) is a displayed polynomial calculation [MATH], conditional on that cubic and the stated matrix-map convention. Trace differentiation in this map direction transposes the entrywise adjoint gradient. The common-adjoint value on a simple regular component uses Schur's lemma; interpreting it as the spectator position uses the inherited D3 scalar/position dictionary. An exact primary passage for that interpretation has not been verified here; the projection sources above provide context, not its derivation.

§VI.3.5 The classification and the regular brane. The finite-group/ADE classification, regular-character identity, $\sum_i d_i^2 = |\Gamma|$, and the dimension-vector relation $\hat{C}\delta = 0$ in (VI.3.21)–(VI.3.24) are mathematical atoms of [MATH]. The general classification is cited ((McKay 1980)); the null relation is derived here by taking dimensions of $Q \otimes R_i$. the finite calculation and the symbolic calculation test the worked groups only. Choosing the regular representation as the Chan–Paton representation of a mobile bulk brane and reading its multiplicities as gauge ranks is The separate physical atom [WS] (quiver gauge groups and ranks; Billo et al. 2001, §4.3, pp. 19–20). The primitive positive null vector is normalized at the trivial representation; the finite-versus-affine distinction is the stated distinction.

§VI.3.6 The D series. The presentation and matrices (VI.3.25)–(VI.3.26), irreducible characters (VI.3.28), Burnside sum and chain/fork products (VI.3.29)–(VI.3.30) are The mathematical atoms [MATH], calculated here for $n \geq 2$ with the endpoint formula restricted to $n \geq 3$. The explicit character products give Figure VI.3.2; the $n = 2, 3$ instances are checked by the finite calculation and the symbolic calculation. The general McKay classification remains cited (McKay 1980), rather than proved by those two instances. The identification of this graph with the D-brane spectrum is the physical atom [WS] supported by the non-abelian projection (Billo et al. 2001, §4.3.1), not a binary-dihedral calculation in Douglas–Moore's cyclic section.

§VI.3.7 The E series. The explicit binary-tetrahedral group, character construction, (VI.3.31)–(VI.3.36), and the $\hat{E}_6$ marks and graph are The mathematical atoms [MATH], derived here from Q_8, its order-three extension and character orthogonality. the finite calculation and the symbolic calculation reconstruct the seven characters and adjacency. The regular-rank gauge theory (VI.3.38) uses the physical Chan–Paton dictionary [WS] (Billo et al. 2001, §4.3.1; McKay multiplicities, quiver gauge groups and ranks). The classification of $2O, 2I$ as $\hat{E}_7, \hat{E}_8$ is cited [MATH], not worked here; its character tables are deferred to VI.11. These mathematical calculations are not attributed to Douglas–Moore's $\mathbb{Z}_n$ examples.

§VI.3.8 The worldsheet origin. Optional capstone. The open-string projection (VI.3.40) of $K \otimes \bar{K} \otimes Q$ giving the bifundamentals with the McKay multiplicity, the Ramond-sector pseudoreal-Q pairing into the $\mathcal{N} = 2$ hyper with the full $\mathcal{N} = 2$ R-symmetry $SU(2)_R \times U(1)_r$ (VI.3.42) (the $U(1)_r$ rotating the spectator line), the *schematic* boundary state (VI.3.44) expanded over conjugacy classes (sector-dependent normalization, character-weighted), the regular brane's vanishing twisted charge (VI.3.45) (mobile) against the fractional brane's nonzero twisted-charge *vector* (pinned; individual components may vanish for non-abelian χ_i), and the open-closed duality (VI.3.47) are the non-abelian refinement of the worldsheet-origin of VI.2 [WS] (Douglas and Moore 1996, §2; fractional branes as twisted boundary states, Diaconescu and Gomis 2000; open-closed/Cardy duality, Billo et al. 2001, §4.3, Eqs. (4.40)–(4.44); the distinction between open-string projection and closed twisted sectors is essential; the character multiplicities are checked by the symbolic calculation; this file does not check boundary-state normalization, the cylinder amplitude, or the regular-character identity). The underlying GSO, boundary-state, and orbifold-CFT machinery is not re-derived (orbifold CFT and boundary states, home Vol. II ch. 6 / Vol. III).

§VI.3.9 The Higgs branch is the ALE space. The active-versus-full-branch clarification (the Higgs branch reconstructs the active $\mathbb{C}^2/\Gamma$ (VI.3.48), the spectator $\mathbb{C}_{z_3}$ riding the vector-multiplet adjoint Φ_i, the full branch mixed (VI.3.49), the Φ_i not entering the hypermultiplet quotient, forced to a common value by the hyper F-terms (VI.3.20)), the hyperkähler quotient (VI.3.50) by $G = (\prod U(N_i))/U(1)_{\text{diag}}$ with the $\mathcal{N} = 2$ FI triplets obeying $\sum_i N_i \vec{\zeta}_i = 0$ (VI.3.51), the single-regular-brane dimension count (VI.3.52)–(VI.3.54) have separate roles. The trace constraint and conditional dimension arithmetic are local derivations [MATH]; the D-brane interpretation of the quotient is [WS]. The mathematical identification with the ALE space is the cited Kronheimer theorem [MATH], under the regular dimension vector, FI trace constraint, and genericity conditions stated above (Douglas and Moore 1996, §8, Eqs. (8.7)–(8.9); (Kronheimer 1989) for the ALE/hyperkähler-quotient theorem, cited here and constructed in VI.4; the Higgs-dimension identity, the hyper F-terms, the diagonal-$U(1)$/FI constraint, the N-brane Sym^N dimension, and the per-node $\mathcal{N} = 2$ marginality $2N_i - \sum_j a_{ij} N_j = 0$ evaluated, the symbolic calculation). The single-brane restriction and the N-brane symmetric product $\text{Sym}^N(\mathbb{C}^2/\Gamma)$ with its larger generic stabilizer are inherited physical premises from VI.1 . Their exact primary support remains unresolved here; the quotient citations do not establish the full symmetric-product identification. Only dimension arithmetic conditional on that stabilizer is checked. The Higgs-not-Coulomb naming is the SCFT identification of the regular-rank quivers as orbifold daughters of $\mathcal{N} = 4$ is the engine-chapter statement of what the theory is, the conformal-manifold dynamics routing to Part III (Vol XIV).

§VI.3.10 What the construction does and does not give. The Higgs branch named not constructed (the hyperkähler quotient, FI resolution, exceptional cycles, and metric are VI.4); the holomorphic, probe-visible reconstruction and its α'/g_s caveats (the stated distinction, inherited from VI.1); the geometric McKay correspondence cited not proved, and the affine-McKay-versus-finite-intersection-graph distinction (the stated distinction; the finite-group and geometric McKay correspondence, home Vol. IV); $2O/2I$ and $\hat{E}_7/\hat{E}_8$ stated not worked (atlas, VI.11); the $\mathbb{C}^3/\Gamma$ thread, abelian $\mathbb{Z}_m \times \mathbb{Z}_n$ and non-abelian alike (VI.6; the toric cases also Vol. VII). The generic $SU(3)$ four-supercharge count and potentially directed spectrum are inherited physical premises here, without a local invariant-spinor derivation or verified exact primary locator. The cited $SU(2)$ McKay formulas do not establish that count.

References

Billo, M., B. Craps, and F. Roose (2001). "Orbifold boundary states from Cardy's condition". In: *JHEP* 01, p. 038. DOI: 10.1088/1126-6708/2001/01/038. arXiv: hep-th/0011060.

Diaconescu, D.-E. and J. Gomis (2000). "Fractional branes and boundary states in orbifold theories". In: *JHEP* 10, p. 001. DOI: 10.1088/1126-6708/2000/10/001. arXiv: hep-th/9906242.

Douglas, M. R. and G. W. Moore (1996). "D-branes, quivers, and ALE instantons". In: arXiv preprint; not published in a journal. arXiv: hep-th/9603167.

Kronheimer, P. B. (1989). "The construction of ALE spaces as hyper-Kähler quotients". In: *J. Differential Geom.* 29.3, pp. 665–683.

McKay, J. (1980). "Graphs, singularities, and finite groups". In: *Proc. Symp. Pure Math.* 37. American Mathematical Society, pp. 183–186.

Chapter VI.4

Moduli spaces: Higgs branches as resolved orbifolds and hyperkähler quotients

VI.4.1 The moduli space of vacua

A regular D-brane can move away from the orbifold point. Its position must therefore appear among the vacuum expectation values of the quiver fields. Chapter 3 supplied those fields for $\mathbb{C}^2/\Gamma$; we now recover the surface on which the brane moves by solving their vacuum equations. The active surface is the Higgs-branch factor. The spectator $\mathbb{C}_{z_3}$ lies in the vector-multiplet adjoints and is held fixed throughout this construction.

The vacuum equations do more than count position coordinates. Gauge-invariant products of hypermultiplets reconstruct the singular surface at zero Fayet–Iliopoulos level. A real level changes which gauge orbits survive, replacing the singular point by compact curves. A complex level changes the holomorphic equations themselves. Keeping these operations distinct lets us recover both the orbifold and its smooth relatives from one gauge theory.

With eight supercharges, the real D-term and complex adjoint F-term form the three moment-map conditions of a hyperkähler quotient. We first compute this quotient for one regular $\mathbb{Z}_2$ brane. Its mesons give $uv = w^2$, and its nonzero real level gives $T^*\mathbb{P}^1$. The general ADE construction then uses the same equations with matrix-valued fields. Identifying the resulting metric as an ALE metric requires the mathematical theorem stated below, beyond the vacuum equations or the dimension count alone.

The moduli space, in one line.

The Higgs branch at fixed vector-multiplet scalars is {D-flat and F-flat}/gauge. With $\mathcal{N}=2$ (eight supercharges) the real D-term and complex adjoint F-term assemble into a triplet of *moment maps* $\vec{\mu}$, and the moduli space is the *hyperkähler quotient* $\vec{\mu}^{-1}(\vec{\zeta})/G$: solve $\vec{\mu}=\vec{\zeta}$, divide by G. The Fayet–Iliopoulos levels $\vec{\zeta}$ are the parameters that generically smooth the singularity (special levels on a wall may leave it partly singular; resolve or deform, separated in §VI.4.8).

The plan is concrete-first. We set up the hyperkähler quotient for the quiver (§VI.4.2); then work the smallest case entirely by hand, the $\mathbb{Z}_2$ orbifold whose resolution is the Eguchi–Hanson space, so that every later abstraction has a worked instance behind it (§VI.4.3); then state Kronheimer's theorem, which says the same computation runs uniformly over the whole ADE list (§VI.4.4); read off the exceptional curves and meet the geometric face of the McKay correspondence (§VI.4.7); separate the two ways of smoothing the singularity, resolution and deformation (§VI.4.8); and mark the boundary of what has and has not been built (§VI.4.9). The heavier differential geometry is named and routed to its home in Part I; the vacuum equations supply the physical route into that geometry.

Geometry vocabulary (recalled from Part I).

The construction below is elementary gauge theory; the geometry it produces is developed in Part I (Volume IV) and the ADE representation theory in Chapter 3. A first reading may take the following on faith and skip the asides marked *optional*.

- **Orbifold $\mathbb{C}^2/\Gamma$:** $\mathbb{C}^2$ divided by a finite group; the active factor used here is smooth except for the singular origin (the fixed point).
- **Resolution:** a smooth space that replaces that one point by a finite-size compact piece and agrees with $\mathbb{C}^2/\Gamma$ everywhere else.
- **Exceptional curve, intersection form:** the inserted pieces are two-spheres $\mathbb{P}^1$; an integer matrix records how many there are and how they meet.
- **ALE space:** smooth in the interior, approaching flat $\mathbb{C}^2/\Gamma$ far away ("asymptotically locally Euclidean").
- **Hyperkähler quotient:** the geometry eight supercharges give on a smooth Higgs branch (Ricci-flat, a triplet of complex structures); the *quotient* is just "solve the moment maps, divide by the gauge group", the geometric name for D-flat $\cap$ F-flat / gauge.

VI.4.2 The moduli space is a hyperkähler quotient

Recall the data of the previous chapter. The affine ADE quiver has a gauge group $\prod_i U(N_i)$ over the irreducible representations R_i of Γ, a hypermultiplet on every edge of the diagram, written as a conjugate pair of bifundamentals $(X_a, \widetilde{X}_a)$, and one adjoint chiral multiplet Φ_i per node, the scalar of the $\mathcal{N}=2$ vector multiplet, carrying the inert spectator direction $\mathbb{C}_{z_3}$ transverse to the active $\mathbb{C}^2/\Gamma$. The active surface is reconstructed by the hypermultiplets; the adjoints Φ_i carry the spectator line and are

set to their common value, so they sit outside the quotient we are about to take. We work on the Higgs branch, Φ_i fixed. Chapter 3 already identified this branch, wrote it as a hyperkähler quotient, and counted its dimension; what was *named* there is what we *construct* here, so the quotient is recalled briefly below and the chapter is spent on the metric and the resolution geometry it was promised to carry.

Eight supercharges organize the supersymmetric vacuum conditions into three real equations per node, a triplet under the $SU(2)_R$ R-symmetry. Reading the $\mathcal{N}=2$ theory in $\mathcal{N}=1$ language, one is the real D-term of the $\mathcal{N}=1$ vector multiplet, the other two the complex F-term of its adjoint partner Φ_i; together they are the three components of a *moment map* $\vec{\mu}_i = (\mu_i^{\mathbb{R}}, \mu_i^{\mathbb{C}})$ valued in the adjoint of $U(N_i)$. Orient each edge once, $a\colon i \to j$, writing the hypermultiplet as $X_a\colon V_i \to V_j$ and $\widetilde{X}_a\colon V_j \to V_i$ with $V_i = \mathbb{C}^{N_i}$; the orientation only assigns names to the two maps, since the $\mathcal{N}=2$ hypermultiplet contains both directions. Collecting the edges incoming to $(h(a)=i)$ and outgoing from $(t(a)=i)$ node i with opposite signs, so that every term is an endomorphism of V_i,

$$\begin{aligned} \mu_i^{\mathbb{C}} &= \sum_{h(a)=i} X_a \widetilde{X}_a - \sum_{t(a)=i} \widetilde{X}_a X_a, \\ \mu_i^{\mathbb{R}} &= \sum_{h(a)=i} \big(X_a X_a^\dagger - \widetilde{X}_a^\dagger \widetilde{X}_a \big) + \sum_{t(a)=i} \big(\widetilde{X}_a \widetilde{X}_a^\dagger - X_a^\dagger X_a \big), \end{aligned} \tag{VI.4.1}$$

the complex one being the F-term $\partial W/\partial \Phi_i$ of the $\mathcal{N}=2$ superpotential $W = \sum_i \operatorname{Tr} \Phi_i \mu_i^{\mathbb{C}}$ inherited from Chapter 3. For the abelian double edge of §VI.4.3 these collapse to $\mu^{\mathbb{R}} = \sum_\alpha (|a_\alpha|^2 - |b_\alpha|^2)$ and $\mu^{\mathbb{C}} = \sum_\alpha a_\alpha b_\alpha$. Why three, and why a triplet: eight supercharges make the target *hyperkähler*, carrying three complex structures rotated into one another by the $SU(2)_R$ R-symmetry, and there is one moment map for each. The D-term is the moment map for one complex structure, the real and imaginary parts of the F-term the moment maps for the other two; together they transform as a vector of $SU(2)_R$, which is what the arrow on $\vec{\mu}_i$ records. There is a normalization to keep when rotating these equations. With the flat hypermultiplet metric $\sum_a (\|\mathrm{d}X_a\|^2 + \|\mathrm{d}\widetilde{X}_a\|^2)$, the equally normalized real components are $(\mu^{\mathbb{R}}, 2\operatorname{Re}\mu^{\mathbb{C}}, 2\operatorname{Im}\mu^{\mathbb{C}})$, up to a common factor and an orientation choice. We retain the displayed F-term normalization, so $(\zeta_R, \zeta_{\mathbb{C}})$ denotes one real and one complex level, with the same factor of two understood when forming a Euclidean triplet. For one charged hypermultiplet the identity $(|a|^2-|b|^2)^2 + 4|ab|^2 = (|a|^2+|b|^2)^2$ makes this relative factor visible. The Higgs branch is the hyperkähler quotient: the level set of the moment maps, divided by the gauge group with its trivially-acting overall diagonal $U(1)$ removed,

$$\mathcal{M}(\vec{\zeta}) \;=\; \big\{\, \vec{\mu}_i = \vec{\zeta}_i \mathbb{1}_{N_i} \text{ for all } i \,\big\} \,/\, G, \qquad G = \Big(\textstyle\prod_i U(N_i) \Big) / U(1)_{\mathrm{diag}}. \tag{VI.4.2}$$

The right-hand sides are the *Fayet–Iliopoulos levels* $\vec{\zeta}_i$, one real triplet per node, set central (proportional to the identity $\mathbb{1}_{N_i}$). They are the smoothing (Kronheimer) parameters: the real part resolves and the complex part deforms (§VI.4.8). The overall diagonal $U(1) \subset \prod_i U(N_i)$ acts trivially on every bifundamental, since each X_a carries opposite charges at its two endpoints, so its moment map is identically zero. Tracing

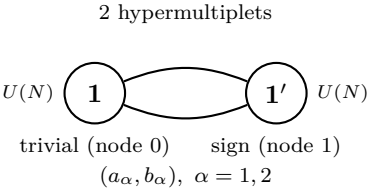


Figure VI.4.1: The $\hat{A}_1$ McKay quiver of $\mathbb{Z}_2 \subset SU(2)$: two nodes joined by a double edge, i.e. two hypermultiplets, each a conjugate pair (a_α, b_α), $\alpha = 1, 2$. The edges are *undirected*: an $\mathcal{N} = 2$ hypermultiplet is a non-chiral pair, not a directed (chiral) bifundamental, so no arrow is drawn (Chapter 3). The single nontrivial node (the sign representation) will carry the single exceptional curve; the trivial node carries none.

the level conditions over each node and summing isolates exactly this combination,

$$\sum_i \mathrm{Tr}_{N_i}\, \vec{\mu}_i \;=\; 0 \quad\Longrightarrow\quad \sum_i \mathrm{Tr}\left(\vec{\zeta}_i\, \mathbb{1}_{N_i}\right) = \sum_i N_i\, \vec{\zeta}_i \;=\; 0, \tag{VI.4.3}$$

one linear constraint on the levels, so that of the #{nodes} triplets only #{nodes} $-\,1$ are independent. We will see in §VI.4.7 that this is exactly the number of compact curves in the resolution.

Dictionary: gauge theory ↔ geometry parameter.
The *moment map* $\vec{\mu}$ is the $\mathcal{N} = 2$ triplet of vacuum equations: $\mu^{\mathbb{R}}$ is the D-term, $\mu^{\mathbb{C}}$ the F-term. The *hyperkähler quotient* is "solve $\vec{\mu} = \vec{\zeta}$, divide by gauge". The *Fayet–Iliopoulos level* $\vec{\zeta}$ is the tunable parameter: $\vec{\zeta} = 0$ leaves the singular orbifold, generic $\vec{\zeta} \neq 0$ smooths it (special levels on a wall leave a partial resolution, §VI.4.7).

VI.4.3 The smallest case: $\mathbb{C}^2/\mathbb{Z}_2$ and the Eguchi–Hanson space

Everything in the general construction is visible in the smallest orbifold, so we do it by hand before saying anything general. Let $\Gamma = \mathbb{Z}_2 = \{\pm\mathbb{1}\}$ act on $\mathbb{C}^2$ by $(z_1, z_2) \mapsto (-z_1, -z_2)$. The McKay quiver, from the A series of Chapter 3, is the affine $\hat{A}_1$ diagram: two nodes, the trivial and the sign representation, joined by a *double* edge (Figure VI.4.1). The regular brane has ranks $(1, 1)$, gauge group $U(1) \times U(1)$, and the diagonal $U(1)$ acts trivially, so the surviving gauge symmetry is a single $U(1)$.

The double edge is two hypermultiplets (a_α, b_α), $\alpha = 1, 2$, with a_α of charge $+1$ and b_α of charge -1 under the surviving $U(1)$. The moment maps (VI.4.1) collapse to the abelian

$$\mu^{\mathbb{R}} = \sum_{\alpha=1,2} \left(|a_\alpha|^2 - |b_\alpha|^2\right), \qquad \mu^{\mathbb{C}} = \sum_{\alpha=1,2} a_\alpha b_\alpha, \tag{VI.4.4}$$

and the Higgs branch is their common level set divided by $U(1)$. The four complex hypermultiplet coordinates, eight real, lose three real moment-map conditions and one

real gauge angle, $8-3-1=4$ real, quaternionic dimension one, as the general count will confirm.

Take $\vec{\zeta}=0$ first. The gauge-invariant functions of charge zero are the *mesons* $M_{\alpha\beta}=a_\alpha b_\beta$, a 2×2 matrix. Being an outer product it has rank at most one, so it obeys

$$\det M = a_1b_1\,a_2b_2 - a_1b_2\,a_2b_1 = 0, \tag{VI.4.5}$$

and the complex moment-map condition $\mu^{\mathbb{C}}=\operatorname{Tr}M=0$ makes M traceless. Writing the independent invariants as $u=M_{12}$, $v=-M_{21}$, $w=M_{11}=-M_{22}$, the rank-at-most-one condition (VI.4.5) reads $-w^2+uv=0$, i.e. the standard A_1 form

$$uv=w^2. \tag{VI.4.6}$$

This is precisely the orbifold. The $\mathbb{Z}_2$-invariant polynomials on $\mathbb{C}^2$ are generated by

$$u=z_1^2,\qquad v=z_2^2,\qquad w=z_1z_2,\qquad \text{with the single relation}\qquad uv=w^2, \tag{VI.4.7}$$

since $z_1^2z_2^2=(z_1z_2)^2$. Every invariant monomial has even total degree, so its two exponents are either both even or both odd. It is therefore a product of u,v times either 1 or w. Reducing by $w^2=uv$ gives distinct monomials of these two types in z_1,z_2, so there is no further relation. The mesonic gauge invariants and the orbifold invariants satisfy the same equation: the gauge theory has rebuilt the geometry. The zero-level Higgs branch is the affine variety $\{uv=w^2\}$, the A_1 Kleinian (du Val) surface singularity, with its node at the origin: the probe at $\vec{\zeta}=0$ sees the singular $\mathbb{C}^2/\mathbb{Z}_2$ itself.

It is singular for one sharp reason. At $\vec{\zeta}=0$ the origin $a_\alpha=b_\alpha=0$ solves the moment-map conditions and is fixed by the whole $U(1)$, an orbit of zero size where the quotient pinches: that fixed point is the tip of the cone, the orbifold's singularity. Turn on a generic level $\vec{\zeta}\neq 0$ and the conditions $\mu_{\mathbb{R}}=\zeta_R$, $\mu_{\mathbb{C}}=\zeta_C$ forbid $a_\alpha=b_\alpha=0$, so no point of the level set is fixed by a phase, the $U(1)$ acts freely, and the quotient is a smooth four-manifold. It carries the unique ALE metric of type A_1, the *Eguchi–Hanson* metric, whose standard closed form we quote,

$$\mathrm{d}s^2=\Big(1-\tfrac{a^4}{r^4}\Big)^{-1}\mathrm{d}r^2+\tfrac{r^2}{4}\Big(1-\tfrac{a^4}{r^4}\Big)\sigma_3^2+\tfrac{r^2}{4}\big(\sigma_1^2+\sigma_2^2\big), \tag{VI.4.8}$$

where the σ_i are the left-invariant one-forms on $SU(2)$, with the angle conjugate to σ_3 given half its usual period so that the principal orbits are $SU(2)/\mathbb{Z}_2$; this half-period is what makes the bolt smooth and the boundary at infinity $S^3/\mathbb{Z}_2$. The *bolt* radius is set by the level, $a^2\propto|\vec{\zeta}|$, matching the exceptional area below. At $r=a$ the circle generated by σ_3 shrinks and the surface caps off on a round $\mathbb{P}^1$ of area proportional to a^2, the *exceptional curve*; as $r\to\infty$ the metric approaches flat $\mathbb{C}^2/\mathbb{Z}_2$, the orbifolded sphere $S^3/\mathbb{Z}_2$ at infinity, which is what "asymptotically locally Euclidean" (ALE) means. The metric is Ricci-flat, as a hyperkähler metric must be; one can check this directly from the displayed form. Deriving the metric *from the quotient* is the hyperkähler-geometry computation routed to §VI.4.9 and Part I; here it is quoted. In the resolution frame $\zeta_{\mathbb{C}}=0$, $\zeta_R>0$ this space is holomorphically the cotangent bundle $T^*\mathbb{P}^1$, the minimal resolution carrying the exceptional $\mathbb{P}^1$; a general $\vec{\zeta}$ gives the same metric in a

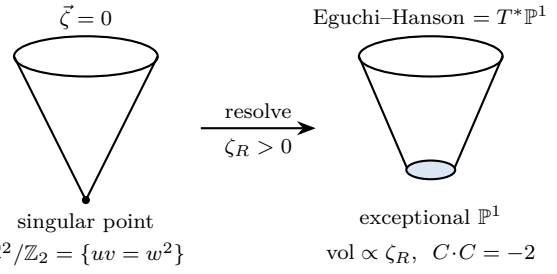


Figure VI.4.2: Resolving the A_1 orbifold (schematic). At $\vec{\zeta} = 0$ the Higgs branch is the singular cone $\mathbb{C}^2/\mathbb{Z}_2$; turning on $\zeta_R > 0$ replaces the tip by a finite $\mathbb{P}^1$ of area $\propto \zeta_R$, giving the smooth Eguchi–Hanson space. The drawing collapses the four real dimensions to a cartoon; the one exceptional curve is the single nontrivial node of Figure VI.4.1.

hyperkähler-rotated complex structure (§VI.4.8). Figure VI.4.2 is the picture to keep: the singular cone has its tip replaced by a finite-size sphere.

The curve count matches the quiver. One regular $\mathbb{Z}_2$ brane gives one compact $\mathbb{P}^1$, dual to the one nontrivial node; the trivial node contributes no curve. The self-intersection of that curve is $C\cdot C = -2$, the hallmark of an A_1 resolution. Both numbers, the single curve and its -2, will reappear as the general rule.

(Optional: how the quotient becomes $T^*\mathbb{P}^1$.) The holomorphic identification asserted at (VI.4.8), that the resolved branch is $T^*\mathbb{P}^1$, can be read off the quotient directly, without the metric. In the chamber $\zeta_{\mathbb{C}} = 0$, $\zeta_R > 0$ the Higgs branch is the GIT quotient of the (a_α, b_α) by the complexified $\mathbb{C}^\times$, with ζ_R the stability parameter. Here GIT means that the complex gauge orbits are restricted by stability before their quotient is taken. The complex moment map keeps

$$\mu^{\mathbb{C}} = a_1 b_1 + a_2 b_2 = 0, \tag{VI.4.9}$$

and $\zeta_R > 0$ forbids the charge-$(+1)$ fields from vanishing together, since $a_1 = a_2 = 0$ would give $\mu^{\mathbb{R}} = -\sum_\alpha |b_\alpha|^2 \le 0 < \zeta_R$. Dividing the nonzero pair (a_1, a_2) by the $\mathbb{C}^\times$ scaling leaves

$$[a_1 : a_2] \in \mathbb{P}^1, \tag{VI.4.10}$$

the base of the cotangent bundle. Its zero section is the exceptional curve, of area $\propto \zeta_R$. Over each point the charge-(-1) fields b_α are cut by (VI.4.9) to the one-dimensional space $\{b : \sum_\alpha a_\alpha b_\alpha = 0\}$ and carry the opposite $\mathbb{C}^\times$ weight, exactly a cotangent covector at $[a]$, so the branch is the total space

$$\mathcal{M}_{\zeta_R > 0} = T^*\mathbb{P}^1, \tag{VI.4.11}$$

with the zero section $b_\alpha = 0$ the exceptional $\mathbb{P}^1$ and the fibres restoring the smooth cone away from it. Concretely, on the patch $a_1 \neq 0$ fix the gauge $a_1 = 1$, write $s = a_2$, and solve (VI.4.9) for $b_1 = -s\, b_2$; with $t = b_2$ the invariants $u = z_1^2, v = z_2^2, w = z_1 z_2$ of (VI.4.6) become

$$(u, v, w) = \big(t,\ s^2 t,\ -s\, t\big), \qquad uv = w^2, \tag{VI.4.12}$$

so (s,t) are smooth coordinates on the resolution, the exceptional curve is $t=0$ (the whole $\mathbb{P}^1$ of s collapsing to the origin $u=v=w=0$), and $t\neq 0$ recovers the $u\neq 0$ part of the punctured cone, the complementary patch $a_2\neq 0$ covering the rest. The Eguchi–Hanson metric (VI.4.8) is the hyperkähler metric on this $T^*\mathbb{P}^1$; only its closed form, not this holomorphic identification, was quoted. The second patch has coordinate $s'=1/s$ and fibre coordinate $t'=-s^2t$. Indeed, after setting $a_2=1$ one has $b_1=t'$ and $b_2=-s't'$. Thus $t'\,\mathrm{d}s'=t\,\mathrm{d}s$, the cotangent transition law. The normal bundle of the zero section is consequently $T^*\mathbb{P}^1=\mathcal{O}(-2)$, giving its self-intersection -2. The distinction matters even though the global holomorphic functions still obey $uv=w^2$. That ring describes the affine surface obtained by contracting the zero section. It does not distinguish points along the exceptional curve; the stable quotient and its two coordinate patches do. The metric is further information on the smooth variety, not part of its affine coordinate ring.

VI.4.4 Kronheimer's construction in general

Nothing in §VI.4.3 used that Γ was $\mathbb{Z}_2$ beyond writing the $\hat{A}_1$ quiver. For any finite $\Gamma\subset SU(2)$ the recipe is the same: take the affine ADE quiver of Chapter 3, form the moment maps (VI.4.1), and build the hyperkähler quotient (VI.4.2). This is Kronheimer's construction, read as the gauge theory on the regular brane.

The dimension is the same for every type, and Chapter 3 already ran the count; we recall it in one line because Kronheimer's theorem now identifies the quotient that carries it as a complete ALE metric. The bifundamentals span a flat quaternionic vector space $\mathbb{V}_{\mathrm{hyp}}$, one Hom pair per edge, on which G acts (we keep $\mathcal{M}$ for the quotient and write $\mathbb{V}_{\mathrm{hyp}}$ for the prequotient space),

$$\dim_{\mathbb{H}}\mathbb{V}_{\mathrm{hyp}}=\sum_{\text{edges}}\delta_i\delta_j,\qquad \dim_{\mathbb{R}}G=\sum_i\delta_i^2-1, \tag{VI.4.13}$$

and on a smooth locus where the effective gauge action is free, the hyperkähler quotient removes one quaternionic dimension per gauge generator (three real moment-map conditions and one gauge angle). With one regular brane the ranks are the Dynkin marks, $N_i=\delta_i=\dim R_i$, so the quaternionic dimension is the edge count minus the gauge count,

$$\dim_{\mathbb{H}}\mathcal{M}=\sum_{\text{edges}}\delta_i\delta_j-\Big(\sum_i\delta_i^2-1\Big). \tag{VI.4.14}$$

The edge sum is fixed by the null-vector identity $\sum_j a_{ij}\delta_j=2\delta_i$ of Chapter 3, the relation that made the diagram affine,

$$\sum_{\text{edges}}\delta_i\delta_j=\tfrac{1}{2}\sum_{i,j}a_{ij}\delta_i\delta_j=\tfrac{1}{2}\sum_i\delta_i(2\delta_i)=\sum_i\delta_i^2, \tag{VI.4.15}$$

so the two large sums in (VI.4.14) cancel and $\dim_{\mathbb{H}}\mathcal{M}=1$, four real dimensions, for A, D, and E alike. The same identity that made the McKay quiver affine fixes the smooth quotient dimension. It does not imply smoothness at zero level, where stabilizers remain. One regular brane sees one copy of the surface it probes.

Kronheimer's theorem supplies what the gauge theory cannot prove on its own, that the quotient is a complete metric of the expected type and that it exhausts the possibilities. For generic $\vec{\zeta}$ the hyperkähler quotient (VI.4.2) of the affine ADE quiver is a smooth, complete, hyperkähler four-manifold asymptotic to $\mathbb{C}^2/\Gamma$, an ALE gravitational instanton; as $\vec{\zeta}$ ranges over the level space it sweeps out the family of such metrics, with the minimal resolution of $\mathbb{C}^2/\Gamma$ appearing at generic real level and vanishing complex level; and every ALE hyperkähler four-manifold (ALE gravitational instanton) asymptotic to $\mathbb{C}^2/\Gamma$ arises this way, up to the Weyl identifications below. The resolution parameters are the levels themselves, a triplet per node modulo the constraint (VI.4.3),

$$\vec{\zeta} \;\in\; \mathbb{R}^3 \otimes \mathfrak{h}, \qquad \dim \mathfrak{h} = r = \#\{\text{nodes}\} - 1 = \text{rank}, \tag{VI.4.16}$$

with $\mathfrak{h}$ the Cartan subalgebra of the finite ADE algebra; the three copies are the $SU(2)_R$ triplet taken apart in §VI.4.8, and the metric degenerates where a curve collapses, the chamber walls of §VI.4.7. *(Optional: those walls on the real slice are the root hyperplanes in $\mathfrak{h}$. In the full triplet space a root must pair to zero with all three components for a degeneration. The levels are counted up to the Weyl group W.)* The construction is uniform across the ADE list, which is its point. The explicit closed-form metric, on the other hand, is elementary only for the A series: A_1 is Eguchi–Hanson (VI.4.8), and the general A_{n-1} space is the multi-centred Gibbons–Hawking metric with n centres. For the D and E spaces the quotient still produces the metric, but no comparably elementary formula is written; we keep the uniform quotient statement and do not chase the D, E metrics here.

VI.4.5 The A series in closed form: multi-centre metrics

The A series is worth seeing in full, because there the metric is as explicit as the algebra and the resolution is a picture one can draw. Let $\Gamma = \mathbb{Z}_n$ act on $\mathbb{C}^2$ by $(z_1, z_2) \mapsto (\omega z_1, \omega^{-1} z_2)$ with $\omega = e^{2\pi i/n}$, the cyclic subgroup of $SU(2)$ from Chapter 2. The invariant ring is generated by

$$x = z_1^n, \qquad y = z_2^n, \qquad w = z_1 z_2, \qquad \text{with} \qquad xy = w^n, \tag{VI.4.17}$$

the A_{n-1} Kleinian singularity. The ring itself is not new: Chapter 2 already obtained $\{xy = w^n\} \times \mathbb{C} = (\mathbb{C}^2/\mathbb{Z}_n) \times \mathbb{C}$ as the mesonic branch of the necklace quiver, with $\mathbb{Z}_2$'s $uv = w^2$ the smallest case. What is new here is the *metric* on the resolved space, and the chain of curves that carries it. The McKay quiver is the affine $\hat{A}_{n-1}$ cycle, n nodes, all of mark one; the regular brane has gauge group $U(1)^n/U(1)_{\text{diag}} = U(1)^{n-1}$, and the resolution carries $n-1$ exceptional curves, one per nontrivial node, in a chain.

The explicit ALE metric is the Gibbons–Hawking form, which trades the four-dimensional problem for a harmonic function on $\mathbb{R}^3$. Write the metric as a circle of coordinate τ fibred over a flat base $\vec{x} \in \mathbb{R}^3$,

$$\mathrm{d}s^2 = V(\vec{x})^{-1} \big(\mathrm{d}\tau + \vec{\omega} \cdot \mathrm{d}\vec{x}\big)^2 + V(\vec{x})\, \mathrm{d}\vec{x} \cdot \mathrm{d}\vec{x}, \qquad \vec{\nabla} \times \vec{\omega} = \vec{\nabla} V, \tag{VI.4.18}$$

where the curl condition forces V to be harmonic, $\nabla^2 V = 0$, and together with the circle fibration this condition makes the four-manifold hyperkähler, hence Ricci-flat, on regions where $V > 0$, away from its sources. The ALE A_{n-1} space is the choice with n unit point sources and no constant term at infinity,

$$V(\vec{x}) = \sum_{i=1}^{n} \frac{1}{|\vec{x} - \vec{x}_i|}, \tag{VI.4.19}$$

at n distinct centres $\vec{x}_i$, each of unit charge, so that with the period of τ fixed to 4π (the value that makes a unit centre smooth for this normalization of V) the circle shrinks *smoothly* at every centre: each centre is then an ordinary point of the smooth space, not a singularity, the apparent puncture a coordinate artefact of the fibration. Here the smooth extension and the asymptotic lens space are quoted geometric results for unit charges and this period. Between two consecutive centres the τ-circle, fibred over the segment joining them and capping off at both ends, sweeps out a two-sphere. The n centres give $n-1$ such independent spheres, the exceptional curves $C_1, \ldots, C_{n-1}$ in a chain (Figure VI.4.3); placing the centres on a line (the geometric chamber, the real slice of the levels) their areas are set by the separations,

$$\mathrm{vol}(C_i) \;\propto\; |\vec{x}_{i+1} - \vec{x}_i| \;\propto\; \zeta_i^{\mathbb{R}}, \tag{VI.4.20}$$

the geometric reading of the Fayet–Iliopoulos levels. More precisely the $n-1$ relative position three-vectors $\vec{x}_{i+1} - \vec{x}_i \in \mathbb{R}^3$ are proportional to the equally normalized A_{n-1} FI triplets in the simple-root basis: collinear centres are the real slice $\zeta_i^{\mathbb{C}} = 0$ of §VI.4.8, and letting the centres move off the line in $\mathbb{R}^3$ restores the full $SU(2)_R$ triplet. Consecutive spheres share the one centre between them and so meet once, while non-consecutive spheres are disjoint, which is the A_{n-1} chain: the intersection matrix is $C_i \cdot C_j = -2$ on the diagonal and $+1$ on the off-diagonal of neighbours, the statement (VI.4.33) of the next section specialised to type A. Collapsing all centres to one point sends every area to zero and returns the singular $\{xy = w^n\}$.

The smallest case closes the loop with the previous section: two centres, $n = 2$, give the single sphere of the Eguchi–Hanson space, and the metric (VI.4.18) is then (VI.4.8) in disguise, the bolt being the sphere over the one segment between the two centres. These normalizations can be compared without finding the coordinate transformation. On a segment of length L choose a gauge in which the connection has no tangential component. The induced metric is $V\,\mathrm{d}\ell^2 + V^{-1}\mathrm{d}\tau^2$, so its area element is $\mathrm{d}\ell\,\mathrm{d}\tau$ and its area is $4\pi L$. In (VI.4.8), use $\sigma_1^2 + \sigma_2^2 = \mathrm{d}\theta^2 + \sin^2\theta\,\mathrm{d}\phi^2$ and $\sigma_3 = \mathrm{d}\psi + \cos\theta\,\mathrm{d}\phi$, with ψ of period 2π. The bolt has radius $a/2$, area πa^2, and hence $a^2 = 4L$ in the two-centre normalization above. This fixes a metric comparison, not the conversion between field-theory scalar units and spacetime lengths. The displayed Eguchi–Hanson metric has vanishing Ricci tensor; the multi-centre family (VI.4.18) is Ricci-flat by the same harmonic-function mechanism, which we quote rather than recompute for general n.

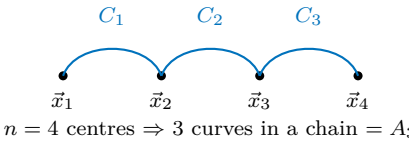


Figure VI.4.3: The A_{n-1} resolution as a multi-centre Gibbons–Hawking space (schematic, $n = 4$). Each τ-circle caps off over a centre $\vec{x}_i$; the circle fibred over the segment between consecutive centres is an exceptional $\mathbb{P}^1$ (here C_1, C_2, C_3). Consecutive spheres share a centre and meet once, giving the A_{n-1} chain; their areas $\propto |\vec{x}_{i+1} - \vec{x}_i| \propto \zeta_i^{\mathbb{R}}$. The three-dimensional base is drawn as a line.

VI.4.6 Non-abelian examples: the D_4 and E_6 singularities

Every explicit worked case so far has been abelian, the cyclic $\mathbb{Z}_n$ with its one-dimensional representations and its elementary multi-centre metric. The construction was built for any $\Gamma \subset SU(2)$, so we now take the two smallest non-abelian cases in parallel, the quaternion group Q_8 and the binary tetrahedral group $2T$, both to see the quotient turn genuinely non-abelian and to watch the invariant ring climb in degree. Their quivers are the $\hat{D}_4$ and $\hat{E}_6$ diagrams of Chapter 3, with central nodes of dimension two and (for $2T$) three; a $U(N_i)$ node with $N_i > 1$ makes the hyperkähler quotient genuinely non-abelian, its moment map an $N_i \times N_i$ matrix set to $\vec{\zeta}_i \mathbb{1}_{N_i}$. The quaternionic dimension is still one by the count of §VI.4.4 (for Q_8, $\sum_i \delta_i^2 = 1{+}1{+}1{+}1{+}4 = 8 = |Q_8|$ and the edge sum $4 \cdot (1 \cdot 2) = 8$ give $\dim_{\mathbb{H}} = 8 - (8 - 1) = 1$; likewise for $2T$): one regular brane, one copy of the surface. What is new is the non-abelian quotient. For Q_8 we compute the Higgs branch from the quiver by hand, as §VI.4.3 did for $\mathbb{Z}_2$, and recover the D_4 geometry directly; for $2T$ we exhibit the geometry and lean on Kronheimer's theorem, the E_6 quotient being heavier. In both, only the algebra is elementary, not the metric.

Take first $\Gamma = Q_8$. Acting on $\mathbb{C}^2$ by the unit quaternions $a = \mathrm{diag}(i, -i)$ and $b = \left(\begin{smallmatrix} 0 & 1 \\ -1 & 0 \end{smallmatrix}\right)$, it leaves invariant

$$x = z_1 z_2 \, (z_1^4 - z_2^4), \qquad y = z_1^2 z_2^2, \qquad z = z_1^4 + z_2^4, \tag{VI.4.21}$$

of degrees six, four, and four, which obey the single relation

$$x^2 = y\, z^2 - 4\, y^3 \qquad \Longleftrightarrow \qquad x^2 = y\,(z - 2y)(z + 2y), \tag{VI.4.22}$$

the D_4 du Val singularity. The cubic on the right factors into three lines through the origin, a mnemonic for the D_4 shape and the geometric echo of the central two-dimensional representation; the actual trivalent D_4 configuration of exceptional curves appears only after the resolution of §VI.4.7, not in this zero-level branch locus. Beside the abelian $uv = w^2$ this is the same kind of statement, one equation in three generators, but the generators now run to degree six and the surface is a D_4, not an A.

That equation is the geometry; now we earn it from the gauge theory. We do for Q_8 what §VI.4.3 did for $\mathbb{Z}_2$: build the Higgs branch from the $\hat{D}_4$ quiver and watch

$\{x^2 = yz^2 - 4y^3\}$ reappear as the ring of gauge invariants. Label the four edges $i = 1, \ldots, 4$, each a hypermultiplet (A_i, B_i) running from the central $U(2)$ node to outer node i and back, $A_i \colon \mathbb{C}^2 \to \mathbb{C}$ and $B_i \colon \mathbb{C} \to \mathbb{C}^2$. From each edge we can form a single $U(2)$-covariant matrix,

$$C_i := B_i A_i \in \mathrm{End}(\mathbb{C}^2), \tag{VI.4.23}$$

and the moment maps pin it down. The outer F-term sets its trace to zero, $\mu_i^{\mathbb{C}} = A_i B_i = \mathrm{Tr}\, C_i = 0$, and as an outer product of a column and a row C_i has rank at most one, hence vanishing determinant; a traceless 2×2 matrix of zero determinant is nilpotent,

$$\mathrm{Tr}\, C_i = 0, \qquad C_i^2 = 0, \tag{VI.4.24}$$

while the central F-term sets their sum to zero, $\mu_c^{\mathbb{C}} = \sum_i B_i A_i = \sum_i C_i = 0$. At zero FI level the affine complex quotient is thus four nilpotent elements of $\mathfrak{sl}_2$ summing to zero, modulo complexified $GL(2, \mathbb{C})$ conjugation in the affine invariant-ring sense (the node $U(1)$'s act trivially on C_i). Its coordinate ring is generated by the conjugation invariants, the traces of products; since $\mathrm{Tr}\, C_i = 0$, the lowest of these are the *two-loops* and the *three-loop*

$$p_{ij} = \mathrm{Tr}(C_i C_j), \qquad q = \mathrm{Tr}(C_1 C_2 C_3). \tag{VI.4.25}$$

Writing each rank-at-most-one nilpotent in terms of a two-vector, $C_i = \left(\begin{smallmatrix} \alpha_i\beta_i & -\alpha_i^2 \\ \beta_i^2 & -\alpha_i\beta_i \end{smallmatrix}\right)$, every trace collapses to the bracket $\langle i, j\rangle = \alpha_i\beta_j - \alpha_j\beta_i$,

$$p_{ij} = -\langle i, j\rangle^2, \qquad q = -\langle 1,2\rangle\langle 2,3\rangle\langle 3,1\rangle \quad \Longrightarrow \quad q^2 = -\,p_{12}p_{13}p_{23}, \tag{VI.4.26}$$

an identity among the invariants. The remaining relation is the nilpotency of the fourth edge, $C_4 = -(C_1 + C_2 + C_3)$: from $\det C_4 = -(p_{12} + p_{13} + p_{23})$ its vanishing forces $p_{12} + p_{13} + p_{23} = 0$. Eliminating p_{23} and setting

$$x = 4q, \qquad y = p_{12}, \qquad z = 2p_{12} + 4p_{13}, \tag{VI.4.27}$$

the two relations fuse into the single equation $x^2 = yz^2 - 4y^3$, the D_4 ring (VI.4.22) again. The non-abelian quiver has rebuilt the orbifold exactly as the abelian A_1 quiver rebuilt $\{uv = w^2\}$: the two-loops and the three-loop of $\hat{D}_4$ are the degree-four invariants y, z and the degree-six invariant x, and their one relation is the D_4 singularity. This is Kronheimer's theorem made explicit in the smallest non-abelian case. The E_6 case runs the same way: integrating out each arm of the $\hat{E}_6$ quiver leaves the central $U(3)$ carrying three nilpotents of $\mathfrak{sl}_3$ summing to zero, $N_a^3 = 0$ and generically regular ($N_a^2 \neq 0$), whose conjugation invariants cut out the E_6 surface (the orbit closures include non-regular configurations). The arm relation $c = AB$, $c^2 = 0$ gives $N^3 = Bc^2A = 0$, while $N^2 = BcA$ need not vanish. This proves the nilpotency implication, not a full presentation of the quotient ring. The exact elimination from these three central matrices to the E_6 generators is not carried out here. Below we instead compute the invariant polynomials in the original orbifold coordinates.

Now $\Gamma = 2T$, of order 24, the $\hat{E}_6$ quiver with its trivalent mark-three node. Here the generators need not be guessed. The *Reynolds operator*, the averaging projection of a polynomial onto its Γ-invariant part,

$$R(f)(z) = \frac{1}{|\Gamma|} \sum_{g \in \Gamma} f(g^{-1} z), \tag{VI.4.28}$$

applied to the monomials of each degree returns the invariants of that degree: a one-dimensional space at degree six, one at degree eight, and a new one at degree twelve (none at degree four),

$$f_6 = z_1 z_2 (z_1^4 - z_2^4), \quad g_8 = z_1^8 + 14 z_1^4 z_2^4 + z_2^8, \quad H_{12} = z_1^{12} - 33 z_1^8 z_2^4 - 33 z_1^4 z_2^8 + z_2^{12}, \tag{VI.4.29}$$

Direct expansion of these polynomials gives the relation

$$H_{12}^2 = g_8^3 - 108\, f_6^4 \qquad \Longleftrightarrow \qquad x^2 = y^3 - 108\, z^4, \tag{VI.4.30}$$

with $x = H_{12}$, $y = g_8$, $z = f_6$ of degrees twelve, eight, six. Rescaling $y \to -y$ and absorbing the 108 into z puts it in the standard form $x^2 + y^3 + z^4 = 0$: the E_6 du Val singularity. Every term has degree twenty-four, the order of $2T$, a consistency of the weighted relation. The averaging computation, rather than the group order alone, determines the first invariant degrees.

The pattern across the worked cases is now plain. The invariant ring of $\mathbb{C}^2/\Gamma$ is one weighted-homogeneous equation in three generators, an A, D, or E surface, whose degrees are fixed by Γ and climb across the examples: $uv = w^n$ for the cyclic $\mathbb{Z}_n$, $x^2 = yz^2 - 4y^3$ for the quaternionic Q_8, $x^2 = y^3 - 108z^4$ for the tetrahedral $2T$. At zero level each quotient is the singular $\mathbb{C}^2/\Gamma$; at generic level it is a smooth D_4 or E_6 ALE space. In the real resolution chamber it carries the four or six holomorphic exceptional (-2)-curves whose pattern the next section reads off. Unlike the A series, the D and E metrics have no elementary closed form: the quotient produces them and Kronheimer's theorem guarantees them, but we write only the algebra, the invariant rings (VI.4.22) and (VI.4.30) that the probe reconstructs.

VI.4.7 The exceptional cycles and the geometric McKay correspondence

Set the complex level to zero and turn on a generic real level, $\zeta_i^{\mathbb{R}} > 0$ over the nontrivial nodes. This is the *geometric* chamber: the quotient is the minimal resolution of $\mathbb{C}^2/\Gamma$, and it carries one compact exceptional curve $C_i \cong \mathbb{P}^1$ for each nontrivial node, of area proportional to the level,

$$\mathrm{vol}(C_i) \;\propto\; \zeta_i^{\mathbb{R}}. \tag{VI.4.31}$$

There are $r = \#\{\text{nodes}\} - 1$ of them, exactly the number of independent levels left by the constraint (VI.4.3), and exactly the rank of the finite ADE algebra. The dictionary between nodes and curves is simple to state: one compact curve C_i for each nontrivial representation R_i, the trivial representation contributing none. *(Optional.)* The precise pairing is through the *tautological bundle* $\mathcal{T}_j$ that the resolution attaches to R_j, a vector bundle on the resolved surface rather than the representation itself, whose first Chern class is dual to the exceptional curves,

$$\int_{C_i} c_1(\mathcal{T}_j) = \delta_{ij}, \tag{VI.4.32}$$

established in Part I. Sending some $\zeta_i^{\mathbb{R}} \to 0$ collapses the matching curves, a partial resolution we lay out below.

How these curves sit against one another is fixed, and it is the geometric content of the McKay correspondence. Each is a rational curve of self-intersection -2, and two of them meet transversally exactly when their nodes are adjacent, so the matrix of intersection numbers is

$$C_i \cdot C_j \;=\; -\,C_{ij}^{\text{fin}}, \tag{VI.4.33}$$

minus the *finite* ADE Cartan matrix: diagonal -2, off-diagonal $+1$ for adjacent curves and 0 otherwise. The dual graph of the exceptional divisor, a node per curve and an edge per intersection, is therefore the finite ADE Dynkin diagram. Compare this with the McKay quiver of Chapter 3, which was the *affine* Dynkin diagram, $a_{ij} = 2\delta_{ij} - \hat{C}_{ij}$ with $\hat{C}$ the affine Cartan matrix. The two differ by exactly one node:

$$C^{\,\text{fin}} \;=\; \big(2\,\mathbb{1} - a\big) \text{ with the trivial-irrep row and column deleted.} \tag{VI.4.34}$$

The trivial representation is the affine node, and it has no exceptional curve. The McKay quiver is the intersection graph plus that one extra node (Figure VI.4.5).

Return to the Q_8 example of the previous section and read off how its curves meet. Deleting the affine node, the trivial representation, from the five-node $\hat{D}_4$ leaves the four-node D_4: a central curve C_c (the subscript c for "central", not the deleted affine node 0), dual to the two-dimensional representation, met by three outer curves C_1, C_2, C_3, dual to the three nontrivial one-dimensional representations. The four are (-2)-curves with the D_4 intersection form,

$$C_i \cdot C_j = -C_{ij}^{\text{fin}}(D_4), \qquad \det\big(-\,C_i \cdot C_j\big) = \det C^{\,\text{fin}}(D_4) = 4, \tag{VI.4.35}$$

so the resolution of $\mathbb{C}^2/Q_8$ has four spheres, three meeting a central one, dual to the four nontrivial representations of Q_8. The same deletion carries $\hat{E}_6$ to E_6, turning the six nontrivial representations of $2T$ into six curves, and runs the same way down the list; the determinant of the intersection form, $\det C^{\,\text{fin}}$, the order of the discriminant group of the ADE root lattice (equally the centre of the simply-connected ADE group), is the ADE index, n for A_{n-1}, 4 for D, and $3, 2, 1$ for $E_{6,7,8}$.

The real levels carry a chamber structure that records how the resolution degenerates. For one regular brane the independent real levels are the r numbers $\zeta_i^{\mathbb{R}}$, one per curve, and the *geometric chamber* is the positive orthant

$$\zeta_i^{\mathbb{R}} > 0 \;\text{ for all } i, \tag{VI.4.36}$$

where every curve has positive area (VI.4.31) and the resolution is the full minimal one. On a wall some $\zeta_i^{\mathbb{R}}$ vanish, the matching curves collapse to zero size while the rest stay finite, leaving a partial resolution with only the nonzero-level curves; the origin, all levels zero, is the unresolved orbifold. For A_2, two curves, the picture is the plane of Figure VI.4.4: the open first quadrant is the smooth surface carrying both curves, each positive axis is a partial resolution with one curve left, and the origin is $\mathbb{C}^2/\mathbb{Z}_3$. Restoring the complex levels $\zeta_i^{\mathbb{C}}$ fattens each real ray into the full triplet of §VI.4.8, trading a collapsed curve for a deformation; the figure is the real slice.

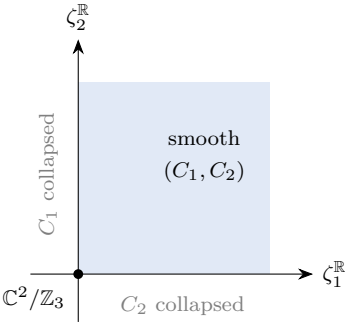


Figure VI.4.4: The Fayet–Iliopoulos chamber for A_2 (real slice, schematic). The open first quadrant $\zeta_1^{\mathbb{R}}, \zeta_2^{\mathbb{R}} > 0$ is the full minimal resolution with both (-2)-curves; on each axis one level vanishes and the corresponding curve collapses, a partial resolution; the origin is the singular orbifold $\mathbb{C}^2/\mathbb{Z}_3$. The complex levels, suppressed here, complete each ray to the $SU(2)_R$ triplet of §VI.4.8.

That the two graphs agree as ADE types is the geometric McKay correspondence, a theorem of the mathematics of surface singularities. We use its statement, the intersection matrix identity (VI.4.33), and route the proof to its home in Part I. What the gauge theory has shown directly is the dual fact, that the resolution computed as the quotient has the right number of curves with the right dimension; the precise intersection form is the geometric input we are matching to.

VI.4.8 Resolution versus deformation

The Fayet–Iliopoulos level is a triplet, $\vec{\zeta} = (\zeta_R, \zeta_{\mathbb{C}})$, one real component and one complex, three real parameters rotated into one another by the $SU(2)_R$ R-symmetry. The two pieces smooth the singularity in two different-looking ways, and keeping them apart is worth a moment.

The split is, before it is geometric, a split in the $\mathcal{N} = 2$ vacuum equations: the two components are the two faces of the Fayet–Iliopoulos coupling and enter different conditions (recall §VI.4.2). The real level ζ_R is the ordinary D-term FI parameter; it sits in the real moment map, deforming D-flatness to $\mu^{\mathbb{R}} = \zeta_R$. The complex level $\zeta_{\mathbb{C}}$ is the complex FI, which in $\mathcal{N} = 1$ language is a *linear* term added to the superpotential,

$$W = \sum_i \operatorname{Tr} \Phi_i \, \mu_i^{\mathbb{C}} \;\longrightarrow\; \sum_i \operatorname{Tr} \Phi_i \big(\mu_i^{\mathbb{C}} - \zeta_{\mathbb{C},i}\, \mathbb{1}\big), \tag{VI.4.37}$$

so that its F-term $\partial W/\partial \Phi_i = \mu_i^{\mathbb{C}} - \zeta_{\mathbb{C},i}$ deforms F-flatness to $\mu^{\mathbb{C}} = \zeta_{\mathbb{C}}$. Both are FI couplings of the node central $U(1)$'s, with no analogue for the trace-free $SU(N_i)$ parts (§VI.4.2), and the eight supercharges unite them into the one $SU(2)_R$ triplet. In case it is not obvious why a superpotential coupling should count as an FI parameter: the $\mathcal{N} = 2$ FI parameter is an $SU(2)_R$ triplet, not a single real number. An $\mathcal{N} = 1$ $U(1)$ admits one real FI, the D-term constant ζ_R; $\mathcal{N} = 2$ promotes it to a triplet whose extra

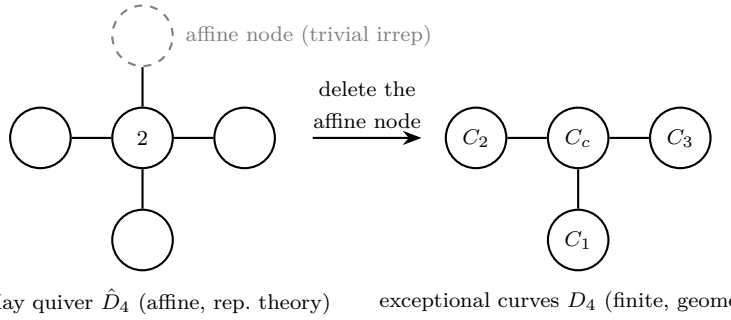


Figure VI.4.5: The geometric McKay correspondence (schematic, drawn for $\Gamma = 2D_2 = Q_8$). Left: the affine $\hat{D}_4$ McKay quiver of Chapter 3, a node per irreducible representation. Right: the dual graph of the exceptional curves of the resolution, a node per (-2)-curve, with edges the intersections (VI.4.33); it is the finite D_4 Dynkin diagram. The two coincide once the affine node, the trivial representation that carries no curve, is removed. Node labels on the left are the Dynkin marks (here only the central 2 is shown).

complex component cannot sit in the D-term and surfaces instead as the linear coupling $\zeta_{\mathbb{C}} \operatorname{Tr} \Phi$, gauge-invariant precisely because $\operatorname{Tr} \Phi$ is. So the resolution is the D-term FI and the deformation is the F-term FI, two faces of one multiplet; the geometric statements below are these two field-theory deformations read off the moduli space.

Turning on the real part ζ_R, with $\zeta_{\mathbb{C}} = 0$, is the *resolution*. The holomorphic moment-map equation is unchanged, while stability and the Kähler class change. The singular point is blown up into the exceptional curves of §VI.4.7, of area $\propto \zeta_R$. Turning on the complex part $\zeta_{\mathbb{C}}$ instead is the *deformation*. Now the defining equation itself changes; for A_1 it smooths from the cone to a nonsingular affine quadric,

$$uv = w^2 \;\longrightarrow\; uv = w^2 + t, \tag{VI.4.38}$$

which has no singular point for $t \neq 0$. Its gradient,

$$\nabla\big(uv - w^2 - t\big) = (v,\, u,\, -2w), \tag{VI.4.39}$$

vanishes only at $u = v = w = 0$, where the equation reads $-t \neq 0$, so the would-be singular point is off the surface. The parameter t is not the raw complex level but a Weyl-invariant function of it: imposing $\mu^{\mathbb{C}} = \operatorname{Tr} M = \zeta_{\mathbb{C}}$ on the rank-at-most-one meson matrix gives $uv = w^2 - \zeta_{\mathbb{C}} w$, and completing the square ($w' = w - \frac{1}{2}\zeta_{\mathbb{C}}$) turns this into $uv = w'^2 + t$ with $t = -\frac{1}{4}\zeta_{\mathbb{C}}^2$, so $t \propto \zeta_{\mathbb{C}}^2$ here. This is the A_1 Weyl group $\mathbb{Z}_2$ acting as $\zeta_{\mathbb{C}} \to -\zeta_{\mathbb{C}}$, with t its invariant. The resolution keeps the affine holomorphic equation and changes its stable quotient, adding an exceptional curve and a Kähler class; the deformation changes the complex structure without switching on a Kähler resolution class in it. At fixed complex structure these are genuinely different operations.

They nevertheless give the same Riemannian manifold. The hyperkähler metric is unchanged when all the levels are rotated together by a common $SU(2)_R$ element. For

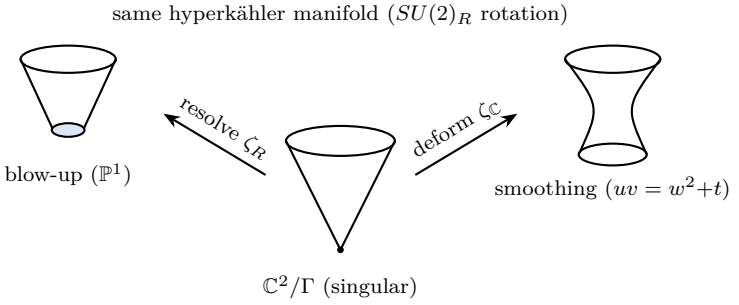


Figure VI.4.6: Resolution and deformation in the A_1 model (schematic). The Kähler resolution (ζ_R, left) blows the tip up into a $\mathbb{P}^1$; the complex deformation ($\zeta_{\mathbb{C}}$, right) smooths the defining equation to a quadric with a neck. For levels related by a common $SU(2)_R$ rotation the two are the same Riemannian four-manifold (for the single A_1 triplet, equal $|\vec{\zeta}|$); the picture distinguishes operations at fixed complex structure, not spaces.

a single triplet, the A_1 case with its one curve, that common rotation preserves only the length

$$|\vec{\zeta}|^2 = \zeta_R^2 + 4|\zeta_{\mathbb{C}}|^2, \tag{VI.4.40}$$

so there the metric depends on the level through $|\vec{\zeta}|$ alone, and a pure resolution ($\zeta_{\mathbb{C}} = 0$) and a pure deformation ($\zeta_R = 0$) of equal $|\vec{\zeta}|$ are the same hyperkähler four-manifold in two frames, related by a hyperkähler rotation (Figure VI.4.6); for higher rank the invariant is the common $SU(2)_R$ orbit of the whole set of triplets, not one scalar. For A_1 (a single triplet) this is why one space can be called the resolution of $\mathbb{C}^2/\Gamma$ or its smoothing with equal right: the names refer to which corner of the triplet is switched on, a choice of $SU(2)_R$ frame. For higher-rank ADE with non-collinear triplets the relative angles are genuine metric data, and resolution and deformation, while still two faces of one hyperkähler family, are not interchangeable descriptions of a single fixed space.

Resolution versus deformation: two frames of the A_1 metric.

	resolution	**deformation**
FI part on	ζ_R (real)	$\zeta_{\mathbb{C}}$ (complex)
affine equation	kept, stability changed	deformed
Kähler class	turned on (curve gains volume)	unchanged
A_1 model	exceptional $\mathbb{P}^1$ (an S^2)	$uv = w^2{+}t$, $t \propto \zeta_{\mathbb{C}}^2$ (T^*S^2)

These are genuinely different operations at *fixed* complex structure, but they build the *same* hyperkähler four-manifold: a common $SU(2)_R$ rotation exchanges $\zeta_R \leftrightarrow 2\,\mathrm{Re}\,\zeta_{\mathbb{C}}$ and leaves the metric fixed (for one A_1 triplet, the invariant is $|\vec{\zeta}|$). The exceptional $\mathbb{P}^1$ of the blow-up and the vanishing cycle of the smoothing are then the *same* two-sphere S^2 in two frames. "Resolution" and "deformation" name which corner of the triplet is on, not two different spaces. For higher-rank ADE this equivalence holds only for FI data in a common $SU(2)_R$ orbit; a set of non-collinear triplets has relative angles that are genuine metric data, not removable by one rotation.

VI.4.9 What the construction does and does not give

The construction delivers the Higgs branch of the regular-brane $\mathcal{N} = 2$ quiver as a hyperkähler quotient, with the smallest case worked in closed form: the moment-map level set (VI.4.2), the quaternionic dimension one, the $\mathbb{Z}_2$ quotient yielding $\{uv = w^2\}$ at zero level and the Eguchi–Hanson metric at generic level, the exceptional curves and their intersection form, and the resolution/deformation split. It is worth marking where the elementary part stops.

The existence and completeness of the metric, and the statement that the quotient exhausts the ALE hyperkähler spaces (the gravitational instantons of §VI.4.4), are Kronheimer's theorem, quoted and not proved here; that mathematics, the hyperkähler quotient as differential geometry and the classification of ALE gravitational instantons, has its home in Part I. No explicit metric beyond the A series was written: the quotient is uniform across ADE, but only the A series has an elementary closed form, the Gibbons–Hawking multi-centre family of §VI.4.5, and the D, E metrics were left as the quotient defines them. The Eguchi–Hanson metric (VI.4.8) we did write was presented and checked Ricci-flat, the consistency a hyperkähler metric demands; it was not re-derived from the quotient by a metric computation, which is Kronheimer's content, and the agreement of the two is the standard result we are using.

The distinction between the field-theory metric and the closed-string metric of Chapter 1 remains. The hyperkähler metric of the field-theory Higgs branch is itself an $\mathcal{N} = 2$-protected quantity, fixed by the quiver data and computed by the quotient in the rigid four-dimensional theory under discussion. The caveat is the identification of that branch with the geometry the closed strings see: the probe extracts the holomorphic data encoded in the chiral ring, while the identification with a closed-string target metric additionally requires the probe limit and a choice of string background. The quotient calculation alone does not determine finite-α' or finite-g_s corrections. The count above

was for one regular brane. For N regular branes we assume the unframed quiver with ranks $N\delta_i$, the same canonical hypermultiplet metric and a common fixed spectator. On this branch the regular one-brane level is kept fixed. The branch of separated regular summands and its closure is Sym^N of the ALE surface, with quaternionic dimension N. The generic stabilizer inside $(\prod_i U(N\delta_i))/U(1)_{\mathrm{diag}}$ is $U(1)^{N-1}$. Blindly substituting $N\delta_i$ into (VI.4.14) would still give one, because that subtraction assumed a free action. The stabilizer restores the missing $N-1$ dimensions. At coincident points the symmetric product is singular; this construction is not the Hilbert-scheme resolution, and does not describe all mixed or fractional-brane branches at a wall.

Two threads are left open by design. The exceptional curves built here are the geometric support for the *fractional* branes of the next chapter: after resolution a fractional brane admits a description as a brane (or brane complex) supported on the exceptional cycles, with flux and B-field data carrying the lower-dimensional charges, and at the orbifold point the cycles collapse and the object is pinned to the singular locus; Chapter 5 gives this geometric and derived-category reading. A second thread concerns B-type data, where two notions must not be merged. The *continuous* B-field periods through the exceptional curves complexify the Kähler/Fayet–Iliopoulos parameters and return with the fractional-brane charges of Chapter 5. *Discrete torsion* is a different choice: a projective phase in the orbifold/Chan–Paton action that can change the quiver projection itself, treated in Chapter 9. Here the geometry has been built; there it is populated and twisted.

Status and sources

The mathematical tag ([MATH], with proof status stated) and the physical-input descriptions, the convention pointers, and the source anchors are collected here, keyed by section. The construction is the hyperkähler-quotient realization of the regular-brane Higgs branch, Kronheimer (1989b) read through the brane probe of Douglas and Moore (1996), with the graph correspondence of McKay (1980) and the geometric bundle theorem of Gonzalez-Sprinberg and Verdier (1983); it continues the $\mathbb{C}^2/\Gamma$ thread of Chapter 3 and uses the resolution and Fayet–Iliopoulos data conventions at their first load-bearing chapter. Selected calculations in the dimension count, the finite-versus-affine Cartan identity, the $\mathbb{Z}_2$ invariant relation $uv = w^2$, the $U(1)$ quotient charts and all ten components of the Eguchi–Hanson Ricci tensor are evaluated for the stated local metric.

The finite calculations are not as a proof of every statement above. In particular, their orthogonality test uses an abstract Euclidean three-vector and does not fix the relative normalization of the displayed real and complex moment maps. Equation (VI.4.40) uses the normalization derived in §VI.4.2. The stated formula gives this identity directly, together with three bounded exercises. Stored supersymmetry labels and curve-area signs remain imported physical or geometric premises. The geometric McKay theorem, invariant-ring generation for D_4, E_6, ALE classification, and the metric/probe dictionary are not established by a finite set of matrix or polynomial evaluations. Source locators are specified below. Other imported claims retain explicit locator debt in the accompanying inventory. Physical dictionary statements have unresolved primary classification; none inherits [MATH] from an adjacent algebraic result. Overview boxes and repeated section summaries retain these same premises. The outer-product determinant calculation also applies at the zero meson. No physical-worldsheet derivation is performed in this chapter.

§VI.4.1 The moduli space of vacua. Framing and the recipe box (moduli space = D/F-flat / gauge = hyperkähler quotient), continuing Chapter 3's named Higgs branch. These repeat the physical assumptions of the action and fixed adjoints, with no new evidence class.

§VI.4.2 The moduli space is a hyperkähler quotient. The moment maps (VI.4.1), the hyperkähler quotient (VI.4.2), and the Fayet–Iliopoulos constraint (VI.4.3) are physical input (resolution and discrete data, the FI level/triplet and the full-U quotient with $\sum_i N_i\zeta_i = 0$; quiver gauge groups and ranks the gauge data; superpotential normalization the F-term moment map; spinor and supersymmetry counting the eight supercharges giving the $SU(2)_R$ triplet). The trivially-acting diagonal $U(1)$ and the resulting constraint are evaluated; the moment map is the $\mathcal{N} = 2$ object inherited from Chapter 3.

§VI.4.3 The smallest case: $\mathbb{C}^2/\mathbb{Z}_2$ and Eguchi–Hanson. The $\hat{A}_1$ quiver (Figure VI.4.1), the abelian moment maps (VI.4.4), the rank-at-most-one meson relation (VI.4.5) and the invariant ring $uv = w^2$ (VI.4.6), and the Eguchi–Hanson metric (VI.4.8) with its bolt $\mathbb{P}^1$ (Figure VI.4.2) are the worked instance, physical input for the brane spectrum and FI dictionary. The determinant and chart derivations are [MATH]; the metric and smooth-bolt statement are quoted mathematics from Eguchi and Hanson (1978). The $\mathbb{Z}_2$ invariant polynomials and relation, the local quotient charts, and local Ricci-flatness of (VI.4.8) have algebraic checks; the two-patch bundle argument establishes the (-2)-curve. The checks are.

§VI.4.4 Kronheimer's construction in general. The uniform quotient, the dimension count (VI.4.14)–(VI.4.15) giving $\dim_{\mathbb{H}} = 1$ via the Chapter 3 null vector, and Kronheimer's existence/completeness/classification have different roles. The brane interpretation /Q2 is physical input. The dimension identity is a conditional [MATH] derivation. The existence/completeness construction is imported mathematics from Kronheimer (1989b); exhaustive classification and period uniqueness use the separate Kronheimer (1989a) (resolution and discrete data; the ALE hyperkähler construction, home Vol. IV). Their exact theorem locators remain unresolved here. The inspected Douglas and Moore (1996, §2.1 and §8.1, eqs. (8.11)–(8.12)) distinguishes the period theorem and cyclic probe comparison and cites both works. For the ADE physical construction, Johnson and Myers (1996, §§2.3–2.4 and 3.2–3.3) gives the regular representation, hypermultiplets and FI quotient for a D1 probe. Its extension to this chapter's prescribed D3 action remains a physical premise, with its D3 source support still unresolved. The dimension is obtained from both graph descriptions. The dimension count and the quotient formula are recalled from Chapter 3; the new content of this chapter is the metric and the resolution geometry.

§VI.4.5 The A series in closed form. The $\mathbb{Z}_n$ invariant ring $xy = w^n$ (VI.4.17) is recalled from VI.2 (the necklace mesonic branch); new here are the Gibbons–Hawking metric (VI.4.18) with its n centres (VI.4.19) and the $n-1$ chain of curves with vol $\propto$ centre separation (VI.4.20),. The GH ansatz, smooth period and lens end are quoted [MATH] geometry (Gibbons and Hawking (1978); resolution and discrete data), with precise locator debt. The segment-area determinant and EH bolt-area comparison are conditional mathematical derivations. The FI-to-centre map remains physical input. The exercise computes the areas and bolt scale from that metric. The displayed cyclic invariant polynomials and their relation are checked for $n = 2$–5; A_1 = two-centre = Eguchi–Hanson, and the general-n Ricci-flatness is the standard harmonic-function statement with the A_1 instance verified.

§VI.4.6 Non-abelian examples: D_4 and E_6. The two non-abelian worked instances, physical input (McKay multiplicities, resolution and discrete data): the Q_8 invariant ring $x^2 = yz^2 - 4y^3$ (VI.4.22) (the D_4 du Val) with its generators (VI.4.21) and three-line factorization, the genuinely non-abelian matrix-node $(U(2), U(3))$ quotient with $\dim_{\mathbb{H}} = 1$; and the $2T$ ring $x^2 = y^3 - 108z^4$ (VI.4.30) (the E_6 du Val) with generators f_6, g_8, H_{12} (VI.4.29) of degrees $6, 8, 12$ obtained by Reynolds averaging over the twenty-four elements. For Q_8 the Higgs branch is computed *from the quiver* ((VI.4.23)–(VI.4.27)): the per-edge $C_i = B_iA_i$ are rank-at-most-one nilpotent $\mathfrak{sl}_2$ elements ($\mathrm{Tr}\, C_i = 0$, $C_i^2 = 0$) summing to zero by the F-terms, and the two-loop/three-loop invariants $p_{ij} = \mathrm{Tr}(C_iC_j)$, $q = \mathrm{Tr}(C_1C_2C_3)$ obey $q^2 = -p_{12}p_{13}p_{23}$ with $\sum p_{ij} = 0$, which the change (VI.4.27) turns into the same D_4 ring (VI.4.22) (the non-abelian counterpart of the A_1 meson computation of §VI.4.3, resting on Kronheimer's theorem made explicit). The displayed ring relations and the generators' Γ-invariance (the $2T$ case built literally by averaging over the 24 matrices, with closure and $SU(2)$ membership guarded), and the displayed Q_8 matrix identities (each C_i nilpotent, the loop identities, $\det C_4 = -(\sum p_{ij})$, and the $x^2 = yz^2 - 4y^3$ relation) are evaluated; the four / six D_4 / E_6 curves and intersection forms are the finite calculation. Full ring generation is imported, not established by those identities. For E_6 the arm nilpotency implications are verified symbolically (each arm integrated out gives a nilpotent $N_a = B_aA_a \in \mathfrak{sl}_3$ with $N_a^3 = 0$ and $N_a^2 = B_acA_a$ generically nonzero (regular), summing to zero). The full central affine quotient and its orbit closures remain imported geometry. Compatibility with the E_6 surface $x^2 = y^3 - 108z^4$ is tested on numerical samples (the numerical calculation: a fit of conjugation

invariants on sampled regular configurations is compatible with an E_6-type relation, the -108 being the $f_6/g_8/H_{12}$ normalization); the exact-symbolic $\mathfrak{sl}_3$ invariant ring is left as the reader's exercise. The D and E metrics are not elementary (quotient plus Kronheimer); only the algebra is written there.

§VI.4.7 The exceptional cycles and the geometric McKay correspondence. The exceptional curves with $\mathrm{vol}(C_i) \propto \zeta_i^{\mathbb{R}}$ in the geometric chamber (VI.4.31), the count $r = \#\text{nodes} - 1 = \text{rank}$, the node-curve pairing by the tautological-bundle Chern class (VI.4.32), the intersection matrix $C_i \cdot C_j = -C_{ij}^{\text{fin}}$ (VI.4.33), and the finite-as-affine-minus-affine-node identity (VI.4.34) are physical input for the FI/area identification. The mathematical graph statement is in McKay (1980); the tautological-bundle theorem is [MATH], quoted from Gonzalez-Sprinberg and Verdier (1983, Theorem 2.2(i), p. 415, §2.7 and Corollary 2.9, pp. 417–418). Its bundle convention and the dual Picard basis give (VI.4.32) (McKay multiplicities, resolution and discrete data; the finite-group and geometric McKay correspondence, home Vol. IV; the tautological bundle and its duality are the mathematical input, proof routed to Part I). The intersection matrix computed two independent ways (finite Dynkin graph versus the affine McKay adjacency with the trivial node deleted), the determinant for the stated examples, and the trivial-node identification (via the all-ones character of the constructed Γ) are obtained directly from the character data. The geometric intersections and chamber signs are inputs to these comparisons; The finite determinant comparisons do not cover E_7 and E_8. The affine-McKay-versus-finite-intersection distinction is (refines the stated distinction); its keybox statement is in Chapter 3.

§VI.4.8 Resolution versus deformation. The triplet split $\vec{\zeta} = (\zeta_R, \zeta_{\mathbb{C}})$, the resolution (blow-up, ζ_R) against the deformation (smoothing $uv = w^2 + t$ with the Weyl-invariant parameter $t \propto \zeta_{\mathbb{C}}^2$, (VI.4.38)), and their identification by hyperkähler rotation are physical input (resolution and discrete data, resolutions at $\zeta_{\mathbb{C}} = 0$ and the $SU(2)_R$ frame). The deformation's smoothness for $t \neq 0$, the $t = -\frac{1}{4}\zeta_{\mathbb{C}}^2$ relation from the meson ring at $\mu^{\mathbb{C}} = \zeta_{\mathbb{C}}$, and the A_1 blow-up chart identities are machine/This files (the counterpart of the resolution and discrete data convention "resolutions at $\zeta_{\mathbb{C}} = 0$").

§VI.4.9 What the construction does and does not give. The metric existence/completeness and separate Torelli/classification results are cited, not proved (Kronheimer, the ALE hyperkähler construction, Vol. IV); the explicit D, E metrics not written (uniform quotient only; the A-series Gibbons–Hawking named); the Eguchi–Hanson metric verified Ricci-flat but not re-derived from the quotient; the probe-limit α'/g_s caveat and the Sym^N branch for N regular branes at ranks $N\delta_i$, conditional on separated regular summands and their geometric closure (the stated distinction, inherited from VI.1; primary physical classification unresolved); the Higgs-not-Coulomb naming. Forward references: fractional/wrapped branes on the exceptional cycles and their derived-category reading are Chapter 5; the continuous B-field/Kähler periods and the separate discrete-torsion (projective Chan–Paton) orbifold phase are Chapter 9.

References

Douglas, M. R. and G. W. Moore (1996). "D-branes, quivers, and ALE instantons". In: arXiv preprint; not published in a journal. arXiv: hep-th/9603167.

Eguchi, T. and A. J. Hanson (1978). "Asymptotically Flat Selfdual Solutions to Euclidean Gravity". In: *Phys. Lett. B* 74, pp. 249–251. DOI: 10.1016/0370-2693(78)90566-X.

Gibbons, G. W. and S. W. Hawking (1978). "Gravitational Multi-Instantons". In: *Phys. Lett. B* 78, pp. 430–432. DOI: 10.1016/0370-2693(78)90478-1.

Gonzalez-Sprinberg, G. and J.-L. Verdier (1983). "Construction géométrique de la correspondance de McKay". In: *Annales scientifiques de l'École Normale Supérieure*. 4th ser. 16.3, pp. 409–449.

Johnson, C. V. and R. C. Myers (1996). "Aspects of Type IIB Theory on ALE Spaces". In: arXiv: hep-th/9610140.

Kronheimer, P. B. (1989a). "A Torelli-type theorem for gravitational instantons". In: *Journal of Differential Geometry* 29.3, pp. 685–697. DOI: 10.4310/jdg/1214443067.

Kronheimer, P. B. (1989b). “The construction of ALE spaces as hyper-Kähler quotients”. In: *J. Differential Geom.* 29.3, pp. 665–683.
McKay, J. (1980). “Graphs, singularities, and finite groups”. In: *Proc. Symp. Pure Math.* 37. American Mathematical Society, pp. 183–186.

Chapter VI.5

Fractional branes and the wrapped-brane interpretation

VI.5.1 What is left to say about the fractional brane

The orbifold D3 probe has one fractional brane for each irreducible representation of $\Gamma \subset SU(2)$, yet resolving $\mathbb{C}^2/\Gamma$ produces one fewer exceptional curves. The missing direction is the point charge of a mobile D3. A fractional brane generally has both point and wrapped charge; the regular combination cancels the wrapped charge and can leave the fixed locus. To see why, we first recall how the two descriptions arise.

Chapter 2 put a D-brane at the $\mathbb{C}^2/\Gamma$ singularity and read off, from the orbifold projection, an *operational* fractional brane: a single irreducible representation R_i in the Chan–Paton choice, the rank vector $(0, \dots, 1, \dots, 0)$, the smallest piece into which the regular brane decomposes. It came with two slogans, "it wraps a collapsed cycle" and "it is stuck," used as names, not as statements. Chapter 3 organized the $r{+}1$ pieces into the nodes of the affine ADE quiver, with the Dynkin marks $m_i = \dim R_i$ as multiplicities. Chapter 4 resolved the singularity and built the geometry the pieces were meant to live on, the ALE (asymptotically locally Euclidean) space, but produced only r compact exceptional curves $C_a \cong \mathbb{P}^1$, one per *nontrivial* node, paired by an intersection form equal to minus the finite ADE Cartan matrix. So the first slogan cannot literally mean "one independent curve per fractional brane": there are $r{+}1$ fractional branes and only r curves. Resolving that mismatch, by computing the actual charge vectors, is the whole of this chapter.

Recalled from Chapters 1–4 (used, not re-derived).

Ch. 1 the D3 probe and its worldvolume gauge theory; moduli space = transverse geometry; the probe reads the local geometry up to α'/g_s corrections.
Ch. 2 the operational fractional brane = one irrep in the Chan–Paton choice, rank vector $(0,\dots,1,\dots,0)$; the regular brane = the regular representation = a bound state of fractionals; the twisted-sector boundary state; "stuck at the singularity."
Ch. 3 the affine ADE McKay quiver: nodes = irreps R_i, Dynkin marks $\dim R_i$, adjacency a_{ij}; the marks are the null vector of the affine Cartan matrix.
Ch. 4 the resolved $\mathbb{C}^2/\Gamma$ (the ALE space): $r = (\#\text{nodes} - 1)$ exceptional curves $C_i \cong \mathbb{P}^1$, one per nontrivial node; $\mathrm{vol}(C_i) \propto \zeta_i^{\mathbb{R}}$; intersection form $C_i \cdot C_j = -C_{ij}^{\mathrm{fin}}$ (the (-2)-curves of the du Val resolution).

The question is not whether the fractional branes are "wrapped branes," a name already in hand, but what their actual charge *vectors* are. The answer, derived below, is that the charge calculation uses the rank-$(r{+}1)$ point-and-curve lattice $H_0(X) \oplus H_2(X)$. In the torsion-free local sector, the fractional classes form a different integral basis after a charge convention is chosen. Their *projections* to the root lattice, rather than the full classes, obey the affine-root relation:

$$\pi_{H_2}(f_a) = C_a \quad (a = 1,\dots,r), \qquad \pi_{H_2}(f_0) = -\theta = -\sum_{a=1}^{r} m_a C_a,$$
$$R_{\mathrm{reg}} = \sum_{i=0}^{r} m_i f_i \in H_0(X), \tag{VI.5.1}$$

The nontrivial nodes project to simple curves, the affine node to minus the highest root θ, and their marks-weighted sum to zero. That sum is the mobile bulk D3. The A_1 and D_4 examples compute these relations and separate collapsed area from finite fractional-brane tension.

We start with the A_1 counterexample (§VI.5.2), then use the wrapped-D5 coupling and the charge lattice to identify the affine node (§VI.5.3–§VI.5.4). The tension and continuation sections explain what changes as the curve collapses (§VI.5.5–§VI.5.6). Worked A_1 and D_4 examples follow (§VI.5.7); the optional K-theory section refines the charge description (§VI.5.8).

VI.5.2 The first puzzle: $r{+}1$ fractional branes, r curves

The mismatch of §VI.5.1 is the place to start, because the obvious way to fix it is wrong, and seeing exactly why is most of the construction. The naive dictionary matches each fractional brane to a homology generator, the affine node to the point class and each nontrivial node to its curve,

$$f_0 \stackrel{?}{=} [\mathrm{pt}] \in H_0, \qquad f_a \stackrel{?}{=} [C_a] \in H_2 \quad (a = 1,\dots,r). \tag{VI.5.2}$$

It has the right count, one point direction and r curves filling out a rank-$(r{+}1)$ lattice, and it is what "f_0 is the trivial representation, so it carries no curve" seems to suggest. It is also false, and A_1 kills it in two lines.

For $A_1 = \mathbb{C}^2/\mathbb{Z}_2$ there are two nodes and one curve C. The charge pairing on the fractional branes is the affine Cartan matrix of the $\widehat{A}_1$ quiver (the identity charge pairing = affine Cartan is derived in §VI.5.4; here we just use it),

$$\widehat{C} = \begin{pmatrix} 2 & -2 \\ -2 & 2 \end{pmatrix}. \tag{VI.5.3}$$

If f_0 were the pure point charge it would lie in the *radical* of this pairing, pairing to zero with every node: a point charge wraps nothing, so it meets no curve. But $\widehat{C}_{01} = -2 \neq 0$, so f_0 pairs nontrivially with f_1 and is not in the radical. The vector that does pair to zero with both nodes is the null vector,

$$\widehat{C}\begin{pmatrix} 1 \\ 1 \end{pmatrix} = 0, \tag{VI.5.4}$$

namely $f_0 + f_1$, the *regular* brane, not f_0. The pure point charge is a marks-weighted *combination* of fractional branes, never a single one. That two-line calculation forces the chapter: the fractional branes are one basis of the charge lattice, the homological generators $H_0 \oplus H_2$ are another, and the two bases are not aligned.

Three descriptions of the fractional charge fix vocabulary for what follows; two are recalled, the third is the new one.

face	description	natural regime
algebraic (Ch. 2)	irrep R_i, a simple Chan–Paton choice	the quiver
worldsheet (Ch. 2)	twisted Cardy state $\|R_i\rangle\!\rangle$, twisted RR charge	orbifold point
geometric (this ch.)	charge vector $f_i \in H_0(X) \oplus H_2(X)$	large radius

The geometric face is the new content, and the table already flags the trap: it is a *charge vector*, not "one curve per node." Its wrapped projection is C_a for a nontrivial node and $-\theta$ for the affine node (§VI.5.4); only the marks-weighted regular representation,

$$R_{\text{reg}} = \bigoplus_i (\dim R_i)\, R_i, \qquad \sum_i (\dim R_i)^2 = |\Gamma|, \tag{VI.5.5}$$

has the charge of a mobile point brane. The three faces match conserved charge classes; the module and binding maps that specify an object enter in §VI.5.8. Their natural regimes are compared in §VI.5.6. The rest of the chapter builds the dictionary: the wrapped-brane interpretation (§VI.5.3), the charge it carries (§VI.5.4), its tension (§VI.5.5), and the continuation of the orbifold-point and large-radius faces into one another (§VI.5.6).

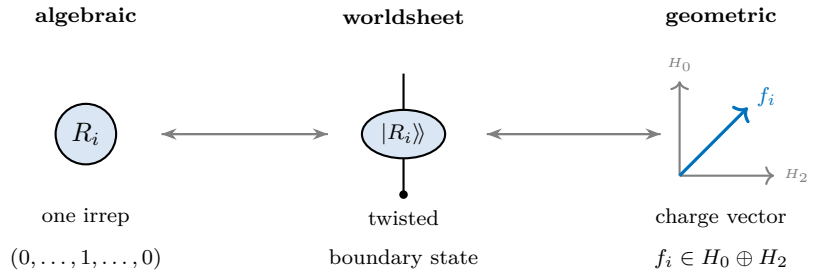


Figure VI.5.1: Three descriptions of a fractional-brane charge (schematic). The algebraic face (an irrep / a one-entry rank vector) and the worldsheet face (a twisted-sector boundary state) are the orbifold-point descriptions of Chapter 2; the geometric face is the large-radius description of this chapter, a *charge vector* $f_i \in H_0 \oplus H_2$, not one independent curve per node. Its wrapped projection is $\pi_{H_2}(f_a) = C_a$ for a nontrivial node and $\pi_{H_2}(f_0) = -\theta$ for the affine node, and only the marks-weighted regular brane is a pure point charge (§VI.5.4). The double arrows match conserved charge classes across descriptions. The binding data needed to specify an object are discussed in §VI.5.8.

Warm-up: $A_1 = \mathbb{C}^2/\mathbb{Z}_2$ at a glance.

This calculation already gives the answer for the smallest orbifold: two irreps (trivial and sign), marks $(m_0, m_1) = (1, 1)$, one exceptional curve C. Writing π_{H_2} for the wrapped (H_2) charge (made precise in §VI.5.4):

brane	Chan–Paton	π_{H_2}	mobility
f_0	trivial	$-C$	stuck
f_1	sign	$+C$	stuck
$R_{\text{reg}} = f_0 + f_1$	regular	0	bulk-D3 charge

Both fractional branes wrap the single curve with opposite charge; only their marks-weighted sum, the null vector $(1, 1)$ of $\widehat{C}$ above, has zero wrapped charge. The corresponding mobile point object also requires binding maps. The general $\pi_{H_2}(f_0) = -\theta$ of §VI.5.4 is just "$-C$" here. We return to A_1 as a running check, and in full in §VI.5.7.

VI.5.3 The wrapped-brane identity

Why is the wrapped object a $D(p{+}2)$, and what kind of D3 charge can it carry? The first question begins with dimensions. A Dp-brane fills $p{+}1$ noncompact worldvolume directions; if the same brane is really a $D(p{+}q)$ wrapping a compact q-cycle in the internal space, then to an observer in the noncompact directions it still looks like a Dp-brane, because

$$(p{+}q){+}1 = (p{+}1) + q, \tag{VI.5.6}$$

the q wrapped directions being invisible at long distance. The geometry must supply the compact cycle. This count alone does not establish a decoupled worldvolume theory for every p; the D3 probe is the case used here.

The resolved ALE space answers it. Its compact homology is

$$H_0(X) \oplus H_2(X), \qquad \operatorname{rank} H_2(X) = r = \#\text{nodes} - 1, \qquad H_4(X) = 0, \tag{VI.5.7}$$

a non-compact four-manifold whose only compact cycles are the point class and the r exceptional curves; there is no compact four-cycle. A brane can sit at a point (it does not wrap) or wrap a 2-cycle, and nothing else. Within this wrapped-brane interpretation $q = 2$,

$$\text{fractional } Dp \;=\; D(p{+}2) \text{ wrapped on a compact 2-cycle.} \tag{VI.5.8}$$

For the D3 probe of Chapters 1–4, $p = 3$, so the wrapped brane is a D5, whose six-dimensional worldvolume splits as

$$(\text{D5 worldvolume}) \;=\; \mathbb{R}^{1,3} \times C_a, \qquad \text{at a point of } \mathbb{C}_{z_3}, \tag{VI.5.9}$$

filling the four spacetime directions of the probe and wrapping the two real dimensions of a curve C_a, at a fixed point of the spectator line $\mathbb{C}_{z_3}$. From four dimensions it looks like a spacetime-filling D3, but it is a wrapped D5. The familiar template, named once, is the conifold: a fractional brane there is a D5 wrapping the single $\mathbb{P}^1$ of the resolved conifold, a Calabi–Yau threefold treated on its own terms in Chapter 6; we borrow only the picture, a D5 on a small two-sphere.

A wrapped D5 is never *only* a wrapped class, and this too is forced, by its couplings. Through the Wess–Zumino term a D-brane couples to the Ramond–Ramond potentials as

$$S_{\mathrm{WZ}} = \mu_5 \int_{\mathbb{R}^{1,3}\times C} \sum_q C_q \wedge e^{B+2\pi\alpha' F}, \tag{VI.5.10}$$

so the C_4 coupling picks up a signed flux period over the oriented cycle. Its brane-source contribution is

$$Q_{\mathrm{D3}}^{\mathrm{source}} \;\propto\; \int_C \big(B + 2\pi\alpha' F\big), \tag{VI.5.11}$$

Reversing the orientation of C reverses this signed period. The B-dependent source coupling is distinct from quantized Page charge: in a fixed B gauge the latter removes the B factor from the RR charge vector and retains the worldvolume flux, including any required shifts. The lattice below concerns integral charge classes, while the displayed C_4 coupling can vary with B. A wrapped D5 can have both point and wrapped components, and a combination can cancel the wrapped part.

The orbifold boundary state supplies a separate normalization. Assign unit untwisted charge to one bulk D3. A single irrep-labelled constituent then carries

$$Q_{\mathrm{untw}}(f_i) = \frac{\dim R_i}{|\Gamma|}, \qquad Q_{\mathrm{untw}}(R_{\mathrm{reg}}) = \sum_i (\dim R_i)\frac{\dim R_i}{|\Gamma|} = 1. \tag{VI.5.12}$$

The first $\dim R_i$ measures one constituent's untwisted charge; the second is its multiplicity in the regular representation. This normalization alone does not select an integer Page-flux representative at large radius.

That combination is the marks-weighted regular brane,

$$[\text{mobile D3}] \;=\; [R_{\text{reg}}] \;=\; \sum_i (\dim R_i)\,[f_i], \tag{VI.5.13}$$

a combination of $\sum_i \dim R_i$ fractional constituents of Chapter 2. The number $|\Gamma| = \sum_i (\dim R_i)^2$ instead counts Chan–Paton dimensions; this is where the name comes from, each f_i carrying only a *fraction* of the mobile brane's charge, so that it takes the whole marks-weighted set to assemble a brane that can leave the fixed point, and conversely a single regular D3 brought to the singularity can split into them. "D5 on a curve" is still shorthand, though. The next section computes the actual H_2 projections of all $r{+}1$ fractional branes, and shows in particular that the affine node is *not* a pure point charge but carries wrapped charge $-\theta$; which brane carries which charge, and which one moves, is settled there.

VI.5.4 The charge lattice

This is the main derivation, and it is pure linear algebra. There are two ways to label charges and they must be kept apart. The *geometric* basis is the local homological approximation $H_0(X) \oplus H_2(X)$: one point-charge direction and the r exceptional curves. The *fractional-brane* basis is the $r{+}1$ simple branes f_i, one per node. Let $\pi_{H_2} : H_0 \oplus H_2 \to H_2$ forget the point component and record only the wrapped part. The mismatch of §VI.5.2 is now sharp: π_{H_2} sends $r{+}1$ fractional branes into a rank-r wrapped lattice, so the f_i cannot project to independent curves. §VI.5.3 supplied the extra rank: a wrapped D5 carries an induced point charge (VI.5.11), so the point-and-curve charge lattice used here is

$$\text{charge lattice} \;=\; H_0(X) \oplus H_2(X), \qquad \text{rank} = r + 1 = \#\text{nodes}, \tag{VI.5.14}$$

the r curves spanning the wrapped sublattice H_2 and the point class supplying the extra rank-one direction.

Fix the convention on the nontrivial nodes,

$$\pi_{H_2}(f_a) = C_a \qquad (a = 1, \dots, r). \tag{VI.5.15}$$

The affine node's projection is then *forced*, not chosen. The mobile brane is the marks-weighted regular brane $R_{\text{reg}} = \sum_i m_i f_i$ (marks $m_i = \dim R_i$, $m_0 = 1$), and a point brane in the bulk wraps nothing, $\pi_{H_2}(R_{\text{reg}}) = 0$; expanding,

$$0 = \pi_{H_2}(R_{\text{reg}}) = m_0\,\pi_{H_2}(f_0) + \sum_{a=1}^{r} m_a C_a \quad\Longrightarrow\quad \pi_{H_2}(f_0) = -\sum_{a=1}^{r} m_a C_a = -\theta, \tag{VI.5.16}$$

minus the highest root $\theta = \sum_a m_a C_a$. The affine node thus has no curve of its own yet carries a definite wrapped charge: a genuine fractional brane, not a point brane. The $r{+}1$ fractional classes span the point-and-curve lattice, while their wrapped projections are affine roots satisfying one relation. Their point components lift that relation, so the full classes remain independent. No single f_i is the mobile point brane.

The pairing makes this rigid. In the fractional-brane basis the charge pairing is the symmetric Calabi–Yau-two Euler form, which equals the affine Cartan matrix

$$\widehat{C}_{ij} \;=\; 2\delta_{ij} - a_{ij}, \tag{VI.5.17}$$

with a_{ij} the McKay adjacency of Chapter 3. Set $\alpha_a = C_a$ $(a = 1, \dots, r)$ and $\alpha_0 = -\theta$, so $(\alpha_i, \alpha_j) = \widehat{C}_{ij}$. The projection (VI.5.16) is exactly the affine-root relation

$$\sum_{i=0}^{r} m_i\, \alpha_i \;=\; m_0\alpha_0 + \sum_{a=1}^{r} m_a\alpha_a \;=\; -\theta + \theta \;=\; 0, \tag{VI.5.18}$$

and pairing it with each α_j gives the regular brane's pairing with every node,

$$\mathbf{m}^{\mathsf{T}}\widehat{C} = 0, \tag{VI.5.19}$$

so the marks-weighted regular brane carries *zero net wrapped charge*. Equivalently, since $\widehat{C}$ is symmetric,

$$\widehat{C}\,\mathbf{m} = 0, \qquad \mathbf{m} = (\dim R_i)_i, \qquad \det \widehat{C} = 0 : \tag{VI.5.20}$$

the marks are the one-dimensional null vector, and the regular brane spans the radical of the charge pairing. This is the same null vector Chapter 3 read off the representation theory: from $Q \otimes R_i = \bigoplus_j a_{ij} R_j$, taking dimensions with $\dim Q = 2$,

$$2\dim R_i = \sum_j a_{ij} \dim R_j \quad\Longleftrightarrow\quad \sum_j \widehat{C}_{ij}\, m_j = 0, \tag{VI.5.21}$$

the McKay dimension identity, agreeing with (VI.5.20). The one-dimensional regular radical gives the charge-level condition for a bulk D3 branch: motion in the transverse geometry requires no net wrapped charge. A mobile point object also requires nontrivial quiver maps, as the A_1 example in §VI.5.8 shows.

Quotient the lattice by this radical. The images of the nontrivial nodes form a basis of the finite root lattice; deleting the affine row and column displays its non-degenerate Cartan matrix $C^{\,\mathrm{fin}}$, with

$$\det C^{\,\mathrm{fin}} = (\text{ADE index}), \qquad C_a \cdot C_b = -C^{\mathrm{fin}}_{ab}, \tag{VI.5.22}$$

the right-hand identity being Chapter 4's intersection form on the exceptional curves: (-2) on the diagonal (the self-intersection of each $\mathbb{P}^1$), the McKay adjacency off it. So the wrapped sublattice H_2 is the finite ADE root lattice with Chapter 4's pairing, and the whole charge lattice assembles as

$$\underbrace{H_0(X)}_{\text{radical} \,=\, \text{marks} \,=\, \text{D3 charge}} \quad\oplus\quad \underbrace{H_2(X)}_{\text{root lattice, pairing } -C^{\,\mathrm{fin}}}, \tag{VI.5.23}$$

rank $1 + r$. Three pairings are in play and must not be conflated: the symmetric CY_2 Euler form $\widehat{C}$ in the fractional basis (degenerate, its radical the regular brane), the geometric intersection form $-C^{\,\mathrm{fin}}$ on the wrapped sublattice H_2 alone (non-degenerate),

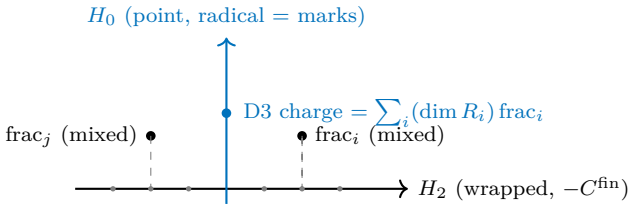


Figure VI.5.2: The fractional-brane charge lattice $H_0 \oplus H_2$ (schematic). The vertical axis is the pure point direction H_0, the radical of the affine Cartan pairing; the horizontal plane is the wrapped sublattice H_2, the finite ADE root lattice with pairing $-C^{\,\mathrm{fin}}$. Individual fractional branes have nonzero wrapped charge and may have a point component; the marks-weighted regular class lands on the H_0 axis with zero wrapped charge, as a mobile bulk D3 does. This equality of classes does not specify the point object. For A_1 the reading is $\pi_{H_2}(f_1) = +C$, $\pi_{H_2}(f_0) = -C$, and $f_0 + f_1$ vertical. The exact classes are basis-dependent (§VI.5.8); the radical and the H_2 pairing are not.

and the point direction H_0 that decouples from both. Nothing here is new geometry: it is Chapter 4's intersection form read as a charge pairing, with the one extra point-charge direction the bulk D3 occupies.

Two bases, and which brane is which.

The same rank-$(r{+}1)$ lattice has two charge descriptions. The *geometric* basis is $H_0 \oplus H_2$: one point direction and the r curves. The *fractional-brane* basis is the $r{+}1$ simple branes f_i, with $\pi_{H_2}(f_a) = C_a$ and $\pi_{H_2}(f_0) = -\theta$; the wrapped projections obey an affine-root relation and are *not* the $H_0 \oplus H_2$ coordinates. Per brane:

Nontrivial node a: $\pi_{H_2} = C_a$, with a convention-dependent point component; stuck.
Affine node 0: $\pi_{H_2} = -\theta$, with a convention-dependent point component, *not* a point brane; stuck.
Regular class $\sum_i m_i[f_i]$: $\pi_{H_2} = 0$, the radical of $\widehat{C}$, the pure-H_0 D3 charge.

VI.5.5 Tension, and what "stuck" means

The wrapped-brane picture invites a quick and wrong conclusion. A D5 wrapping a curve C_a has a leading geometric tension equal to the brane tension times the wrapped area,

$$T_{\mathrm{area}} \;=\; T_{\mathrm{D5}}\ \mathrm{vol}(C_a), \qquad \mathrm{vol}(C_a) \propto \zeta_a^{\mathbb{R}} \xrightarrow[\zeta \to 0]{} 0, \tag{VI.5.24}$$

the exceptional area being proportional to the real Fayet–Iliopoulos level in the chosen local Kähler chamber (Chapter 4). As the cycle collapses at the orbifold point $\zeta \to 0$ this *geometric area term* vanishes, and one might conclude that the fractional brane becomes tensionless. That is wrong, and the reason is the heart of what "stuck" means.

For the standard orbifold constituents the full tension stays finite. A BPS wrapped

brane has tension given by the modulus of a central charge,

$$T_{\mathrm{frac},i} \;=\; |Z_i|. \tag{VI.5.25}$$

Write the fractional charge schematically as a point part plus a wrapped part, and the complexified Kähler parameter of each curve as $t_a = b_a + i\, j_a$, with $j_a = (4\pi^2\alpha')^{-1}\int_{C_a} J$ and $b_a = (4\pi^2\alpha')^{-1}\int_{C_a} B$ the dimensionless periods. In the chosen local real-FI/Kähler chamber, j_a is proportional to $\zeta_a^{\mathbb{R}}$:

$$\Gamma_i = q_{0,i}\,[\mathrm{pt}] + \sum_a q_{a,i}\,[C_a], \qquad Z_i(t) = q_{0,i} + \sum_a q_{a,i}\, t_a + \cdots, \tag{VI.5.26}$$

the dots standing for corrections to this leading large-radius expression (§VI.5.9). The fixed coefficients are charge data in a specified frame; the B-dependent central charge is not the Page charge. The geometric area piece is the imaginary part, $\sum_a q_{a,i}\, j_a$. At the orbifold point the metric area collapses, $j_a \to 0$, but the B-period stays nonzero, $b_a = b_a^{\mathrm{orb}} \neq 0$ (in a standard normalization $b = \frac{1}{2}$ for A_1, the value at which the orbifold conformal field theory is non-singular). In A_1 the wrapped contribution is proportional to $t = b + ij = \frac{1}{2} + i\,0 \neq 0$. It must be combined with the point term in the same charge frame; the explicit frame comparison appears in §VI.5.8. The area piece vanishes while each standard orbifold constituent has the nonzero untwisted normalization of (VI.5.12). Thus the two statements sit side by side,

$$\zeta \to 0: \qquad T_{\mathrm{area}} = T_{\mathrm{D5}}\,\mathrm{vol}(C_a) \longrightarrow 0, \qquad \text{but} \qquad T_{\mathrm{frac},i} = |Z_i| \longrightarrow \text{finite}. \tag{VI.5.27}$$

The collapse of the cycle is the collapse of one term in Z_i, not of the brane. The exact Z_i, with its normalization and induced charges, requires further stringy input deferred to §VI.5.9; (VI.5.26) keeps only the leading point and wrapped terms.

So "stuck at the singularity" is not "tensionless," and the worldsheet face says why in one line. In the sector twisted by a nontrivial group element $g \neq e$, the fractional brane f_i carries twisted Ramond–Ramond charge proportional to the character $\chi_i(g)$; the regular brane, the marks-weighted sum, therefore carries

$$Q_{\mathrm{tw}}(R_{\mathrm{reg}}; g) \;\propto\; \sum_i (\dim R_i)\,\chi_i(g) \;=\; \chi_{\mathrm{reg}}(g) \;=\; 0 \qquad (g \neq e), \tag{VI.5.28}$$

since the regular-representation character vanishes off the identity. The regular brane thus has *no* net twisted charge and is free to move into the bulk, while an individual fractional brane generically does carry twisted charge. That twisted charge is localized at the fixed locus, where the twisted sectors live, and an ordinary bulk D3 cannot carry it off, so the fractional brane is pinned there by charge conservation, with a finite BPS tension rather than a vanishing one. This is the geometric face of the operational "stuck" of Chapter 2. The main calculation isolates the geometric area term; the precise central charge is a deferred refinement (§VI.5.9).

VI.5.6 The worldsheet and geometric charge descriptions

How does the charge of an orbifold boundary state, where the curve has collapsed, compare with the charge of a large-radius wrapped brane? The common quantity in this comparison is the conserved charge class; its representative and central charge depend on the chamber:

$$\Gamma_i \in H_0 \oplus H_2 \text{ fixed;} \qquad Z_i(t) \text{ varies with } t; \\ \text{the convenient description varies with } t. \tag{VI.5.29}$$

The parameter is the complexified Kähler class $t = b + ij$ of §VI.5.5, the metric area j complexified by the B-period b. The charge descriptions at the two ends are:

region	best description	what is fixed
$j = 0,\ b = b^{\text{orb}}$	twisted Cardy state $\lvert R_i\rangle\!\rangle$	Γ_i, the twisted charge
j large	large-radius brane object	Γ_i, its H_2 projection

Crucially the orbifold point is *not* $t = 0$: the area $j \to 0$, but the B-period $b = b^{\text{orb}} \neq 0$ (for A_1, $b = \frac{1}{2}$) keeps the conformal field theory non-singular, and gives the standard constituents finite leading central charges there (§VI.5.5). The two faces are not "before and after a singularity" but the two ends of a charge comparison in the Kähler moduli space. Existence and stability of a particular object along a path require further data.

This charge-level continuation is the brane-level McKay dictionary used here. The twisted boundary state is not literally a D5 wrapping C_a at the orbifold point, where there is no C_a to wrap. The derived McKay equivalence in §VI.5.8 supplies a categorical setting, but charge matching alone does not identify objects. The correspondence of Chapter 3 (irreps $\leftrightarrow$ nodes) and Chapter 4 (geometric McKay, nontrivial irreps $\leftrightarrow$ exceptional curves) is thereby lifted from representations and cycles to the D-brane charge classes,

$$\underbrace{\text{twisted boundary state } \lvert R_a\rangle\!\rangle}_{\text{orbifold point}} \longleftrightarrow \underbrace{\text{large-radius brane, } \pi_{H_2} = C_a}_{\text{large radius, node } a}, \tag{VI.5.30}$$

and the same way for the affine node, whose large-radius projection is $-\theta$ rather than a curve of its own. The marks-weighted sum has bulk-D3 charge at both ends: its twisted charge cancels at the orbifold point and its wrapped charge vanishes at large radius. A mobile point object also needs the appropriate quiver module or extension maps.

What is identified in this comparison is the conserved charge class. The twisted boundary state carries a definite twisted Ramond–Ramond charge labelled by R_i, the large-radius brane a definite class in $H_0 \oplus H_2$ (§VI.5.4), and the continuation identifies them,

$$\Gamma\big(\,\lvert R_i\rangle\!\rangle\,\big)\Big|_{\text{orbifold}} \;=\; \Gamma\big(f_i\big)\Big|_{\text{large radius}} \;\in\; H_0 \oplus H_2, \tag{VI.5.31}$$

the same class in a chosen charge frame. This is what "charge-preserving" means: $Z_i(t)$

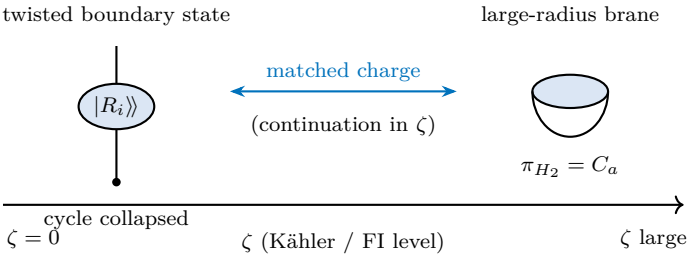


Figure VI.5.3: The charge dictionary in two regimes (schematic), drawn for a nontrivial node a. At $\zeta = 0$ (orbifold point) the fractional brane is the twisted-sector boundary state $|R_a\rangle\!\rangle$ of Chapter 2; at large ζ (resolved) it is a large-radius brane object with H_2 projection C_a (the affine node i=0 continues the same way, to its projection $-\theta$, with no curve of its own). Along the arrow the charge Γ_i is fixed, the central charge $Z_i(t)$ varies, and the convenient description changes; the arrow tracks the conserved class. It does not identify a unique object or establish stability along the path.

varies continuously, but the class in the lattice does not[1]. The fractional branes carry the indivisible classes, the regular brane the radical class, at both ends. In A_1 the brane whose large-radius projection is $+C$ becomes the Cardy state at $j = 0$, $b = \frac{1}{2}$; its companion projects to $-C$; their sum is the point charge at every t. The three readings of one McKay correspondence line up: representations → nodes (Chapter 3), geometry → finite curves (Chapter 4), branes → charge classes (here).

VI.5.7 Worked examples: A_1 and D_4

$A_1 = \mathbb{C}^2/\mathbb{Z}_2$: the template

The general derivation runs the same way on every case, and A_1 shows the full procedure on the smallest one. Tabulate the data; there is a single curve C:

node	irrep	mark
0	trivial	1
1	sign	1

The highest root is the marks-weighted sum of the finite curves, here $\theta = m_1 C = C$, so the projections are

$$\pi_{H_2}(f_1) = C_1, \qquad \pi_{H_2}(f_0) = -\theta = -C_1. \tag{VI.5.32}$$

Build the Cartan matrix from the root pairing, in which each curve is a root of squared length $(\alpha, \alpha) = 2 = -(C{\cdot}C)$, minus its self-intersection -2. With $\alpha_1 = C$ and the affine

[1]Which bound states are *stable* can change along the path, at walls of marginal stability; that concerns the BPS spectrum, not the charge lattice, and belongs to the dynamics of later volumes. Here we follow only the conserved charge.

root $\alpha_0 = -\theta = -C$,

$$(\alpha_1,\alpha_1) = 2, \quad (\alpha_0,\alpha_1) = (-C,C) = -2, \quad (\alpha_0,\alpha_0) = 2 \implies \widehat{C} = \begin{pmatrix} 2 & -2 \\ -2 & 2 \end{pmatrix}, \tag{VI.5.33}$$

whose null vector is the marks $(1,1)$, the regular brane,

$$R_{\text{reg}} = f_0 + f_1, \quad \pi_{H_2}(R_{\text{reg}}) = -C_1 + C_1 = 0, \quad \widehat{C}\,(1,1)^{\mathsf{T}} = 0, \qquad \sum_i (\dim R_i)^2 = 2 = |\mathbb{Z}_2|, \tag{VI.5.34}$$

not either node alone: were the naive $f_0 = H_0$ true, f_0 would be the radical, but $(\alpha_0,\alpha_1) = -2 \neq 0$ rules it out. Deleting either node leaves the 1×1 finite Cartan $C^{\,\text{fin}} = (2)$, so the A_1 index is $\det C^{\,\text{fin}} = 2$ and the curve has self-intersection $C{\cdot}C = -2$.

$D_4 = \mathbb{C}^2/Q_8$: the same template, non-abelian

The non-abelian case runs identically, with one node of mark 2. The binary group Q_8 has five irreps, four of dimension one and one of dimension two, so the quiver is affine $\hat{D}_4$, a central node (the two-dimensional irrep, mark 2) joined to four outer nodes (the one-dimensional irreps, marks 1). Take the trivial node as one outer node; the marks are $(1,1,1,1,2)$,

$$\sum_i (\dim R_i)^2 = 1+1+1+1+4 = 8 = |Q_8|, \tag{VI.5.35}$$

The normalized untwisted charges of the four outer constituents are each $1/8$, whereas the central constituent has charge $2/8 = 1/4$. The regular brane has five irrep types but six constituents, including two central ones; its Chan–Paton dimension is eight, and its untwisted charge is $4(1/8) + 2(1/4) = 1$. The central mark is a multiplicity in this sum, not an extra factor in one constituent's charge. The resolution has $r = 4$ curves, three outer C_1, C_2, C_3 and the central C_{c}. The highest root weights the central curve by its mark,

$$\theta = C_1{+}C_2{+}C_3{+}2C_{\text{c}}, \qquad \pi_{H_2}(f_a) = C_a \ (a = 1,2,3,\text{c}), \qquad \pi_{H_2}(f_0) = -\theta, \tag{VI.5.36}$$

the affine node again not a point charge. To see *why* the affine node attaches to the central node, compute its pairings from the finite D_4 root data $(C_a,C_a) = 2$, $(C_a,C_{\text{c}}) = -1$, $(C_a,C_b) = 0$ for outer $a \neq b$, and $(C_{\text{c}},C_{\text{c}}) = 2$:

$$\begin{aligned} (-\theta,C_a) &= -\big[(C_a,C_a) + 2(C_{\text{c}},C_a)\big] = -(2-2) = 0 \quad (a=1,2,3), \\ (-\theta,C_{\text{c}}) &= -\big[3(-1) + 2\cdot 2\big] = -1, \end{aligned} \tag{VI.5.37}$$

so $\alpha_0 = -\theta$ is orthogonal to the outer roots and meets only the central one. That gives the affine $\hat{D}_4$ Cartan matrix in node order $(0,1,2,3,\text{c})$,

$$\widehat{C}_{\hat{D}_4} = \begin{pmatrix} 2 & 0 & 0 & 0 & -1 \\ 0 & 2 & 0 & 0 & -1 \\ 0 & 0 & 2 & 0 & -1 \\ 0 & 0 & 0 & 2 & -1 \\ -1 & -1 & -1 & -1 & 2 \end{pmatrix}, \qquad \widehat{C}_{\hat{D}_4}\,(1,1,1,1,2)^{\mathsf{T}} = 0, \tag{VI.5.38}$$

with the marks as its null vector. The regular brane is therefore

$$R_{\rm reg} = f_0+f_1+f_2+f_3+2\,f_{\rm c}, \qquad \pi_{H_2}(R_{\rm reg}) = -\theta+(C_1+C_2+C_3+2C_{\rm c}) = 0, \tag{VI.5.39}$$

the mark 2 of the central node a line of linear algebra, not just a Dynkin label. Deleting the affine node leaves the finite D_4 Cartan with

$$\det C^{\rm fin}_{D_4} = 4, \tag{VI.5.40}$$

the D_4 index. Per node, and side by side with A_1:

node	mark	π_{H_2}
0	1	$-(C_1+C_2+C_3+2C_{\rm c})$
$1,2,3$	1	$C_1,\ C_2,\ C_3$
c	2	$C_{\rm c}$
$R_{\rm reg}$	(sum)	0

feature	A_1	D_4
# curves	1	4
# fractional types	2	5
nontrivial marks	1	$1,1,1,2$
affine π_{H_2}	$-C$	$-(C_1+C_2+C_3+2C_{\rm c})$
$\det C^{\rm fin}$	2	4

The reader can run the same template on $A_2 = \mathbb{C}^2/\mathbb{Z}_3$: three nodes, two curves C_1, C_2, marks $(1,1,1)$, highest root $\theta = C_1 + C_2$, so $\pi_{H_2}(f_0) = -(C_1 + C_2)$ and the regular brane $R_{\rm reg} = f_0 + f_1 + f_2$ has zero wrapped charge, the marks $(1,1,1)$ the null vector of the affine $\widehat{A}_2$ Cartan. In every case the charge lattice is $H_0 \oplus H_2$ of rank $r+1$ in the stated local homological approximation; the arithmetic is Chapter 4's, read now as the charges of the fractional branes rather than the geometry of the curves.

*VI.5.8 D-brane charges and the derived category

(Optional.) This section may be skipped on a first reading. The main line used only the homological lattice $H_0(X) \oplus H_2(X)$ and the Chapter 4 intersection form, the right level for the wrapped-brane interpretation. The price was two suppressed structures: the integral charge group, and the open strings between branes. We record both in the smallest form the chapter needs, with one explicit A_1 calculation. Homology records the Chern-character image, K-theory the additive charge class, and the derived category the object and maps by which branes bind. A physical B-brane interpretation additionally uses a heart and stability condition.

Dictionary for the optional refinement.

Homology $H_0 \oplus H_2$**:** the Chern-character image of the charge class.
K-theory $K(X)$**:** the additive charge group itself.
Derived category $D^b(\coh X)$**:** the brane object with its open strings.
Ext^1**:** the quiver arrows, the first-order bindings.
Euler form χ**:** the charge pairing, equal to the affine Cartan matrix.
Shift [1]**:** flips the K-theory charge. $\mathcal{O}_p$**:** the point brane, the mobile D3.

From homology charge to K-theory charge

For a B-type brane on the resolved ALE surface X the charge is not a homology class but a class in (compactly supported) topological K-theory, $[E] \in K(X)$, represented by sheaves or complexes supported on the exceptional curves and on points. The homological charge of the main line is its Chern-character image,

$$[E] \in K(X) \;\longmapsto\; \Gamma(E) = \mathrm{ch}(E)\sqrt{\mathrm{Td}(X)} \;\rightsquigarrow\; \Gamma_0(E) + \Gamma_2(E) \in H_0(X) \oplus H_2(X), \tag{VI.5.41}$$

of which only the point and curve components entered §VI.5.4. Two rules suffice. Charge is additive in exact sequences: $0 \to A \to B \to C \to 0$ gives $[B] = [A] + [C]$, the statement that a bound state's charge is the sum of its constituents'; and a shift flips the charge, $[E[1]] = -[E]$, which is how one fractional brane can carry the charge opposite to another. K-theory refines the charge group but still forgets the open strings from E to another brane; for those one needs the category.

The A_1 calculation in K-theory

Everything is transparent for $A_1 = \mathbb{C}^2/\mathbb{Z}_2$, and it reproduces the charge calculation of §VI.5.7 with explicit objects. Let $i : C \hookrightarrow X$ be the exceptional $\mathbb{P}^1$ (normal bundle $\mathcal{O}_C(-2)$), and take, up to convention, the two brane objects

$$F_1 = i_*\mathcal{O}_C, \qquad F_0 = i_*\mathcal{O}_C(-1)[1], \tag{VI.5.42}$$

the shift [1] reversing F_0's charge by $[E[1]] = -[E]$. The point brane follows from the elementary sequence on C (with $p \in C$ a point), the additivity rule applied to it,

$$0 \to \mathcal{O}_C(-1) \to \mathcal{O}_C \to \mathcal{O}_p \to 0 \;\;\Longrightarrow\;\; [\mathcal{O}_p] = [i_*\mathcal{O}_C] - [i_*\mathcal{O}_C(-1)] = [F_1] + [F_0], \tag{VI.5.43}$$

the K-class identity $[R_{\mathrm{reg}}] = [F_0] + [F_1] = [\mathcal{O}_p]$, with the shift turning a difference into a sum. The map $\mathcal{O}_C(-1) \to \mathcal{O}_C$ is nonzero; its cone is $\mathcal{O}_p$. This map supplies binding data beyond the two summands. Indeed $F_0 \oplus F_1$ has the same K-class as $\mathcal{O}_p$ but is not isomorphic to it: the split object has cohomology sheaves in degrees -1 and 0 and two scalar endomorphisms, while $\mathcal{O}_p$ is a degree-zero sheaf with one scalar endomorphism. In the orbifold/quiver heart, the regular dimension vector likewise needs arrow maps or extension data to select a point object. The Chern character reproduces the wrapped charges: with the degree-(-2) normal bundle, $\mathrm{ch}(i_*\mathcal{O}_C) = [C] + [p]$ and

$\mathrm{ch}(i_*\mathcal{O}_C(-1)) = [C]$ (suppressing the common Todd factor), so

$$\mathrm{ch}(F_1) = [C] + [p], \qquad \mathrm{ch}(F_0) = -[C], \qquad \mathrm{ch}(F_0) + \mathrm{ch}(F_1) = [p], \tag{VI.5.44}$$

that is $\pi_{H_2}(F_1) = C$, $\pi_{H_2}(F_0) = -C$, and zero net wrapped charge in the sum, exactly the homological statement of §VI.5.7 lifted to K-theory. These are integral classes in one large-radius frame. To compare their B-dependent source coupling with the orbifold normalization, use the equivalent orbifold representative $b = -\frac{1}{2}$ (rather than $+\frac{1}{2}$ modulo an integral B shift). With the oriented-curve convention of (VI.5.11), their point-plus-B periods are

$$Q_0^{\text{source}}(F_0) = 0 + (-1)(-\tfrac{1}{2}) = \tfrac{1}{2}, \qquad Q_0^{\text{source}}(F_1) = 1 + (+1)(-\tfrac{1}{2}) = \tfrac{1}{2}. \tag{VI.5.45}$$

Their sum is still one D3. Under $b \mapsto b + 1$ the same source period $q_0 + bq_2$ requires $q_0 \mapsto q_0 - q_2$. Thus $b = +\frac{1}{2}$ represents the same background only with this Page-basis change; holding the displayed classes fixed would instead give $-\frac{1}{2}$ and $\frac{3}{2}$. Which node carries which shifted sheaf is a convention; the invariant content is their opposite wrapped projections and point-brane sum.

The Euler form is the affine Cartan matrix

The same objects also carry the open strings, which homology cannot see. A topological B-brane is an object $E \in D^b(\mathrm{coh}\, X)$; the open strings from E to F are counted by $\mathrm{Ext}^k(E, F)$, and their alternating sum is the Euler pairing

$$\chi(E, F) = \sum_k (-1)^k \dim \mathrm{Ext}^k(E, F), \tag{VI.5.46}$$

the categorical version of the charge pairing of §VI.5.4. For the fractional branes choose the orbifold/quiver heart inside the derived category. Its *simple* objects S_i are indexed by irreps R_i. A simple object has only scalar endomorphisms, $\dim \mathrm{Ext}^0(S_i, S_j) = \delta_{ij}$; the surface is Calabi–Yau of dimension two, so Serre duality gives $\mathrm{Ext}^2(S_i, S_j) \cong \mathrm{Ext}^0(S_j, S_i)^*$, hence $\dim \mathrm{Ext}^2(S_i, S_j) = \delta_{ij}$; and the middle group carries the quiver arrows,

$$\dim \mathrm{Ext}^1(S_i, S_j) = \dim \mathrm{Hom}_\Gamma(R_j, Q \otimes R_i) = a_{ij}, \tag{VI.5.47}$$

the McKay adjacency of Chapter 3 read as open-string states. In A_1 this is the same defining representation as just used, $Q = R_1 \oplus R_1$, so $Q \otimes R_0 = 2R_1$ and $Q \otimes R_1 = 2R_0$, giving $a_{01} = a_{10} = 2$ and $a_{00} = a_{11} = 0$. Adding the three groups,

$$\chi(S_i, S_j) = \delta_{ij} - a_{ij} + \delta_{ij} = 2\delta_{ij} - a_{ij} = \widehat{C}_{ij}, \tag{VI.5.48}$$

so the affine Cartan matrix of §VI.5.4 is the symmetric CY_2 Euler form of the simple objects. The Ext^1 matrix is the McKay adjacency a; the distinct Euler/Cartan matrix is $\widehat{C} = 2I - a$. For A_1, these are respectively $\left(\begin{smallmatrix} 0 & 2 \\ 2 & 0 \end{smallmatrix}\right)$ and $\left(\begin{smallmatrix} 2 & -2 \\ -2 & 2 \end{smallmatrix}\right)$. The regular brane, whose class is the regular representation, has the marks as the null vector of $\widehat{C}$; under the large-radius dictionary a point object $\mathcal{O}_p$ has this class. The module or extension data distinguish it from the split regular-class object.

The derived McKay statement

The precise statement behind these calculations is the derived McKay correspondence: for $\Gamma \subset SU(2)$ with minimal resolution $X \to \mathbb{C}^2/\Gamma$ there is an equivalence

$$D^b_\Gamma(\mathrm{coh}\,\mathbb{C}^2) \;\simeq\; D^b(\mathrm{coh}\,X), \tag{VI.5.49}$$

the orbifold/quiver side on the left, the resolved geometry on the right. With the chosen heart and conventions, the simple objects S_i correspond to the fractional objects F_i. A Γ-cluster has regular global representation together with its scheme/module structure, and its image is a point object $\mathcal{O}_p$; the regular representation alone fixes only the K-class. The equivalence is quoted, not proved (its home is the B-brane machinery of Volume V, the K-theory of D-brane charge that of Volume III); what matters here is that it preserves the two structures we use, the K-theory classes (the charge lattice) and the Ext groups (the arrows and the Euler form). This is the formal version of the brane-level McKay dictionary of §VI.5.6.

For larger ADE the mechanism is the same: the theorem supplies objects F_i whose Ext-quiver is the affine ADE diagram and whose classes project to $\pi_{H_2}(F_a) = C_a$ and $\pi_{H_2}(F_0) = -\theta = -\sum_a m_a C_a$, with $\sum_i m_i[F_i] = [\mathcal{O}_p]$ as a class. The point object requires corresponding nontrivial maps; stability remains a separate physical question. The derived category is used here only as the precise language for three structures already used in the main line: the charges (here K-theory classes), the quiver arrows (here Ext^1 open strings), and the affine Cartan matrix (here their Euler pairing).

VI.5.9 What the construction does and does not give

With the charge lattice in hand the reader can now compute the fractional-brane data for any ADE case: write the mobile brane $R_{\mathrm{reg}} = \sum_i m_i f_i$ from the marks, obtain the affine node's projection $\pi_{H_2}(f_0) = -\theta$ as forced by $\pi_{H_2}(R_{\mathrm{reg}}) = 0$, verify the null-vector relation $\widehat{C}\,\mathbf{m} = 0$, read the mobile brane off as the pure-H_0 radical, and tell the vanishing wrapped *area* at the orbifold point from the finite brane *tension* there. That is the charge dictionary promised at the outset, (VI.5.1): the fractional classes span the rank-$(r{+}1)$ point-and-curve lattice, their wrapped projections obey the affine-root relation, and the wrapped H_2 sublattice carries Chapter 4's intersection form. The marks span the radical. Four limits of this calculation remain.

First, the tension. The main line controls only the geometric area term $\propto \mathrm{vol}(C_a) \propto \zeta_a^{\mathbb{R}}$, which vanishes as the cycle collapses; the *full* tension does not. The collapsed cycle keeps a B-period (the half-integer value for A_1) and the brane carries induced lower charges, so the BPS central charge $Z_i \sim \int_C (B + iJ) + (\text{induced}) + \cdots$ is finite there: "stuck" is the localization of the conserved twisted charge at the fixed point, a finite tension, not tensionlessness. The exact Z_i with all normalizations is a stringy refinement living in Volumes III and IV, and the probe caveat of Chapter 1 stands: the probe reads the holomorphic charge while the full metric and tension are leading classical statements, corrected at finite α' and g_s.

Second, the categorical statement. The optional §VI.5.8 derives the Ext-quiver and the Euler-form = affine-Cartan identity and works the A_1 K-theory calculation in full,

but the derived McKay *equivalence* is quoted, not proved, its proof routed to Volume V and the K-theory refining the homology to Volume II. The main-line charge arithmetic follows from homology and the Chapter 3–4 data alone.

Third, a distinction not to blur. The wrapped branes here are *probe constituents*, pieces of the probe brane whose worldvolume gauge theory is the quiver of Chapters 2–3. They are not spacetime states: the enhanced ADE gauge symmetry that arises when a wrapped brane becomes a massless *spacetime* particle as a cycle shrinks, the W-bosons of geometric engineering, is a different construction with its home in Volume IX. The two share the ADE label but are physically distinct; this chapter is about the worldvolume side.

Finally, the construction here uses ordinary finite $SU(2)$ orbifolds, for which nontrivial discrete torsion does not occur. Chapter 9 changes the orbifold class, for example to a suitable finite $SU(3)$ action with nontrivial $H^2(\Gamma, U(1))$. There the Chan–Paton representations are projective and the quiver and charge dictionary change.

Status and sources

The evidence-code tags ([WS] physical worldsheet derivation, [MATH] cited mathematical theorem), the convention pointers, and the source anchors are collected here, keyed by section. The chapter gives the geometric identity of the fractional brane of Chapter 2 on the resolved ALE space of Chapter 4: a wrapped D-brane on an exceptional cycle (the fractional branes spanning $H_0 \oplus H_2$ with affine-root wrapped projections, the affine node projecting to $-\theta$, the marks-weighted regular brane the pure-H_0 mobile D3), after Diaconescu and Gomis (2000) (boundary states $\leftrightarrow$ branes on holomorphic cycles) and the fractional-brane / wrapped-brane analyses of Bertolini et al. (2002), read through the probe of Douglas and Moore (1996). It recalls Chapter 2 (operational fractional brane, orbifold action), Chapter 3 (McKay quiver, marks, adjacency, McKay multiplicities), and Chapter 4 (exceptional cycles and intersection form, resolution and discrete data). The charge-lattice arithmetic (the affine Cartan as the charge Euler form, its radical the marks, the regular brane's zero net wrapped charge, the finite Cartan determinant and the (-2)-curve intersection form, the geometric area term $\propto \zeta$, and the affine-node projection $\pi_{H_2}(f_0) = -\theta$) follows from the stated charge dictionary and the explicit finite examples.

§VI.5.1 What is left to say. Framing: the mismatch of $r{+}1$ fractional branes against r curves, the recall box, and the chapter's deliverable (VI.5.1) (the charge dictionary previewed here, derived in §VI.5.4; orbifold action, McKay multiplicities, resolution and discrete data).

§VI.5.2 The first puzzle. The mismatch $r{+}1$ branes versus r curves and the naive dictionary (VI.5.2), killed on the spot by the A_1 affine Cartan (the radical is $(1,1)$, not f_0) (VI.5.3)–(VI.5.4); the three-face table with the regular decomposition (VI.5.5) (Figure VI.5.1). The first two faces recalled from Chapter 2, the geometric face the new content. No standalone claim-atom; sets up Q1/Q4.

§VI.5.3 The wrapped-brane identity. By dimension counting (VI.5.6) the general rule fractional $Dp = D(p{+}2)$ on a compact 2-cycle (VI.5.8), so a D5 for the D3 probe; the ALE compact homology $H_0 \oplus H_2$ with $H_4 = 0$ (VI.5.7) forcing the 2-cycle; the Wess–Zumino induced point charge (VI.5.10)–(VI.5.11) making the wrapped D5 a charge mixture; and the mobile D3 the marks-weighted regular brane (VI.5.13) (the affine-node wrapped charge $-\theta$, not pure H_0, previewed here and derived in §VI.5.4): (source-backed physical dictionary, without a worldsheet derivation here) (orbifold action, McKay multiplicities, resolution and discrete data; Diaconescu and Gomis (2000), Bertolini et al. (2002); the conifold template Klebanov and Strassler (2000)). The trivial-node / mobile-D3 distinction and the homology rank are This files (the precise sense of "wraps a collapsed cycle": a $D(p{+}2)$ on a 2-cycle, p-dependent; a definite charge; a probe constituent, not a spacetime gauge boson).

§VI.5.4 The charge lattice. The charge lattice $H_0 \oplus H_2$ of rank $r{+}1$ (VI.5.14); the finite-node convention (VI.5.15) forcing the affine-node projection $\pi_{H_2}(f_0) = -\theta$ via $\pi_{H_2}(R_{\text{reg}}) = 0$ (VI.5.16); the

charge Euler form = affine Cartan (VI.5.17); the affine-root relation (VI.5.18) giving the radical = the marks = the mobile D3 (VI.5.19)–(VI.5.20); the non-degenerate quotient = the finite Cartan = minus the intersection form (VI.5.22)–(VI.5.23): [MATH] for the conditional lattice algebra (McKay multiplicities, resolution and discrete data). The identification of this homological group with the full physical charge lattice is a separate physical premise with integral refinements. The finite lattice algebra is $\widehat{C} = 2I - a$, $\widehat{C}\,\mathbf{m} = 0$, $\det \widehat{C} = 0$, $\mathbf{m}^{\mathsf{T}}\widehat{C} = 0$, $\det C^{\,\mathrm{fin}}$ = ADE index, the (-2)-curves. The cycle lattice is the wrapped sublattice, not the whole charge lattice.

§VI.5.5 Tension and "stuck." The geometric area term $T_{\mathrm{D5}}\,\mathrm{vol}(C_a) \propto \zeta_a^{\mathbb{R}} \to 0$ at the orbifold point (VI.5.24), against the finite full BPS tension $|Z_i|$ with $Z_i(t) = q_{0,i} + \sum_a q_{a,i} t_a + \cdots$ (VI.5.26) (area part $\sum_a q_{a,i} j_a \to 0$, b_a and induced charges remaining); the regular brane's twisted charge cancels by $\chi_{\mathrm{reg}}(g{\neq}e) = 0$ (VI.5.28); "stuck" = twisted-charge localization, not tensionlessness: ([MATH] only for the conditional area limit; the area/FI identification and full tension are physical premises; [WS] only for the recalled twisted-sector charge). The area term's vanishing at $\zeta = 0$ is evaluated, and only the area term: the full tension is finite there, the honest gap, with no "full tension = 0" check. The mass dimensions $[T_{\mathrm{D5}}] + [\mathrm{vol}] = [\mathrm{tension}_{4d}]$ are in the dimensional and consistency checks.

§VI.5.6 The charge descriptions. The fixed-charge invariant (VI.5.29) (Γ_i fixed, $Z_i(t)$ varying, the description varying); the twisted boundary state (orbifold point) $\leftrightarrow$ the large-radius brane (projection C_a for a nontrivial node, $-\theta$ for the affine node) as the matched conserved class across ζ (VI.5.30), the brane-level McKay dictionary, a charge-preserving continuation (the precise derived statement is §VI.5.8), not a literal naive D5 on a curve: (source-backed continuation; [WS] applies to the orbifold boundary state) (Diaconescu and Gomis (2000); McKay multiplicities; recall orbifold CFT and boundary states for the boundary-state side, home Vol. II/II). The continuation statement is qualitative (no separate machine check); its consistency is the Ext-quiver of §VI.5.8.

§VI.5.7 Worked A_1 and D_4. The two worked instances, [MATH] for the displayed arithmetic (McKay multiplicities, resolution and discrete data): $A_1 = \mathbb{C}^2/\mathbb{Z}_2$ (two fractional types, the affine Cartan $\left(\begin{smallmatrix} 2 & -2 \\ -2 & 2 \end{smallmatrix}\right)$ with radical $(1,1)$, the single (-2)-curve, $\det C^{\,\mathrm{fin}} = 2$, the regular brane the mobile-D3 charge) (VI.5.32)–(VI.5.34); and $D_4 = \mathbb{C}^2/Q_8$ (five types, six regular constituents, eight Chan–Paton dimensions, the mark-2 central node, $\sum(\dim R_i)^2 = 8$, four D_4 curves, $\det C^{\,\mathrm{fin}} = 4$, the regular brane $f_0{+}f_1{+}f_2{+}f_3{+}2f_{\mathrm{centre}}$) (VI.5.35)–(VI.5.39). The identities hold in the three finite examples ($\mathbb{Z}_2$, $\mathbb{Z}_3$, Q_8) by using the McKay and intersection data of Chapters 3 and 4.

§VI.5.8 D-brane charges and the derived category. K-theory as the decategorified charge, the Chern-character image (VI.5.41) ($\to$ Vol. III; Minasian and Moore (1997), Witten (1998)), and the bounded derived category $D^b(\mathrm{coh}\,X)$ as the full brane data: the Euler pairing (VI.5.46) of the simple objects S_i (with $\dim \mathrm{Ext}^0 = \dim \mathrm{Ext}^2 = \delta_{ij}$ by Serre duality on the CY_2 surface and $\dim \mathrm{Ext}^1 = a_{ij}$ (VI.5.47)) *equals* the affine Cartan matrix $\widehat{C} = 2\delta - a$ (VI.5.48); the derived McKay equivalence $D^b_\Gamma(\mathbb{C}^2) \simeq D^b(X)$ (VI.5.49) ($S_i \leftrightarrow F_i$ in a chosen heart; a regular-class cluster with its module structure maps to $\mathcal{O}_p$); and the worked A_1 K-theory calculation, the exact sequence $0 \to \mathcal{O}_C(-1) \to \mathcal{O}_C \to \mathcal{O}_p \to 0$ giving $[\mathcal{O}_p] = [F_1]{+}[F_0]$ (VI.5.43) and the Chern characters $\mathrm{ch}(F_1) = [C]{+}[p]$, $\mathrm{ch}(F_0) = -[C]$ (VI.5.44): [MATH] only for the exact-sequence, conditional Euler-sum, and quoted derived-equivalence statements; the physical K-theory/B-brane identification and stability remain separate unclassified premises (Bridgeland et al. (2001); the B-brane formulation Aspinwall (2004); the surface derived McKay correspondence, home Vol. V ch. 6). The derived equivalence is quoted, not proved; the Ext-quiver = affine Dynkin / Euler form = affine Cartan consistency is evaluated, not a proof of the equivalence. The shift rule $[E[1]] = -[E]$ and additivity in exact sequences are the two K-theory facts used. This files (K-theory = the charge / the decategorified class; the derived category retains maps and Ext beyond the charge; the charge is not the complete information).

§VI.5.9 What it does and does not give. The full tension finite at the orbifold point (the exact central charge $\to$ Vol. III/IV; the probe α'/g_s caveat, the stated distinction from Chapter 1); the derived equivalence quoted not proved (the surface derived McKay correspondence, Vol. V); the probe-constituent (worldvolume) versus geometric-engineering (spacetime) distinction, enhanced ADE gauge symmetry deferred to Volume IX.

References

Aspinwall, P. S. (2004). "D-branes on Calabi-Yau manifolds". In: Lectures, TASI 2003; published in Recent Trends in String Theory, pp. 1–152. DOI: 10.1142/9789812775108_0001. arXiv: hep-th/0403166.

Bertolini, M. et al. (2002). "N=2 gauge theories on systems of fractional D3/D7 branes". In: *Nucl. Phys. B* 621, pp. 157–178. DOI: 10.1016/S0550-3213(01)00568-5. arXiv: hep-th/0107057.

Bridgeland, T., A. King, and M. Reid (2001). "The McKay correspondence as an equivalence of derived categories". In: *J. Amer. Math. Soc.* 14. American Mathematical Society, pp. 535–554. DOI: 10.1090/S0894-0347-01-00368-X. arXiv: math/9908027.

Diaconescu, D.-E. and J. Gomis (2000). "Fractional branes and boundary states in orbifold theories". In: *JHEP* 10, p. 001. DOI: 10.1088/1126-6708/2000/10/001. arXiv: hep-th/9906242.

Douglas, M. R. and G. W. Moore (1996). "D-branes, quivers, and ALE instantons". In: arXiv preprint; not published in a journal. arXiv: hep-th/9603167.

Klebanov, I. R. and M. J. Strassler (2000). "Supergravity and a confining gauge theory: Duality cascades and chi SB resolution of naked singularities". In: *JHEP* 08, p. 052. DOI: 10.1088/1126-6708/2000/08/052. arXiv: hep-th/0007191.

Minasian, R. and G. W. Moore (1997). "K theory and Ramond-Ramond charge". In: *JHEP* 11, p. 002. DOI: 10.1088/1126-6708/1997/11/002. arXiv: hep-th/9710230.

Witten, E. (1998). "D-branes and K theory". In: *JHEP* 12, p. 019. DOI: 10.1088/1126-6708/1998/12/019. arXiv: hep-th/9810188.

Chapter VI.6

$\mathbb{C}^3/\Gamma$: $\mathcal{N}{=}1$ quivers and superpotentials

VI.6.1 Out of the ADE miracle

The $\mathbb{C}^2/\Gamma$ chapters linked a D3-brane quiver to an affine ADE diagram and an ALE space. In three complex dimensions the same projection still gives a quiver, but its defining representation can be complex, so arrows need not pair. The cubic superpotential then carries geometric information that the graph alone lacks.

The previous block told a tidy story. When Γ is a finite subgroup of $SU(2)$, the McKay graph of the orbifold $\mathbb{C}^2/\Gamma$ is exactly an affine ADE Dynkin diagram; the brane probe is an $\mathcal{N}{=}2$ quiver gauge theory whose nodes, edges and ranks are read off a Cartan matrix, and whose Higgs branch is the resolved ALE space. The classification of the singularities, of the gauge theories, and of the resolutions all collapse onto the single A–D–E list. That triple coincidence is the reason the $\mathbb{C}^2$ story felt inevitable. It is also special to two complex dimensions, and this chapter is about what happens when it goes away.

It is worth placing the chapter in the arc of the volume. Chapter 2 built the orbifold projection machine and ran it on small abelian examples. Chapter 3 turned the non-abelian $\mathbb{C}^2/\Gamma$ into the affine ADE quivers and read the McKay correspondence as gauge theory. Chapter 4 gave those quivers their geometry, the ALE moduli spaces as hyperkähler quotients, and Chapter 5 the fractional branes wrapping the exceptional cycles. Those four chapters are the $\mathbb{C}^2/\Gamma$, $\mathcal{N}{=}2$ block, organized from beginning to end by ADE. The present chapter opens the parallel $\mathbb{C}^3/\Gamma$, $\mathcal{N}{=}1$ block, and the first thing to absorb is that the organizing diagram is gone.

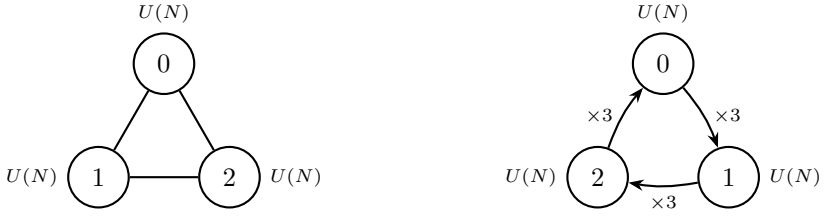
The construction machine itself does not change. The worldvolume theory is still obtained by the orbifold projection of Chapter 2, the nodes are still the irreducible representations of Γ, and the arrows are still counted by tensoring with the defining representation. What changes is the defining representation, which we call Q throughout: the **2** of $SU(2)$ or the **3** of $SU(3)$, the representation by which Γ acts on the transverse coordinates. (Here and below Q is a representation of Γ, the data that draws the quiver;

it is not a supercharge.) For $SU(2)$ it is the two-dimensional **2**, which is pseudoreal, and pseudoreality is what forced the McKay graph to be undirected. For $SU(3)$ it is the three-dimensional **3**, and its restriction to a typical subgroup is a *complex* representation, not equivalent to its conjugate. The McKay graph therefore acquires an orientation, the gauge theory can become *chiral*, and there is no Cartan matrix and no Dynkin classification to lean on. Table VI.6.1 lines up the two cases.

	$\mathbb{C}^2/\Gamma$ (Chapters 3–5)	$\mathbb{C}^3/\Gamma$ (this chapter)
ambient group	$\Gamma \subset SU(2)$	$\Gamma \subset SU(3)$
defining rep Q	**2**	**3**
reality of Q	pseudoreal	generically complex
McKay graph	undirected	directed quiver
supersymmetry	$4d$ $\mathcal{N}$=2	$4d$ $\mathcal{N}$=1 when $Q^\Gamma = 0$
organizing object	affine ADE Cartan matrix	adjacency a_{ij} + cubic W
typical matter	non-chiral hypermultiplets	chiral bifundamentals
geometry	ALE resolution	CY_3 orbifold / resolution chambers

Table VI.6.1: The two orbifold blocks. The right column describes an $SU(3)$ action with no invariant vector in Q. A subgroup fixing a complex direction preserves more supersymmetry.

Figure VI.6.1 makes the same contrast visually: the $\mathbb{C}^2$ McKay graph is an undirected ADE diagram, where each edge is one hypermultiplet, or a conjugate pair of chiral multiplets; the $\mathbb{C}^3$ quiver is directed, and the arrows need not pair.



$\mathbb{C}^2/\mathbb{Z}_3$: undirected

$\mathbb{C}^3/\mathbb{Z}_3$: directed

Figure VI.6.1: The same cyclic group $\mathbb{Z}_3$ gives an undirected McKay graph in $SU(2)$ (left, the affine $\widehat{A}_2$, edges drawn undirected as in Chapter 3, non-chiral) and a directed quiver in $SU(3)$ (right, the dP_0 triple-arrow triangle drawn as in Chapter 2, $\times 3$ the three chiral fields per edge, chiral). The orientation is the whole difference.

The loss of ADE is not a defect, and it helps to say why. The representation-theoretic tensor-product rule that produced the quiver is unchanged and still runs for every finite $\Gamma \subset SU(3)$: write the irreducibles, tensor with **3**, read off the arrows. What disappears is only the miraculous *collapse* of that output onto a finite Dynkin list. In three complex dimensions there is no such list; there are instead a few named families of subgroups, and the quivers are as varied as the groups. Our task is to compute the

directed adjacency and the inherited cubic, then read the regular-brane geometry from their vacuum equations.

Take-home message of this chapter

In $\mathbb{C}^2/\Gamma$ the McKay correspondence lands on affine ADE. In $\mathbb{C}^3/\Gamma$ the same projection still works, but the defining **3** of $SU(3)$ is generically complex, so the McKay graph is naturally *directed*, the four-dimensional theory can be *chiral*, and the organizing data is the directed McKay quiver together with the cubic superpotential inherited from the $\mathcal{N}$=4 parent, not a Cartan matrix. *Do not look for a Cartan matrix in this chapter; the adjacency a_{ij} is the object.*

Two things must therefore be supplied that the ADE story handed us for free. The first is the orientation of the quiver, which carries the chirality and is the genuinely new content. The second is the superpotential: in $\mathcal{N}$=1 the cubic coupling is not decoration, it is the projected image of the unique cubic invariant of $SU(3)$, and without it the quiver is not the theory. The path of the chapter is to run the projection slowly in the $\mathbb{C}^3$ language (§VI.6.2); build the directed McKay quiver (§VI.6.3); read off chirality and the anomaly (§VI.6.4); derive the cubic superpotential (§VI.6.5); and then work a deliberately graded set of examples, two abelian ones, the recalled dP_0 and the non-isolated $\mathbb{C}^3/(\mathbb{Z}_2 \times \mathbb{Z}_2)$ (§VI.6.6), and the non-abelian $\Delta(27)$ with A_4 as a foil and the exceptional $\Sigma(168)$ as a closing taste (§VI.6.7), before turning to the Higgs branch (§VI.6.8) and the limits of the construction (§VI.6.9). A word on the classification, since there is no A–D–E list: the finite subgroups of $SU(3)$ come in the diagonal abelian groups $\mathbb{Z}_m \times \mathbb{Z}_n$, the trihedral series $\Delta(3n^2)$ and $\Delta(6n^2)$, and a finite set of exceptionals Σ. We will name these as a map and work representatives; the full taxonomy, and the resolution geometry, belong to later volumes. The ADE miracle was special to $SU(2)$. For an $SU(3)$ action with $Q^\Gamma = 0$, the projection gives an $\mathcal{N}$=1 theory; its directed quiver is chiral when Q is complex.

VI.6.2 The D3-brane projection, slowly

The projection is the same machine introduced in Chapter 2, but it is worth running once slowly in the $\mathbb{C}^3$ language, because every new feature of this chapter enters through the representation $Q = \mathbf{3}$. We begin before the orbifold and add it in.

Before projection, N regular D3-branes at an orbifold point are represented on the covering space by $K = N|\Gamma|$ images. Their flat-space parent carries $4d$ $\mathcal{N}$=4 $U(K)$ super Yang–Mills. In $\mathcal{N}$=1 language its fields are one vector multiplet A_μ and three adjoint chiral multiplets Φ_1, Φ_2, Φ_3, the latter the three complex coordinates of the transverse $\mathbb{C}^3$; as a triple the Φ_a form the defining **3** of the $SU(3)$ flavour symmetry that rotates the transverse space. Placing the branes at the tip of $\mathbb{C}^3/\Gamma$ with $\Gamma \subset SU(3)$ introduces two simultaneous actions of Γ:

- a *geometric* action $Q(g)$ on the transverse index $a = 1, 2, 3$, the defining **3** restricted to Γ;
- a *Chan–Paton* action $\gamma(g) \in U(K)$ on the brane labels, the representation $\gamma : \Gamma \to U(K)$ carried by the open-string endpoints.

The orbifold keeps exactly the fields on which the two actions compensate:

$$A_\mu = \gamma(g)\, A_\mu\, \gamma(g)^{-1}, \qquad \Phi_a = Q(g)_{ab}\, \gamma(g)\, \Phi_b\, \gamma(g)^{-1}, \qquad g \in \Gamma. \tag{VI.6.1}$$

The gauge field, a Chan–Paton matrix with no transverse index, survives where it commutes with $\gamma(g)$ for all g. The scalars, which carry the extra factor $Q(g)$, survive only in the combinations that the geometric and Chan–Paton rotations leave invariant together. That single difference, the presence or absence of the factor $Q(g)$, is the whole content of the projection. Figure VI.6.2 shows the three stages of the construction.

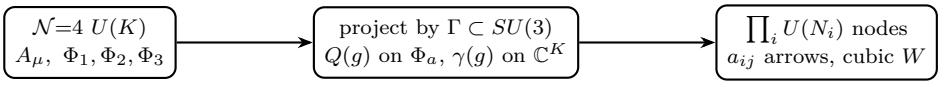


Figure VI.6.2: The orbifold projection from the flat-space $\mathcal{N}$=4 parent, the two Γ-actions of (VI.6.1), and the quiver they leave invariant. It has exactly $\mathcal{N}$=1 when $Q^\Gamma = 0$. Only the chiral fields carry the geometric factor $Q(g)$, which is what makes the matter (the arrows) sensitive to Q while the gauge group (the nodes) is not.

The gauge group from Schur's lemma. Decompose the Chan–Paton space into the isotypic blocks of Γ,

$$\mathbb{C}^K = \bigoplus_i \mathbb{C}^{N_i} \otimes R_i, \qquad R_i \text{ the irreducibles of } \Gamma, \tag{VI.6.2}$$

where R_i is the space on which Γ acts irreducibly and $\mathbb{C}^{N_i}$ is the multiplicity space it does not touch. A surviving gauge field commutes with every $\gamma(g)$, that is, it is an endomorphism of $\mathbb{C}^K$ intertwining the Γ-action. Schur's lemma says such intertwiners act as scalars on each irreducible and freely on each multiplicity space, so the commutant is block-diagonal and the gauge group is one unitary factor per irreducible,

$$\begin{aligned} \mathrm{End}_\Gamma(\mathbb{C}^K) = \bigoplus_i \mathrm{Mat}_{N_i}(\mathbb{C}) \implies G = \prod_i U(N_i), \\ N_i = N\, \dim R_i, \qquad K = \sum_i N_i \dim R_i = N\,|\Gamma|. \end{aligned} \tag{VI.6.3}$$

The second line records the *regular* brane, the case $\gamma =$ the regular representation $\mathbb{C}[\Gamma]$, in which each irreducible R_i appears with multiplicity equal to its own dimension and the ranks are $N_i = N \dim R_i$. A small picture fixes this: for an abelian Γ with four one-dimensional irreducibles, the regular Chan–Paton space of one brane is four one-dimensional blocks, and (VI.6.3) gives four $U(1)$ factors, one sitting on each block. For N branes the same four blocks become four $U(N)$ factors.

A regular brane is, physically, an ordinary bulk D3-brane that happens to sit at the singularity: it can move off into $\mathbb{C}^3/\Gamma$, and its γ is the regular representation. A *fractional* brane instead occupies a single isotypic block and has γ supported on one irreducible. By itself it cannot move to a generic bulk point; on a non-isolated quotient it may move along a fixed locus. We will use only the regular brane in this chapter, and recall the fractional vocabulary only so the later references make sense; the geometry of fractional branes was the subject of Chapter 5 in the $\mathbb{C}^2$ case.

How many supercharges survive. The geometric action on Q is a physical premise of the orbifold construction; the dimension sum in (VI.6.3) says nothing about supersymmetry. The positive-chirality transverse spinor of $Spin(6) \simeq SU(4)$ restricts under $SU(3)$ as $\mathbf{4} = \mathbf{1} \oplus \mathbf{3}$. The singlet leaves one $4d$ supersymmetry multiplet, and every invariant vector of $Q = \mathbf{3}|_\Gamma$ leaves another. Thus the preserved count is

$$\mathcal{N} = 1 + \dim_{\mathbb{C}} Q^\Gamma. \tag{VI.6.4}$$

For the examples below, $Q^\Gamma = 0$ and the result is exactly $\mathcal{N}$=1. If Γ fixes a complex direction, its action is conjugate into an $SU(2)$ subgroup and the count rises to $\mathcal{N}$=2; the trivial action gives the flat $\mathcal{N}$=4 parent. The invariant holomorphic three-form follows from $\det Q(g) = 1$ and ensures at least the first singlet. It does not exclude these enhancements. The group embedding, rather than the character-degree identity, chooses the supercharges.

Projection checklist

To build the probe of $\mathbb{C}^3/\Gamma$: (1) choose $\Gamma \subset SU(3)$ and check $Q^\Gamma = 0$ for exactly $\mathcal{N}$=1; (2) restrict the defining $\mathbf{3}$ to Γ to get Q; (3) choose the Chan–Paton representation γ (regular, for a regular brane); (4) decompose γ into irreducibles, fixing the gauge group $\prod_i U(N_i)$; (5) keep the invariant gauge fields and the invariant chiral fields. Steps (4) and (5) are the next two sections.

The matter is what (VI.6.1) keeps among the scalars, and the rule is already visible: a chiral field Φ_a survives between block i and block j exactly when the geometric rotation $Q(g)$ can be undone by a Chan–Paton rotation, that is, when R_j sits inside $Q \otimes R_i$. Counting those is the quiver. By this point the reader can already fix the regular-brane gauge group $\prod_i U(N_i)$ from the character degrees of Γ alone, and say why the nodes are blind to Q while only the matter feels it.

VI.6.3 From Chan–Paton blocks to the directed McKay quiver

The matter content is the most important object in the chapter, so we build it carefully. A surviving scalar is a map from one Chan–Paton block to another that carries one unit of the transverse index. Concretely, Φ_a restricted to the pair of blocks (i, j) is a linear map $\mathbb{C}^{N_j} \otimes R_j \to \mathbb{C}^{N_i} \otimes R_i$ that intertwines the Γ-actions after accounting for the geometric factor $Q(g)$. By (VI.6.1), such a map exists precisely when there is a Γ-intertwiner

$$R_j \longrightarrow Q \otimes R_i, \tag{VI.6.5}$$

and the surviving fields between the two blocks are bifundamentals of $U(N_i) \times U(N_j)$, one for each independent intertwiner. We fix the arrow convention once and use it throughout: an arrow $i \to j$ carries a chiral field

$$X_{ij} \in (\Box_i, \overline{\Box}_j), \tag{VI.6.6}$$

the fundamental of $U(N_i)$ times the antifundamental of $U(N_j)$. As a matrix it maps the j multiplicity space to the i multiplicity space; the drawn arrow still runs $i \to j$. This distinction fixes the order of products in W. The dimension of that intertwiner space is the number of fields, so we tensor and decompose,

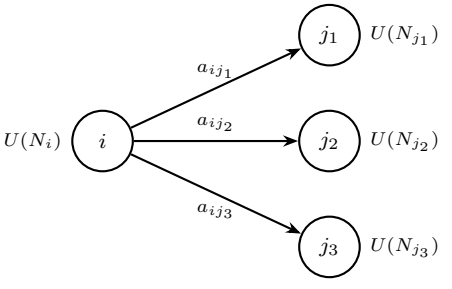
$$Q \otimes R_i \;=\; \bigoplus_j a_{ij}\, R_j, \qquad a_{ij} = \dim \mathrm{Hom}_\Gamma\big(R_j,\; Q \otimes R_i\big). \tag{VI.6.7}$$

The numbers a_{ij} are the McKay multiplicities. They organize the matter into a quiver by the rule:

The McKay rule

Draw one node for each irreducible R_i. Draw a_{ij} arrows from node i to node j, one for each copy of R_j inside $Q \otimes R_i$. Each arrow is a chiral bifundamental $X_{ij} \in (\Box_i, \overline{\Box}_j)$. The defining representation $Q = \mathbf{3}$, not the shape of the singular space, draws the quiver.

A multiplicity larger than one means several arrows, not several gauge groups: a double arrow $a_{ij} = 2$ is two independent chiral fields with the same gauge quantum numbers, and a triple arrow is three. We will meet triple arrows already in dP_0. Figure VI.6.3 shows the rule in action: the decomposition of $Q \otimes R_i$ is literally the list of arrows leaving node i.



$$Q \otimes R_i = a_{ij_1} R_{j_1} \oplus a_{ij_2} R_{j_2} \oplus a_{ij_3} R_{j_3}$$

Figure VI.6.3: The McKay rule: tensor R_i by the defining Q, decompose into irreducibles, and draw a_{ij} arrows from i to each constituent R_j. The outgoing arrows of node i are exactly the summands of $Q \otimes R_i$.

The multiplicity is computed by character orthogonality, which turns the abstract Hom into a sum over the group. Writing χ_i for the character of R_i and using that the multiplicity of R_j in a representation is its inner product with χ_j,

$$a_{ij} = \big\langle \chi_j,\; \chi_Q\, \chi_i \big\rangle = \frac{1}{|\Gamma|} \sum_{g \in \Gamma} \chi_Q(g)\, \chi_i(g)\, \overline{\chi_j(g)}. \tag{VI.6.8}$$

The order of the slots matters: χ_Q and χ_i enter directly, and it is χ_j, the character of the *outgoing* node, that is complex-conjugated. That asymmetry is exactly what will make the quiver directed.

It pays to see (VI.6.8) work once in the simplest setting, an abelian Γ, before the worked examples. There every irreducible is one-dimensional, a character ρ, and tensoring is multiplication of characters. If the defining representation is a sum of three one-dimensional weights,

$$Q = \rho_1 \oplus \rho_2 \oplus \rho_3, \qquad Q \otimes \rho_i = (\rho_i\rho_1) \oplus (\rho_i\rho_2) \oplus (\rho_i\rho_3), \tag{VI.6.9}$$

so from the node ρ_i there is exactly one arrow to each of the three nodes $\rho_i\rho_1, \rho_i\rho_2, \rho_i\rho_3$. The reader can check from (VI.6.8) that the same three arrows come out of the character sum. This one rule already contains both abelian examples below: for $\mathbb{Z}_3$ with all three weights equal it collapses three arrows onto one target, and for $\mathbb{Z}_2 \times \mathbb{Z}_2$ it spreads them onto three distinct targets.

Common misconception: the geometry does not draw the quiver

The quiver is not read off the shape of the singular space. It is fixed by the representation theory of Γ: the nodes are the irreducibles, and the arrows are the decomposition of $Q \otimes R_i$. Two orbifolds with very different singular geometries can share a quiver if they share the representation $Q|_\Gamma$, and the geometry reappears only later, as the moduli space the quiver *produces*. Tensor by Q, decompose, draw arrows: that is the whole construction.

After this section the reader can draw the entire quiver of any $\Gamma \subset SU(3)$ from its character table alone: one node per irreducible, and a_{ij} arrows $i \to j$ read off the decomposition of $Q \otimes R_i$. What the orientation of those arrows means physically is the next section.

VI.6.4 Chirality, the reality of Q, and the anomaly

The quiver of §VI.6.3 has an orientation, and the orientation is the new physics. A chiral bifundamental from node i to node j is not the same field as one from j to i: the two carry conjugate gauge representations, and in four dimensions a left-handed $(\square_i, \overline{\square}_j)$ cannot be traded for a $(\square_j, \overline{\square}_i)$. The net number of chiral arrows between two nodes is therefore the *difference*

$$(a_{ij} - a_{ji}), \tag{VI.6.10}$$

and a theory is chiral when this antisymmetric part is nonzero somewhere. What controls it is the reality of the defining representation. Take the complex conjugate of the character formula (VI.6.8), use $\overline{\chi_Q} = \chi_{Q^\vee}$ for the dual representation, and read the conjugated sum as the same multiplicity formula with i and j exchanged:

$$\overline{a_{ij}(Q)} = \frac{1}{|\Gamma|}\sum_g \overline{\chi_Q}\,\overline{\chi_i}\,\chi_j = \frac{1}{|\Gamma|}\sum_g \chi_{Q^\vee}\,\chi_j\,\overline{\chi_i} = a_{ji}(Q^\vee). \tag{VI.6.11}$$

The multiplicities are non-negative integers, $\overline{a_{ij}} = a_{ij}$, so (VI.6.11) says the adjacency built from the conjugate representation is the transpose of the one built from Q,

$$a_{ij}(Q^\vee) = a_{ji}(Q), \qquad \text{hence} \qquad a - a^{\mathsf{T}} \ \text{ is controlled by } \ Q - Q^\vee. \tag{VI.6.12}$$

If $Q \cong Q^\vee$, that is if χ_Q is real, the adjacency is symmetric and the quiver is non-chiral; the arrows pair up into conjugate pairs, which for $SU(2)$ is exactly the undirected McKay graph of Chapter 3. If Q is genuinely complex the pairing fails, the antisymmetric part is nonzero, and the theory is chiral. The decisive variable is the reality of Q, and the natural guess that chirality follows from Γ being non-abelian is wrong in both directions, as Table VI.6.2 shows.

Γ	reality of Q	abelian?	chiral?
$\mathbb{Z}_3$, weights $(1,1,1)$	complex	yes	yes
$\mathbb{Z}_2 \times \mathbb{Z}_2$	real (sum of three real characters)	yes	no
$\Delta(27)$	complex ($\mathbf{3} \ncong \overline{\mathbf{3}}$)	no	yes
$A_4 = \Delta(12)$	real ($\mathbf{3} \subset SO(3)$)	no	no

Table VI.6.2: Chirality is governed by the reality of Q, not by whether Γ is abelian. The four entries are the worked examples of this chapter.

Common misconception: "non-abelian means chiral"

Chirality of a $\mathbb{C}^3/\Gamma$ quiver is decided by whether the defining $\mathbf{3}$ is complex, not by whether Γ is abelian. The abelian $\mathbb{Z}_3 = (1,1,1)$ is chiral; the abelian $\mathbb{Z}_2 \times \mathbb{Z}_2$ is non-chiral; the non-abelian $\Delta(27)$ is chiral; the non-abelian A_4 is non-chiral, because its $\mathbf{3}$ is the real rotation representation. There is no affine-Dynkin or Cartan structure for $SU(3)$ in any of these cases.

A chiral gauge theory must have its anomalies cancel, and the regular brane does so automatically, for a reason worth seeing. Two dimension identities hold for any $\Gamma \subset SU(3)$. Summing (VI.6.7) against the dimensions reproduces the dimension of $Q \otimes R_i$,

$$\sum_j a_{ij} \dim R_j = (\dim Q)\, \dim R_i = 3 \dim R_i, \tag{VI.6.13}$$

the outgoing arrows weighted by ranks. The incoming arrows obey the same identity, but for a different reason. The regular representation absorbs any tensor factor up to multiplicity,

$$Q \otimes \mathbb{C}[\Gamma] = \mathbb{C}[\Gamma]^{\oplus 3}, \qquad \mathbb{C}[\Gamma] = \bigoplus_i R_i^{\oplus \dim R_i}, \tag{VI.6.14}$$

so the multiplicity of R_i in $Q \otimes \mathbb{C}[\Gamma]$ is $3 \dim R_i$ on the one hand, and $\sum_j a_{ji} \dim R_j$ on the other (reading the second slot of (VI.6.7) through every R_j), giving

$$\sum_j a_{ji} \dim R_j = 3 \dim R_i. \tag{VI.6.15}$$

At the regular ranks $N_i = N \dim R_i$, the cubic $SU(N_i)^3$ gauge anomaly at node i is proportional to the chiral matter leaving the node minus the chiral matter entering it, weighted by the ranks at the other end,

$$\mathcal{A}_i \;\propto\; \sum_j a_{ij} N_j - \sum_j a_{ji} N_j = N\Big(\sum_j a_{ij} \dim R_j - \sum_j a_{ji} \dim R_j\Big) = 0, \tag{VI.6.16}$$

zero by (VI.6.13) and (VI.6.15). The two identities, one from $\dim(Q \otimes R_i)$ and one from the regular representation, are exactly what is needed. Notice that this settles only the non-abelian $SU(N_i)^3$ anomaly; the fate of the $U(1)$ factors, some of which become massive or anomalous, is the consistency question of Chapter 7, not of this chapter.

Rank and anomaly check

For any Γ, three numbers must agree. The dimension sum $\sum_i (\dim R_i)^2 = |\Gamma|$ confirms no irreducible was missed. The two rank-weighted sums $\sum_j a_{ij} \dim R_j$ and $\sum_j a_{ji} \dim R_j$ must each equal $3 \dim R_i$ at every node; their difference is the $SU(N_i)^3$ anomaly, which vanishes at the regular ranks. The reader can carry these three checks through every worked example below; we will point to them as we go. For an abelian Γ with $Q = \rho_1 \oplus \rho_2 \oplus \rho_3$, the row sum is 3 at every node because there are exactly three outgoing arrows, and the reader can check that the adjacency is symmetric precisely when the weight set $\{\rho_1, \rho_2, \rho_3\}$ is closed under inversion, that is when $Q \cong Q^\vee$ is real, recovering (VI.6.12).

VI.6.5 The cubic superpotential, inherited from $\mathcal{N}$=4

The arrows are only half of an $\mathcal{N}$=1 theory. In the $\mathbb{C}^2/\Gamma$ block the geometry was controlled by the hyperkähler quotient, the moment maps of the $\mathcal{N}$=2 structure, and the superpotential was forced by that extended supersymmetry. With only $\mathcal{N}$=1 there is no such crutch: the F-term equations from a genuinely cubic superpotential are an essential part of the data, and the quiver without its superpotential is not a definite theory. It is worth seeing why the bare quiver is not enough. Two orbifolds can share a quiver while differing in their superpotentials, and the difference is physical: it is the F-term relations (VI.6.20) that cut the space of arrow configurations down to the right moduli space, so without W the would-be geometry is far too big and does not reconstruct $\mathbb{C}^3/\Gamma$. The projected superpotential supplies the relations needed for the regular-brane moduli problem in §VI.6.8. Fortunately it is not free to choose; it descends, intact, from the parent.

On the unprojected branes the $\mathcal{N}$=4 theory carries the cubic coupling

$$W_{\text{parent}} = \varepsilon^{abc}\, \mathrm{Tr}\big(\Phi_a \Phi_b \Phi_c\big) = 3\, \mathrm{Tr}\big(\Phi_1 [\Phi_2, \Phi_3]\big), \tag{VI.6.17}$$

the commutator form on the right following from the antisymmetry of ε and the cyclicity of the trace. The three adjoints $\Phi_{1,2,3}$ are the components of the defining $\mathbf{3}$ of the $SU(3)$ flavour symmetry, and the coupling is fixed by that symmetry together with $\mathcal{N}$=4: the only cubic invariant one can form from three copies of the $\mathbf{3}$ is the totally antisymmetric one, the determinant $\Lambda^3 \mathbf{3} = \mathbf{1}$. The tensor ε^{abc} is that invariant, and under $g \in SU(3)$ it transforms by the determinant,

$$\varepsilon^{abc}\, g_a{}^d\, g_b{}^e\, g_c{}^f = \det(g)\, \varepsilon^{def} = \varepsilon^{def}, \tag{VI.6.18}$$

the last step because $\det g = 1$. This is exactly why (VI.6.17) survives the projection by $\Gamma \subset SU(3)$, and it is the algebraic expression of the Calabi–Yau condition: the invariant ε is the holomorphic three-form $dz_1 \wedge dz_2 \wedge dz_3$. (A would-be $U(3)$ element

with $\det g \neq 1$ would not preserve the cubic, so the $SU(3)$ embedding is doing real work here, just as it did for the supersymmetry count.)

Projecting (VI.6.17) splits each adjoint into arrow blocks. Gauge-index contraction requires a closed path $i \to j \to k \to i$, but closure alone does not fix its coupling. Choose a basis α of the intertwiner space for each arrow and let $B^{\alpha}_{ij,a}$ be its component in transverse direction a, with Chan–Paton indices ordered as in (VI.6.6). Restricting the parent trace to these blocks gives the actual coefficient

$$C^{ijk}_{\alpha\beta\gamma} = \varepsilon^{abc}\,\mathrm{tr}_{R_i}\big(B^{\alpha}_{ij,a}B^{\beta}_{jk,b}B^{\gamma}_{ki,c}\big), \qquad W = \frac{1}{3}\sum_{i,j,k}\sum_{\alpha,\beta,\gamma} C^{ijk}_{\alpha\beta\gamma}\,\mathrm{Tr}\big(X^{\alpha}_{ij}X^{\beta}_{jk}X^{\gamma}_{ki}\big). \tag{VI.6.19}$$

The outer sums run over every ordered, composable node and arrow-label triple; terms with no closed path are absent. The factor $1/3$ divides the ordered parent trace by its three cyclic starting positions, counting repeated-arrow words with their actual multiplicity. Equivalently, a cyclic orbit contributes its orbit size divided by three times the displayed C. Thus a word made from one repeated arrow carries weight $1/3$, while a word with three distinct rotations carries weight one. The contraction over a, b, c inside C is a different sum: it selects the inherited coupling and cannot be replaced by a count of triangles. For a non-abelian group the B matrices and their trace must actually be supplied to determine C; the adjacency tells us which channels are available, not whether a particular C vanishes. This distinction matters for the $\Delta(27)$ and exceptional examples below, whose full cubic coefficient tables are not calculated here.

The repeated-arrow issue already appears in the A_4 example below. At its **3** node, choose two self-arrow intertwiners $B^{A}_{a,bc} = \epsilon_{abc}$ and $B^{S}_{a,bc} = |\epsilon_{abc}|$. Their contraction gives $C_{AAA} = C_{ASS} = C_{SAS} = C_{SSA} = 6$. On commuting diagonal test fields A, S, the ordered formula therefore reads $2\,\mathrm{Tr}\,A^3 + 6\,\mathrm{Tr}\,AS^2$, up to the common parent normalization. Taking one unweighted representative would instead give $6\,\mathrm{Tr}\,A^3 + 6\,\mathrm{Tr}\,AS^2$ and change the relative coupling. This finite test fixes the counting convention; it does not supply a general table of non-abelian coefficients.

Differentiating the ordered sum counts every occurrence of the chosen arrow, including repeated occurrences in one word. Cyclicity of the contracted trace combines the three derivative positions. In the following expression the remaining indices still range over every ordered, composable triple,

$$\frac{\partial W}{\partial X^{\alpha}_{ij}} = \sum_{k,\beta,\gamma} C^{ijk}_{\alpha\beta\gamma}X^{\beta}_{jk}X^{\gamma}_{ki}. \tag{VI.6.20}$$

The product runs from j back to i in the drawn-arrow convention. Its order cannot be reversed: cyclicity relates traces of closed words, while this derivative is an open path with fixed endpoints. Vanishing of these derivatives cuts down the space of arrow configurations before the gauge quotient.

For a diagonal abelian action, write the three character weights as q_a. The arrow X^{a}_{i} runs from i to $i + q_a$ and the determinant-one condition reads $q_1 + q_2 + q_3 = 0$ in the character group. In the conventional normalization that counts each cyclic orbit

once, the projected cubic becomes

$$W = \frac{1}{3}\sum_i \varepsilon_{abc}\ \mathrm{Tr}\big(X_i^a\, X_{i+q_a}^b\, X_{i+q_a+q_b}^c\big). \tag{VI.6.21}$$

The factor $1/3$ removes the three cyclic copies of each traced word. It only fixes a common normalization relative to (VI.6.17); it does not change any F-flat equation. After this cyclic reduction each arrow occurs in one positive and one negative cubic word,

$$\#\{\text{distinct cyclic } W \text{ words containing a fixed } X_{ij}^a\} = 2, \qquad \text{with opposite signs.} \tag{VI.6.22}$$

This is the toric incidence property. It holds for these abelian orbifold projections even when two weights coincide, because the arrows retain their transverse labels. The following examples show the two complementary paths in an F-term explicitly.

Warning: a triangle of nodes is not a superpotential term

In an abelian quiver a triangle is almost literally a term: each closed oriented triangle, with its three distinct weights, contributes one word, and (VI.6.21) reads it off the graph. In a non-abelian quiver the arrows carry intertwiner labels, and a term is one ε-contracted invariant built from the arrow channels $\mathrm{Hom}_\Gamma(R_j, Q \otimes R_i)$; a visible triangle of nodes may support several such invariants or none. The cubic coupling is always the projected ε tensor, never a count of triangles in the drawing. The daughter superpotential is not optional data: it is the projected holomorphic three-form coupling of the parent.

By the end of this section the reader can identify allowed cubic paths and their ordered F-terms. For a general non-abelian group, evaluating W also requires the actual intertwiners and their inherited coefficients. In the abelian case, the reader can recognize the toric "two terms per field" pattern that the moduli space will turn back into geometry.

VI.6.6 Abelian examples: isolated versus non-isolated

The two abelian $\mathbb{C}^3$ orbifolds of this chapter run through the identical projection machine yet land at opposite poles: $dP_0 = \mathbb{C}^3/\mathbb{Z}_3$ is chiral and isolated, while $\mathbb{C}^3/(\mathbb{Z}_2 \times \mathbb{Z}_2)$ is non-chiral and non-isolated. Worked side by side they are the chapter's antidote to two tempting heuristics, that abelian should mean non-chiral and that abelian should mean isolated. Both fail, and the quiver registers the difference first.

The isolated, chiral case: $dP_0 = \mathbb{C}^3/\mathbb{Z}_3$

The smallest chiral case was worked in full in Chapter 2, as the cone over $\mathbb{P}^2$, the local dP_0 geometry. We recall it, not to redo it, but to fix orientation and notation and to watch the formulas of §§VI.6.3–VI.6.5 run on a case the reader already trusts. Take $\mathbb{C}^3/\mathbb{Z}_3$ with weights $(1,1,1)$: the generator acts as $\omega\,\mathbb{1}$ with $\omega = e^{2\pi i/3}$, the three one-dimensional irreducibles are $R_k(\omega\mathbb{1}) = \omega^k$, and the defining representation is

$Q = \omega \oplus \omega \oplus \omega$, all three weights equal to 1. The abelian rule (VI.6.9) then collapses the three arrows onto a single target,

$$Q \otimes R_i = 3\, R_{i+1}, \qquad a_{ij} = 3\, \delta_{j,\, i+1 \bmod 3}. \tag{VI.6.23}$$

Three nodes, a triple arrow $i \to i{+}1$ in one common orientation, drawn in Figure VI.6.4; the quiver is manifestly chiral, $a_{ij} \neq a_{ji}$, because the weight set $\{1,1,1\}$ is not closed under inversion. The superpotential is the single ε-contracted triangle, which expands into the six sign-weighted words

$$W = \varepsilon_{abc}\, \mathrm{Tr}\big(X^a_{01} X^b_{12} X^c_{20}\big) = \sum_{(a,b,c)\in \mathrm{cyc}(1,2,3)} \mathrm{Tr}\big(X^a_{01} X^b_{12} X^c_{20} - X^a_{01} X^c_{12} X^b_{20}\big), \tag{VI.6.24}$$

where $\mathrm{cyc}(1,2,3) = \{(1,2,3),(2,3,1),(3,1,2)\}$. The nine fields $X^a_{i,i+1}$ ($a = 1,2,3$, $i = 0,1,2$) each appear in exactly two terms with opposite sign by (VI.6.22). The ordered products cannot be combined into a matrix commutator because their factors connect different pairs of nodes. The dimension checks are immediate, $\sum_i (\dim R_i)^2 = 3 = |\Gamma|$ and $\sum_j a_{ij} \dim R_j = 3$ at each node. Table VI.6.3 packages the data in the format we will reuse for every example.

group	$\mathbb{Z}_3$, weights $(1,1,1)$ (order 3)
irreducibles	R_0, R_1, R_2, all $\dim 1$
defining Q	$\omega \oplus \omega \oplus \omega$ (complex)
adjacency	$a_{ij} = 3\delta_{j,i+1}$ (triple arrow $i \to i{+}1$)
chiral?	yes ($a \neq a^{\mathsf{T}}$)
isolated?	yes (no nontrivial g fixes a line)
role here	the simplest isolated chiral anchor

Table VI.6.3: The recalled $dP_0 = \mathbb{C}^3/\mathbb{Z}_3$ data.

One fact about dP_0 will be the foil for the second example: it is an *isolated* singularity. No nontrivial element of $\mathbb{Z}_3$ fixes any direction, the only fixed point of $\omega\mathbb{1}$ being the origin, so the singular set is a point. The second example changes only the group, not the machine, and both the chirality and the isolation are lost.

The non-isolated, non-chiral case: $\mathbb{C}^3/(\mathbb{Z}_2 \times \mathbb{Z}_2)$

This is the example to dwell on, and we work it in full. Take $\Gamma = \mathbb{Z}_2 \times \mathbb{Z}_2$ generated by

$$g_1 = \mathrm{diag}(1,-1,-1), \qquad g_2 = \mathrm{diag}(-1,1,-1), \qquad g_3 = g_1 g_2 = \mathrm{diag}(-1,-1,1), \tag{VI.6.25}$$

an order-four group inside $SU(3)$ (each generator has determinant $+1$). Being abelian, it has four one-dimensional irreducibles, labeled by the two signs $(s,t) \in \{0,1\}^2$ under (g_1, g_2) via $\chi_{(s,t)}(g_1) = (-1)^s$, $\chi_{(s,t)}(g_2) = (-1)^t$; the trivial one is $(0,0)$. Table VI.6.4 is the character table.

The three transverse coordinates carry the three *nontrivial* characters. Reading (VI.6.25), z_1 is fixed by g_1 and flipped by g_2, so $z_1 = \chi_{(0,1)}$; similarly $z_2 = \chi_{(1,0)}$ and

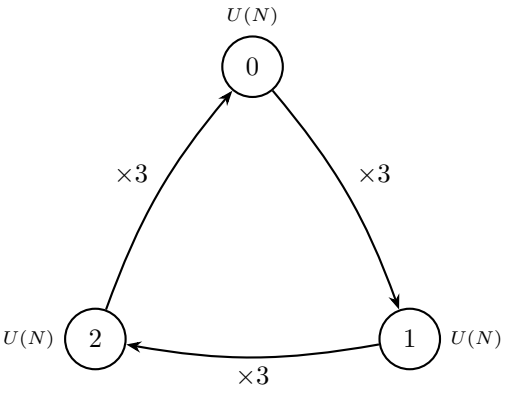


Figure VI.6.4: The $dP_0 = \mathbb{C}^3/\mathbb{Z}_3$ quiver (recalled from Chapter 2, drawn as there): three $U(N)$ nodes joined cyclically $0 \to 1 \to 2 \to 0$ by a triple bifundamental arrow on each edge ($\times 3$ denotes three distinct chiral fields, $a_{ij} = 3\delta_{j,i+1}$, not a charge-three field). No reverse arrows and no adjoint loops: the theory is chiral, isolated.

	e	g_1	g_2	g_3
$\chi_{(0,0)}$	1	1	1	1
$\chi_{(1,0)}$	1	-1	1	-1
$\chi_{(0,1)}$	1	1	-1	-1
$\chi_{(1,1)}$	1	-1	-1	1

Table VI.6.4: Character table of $\mathbb{Z}_2 \times \mathbb{Z}_2$. All entries are real, so every representation is real.

$z_3 = \chi_{(1,1)}$. The defining representation is therefore

$$Q = \chi_{(0,1)} \oplus \chi_{(1,0)} \oplus \chi_{(1,1)}, \tag{VI.6.26}$$

a sum of three *real* characters, so χ_Q is real and the quiver will be non-chiral by (VI.6.12), before we even compute it. Table VI.6.5 records the three weights once, since every arrow below is a shift by one of them.

Now the adjacency. The four characters form the dual group $\widehat{\Gamma} \cong \mathbb{Z}_2 \times \mathbb{Z}_2$, on which tensoring is addition of labels,

$$\chi_{(s,t)} \otimes \chi_{(s',t')} = \chi_{(s+s',\, t+t') \bmod 2}, \qquad Q \otimes \chi_{(s,t)} = \sum_{(u,v)\neq(0,0)} \chi_{(s+u,\, t+v)}. \tag{VI.6.27}$$

Adding the three nonzero labels to a fixed (s,t) lands on the three *other* labels, so from every node there is exactly one arrow to each of the other three and none to itself,

$$a_{ij} = 1 - \delta_{ij}, \qquad \text{i.e.} \qquad a = J - \mathbb{1}_4, \tag{VI.6.28}$$

with J the all-ones matrix. The reader can confirm the same matrix from the character formula (VI.6.8) and the table, and can read it off the explicit projection too: with γ

weight	coordinate	character (s,t)	arrow shift
q_1	z_1	$(0,1)$	$i \to i+(0,1)$
q_2	z_2	$(1,0)$	$i \to i+(1,0)$
q_3	z_3	$(1,1)$	$i \to i+(1,1)$

Table VI.6.5: The three transverse weights of $\mathbb{C}^3/(\mathbb{Z}_2 \times \mathbb{Z}_2)$. Each coordinate z_a carries one nontrivial character, and the McKay arrow of color a shifts a node by that character. The three shifts are distinct and sum to zero in $\mathbb{Z}_2 \times \mathbb{Z}_2$, so from each node the three arrows reach the three other nodes.

diagonal in the four blocks, a field Φ_a survives between blocks whose characters differ by the weight of z_a, and the surviving pattern is exactly the off-diagonal $J - \mathbb{1}$. The quiver is the complete graph on four nodes with a bidirectional arrow on every edge, the "doubled K_4" of Figure VI.6.5. It is symmetric, $a = a^{\mathsf{T}}$, hence non-chiral, just as (VI.6.26) predicted.

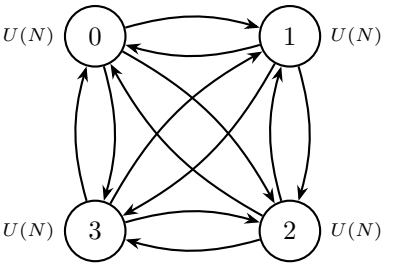


Figure VI.6.5: The $\mathbb{C}^3/(\mathbb{Z}_2 \times \mathbb{Z}_2)$ quiver: four nodes, a bidirectional arrow on every pair (the doubled K_4), $a = J - \mathbb{1}$. Symmetric, hence non-chiral: each edge is two opposite chiral multiplets whose net chirality cancels, not one undirected line. The superpotential triangles are suppressed.

It is worth being careful about what "doubled K_4" means. A symmetric adjacency means one arrow each way on every unordered edge. In the quiver this is *not* an undirected edge: it is two opposite chiral multiplets, X_{ij} and X_{ji}, whose net chirality cancels. The matter is vectorlike rather than chiral, which is the gauge-theory signature of the symmetric Q. Labeling the three arrows out of node 0 by their weights, X_0^1, X_0^2, X_0^3 run to the nodes $0{+}q_1, 0{+}q_2, 0{+}q_3$, that is to the three other nodes, and similarly for every node; this is the concrete content of (VI.6.27).

The superpotential is the toric one of (VI.6.21). The three weights are the three nontrivial labels, which sum to zero in $\mathbb{Z}_2 \times \mathbb{Z}_2$, so $q_1 + q_2 + q_3 = 0$ and the closed triangles are the loops $i \to j \to k \to i$ carrying the three distinct weights. Writing X_{ij}^a for the arrow of weight q_a from i to j, a representative pair of terms makes the toric structure concrete,

$$W \supset \mathrm{Tr}\big(X_{0,2}^1 X_{2,1}^2 X_{1,0}^3\big) - \mathrm{Tr}\big(X_{0,2}^1 X_{2,3}^3 X_{3,0}^2\big), \tag{VI.6.29}$$

the field $X_{0,2}^1$ appearing in both, with opposite sign. Differentiating in it opens both

triangles at that shared arrow,

$$\frac{\partial W}{\partial X^1_{0,2}} = X^2_{2,1}X^3_{1,0} - X^3_{2,3}X^2_{3,0} = 0, \tag{VI.6.30}$$

and the vanishing F-term equates the two length-two paths that return from node 2 to node 0: the path $2 \to 1 \to 0$ equals the path $2 \to 3 \to 0$. Every one of the twelve fields sits in exactly two cyclic words and gives an ordered path relation. These are the projected commuting-coordinate relations used in the regular-brane moduli problem of §VI.6.8. The anomaly check is immediate: every node has rank N, three arrows in and three out, so the rank-weighted sums of (VI.6.13) and (VI.6.15) are $3N$ each way and the difference (VI.6.16) vanishes.

Now the second heuristic. The singularity is *not* isolated. Each generator in (VI.6.25) has an eigenvalue $+1$, so it fixes a whole complex line: g_1 fixes the z_1-axis, along which it acts as $\mathrm{diag}(-1,-1)$ on the transverse (z_2, z_3), that is as $\mathbb{C}^2/\mathbb{Z}_2$. The three generators fix the three coordinate axes, and the singular set of $\mathbb{C}^3/(\mathbb{Z}_2 \times \mathbb{Z}_2)$ is three lines of $\mathbb{C}^2/\mathbb{Z}_2$ singularities meeting at the origin (Figure VI.6.6), not an isolated point. For a faithful finite subgroup of $SU(3)$, the quotient is isolated precisely when no nonidentity element fixes a nonzero vector. The determinant-one condition rules out complex reflections, so a fixed line really contributes to the singular locus. The reader can verify directly that each of g_1, g_2, g_3 has eigenvalue $+1$ and so fixes a line, which is why this quotient is non-isolated while dP_0 was isolated.

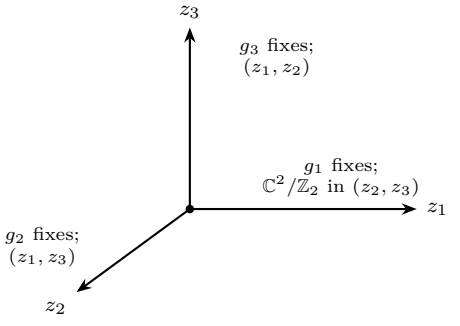


Figure VI.6.6: The non-isolated singular locus of $\mathbb{C}^3/(\mathbb{Z}_2 \times \mathbb{Z}_2)$: each nontrivial generator has eigenvalue $+1$ and fixes a coordinate line, along which the transverse action is $\mathbb{C}^2/\mathbb{Z}_2$. The three lines of singularities meet at the origin. (Schematic: the three complex lines are drawn as real axes.)

Common misconception: "abelian means isolated"

Whether $\mathbb{C}^n/\Gamma$ is an isolated singularity is a property of the action, not of whether Γ is abelian. For the finite $SU(3)$ actions considered here, the quotient is isolated exactly when no nonidentity $g \in \Gamma$ has eigenvalue 1. The abelian $\mathbb{Z}_3 = (1,1,1)$ acts freely and dP_0 is isolated; the abelian $\mathbb{Z}_2 \times \mathbb{Z}_2$ has three fixed lines and is non-isolated. A non-isolated point carries whole lines of lower singularities, and its resolution involves families of cycles rather than a finite set, a structural difference the gauge theory already registers in its vectorlike matter.

Side by side, the two abelian examples isolate the cause. The difference is entirely in the representation Q: complex with a free action for dP_0, real with three fixed lines for $\mathbb{Z}_2 \times \mathbb{Z}_2$, and the quiver sees it first, in the orientation of its arrows.

VI.6.7 Non-abelian examples: $\Delta(27)$ with A_4 as contrast, and the exceptional $\Sigma(168)$

For a genuinely non-abelian chiral example we take the trihedral group $\Delta(27)$, the smallest non-abelian piece of the $\Delta(3n^2)$ series. It is cleanest to define it by its matrices. Inside $SU(3)$ it is generated by a diagonal phase and the cyclic permutation of the three axes,

$$d = \mathrm{diag}(1, \omega, \omega^2), \qquad T = \begin{pmatrix} 0 & 1 & 0 \\ 0 & 0 & 1 \\ 1 & 0 & 0 \end{pmatrix}, \qquad \omega = e^{2\pi i/3}, \quad \det d = \det T = 1. \tag{VI.6.31}$$

The diagonal $SU(3)$ matrices with cube-root entries form a *normal abelian subgroup*,

$$A = \big\{\mathrm{diag}(\omega^a, \omega^b, \omega^c) : a + b + c \equiv 0 \ (\mathrm{mod}\ 3)\big\} = \langle d,\ \omega \mathbb{1}\rangle \cong \mathbb{Z}_3 \times \mathbb{Z}_3 \quad (\text{order } 9), \tag{VI.6.32}$$

and T cyclically permutes its phases, $TdT^{-1} = \mathrm{diag}(\omega, \omega^2, 1) = \omega d$, so T normalizes A. Hence $\Delta(27)$ is an *extension* of the cyclic $\mathbb{Z}_3$ generated by T by the normal $A \cong \mathbb{Z}_3 \times \mathbb{Z}_3$, of order $9 \cdot 3 = 27$. The extension splits, with T a complement, so it is the semidirect product $(\mathbb{Z}_3 \times \mathbb{Z}_3) \rtimes \mathbb{Z}_3$ written in the standard form of $\Delta(3n^2)$. Seen instead through its centre, $\Delta(27)$ is the Heisenberg group over $\mathbb{F}_3$: every commutator lands in the central $Z = \langle \omega \mathbb{1}\rangle \cong \mathbb{Z}_3$, with $[T, d] = TdT^{-1}d^{-1} = \omega \mathbb{1}$, and $\Delta(27)$ is then the *non-split* central extension $1 \to Z \to \Delta(27) \to \mathbb{Z}_3 \times \mathbb{Z}_3 \to 1$ of $\mathbb{Z}_3 \times \mathbb{Z}_3$ by Z. The split extension by the axis permutation and the non-split extension by the centre are the same group of order 27 seen from two angles. (Of the two non-abelian groups of order 27, this is the one of *exponent three*: every non-identity element cubes to the identity, as one checks from the generators, so it has no element of order nine and is the Heisenberg group, not the exponent-nine group $\mathbb{Z}_9 \rtimes \mathbb{Z}_3$.)

The representation content follows from the dimension budget, with no character table needed to start. The commutator subgroup is exactly the centre, so the abelianization is $\Delta(27)/\langle \omega \mathbb{1}\rangle \cong \mathbb{Z}_3 \times \mathbb{Z}_3$, which has nine one-dimensional characters; these pull back to nine one-dimensional irreducibles of $\Delta(27)$. The remaining dimension-squared

budget is $27 - 9 = 18$, and the only way to write 18 as a sum of squares of integers larger than one, consistent with each dimension dividing the order, is $18 = 3^2 + 3^2$. So there are exactly two three-dimensional irreducibles, and a group with a faithful three-dimensional representation that is not real must have them as a complex-conjugate pair: the defining $\mathbf{3}$ and its conjugate $\overline{\mathbf{3}}$. The reader can see in this dimension count why $\Delta(27)$ *cannot* have a single three-dimensional irreducible: 18 is not a perfect square. Table VI.6.6 collects the irreducibles.

irreducibles	dimensions	role in the quiver
nine $\mathbf{1}_{r,s}$	1 each	nine small nodes
$\mathbf{3}$	3	the defining node (Q)
$\overline{\mathbf{3}}$	3	its conjugate
$\sum_i (\dim R_i)^2 = 9 \cdot 1 + 9 + 9 = 27 = \lvert\Gamma\rvert$		

Table VI.6.6: Irreducibles of $\Delta(27)$. The pair $\mathbf{3}, \overline{\mathbf{3}}$ is complex-conjugate, the source of the chirality.

The tensor products are computed cleanly from one fact about the defining character. The diagonal centre acts on $\mathbf{3}$ as $\omega^k \mathbb{1}$, with trace $3\omega^k$; every *non-central* element, being either a non-scalar diagonal like d (trace $1 + \omega + \omega^2 = 0$) or an off-diagonal permutation type like T (trace 0), is traceless. So the defining character is supported on the centre,

$$\chi_{\mathbf{3}}(\omega^k \mathbb{1}) = 3\omega^k, \qquad \chi_{\mathbf{3}}(g) = 0 \ \text{ for non-central } g. \tag{VI.6.33}$$

From (VI.6.33) the products are immediate as functions on the group: $\chi_{\mathbf{3}}(g)^2 = 3\,\chi_{\overline{\mathbf{3}}}(g)$ holds pointwise (both sides are $9\omega^{2k} = 9\overline{\omega^k}\cdot$ on the centre and 0 off it), and $|\chi_{\mathbf{3}}(g)|^2$ equals 9 on the centre and 0 elsewhere, which is the character of the sum of the nine one-dimensional irreducibles. Decoding these as tensor products,

$$\mathbf{3} \otimes \mathbf{3} = 3\,\overline{\mathbf{3}}, \qquad \mathbf{3} \otimes \overline{\mathbf{3}} = \bigoplus_{r,s} \mathbf{1}_{r,s}, \tag{VI.6.34}$$

where $r, s \in \mathbb{Z}_3$ label the nine one-dimensional characters of the abelianisation $\mathbb{Z}_3 \times \mathbb{Z}_3$. Reading (VI.6.34) as McKay data fixes the quiver (Figure VI.6.7). The nine one-dimensional nodes all point to the *same* three-dimensional node: a one-dimensional character is trivial on the centre, where $\chi_{\mathbf{3}}$ is supported by (VI.6.33), so $\chi_{\mathbf{3}} \cdot \chi_{\mathbf{1}} = \chi_{\mathbf{3}}$ as a class function and

$$Q \otimes \mathbf{1}_{r,s} = \mathbf{3} \quad \text{for all nine } \mathbf{1}_{r,s}, \tag{VI.6.35}$$

one arrow from each one-dimensional node to the $\mathbf{3}$. The $\overline{\mathbf{3}}$ node emits one arrow to each of the nine $\mathbf{1}$'s, from $\mathbf{3} \otimes \overline{\mathbf{3}} = \bigoplus_{r,s} \mathbf{1}_{r,s}$; and the $\mathbf{3}$ node emits a triple arrow to the $\overline{\mathbf{3}}$, from $\mathbf{3} \otimes \mathbf{3} = 3\,\overline{\mathbf{3}}$. The three arrow types,

$$\mathbf{1}_{r,s} \longrightarrow \mathbf{3} \xrightarrow{\times 3} \overline{\mathbf{3}} \longrightarrow \mathbf{1}_{r,s}, \tag{VI.6.36}$$

close into one directed cycle, the middle arrow tripled. The adjacency is plainly not symmetric. To see the chirality explicitly, compare the pair $(\mathbf{3}, \overline{\mathbf{3}})$: there is a triple arrow

$\mathbf{3} \to \overline{\mathbf{3}}$ but none in return, $a_{\mathbf{3},\overline{\mathbf{3}}} = 3 \neq 0 = a_{\overline{\mathbf{3}},\mathbf{3}}$, the direct gauge-theory expression of $\mathbf{3} \ncong \overline{\mathbf{3}}$. The dimension checks hold as before: $\sum a_{ij} \dim R_j = 3 \dim R_i$ at every node (for the $\mathbf{3}$ node, $3 \cdot 3 = 9 = 3 \cdot 3$; for a $\mathbf{1}$ node, $3 = 3 \cdot 1$).

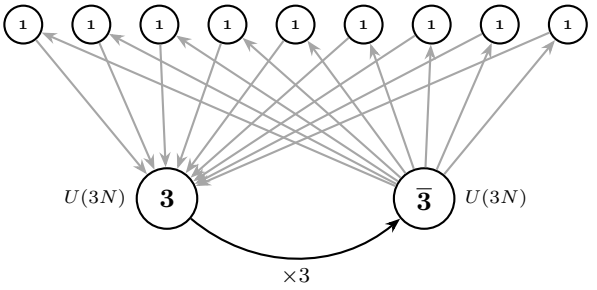


Figure VI.6.7: The $\Delta(27)$ quiver (schematic, the standard McKay quiver of $\Delta(27)$; the nine top nodes are the one-dimensional irreps, each a $U(N)$ factor, the two lower nodes the $\mathbf{3}, \overline{\mathbf{3}}$ with $U(3N)$). The nine one-dimensional nodes (top) each send one arrow to the defining $\mathbf{3}$ (from $Q \otimes \mathbf{1} = \mathbf{3}$); the $\mathbf{3}$ sends a triple arrow to $\overline{\mathbf{3}}$ (from $\mathbf{3} \otimes \mathbf{3} = 3\,\overline{\mathbf{3}}$); and $\overline{\mathbf{3}}$ sends one arrow back to each $\mathbf{1}_{r,s}$ (from $\mathbf{3} \otimes \overline{\mathbf{3}} = \bigoplus_{r,s} \mathbf{1}_{r,s}$). The three layers close into one directed cycle $\{\mathbf{1}\} \to \mathbf{3} \to \overline{\mathbf{3}} \to \{\mathbf{1}\}$; the asymmetry is the chirality.

The contrast that sharpens the lesson is the smaller sibling $A_4 = \Delta(12) = (\mathbb{Z}_2 \times \mathbb{Z}_2) \rtimes \mathbb{Z}_3$, the rotation group of the tetrahedron. It too is non-abelian, with irreducibles $\{\mathbf{1}, \mathbf{1}', \mathbf{1}'', \mathbf{3}\}$. But its three-dimensional representation is the ordinary rotation representation, $A_4 \subset SO(3) \subset SU(3)$, which is *real*: its character is real on every class. The tensor product comes out $\mathbf{3} \otimes \mathbf{3} = \mathbf{1} \oplus \mathbf{1}' \oplus \mathbf{1}'' \oplus \mathbf{3} \oplus \mathbf{3}$, symmetric, so the McKay adjacency is symmetric and the theory is non-chiral: a non-abelian but vectorlike quiver. Table VI.6.7 sets the two trihedral groups against each other.

	$\Delta(27)$	$A_4 = \Delta(12)$
order	27	12
irreducibles	nine $\mathbf{1}$'s $\oplus\, \mathbf{3} \oplus \overline{\mathbf{3}}$	$\mathbf{1}, \mathbf{1}', \mathbf{1}'', \mathbf{3}$
defining $\mathbf{3}$	complex	real ($\subset SO(3)$)
quiver	chiral	non-chiral
lesson	complex Q gives chirality	non-abelian alone does not

Table VI.6.7: $\Delta(27)$ against A_4. The two are both non-abelian trihedral groups; the chirality tracks the reality of the defining $\mathbf{3}$, nothing else.

The lesson of the two trihedral groups

Non-abelian does not imply chiral. $\Delta(27)$ is chiral because its defining $\mathbf{3}$ is genuinely complex, $\mathbf{3} \ncong \overline{\mathbf{3}}$. A_4 is non-chiral because its defining $\mathbf{3}$ is real, $A_4 \subset SO(3)$. Complex Q is the source of chirality, in the abelian and the non-abelian case alike, which is the single message of Table VI.6.2.

This is the first genuinely non-abelian chiral example, and it shows how non-abelian McKay data is computed rather than merely asserted: the dimension budget fixes the irreducibles, one fact about the defining character (supported on the centre) fixes the tensor products, and the arrows follow. A_4 then proves that non-abelianity itself is not the cause of chirality.

The exceptional case: $\Sigma(168) = PSL(2,7)$

We close the non-abelian examples with one exceptional group, to show that the directed McKay construction is not confined to the abelian and trihedral families. The exceptional subgroups of $SU(3)$ are a finite list, and the same formula (VI.6.7) handles each; we sample $\Sigma(168) \cong PSL(2,7)$, the simple group of order 168 and the symmetry group of the Klein quartic. Here $PSL(2,7) = PSL(2,\mathbb{F}_7)$ is the projective special linear group of 2×2 matrices over the field $\mathbb{F}_7 = \mathbb{Z}/7\mathbb{Z}$ (determinant one, modulo $\pm\mathbb{1}$). The reader is not asked to learn its representation theory here, only to see the same construction with more irreducibles.

Its irreducibles have dimensions

$$\Sigma(168): \quad \{\mathbf{1},\mathbf{3},\overline{\mathbf{3}},\mathbf{6},\mathbf{7},\mathbf{8}\}, \qquad 1^2+3^2+3^2+6^2+7^2+8^2 = 168, \tag{VI.6.37}$$

the dimension-squared sum confirming the list is complete. The defining $\mathbf{3}$ and its conjugate $\overline{\mathbf{3}}$ are a complex-conjugate pair, so the probe is again chiral. The complexity of Q is visible on an order-seven element, which sits in the defining representation as the diagonal phase

$$T = \mathrm{diag}(\beta,\beta^2,\beta^4), \qquad \beta = e^{2\pi i/7}, \qquad \chi_{\mathbf{3}}(T) = \beta+\beta^2+\beta^4 = \tfrac{1}{2}\big(-1+i\sqrt{7}\big), \tag{VI.6.38}$$

whose trace is not real; its conjugate $\frac{1}{2}(-1-i\sqrt{7})$ is the value on $\overline{\mathbf{3}}$, and that $\sqrt{-7}$ is the fingerprint of this group. A few rows of the adjacency show the same machine at work; tensoring the defining representation,

$$\mathbf{3}\otimes\mathbf{3} = \overline{\mathbf{3}}\oplus\mathbf{6}, \qquad \mathbf{3}\otimes\overline{\mathbf{3}} = \mathbf{1}\oplus\mathbf{8}, \qquad \mathbf{3}\otimes\mathbf{8} = \mathbf{3}\oplus\mathbf{6}\oplus\mathbf{7}\oplus\mathbf{8}, \tag{VI.6.39}$$

each line obeying the dimension identity (VI.6.13) (for instance $3+6 = 9 = 3\cdot 3$ in the first). Read as arrows: the $\mathbf{3}$ node sends an arrow to $\overline{\mathbf{3}}$ and one to $\mathbf{6}$; the $\overline{\mathbf{3}}$ direction sends to $\mathbf{1}$ and $\mathbf{8}$; the $\mathbf{8}$ sends to $\mathbf{3},\mathbf{6},\mathbf{7},\mathbf{8}$. The six-node directed quiver is recorded in the atlas; explicit inherited cubic coefficients require an intertwiner calculation that is not supplied by these tensor products. The tensor products establish the displayed arrows and their chirality; they do not establish the exceptional superpotential. The point is only that an exceptional $SU(3)$ subgroup requires no new physical idea, just more representation data: the same projection delivers a chiral $\mathcal{N}{=}1$ gauge theory for $PSL(2,7)$ as readily as for $\mathbb{Z}_3$.

By the end of this section the reader can build a non-abelian quiver from a character table, and explain the chapter's sharpest contrast: $\Delta(27)$ is chiral because its $\mathbf{3}$ is genuinely complex ($\mathbf{3} \ncong \overline{\mathbf{3}}$), while A_4 is non-chiral because its $\mathbf{3}$ is the real rotation representation in $SO(3)$, even though both groups are non-abelian. An exceptional group such as $\Sigma(168)$ then adds no new idea, only more representation data.

VI.6.8 The Higgs branch, FI chambers, and what is not proved

We have built the gauge theory; its distinguished regular-brane bulk component probes the geometry. This is the construction of Chapter 1: a D3-brane can move in its transverse space, and its position appears as a scalar vacuum expectation value. We sketch how the classical bulk component recovers the space probed by one regular brane.

The moduli space is carved out by two sets of equations. The F-terms are the derivatives (VI.6.20) of the superpotential,

$$\frac{\partial W}{\partial X_{ij}^{\alpha}} = \sum_{k,\beta,\gamma} C_{\alpha\beta\gamma}^{ijk}\, X_{jk}^{\beta}\, X_{ki}^{\gamma} = 0, \tag{VI.6.40}$$

holomorphic relations among arrows; for the abelian examples they equate two ordered paths with the same endpoints. The D-terms are the moment maps of the gauge group $\prod_i U(N_i)$, set equal to the Fayet–Iliopoulos parameters,

$$\mu_i \;=\; \sum_{\text{arrows out of } i} X X^{\dagger} \;-\; \sum_{\text{arrows into } i} X^{\dagger} X \;=\; \zeta_i\, \mathbb{1}_{N_i}, \qquad \sum_i N_i\, \zeta_i = 0. \tag{VI.6.41}$$

With the usual compatibility of the moment-map and stability parameters, the symplectic quotient has a GIT description. A generic chamber admits a stable-locus description; at a wall, semistable points and their orbit closures must also be included:

$$\mathcal{M}_{\zeta} \;=\; \{X:\; \partial W = 0,\; \mu = \zeta\} \Big/ \prod_i U(N_i) \;\simeq\; \{F\text{-flat}\} \;/\!/_{\zeta}\; \prod_i GL(N_i, \mathbb{C}). \tag{VI.6.42}$$

For one regular brane the ranks are $N_i = \dim R_i$. Moving the brane to a point with trivial stabilizer gives a three-complex-dimensional family of vacua. The finite-group invariant ring has the same dimension, because $\mathbb{C}[z_1, z_2, z_3]$ is integral over $\mathbb{C}[z_1, z_2, z_3]^{\Gamma}$. Thus the bulk component has

$$\dim_{\mathbb{C}} \mathcal{M}_{\text{reg,bulk}} = 3. \tag{VI.6.43}$$

This dimension calculation does not by itself identify an entire moduli scheme. The physical identification of the distinguished one-regular-brane component at zero FI with $\operatorname{Spec} \mathbb{C}[z_1, z_2, z_3]^{\Gamma}$ uses the projected F-term relations and the brane-probe interpretation. Extra branches or nonreduced structure are separate questions. For N regular branes there is a bulk branch $\operatorname{Sym}^N(\mathbb{C}^3/\Gamma)$; it need not exhaust all vacua.

At zero FI the affine invariant ring describes the singular target. A nonzero FI parameter changes the stability condition, and an appropriate chamber can give a crepant resolution. The existence of such a chamber for a specified group and the identification of its quotient with a chosen resolution are geometric results, not consequences of (VI.6.43). In the dP_0 example the familiar resolution is the total space of $\mathcal{O}_{\mathbb{P}^2}(-3)$; for $\mathbb{Z}_2 \times \mathbb{Z}_2$ the fixed lines yield a richer chamber problem. The F-terms are relations in the projected path algebra, and Figure VI.6.8 shows how they enter the quotient.

The recalled dP_0 makes the affine invariant ring concrete. For one regular brane the nine arrows $X_{i,i+1}^{a}$ are complex numbers, and the gauge-invariant data are the closed

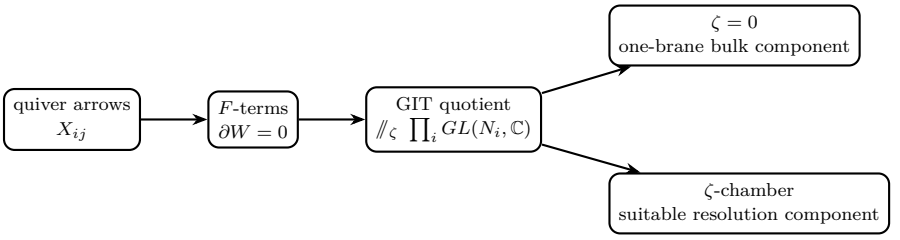


Figure VI.6.8: For one regular brane, the F-term arrows and stability quotient describe a distinguished bulk component. At zero FI parameter, its identification with $\mathbb{C}^3/\Gamma$ uses the physical probe construction; its dimension is derived here. A suitable nonzero-FI chamber can describe a resolution component. The diagram does not identify the full moduli scheme or every chamber.

cubic loops $X_{01}^a X_{12}^b X_{20}^c$. These map to the degree-three $\mathbb{Z}_3$-invariant monomials $z_a z_b z_c$ of $\mathbb{C}^3$ (the ten symmetric cubics $z_1^3,\ z_1^2 z_2,\ \ldots,\ z_1 z_2 z_3$), which generate the coordinate ring of the cone over $\mathbb{P}^2$, subject to their relations,

$$\begin{aligned} \mathcal{R}_{dP_0} &= \mathbb{C}[z_1,z_2,z_3]^{\mathbb{Z}_3} = \mathbb{C}[\, z_a z_b z_c : 1 \le a,b,c \le 3\,], \\ \operatorname{Spec} \mathcal{R}_{dP_0} &= \operatorname{Cone}\big(\nu_3(\mathbb{P}^2)\big). \end{aligned} \tag{VI.6.44}$$

Here ν_3 is the cubic Veronese embedding of $\mathbb{P}^2$. The ring equality establishes the affine quotient independently of the quiver. Matching it to the one-regular-brane moduli component additionally uses the projected F-terms and the gauge quotient; the shared dimension alone would be insufficient. The same logic, with the F-terms and the invariant ring of the relevant group, runs for every example, though for the non-abelian ones the invariant theory is heavier.

That is as far as this chapter goes, and it is worth being explicit about the boundary.

What the Higgs-branch discussion does *not* prove

We identify the distinguished bulk component at zero FI with $\mathbb{C}^3/\Gamma$ under the standard probe construction and check its complex dimension. We do *not* carry out the full GIT quotient, extract the toric fan, build the brane tiling or perfect matchings for the abelian cases, prove the Bridgeland–King–Reid derived equivalence, establish the existence or classification of crepant resolutions, or compute the exact metric. Those are the business of the toric volume and the foundations. In particular we do not assert unconditionally that the Higgs branch *is* the resolved $\mathbb{C}^3/\Gamma$: the one-brane bulk component is identified with the singular quotient at zero FI and can reach a resolution only in an appropriate chamber.

One caveat carries over from Chapter 1. The variety the probe sees is an algebraic object, the classical moduli space; the exact stringy geometry, including the metric, receives α' and g_s corrections, and the bulk-component identification with the orbifold is a leading classical statement. The lesson is that the quiver-with-superpotential is not just a gauge theory: its distinguished regular-brane bulk component remembers the orbifold it was built from. But the machinery that turns that memory into an explicit

resolved geometry is deliberately deferred. In capability terms, the reader can now impose F- and D-flatness on a $\mathbb{C}^3/\Gamma$ quiver, identify the distinguished one-regular-brane bulk component with the orbifold at zero FI under the probe premise, verify that its complex dimension is three, and state exactly where the construction stops short of the resolved geometry.

VI.6.9 What the construction gives, and where it goes next

The reader leaves this chapter with a definite construction. Given any finite $\Gamma \subset SU(3)$, the probe is built in a fixed sequence, with its supersymmetry count checked separately.

Building the $\mathbb{C}^3/\Gamma$ probe

(1) Specify Q and count its invariant vectors using (VI.6.4). (2) Find the irreducibles R_i of Γ. (3) Decompose $Q \otimes R_i = \bigoplus_j a_{ij} R_j$. (4) Draw a_{ij} arrows $i \to j$. (5) Decide chirality from the reality of Q. (6) Project the parent cubic; for a non-abelian group this requires actual arrow intertwiners and their coefficients. (7) Set the regular ranks $N_i = N \dim R_i$. (8) Check $\sum_i (\dim R_i)^2 = |\Gamma|$ and the two rank-weighted identities $\sum_j a_{ij} \dim R_j = \sum_j a_{ji} \dim R_j = 3 \dim R_i$ for the non-abelian cubic anomaly at nodes where it applies. (9) Identify the distinguished one-regular-brane bulk component at zero FI under the standard probe construction, and check its complex dimension is three.

Return for a moment to the opening contrast. In $\mathbb{C}^2$ the A–D–E list packaged the answer: knowing the Dynkin type told you the quiver, the ranks, and the resolved geometry at once. In $\mathbb{C}^3$ the construction above is just as general, but its output is not a Dynkin diagram and does not collapse onto a finite list. The same nine steps run for $\mathbb{Z}_3$, for $\mathbb{Z}_2 \times \mathbb{Z}_2$, for $\Delta(27)$ and for $PSL(2,7)$, and they produce as many different chiral quivers as there are groups.

Several threads are deliberately left for later, and it helps to say what each would answer. The resolution geometry of $\mathbb{C}^3/\Gamma$, its toric fan and brane tiling for the abelian cases, and the three-dimensional derived McKay correspondence are named here and constructed in the toric volume and the foundations: they would turn the "main branch reconstructs $\mathbb{C}^3/\Gamma$" of §VI.6.8 into an explicit resolved Calabi–Yau. The full classification of the finite subgroups of $SU(3)$, the higher trihedral series and the remaining exceptionals, is a map here and a table in the atlas. The infrared dynamics of these chiral quivers, their superconformal points, a-maximization, and the dualities among them, belong to the dynamics volumes; the orbifold construction stops at building the theory and identifying its classical geometry. And the $U(1)$ factors, the tadpoles, and the full quiver-consistency conditions are the subject of Chapter 7, where the twisted-sector calculation at regular rank is extended.

What the chapter does settle is the structural fact that organizes the whole block, and it is worth carrying away in one line: in three complex dimensions the McKay quiver is directed, the theory is chiral exactly when the defining representation is complex, and its cubic superpotential is obtained by projecting the $\mathcal{N}$=4 parent trace.

Status and sources

The source notes distinguish the physical assumptions from the mathematical statements and indicate where a precise source location remains open.

§VI.6.1 Physical setting. The finite-subgroup and quiver context follows Hanany and He (1999) and the orbifold construction of Douglas and Moore (1996). The $SU(2)$ ADE comparison is inherited from earlier chapters. The right column of Table VI.6.1 requires $Q^\Gamma = 0$ for exactly $\mathcal{N} = 1$. The precise primary passage for the spinor branching and enhanced subgroup cases remains to be located.

§VI.6.2 Projection and supercharges. The D3 Chan–Paton projection is a physical input associated with Douglas and Moore (1996) and Lawrence et al. (1998); Schur's-lemma centralizer and regular-representation dimensions are representation arithmetic. Equation (VI.6.4) uses the $SU(4) \downarrow SU(3)$ spinor branching and distinguishes the generic $SU(3)$ case from $SU(2)$ and trivial actions. The spinor branching determines the preserved supercharges independently of the character-degree sum used for the ranks.

§VI.6.3 Directed McKay data. The physical arrow projection is attributed to Douglas and Moore (1996) and the finite-group examples to Hanany and He (1999). The multiplicity and character formulas are exact representation identities once Q, irrep order, and orientation are fixed. The character count and the abelian group law both give the adjacency. Its spectrum alone cannot specify the orientation of a named asymmetric matrix. The nonabelian tables use numerical Dixon diagonalization and rounding, with exact character calculations for the smaller groups. Their adjacency does not determine the cubic intertwiners.

§VI.6.4 Chirality and anomaly. The equality $a(Q^\vee) = a(Q)^\mathsf{T}$ is a character identity; its converse for symmetric a follows from the row of the trivial representation. The two weighted-sum identities use the regular representation. Their field-theory reading as perturbative cubic $SU(N_i)^3$ anomaly cancellation assumes regular ranks and a node with a meaningful cubic anomaly; $U(1)$ and possible global issues belong to Chapter 7. The cubic condition leaves the abelian and global consistency conditions separate.

§VI.6.5 Inherited cubic. The parent $\mathcal{N} = 4$ cubic and its orbifold projection are physical inputs associated with Lawrence et al. (1998). The parent trace identity has an exact cyclic-word proof: three positive permutations become the same trace, as do the three negative permutations. The six 4×4 matrix evaluations illustrate the exact trace identity. Numerical determinant and QR evaluations illustrate the determinant identity. The abelian cubic uses the ordered products, since matching endpoints alone leaves the order undetermined. For nonabelian Γ, the actual coefficients in (VI.6.19) need chosen intertwiners and the parent trace.

§VI.6.6 Abelian examples. The dP_0 orientation recalls Chapter 2. The $\mathbb{Z}_2 \times \mathbb{Z}_2$ character table, $J - I$ adjacency, ordered path pair and fixed axes are finite calculations for the specified generators. The resolution interpretation is associated with Douglas, Greene, et al. (1997); a precise theorem or passage locator remains open. The character and cubic statements here apply to the specified abelian examples.

§VI.6.7 Nonabelian examples. The named subgroup examples are associated with Hanany and He (1999). The $\Delta(27)$ character and tensor identities have a small-group symbolic derivation by character identities; the A_4 comparison is likewise finite. The $PSL(2,7)$ character table and adjacency come from a numerical representation calculation with a specified order-seven class. Exact external support for the displayed exceptional tensor rows needs a locator. None of these adjacency calculations supplies inherited nonabelian cubic coefficients.

§VI.6.8 Moduli and FI chambers. The classical D-brane probe interpretation is associated with Douglas, Greene, et al. (1997). Finite invariant-ring dimension and the displayed dP_0 ring are algebraic statements. Identifying the distinguished zero-FI component with that ring also uses the physical projected-quiver construction. Stability quotients, chamber-to-resolution identifications and the dimension-three derived McKay theorem associated with Bridgeland et al. (2001) are source-only here; no theorem locator or full quotient computation is claimed. the threefold derived McKay correspondence retains the geometric work.

The finite examples cover oriented $\mathbb{Z}_5$ adjacency, cyclic dP_0 words with ordered derivatives and the regular-rank counts for $\Delta(27)$ at fixed N. The invariant-vector counts assume the stated spinor

branching. The parent trace accounts for the factor of three in the abelian cyclic sum. The imported string projection, nonabelian cubic coefficients and source-only moduli identifications require their separate physical or mathematical premises.

References

Bridgeland, T., A. King, and M. Reid (2001). "The McKay correspondence as an equivalence of derived categories". In: *J. Amer. Math. Soc.* 14. American Mathematical Society, pp. 535–554. DOI: 10.1090/S0894-0347-01-00368-X. arXiv: math/9908027.

Douglas, M. R., B. R. Greene, and D. R. Morrison (1997). "Orbifold resolution by D-branes". In: *Nucl. Phys. B* 506, pp. 84–106. DOI: 10.1016/S0550-3213(97)00517-8. arXiv: hep-th/9704151.

Douglas, M. R. and G. W. Moore (1996). "D-branes, quivers, and ALE instantons". In: arXiv preprint; not published in a journal. arXiv: hep-th/9603167.

Hanany, A. and Y.-H. He (1999). "NonAbelian finite gauge theories". In: *JHEP* 02, p. 013. DOI: 10.1088/1126-6708/1999/02/013. arXiv: hep-th/9811183.

Lawrence, A. E., N. Nekrasov, and C. Vafa (1998). "On conformal field theories in four-dimensions". In: *Nucl. Phys. B* 533, pp. 199–209. DOI: 10.1016/S0550-3213(98)00495-7. arXiv: hep-th/9803015.

Chapter VI.7

Tadpoles, anomalies, and quiver consistency

VI.7.1 Why a drawable quiver still needs consistency checks

A brane quiver specifies charged fields and their interactions. Changing the number of branes at one node leaves the arrows in place, but changes how many fermions the neighbouring gauge factors see. A projection that produces a sensible spectrum at regular ranks can therefore produce a gauge anomaly at other ranks. The first task of this chapter is to turn the arrows into conditions on those ranks.

There is a second description of the same branes. Their Chan–Paton representation determines which twisted Ramond–Ramond fields they source. In sectors localized at the orbifold point, the familiar nondegenerate D3-only examples reproduce the full quiver rank equations. When nodes are absent, their gauge anomalies supply no equation and the string constraints must be analyzed for that configuration. Sectors supported along a fixed complex line carry additional information that the four-dimensional cubic anomaly does not measure. Finally, abelian gauge bosons can couple to these closed-string fields and become massive even when their mixed gauge anomalies vanish.

We take the Chapter 6 spectrum and cubic superpotential as given, in four-dimensional $\mathcal{N}=1$ notation, allowing enhanced supersymmetry for special embeddings. We derive the fermion counts, solve representative rank constraints, and evaluate twisted traces. For abelian masses we identify the relevant couplings and state the kinetic assumptions needed to turn them into a mass matrix. Compact charge cancellation requires the rest of the compactification. Table VI.7.1 separates these questions.

consistency notion	gauge-theory side	string side
non-abelian anomaly	$SU(N_i)^3$ cancellation	localized chiral RR tadpoles
$U(1)$ anomaly / mass	anomalous or massive $U(1)$	Green–Schwarz / Stückelberg
global tadpole	compact charge neutrality	orientifolds / flux / flavour

Table VI.7.1: Three levels of consistency. The chapter computes local anomaly coefficients and twisted traces. Abelian masses also require the dynamical closed-string modes and their kinetic terms; compact completion requires global charge data.

Take-home message of this chapter

A quiver is not consistent merely because it can be drawn. For a directed $\mathbb{C}^3/\Gamma$ quiver the *antisymmetric* part of the adjacency, $a - a^{\mathsf{T}}$, controls the four-dimensional non-abelian gauge anomaly, while Chan–Paton traces in the twisted sectors control the Ramond–Ramond tadpoles. The regular brane passes both basic checks automatically; fractional ranks, orientifold projections, or compact embeddings impose real conditions. *Anomaly-freedom is necessary, not sufficient, and "local" is not "compact".*

The chapter is more computational than the slogan suggests, and it helps to say up front which quantities we will actually evaluate. Three objects do all of the work. The first is the *anomaly vector* $(a - a^{\mathsf{T}})N$, an integer vector read off the antisymmetric adjacency acting on the ranks; it gives the cubic coefficient at occupied nodes with $N_i \geq 3$. The second is the family of *twisted Chan–Paton traces* $\operatorname{Tr}\gamma_g = \sum_i N_i \chi_i(g)$, one complex number per group element, which control the twisted Ramond–Ramond tadpoles. The third is the $U(1)$ *coupling matrix* $K_{\lambda,g}$ tying the abelian gauge bosons to the twisted axions, which determines masses once the dynamical axions and their kinetic metric are specified. The rest of the chapter is learning how these three are related, where they differ, and how to compute each in an example. We develop them in turn (§VI.7.2–VI.7.6) and then apply the relevant calculations to three groups (§VI.7.7–VI.7.9) before drawing the local/compact boundary (§VI.7.10).

VI.7.2 Non-abelian anomalies from the antisymmetric adjacency

Recall the field content. To each node i the construction assigns a factor $U(N_i)$, and to each arrow $i \to j$ a chiral multiplet X_{ij} transforming as $(\square_i, \overline{\square}_j)$, a fundamental of $U(N_i)$ and an antifundamental of $U(N_j)$; the number of such arrows is the McKay multiplicity a_{ij}. The cubic anomaly of a four-dimensional gauge theory is carried by the chiral fermions, and only the bifundamentals contribute: the $\mathcal{N}{=}1$ vector multiplet's gaugino sits in the adjoint, a real representation, whose cubic anomaly vanishes.

Fix a node i and count the chiral fermions charged under $SU(N_i)$. Each outgoing arrow $i \to j$ carries X_{ij}, an N_j-plet of fundamentals of $SU(N_i)$; there are a_{ij} such arrows, contributing $a_{ij}N_j$ fundamentals. Each incoming arrow $j \to i$ carries X_{ji} in $(\square_j, \overline{\square}_i)$, an N_j-plet of *anti*fundamentals of $SU(N_i)$; there are a_{ji} of these, contributing $a_{ji}N_j$ antifundamentals. The cubic anomaly index of a representation R is $A(R)$ with

$A(\square) = +1$, $A(\overline{\square}) = -1$; collecting the matter node by node, the $SU(N_i)^3$ anomaly coefficient is the difference,

$$\mathcal{A}_i \;=\; \sum_j a_{ij}N_j - \sum_j a_{ji}N_j \;=\; \sum_j (a_{ij} - a_{ji})\, N_j \;=\; \big[(a - a^{\mathsf{T}})\, N\big]_i. \qquad \text{(VI.7.1)}$$

Table VI.7.2 is the same count laid out as a count of arrows, the format we will reuse. The object that controls the anomaly is therefore the antisymmetric part of the adjacency, $a - a^{\mathsf{T}}$. (We write it out rather than abbreviate it; the letter B is reserved for the Neveu–Schwarz two-form.) Its rows acting on the rank vector $N = (N_i)$ give the anomaly vector $\mathcal{A}$, and, if every node has $N_i \geq 3$, cancellation of all perturbative cubic anomalies is equivalent to

$$(a - a^{\mathsf{T}})\, N \;=\; 0. \qquad \text{(VI.7.2)}$$

arrow at node i	representation of $SU(N_i)$	multiplicity	anomaly sign
$i \to j$ (outgoing)	fundamental $\square_i$	$a_{ij}N_j$	$+$
$j \to i$ (incoming)	antifundamental $\overline{\square}_i$	$a_{ji}N_j$	$-$
net $SU(N_i)^3$ anomaly $\mathcal{A}_i$		$\displaystyle\sum_j (a_{ij} - a_{ji})N_j = \big[(a - a^{\mathsf{T}})N\big]_i$	

Table VI.7.2: The $SU(N_i)^3$ anomaly as a count of arrows at node i. Outgoing arrows bring fundamentals (anomaly $+$), incoming arrows bring antifundamentals (anomaly $-$); each arrow's multiplicity is weighted by the rank N_j at its far end. The cubic interpretation applies to $N_i \geq 3$. The net is the antisymmetric adjacency acting on the ranks.

Chapter 6 established that the regular brane satisfies (VI.7.2) identically, and the argument is worth recalling in one line because the rest of the chapter leans on it. With $d_i = \dim R_i$ the dimension vector, the regular ranks are $N_i = N d_i$, and two rank-weighted sums coincide,

$$\sum_j a_{ij}\, d_j \;=\; 3\, d_i \;=\; \sum_j a_{ji}\, d_j, \qquad \text{(VI.7.3)}$$

the first because tensoring R_i with the three-dimensional Q multiplies its dimension by three, the second because the regular representation obeys $Q \otimes \mathbb{C}[\Gamma] = \mathbb{C}[\Gamma]^{\oplus 3}$. Subtracting the two halves of (VI.7.3) gives, at the regular ranks,

$$(a - a^{\mathsf{T}})\, d = 0, \qquad \mathcal{A} = N\,(a - a^{\mathsf{T}})\, d = 0, \qquad \text{(VI.7.4)}$$

so the regular brane passes the perturbative cubic test for every such Γ. This is the statement Chapter 6 made; here it is the first of the consistency conditions, and the new point is that it is a property of the *direction* d, not of every direction. Where Chapter 6 stopped at the regular ranks, we now ask the general-rank question, and the rank-weighted vector $(a - a^{\mathsf{T}})N$ is the answer.

The interpretation of this vector depends on the rank at the node being tested. For $N_i \geq 3$ it is the cubic $SU(N_i)$ coefficient in the stated normalization. An $SU(2)$ node has no independent cubic invariant. Its separate Witten anomaly tests the parity of the number of doublets. In a quiver with only bifundamentals between distinct nodes, that count is $\sum_{j\neq i}(a_{ij}+a_{ji})N_j$ modulo two; adjoints do not change it. At $N_i = 1$ there is only an abelian factor, and at $N_i = 0$ there is no gauge factor. Thus the full equation (VI.7.2) is a useful rank constraint, but at small or absent nodes it is stronger than the perturbative non-abelian anomaly test itself. Its string interpretation must be supplied by the tadpole conditions, not by a nonexistent cubic Casimir. For example, the formal vector at $N = (1, 1, 2)$ is nonzero, although there is no $SU(N_i \geq 3)$ factor; the $SU(2)$ node has six doublets and passes the parity test.

The smallest chiral example: dP_0

The contrast between "automatic for the regular brane" and "a real condition" is sharpest on the smallest chiral case. For $dP_0 = \mathbb{C}^3/\mathbb{Z}_3$ the weights are $(1, 1, 1)$ and the adjacency is $a_{ij} = 3\,\delta_{j,i+1}$ on three nodes: a single directed triangle, traversed thrice. Its antisymmetric part is $a - a^{\mathsf{T}} = 3(P - P^{\mathsf{T}})$ with P the cyclic shift, so explicitly

$$a = \begin{pmatrix} 0 & 3 & 0 \\ 0 & 0 & 3 \\ 3 & 0 & 0 \end{pmatrix}, \qquad a - a^{\mathsf{T}} = \begin{pmatrix} 0 & 3 & -3 \\ -3 & 0 & 3 \\ 3 & -3 & 0 \end{pmatrix}, \tag{VI.7.5}$$

and the anomaly vector reads

$$\mathcal{A} \;=\; (a - a^{\mathsf{T}})\,N \;=\; 3\,(N_1 - N_2,\; N_2 - N_0,\; N_0 - N_1). \tag{VI.7.6}$$

Demanding $\mathcal{A} = 0$ forces, reading the three components in turn, $N_1 = N_2$, $N_2 = N_0$, $N_0 = N_1$, that is

$$N_0 = N_1 = N_2. \tag{VI.7.7}$$

When every node has rank at least three, the cubic anomalies therefore force the ranks onto the regular line. At smaller positive ranks one may impose the same full equation as the stronger string rank constraint used here; this is not derived from a cubic index. Empty-node configurations need their own string analysis. At $(2, 2, 2)$ the cubic coefficients have no independent anomaly interpretation, while each $SU(2)$ has twelve doublets and passes the separate parity test. These distinctions will matter when a fractional configuration leaves a node empty.

VI.7.3 Fractional ranks and the integer kernel

The anomaly condition (VI.7.2) is a linear equation on the ranks, so its solution set is a question in lattice algebra, and it is worth turning into a method one can run on any quiver. Write a general rank vector as the regular direction plus a deformation,

$$N \;=\; N\,d + M, \qquad d_i = \dim R_i, \tag{VI.7.8}$$

where $N\,d$ is the movable bulk of N regular branes and M is a *fractional-rank* deformation, a redistribution of branes among the nodes that need not be a multiple of d. Because $(a - a^{\mathsf{T}})\,d = 0$, the anomaly of (VI.7.8) depends on M alone,

$$\mathcal{A} \;=\; (a - a^{\mathsf{T}})\,N \;=\; (a - a^{\mathsf{T}})\,M, \tag{VI.7.9}$$

and the full rank equation becomes $(a - a^{\mathsf{T}})\,M = 0$.

The solutions of the full rank equation form the kernel of the antisymmetric adjacency, but the arithmetic must be done over the integers, not the rationals, because a rank vector is a tuple of nonnegative integers. Two refinements matter. First, the relevant object is the *integer* kernel

$$\ker_{\mathbb{Z}}(a - a^{\mathsf{T}}) = \{M \in \mathbb{Z}^{r+1} : (a - a^{\mathsf{T}})M = 0\}, \tag{VI.7.10}$$

a sublattice of $\mathbb{Z}^{r+1}$ ($r+1$ the number of nodes), computed in practice from the Smith normal form of $a - a^{\mathsf{T}}$: the number of zero invariant factors is the rank of the kernel, and the corresponding columns of the transforming matrix are a lattice basis. The diagonal Smith form alone gives the nullity, not the transforming columns. Clearing denominators in a rational basis gives integral kernel vectors, but does not in general prove that they generate the saturated integer kernel. For dP_0, the equations themselves say $M_0 = M_1 = M_2$, proving that $(1,1,1)$ is a primitive lattice generator. For the symmetric four-node example there are no equations, so the standard basis generates all of $\mathbb{Z}^4$. Second, a kernel vector with a negative entry is not by itself a brane configuration; only $N = N\,d + M \geq 0$ component by component is an admissible rank vector. The lattice $\ker_{\mathbb{Z}}(a - a^{\mathsf{T}})$ records the directions solving the full rank equation; intersecting the total-rank lattice with the nonnegative orthant gives the allowed ranks for that equation.

The method has three regimes, set by the chirality. Table VI.7.3 records them on the chapter's examples, and the reader can reproduce each entry directly. Chirality makes the antisymmetric matrix nonzero, but does not fix its nullity. For dP_0 it is one-dimensional, spanned by $d = (1,1,1)$ itself, as (VI.7.6) showed, so there is no further fractional direction solving the full rank equation beyond rescaling the regular brane. For a non-chiral quiver the antisymmetric part vanishes outright, $a = a^{\mathsf{T}}$, the anomaly is identically zero, and the kernel is the whole lattice $\mathbb{Z}^{r+1}$: every rank vector passes the cubic test. A genuinely chiral quiver with a kernel larger than the regular line is the interesting intermediate case; the cleanest small instance is a circulant $\mathbb{C}^3/\mathbb{Z}_n$, which we use as a method drill below.

A method drill: the circulant kernel of a chiral $\mathbb{C}^3/\mathbb{Z}_n$

(Optional computational aside, skippable on a first reading.) The mainline argument needs only the integer kernel $\ker_{\mathbb{Z}}(a - a^{\mathsf{T}})$ and the distinction between its rational span and its integral, nonnegative rank vectors; this drill shows how the Fourier diagonalization of a circulant makes that kernel explicit for the abelian series. For an abelian $\mathbb{C}^3/\mathbb{Z}_n$ with weights (w_1, w_2, w_3) summing to zero mod n, the nodes are labeled by $i \in \mathbb{Z}_n$ and the three arrows out of node i go to $i + w_1, i + w_2, i + w_3$, so the

example	$\ker_{\mathbb{Z}}(a-a^{\mathsf{T}})$	physical meaning
$dP_0=\mathbb{C}^3/\mathbb{Z}_3$	$\mathbb{Z}\cdot(1,1,1)$	only the regular direction
$\mathbb{C}^3/(\mathbb{Z}_2\times\mathbb{Z}_2)$	all of $\mathbb{Z}^4$	no cubic anomaly constraint
chiral $\mathbb{C}^3/\mathbb{Z}_n$	circulant kernel (below)	regular line, sometimes larger

Table VI.7.3: The anomaly-free rank lattice in the three regimes. The chiral examples shown restrict the ranks; a non-chiral quiver imposes no cubic constraint at all; a circulant chiral quiver can have a kernel larger than the regular line, computed from the discrete Fourier transform.

adjacency is a sum of three cyclic-shift powers,

$$a \;=\; P^{w_1}+P^{w_2}+P^{w_3}, \qquad (P)_{ij}=\delta_{j,i+1}, \tag{VI.7.11}$$

a circulant matrix. Circulants are diagonalized by the discrete Fourier transform: the eigenvectors are $v_i^{(\ell)}=\zeta^{\ell i}$ with $\zeta=e^{2\pi i/n}$, and P has eigenvalue ζ^{ℓ} on $v^{(\ell)}$, so

$$(a-a^{\mathsf{T}})\,v^{(\ell)}=\Big(\sum_c \zeta^{\ell w_c}-\sum_c \zeta^{-\ell w_c}\Big)v^{(\ell)}=2i\sum_{c=1}^{3}\sin\frac{2\pi\ell w_c}{n}\;v^{(\ell)}. \tag{VI.7.12}$$

The mode $v^{(\ell)}$ is in the kernel exactly when the bracket vanishes,

$$v^{(\ell)}\in\ker(a-a^{\mathsf{T}}) \quad\Longleftrightarrow\quad S(\ell)\equiv\sum_{c=1}^{3}\sin\frac{2\pi\ell w_c}{n}=0. \tag{VI.7.13}$$

The mode $\ell=0$, the constant vector, is the regular direction $d=(1,\dots,1)$ and is always there, $S(0)=0$; whether any other mode survives is an arithmetic question about the weights. Take the chiral $\mathbb{C}^3/\mathbb{Z}_5$ with weights $(1,1,3)$ (which sum to $5\equiv 0$): the bracket is $S(\ell)=2\sin(2\pi\ell/5)+\sin(6\pi\ell/5)$, and evaluating it on the four nonzero modes,

$$S(1)=2\sin\tfrac{2\pi}{5}+\sin\tfrac{6\pi}{5},\quad S(2)=2\sin\tfrac{4\pi}{5}+\sin\tfrac{12\pi}{5},\quad S(3)=-S(2),\quad S(4)=-S(1), \tag{VI.7.14}$$

none of which vanishes ($S(1)\approx 1.31$, $S(2)\approx 2.13$), so the kernel is again only the regular line. By contrast the weights $(1,2,2)$, summing to 5, give the bracket $\sin(2\pi\ell/5)+2\sin(4\pi\ell/5)$, and pairing ℓ with $5-\ell$ shows the same: nonzero off $\ell=0$. Fourier diagonalization determines the complex kernel and hence the rational nullity of this integer matrix. It does not by itself supply a saturated integer basis. Both weight choices above have only the constant mode, so their integer kernel is exactly the regular line. For a larger kernel, real and imaginary parts of individual Fourier modes need not be rational vectors. One must solve the rational equations and determine the integral lattice, for instance using Smith transformations, before imposing nonnegative ranks.

A deformation M with a nonzero component of $(a-a^{\mathsf{T}})M$ at an occupied $SU(N_i\geq 3)$ node gives a perturbative gauge anomaly in the stated spectrum. Its field-theory anomaly must be cancelled by additional charged sources: flavour branes passing through the

singularity, or an orientifold plane (Chapter 8). Noncompact boundary conditions can accommodate suitable fixed-line flux, but do not remove the fully localized tadpole constraint. Neither kind of background choice is a substitute for cancelling a perturbative gauge anomaly. An anomalous gauge theory is not made consistent by tolerating a noncompact tadpole, and one may then no longer claim a compact or standalone model. Flavour branes are noncompact branes that intersect the probe stack and add fundamental (rather than bifundamental) matter to selected nodes, shifting the anomaly of those nodes by the flavour count; their systematic treatment belongs to the model-building and compact-embedding part of the book and is not developed here. We identify the kernel and stop; the completions, and the renormalization-group cascades that relate different anomaly-free ranks, are not pursued here.

VI.7.4 Twisted Ramond–Ramond tadpoles from the annulus

The gauge-theory anomaly has a string-theoretic origin, and seeing it requires the cylinder amplitude. A pair of D-branes exchange open strings around a loop; read in the dual closed-string channel, the same cylinder is a tree-level exchange of closed strings, including the twisted Ramond–Ramond fields localized at the orbifold fixed locus (Figure VI.7.1). The coefficient with which a brane configuration sources a given twisted field is its *tadpole*, and it must be accounted for exactly as a charge must be conserved. We assemble the tadpole one factor at a time, because each factor teaches a different lesson.

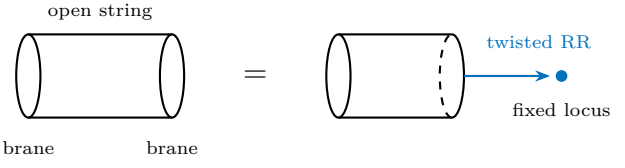


Figure VI.7.1: The cylinder two ways. In the open channel (left) it is a one-loop diagram of open strings stretched between branes; in the dual closed channel (right) it is a tree exchange in which the branes emit a closed string, including the twisted Ramond–Ramond field localized at the orbifold fixed locus. The tadpole is the coefficient of that emission.

The Chan–Paton trace and the regular representation

The piece of the amplitude that depends on the branes is a trace over the open-string Chan–Paton labels of the orbifold group action. In the sector twisted by $g \in \Gamma$ the annulus inserts the Chan–Paton matrix γ_g that represents g on the brane labels, and the boundary contributes its trace. For a configuration carrying N_i branes of type R_i, the representation on the Chan–Paton space is $\bigoplus_i N_i\, R_i$, so the trace is the ranks

weighted by characters,

$$\operatorname{Tr}\gamma_g \;=\; \sum_i N_i\,\chi_i(g). \tag{VI.7.15}$$

This single number per group element is the central object of the section, and three lessons follow from it. First, at the regular ranks $N_i = \dim R_i$ the weighted sum is the character of the regular representation,

$$\operatorname{Tr}\gamma_g \;=\; \sum_i (\dim R_i)\,\chi_i(g) \;=\; |\Gamma|\,\delta_{g,e}, \tag{VI.7.16}$$

the standard fact that $\chi_{\rm reg} = \sum_i (\dim R_i)\chi_i$ vanishes off the identity by column orthogonality. So a stack of regular branes sources *no* twisted Ramond–Ramond field, consistent with its being a mobile bulk brane that can leave the singularity. Second, a fractional brane, with N_i not proportional to $\dim R_i$, gives a nonzero $\operatorname{Tr}\gamma_g$ for some $g \neq e$ and so does source twisted flux; it is pinned to the fixed locus precisely because it carries a charge that lives there. Third, in a *compact* model the total twisted charge summed over all sources must cancel; a noncompact model can retain appropriate fixed-line sources with boundary conditions at infinity. A fully localized uncancelled source cannot be dismissed in that way. The reader can verify the first lesson on the smallest case directly: for $\mathbb{Z}_3$ with characters $1, \omega^k, \omega^{2k}$ on the element θ^k, the regular sum is $1 + \omega^k + \omega^{2k}$, which is 3 at $k = 0$ and 0 at $k = 1, 2$.

The kinematic sine factors

For an abelian $\mathbb{C}^3/\mathbb{Z}_n$, let $g = \theta^k$ rotate the transverse planes by $e^{2\pi i k v_a}$. The annulus factorization gives a weighted cancellation condition of the following form in fully localized sectors. We use $\mathcal{T}_k$ for this weighted condition, rather than a canonically normalized boundary-state charge,

$$\mathcal{T}_k \;\sim\; \left(\prod_{a=1}^{3} 2\sin\pi k v_a\right)\,\operatorname{Tr}\gamma_{\theta^k}, \tag{VI.7.17}$$

one sine factor per transverse plane times the Chan–Paton trace. Each factor of the formula now has a meaning we can read off: $\operatorname{Tr}\gamma_{\theta^k}$ counts how the branes carry the group action, and the sine factors record how the transverse geometry responds to it. The relation to the anomaly can also be seen algebraically. Choose real lifts of the $SU(3)$ weights with $v_1 + v_2 + v_3 = 0$. If $x_a = \pi k v_a$, then $x_3 = -x_1 - x_2$ gives

$$\sum_a \sin(2x_a) = -4\sin x_1 \sin x_2 \sin x_3.$$

Thus the Fourier eigenvalue $2i\sum_a \sin(2x_a)$ is $-i\prod_a 2\sin x_a$ in this lift. Integer shifts of the weight representatives can change the product's sign, so the schematic condition (VI.7.17) does not fix an absolute charge normalization. Its vanishing is unambiguous. If one eigenvalue of g is one, a sine vanishes and the fully localized expression ceases to measure the sector's full source. We now examine the fixed directions that distinguish those cases.

VI.7.5 Localized tadpoles versus fixed-line sectors

The four-dimensional anomaly and the twisted tadpole are not the same statement, and the difference is the most delicate point of the chapter. It turns on which group elements act *freely* away from the origin, and the sine factors in (VI.7.17) decide it.

The multiplicity of the eigenvalue 1 of $g = \theta^k$ on $\mathbb{C}^3$ counts the fixed directions,

$$m_1(g) = \#\{a : kv_a \in \mathbb{Z}\} = \dim_{\mathbb{C}}(\text{fixed locus}), \tag{VI.7.18}$$

and the corresponding sine factor $2\sin\pi kv_a$ vanishes exactly on those directions, since $\sin\pi kv_a = 0$ iff $kv_a \in \mathbb{Z}$. Two cases organize everything. An element with $m_1(g) = 0$, so that no $2\sin\pi kv_a$ vanishes, fixes only the origin: its sector is fully localized and of $\mathcal{N}$=1 type. The whole quotient is isolated only if every nonidentity element has this property. These fully localized sectors are the string-theoretic carriers of the four-dimensional non-abelian cubic anomaly: for the nondegenerate D3-only setup their cancellation gives the full rank condition (VI.7.2). Its identification with the perturbative cubic test retains the occupied-node and rank restrictions stated above. An element with $m_1(g) = 1$, one integral sector weight $kv_a \in \mathbb{Z}$, leaves the a-th complex plane fixed. The corresponding sine factor vanishes, and the sector is supported on a whole complex *line*. Along that line the transverse geometry is a surface singularity with $\mathcal{N}$=2 supersymmetry. A fixed-line sector does not produce a four-dimensional cubic anomaly; it produces logarithmic running, the beta-function data of an $\mathcal{N}$=2-like subsector.

This is the point where the vanishing of a sine factor must be read correctly, and the warning is sharp enough to box. A zero sine factor does not mean "nothing happens" in that sector; it means the schematic localized-tadpole formula (VI.7.17) is computing the wrong quantity for it. The fixed-line sector is genuinely present, carries genuine physics, and needs a different regularization (a six-dimensional or running tadpole, not a four-dimensional localized one); the zero is the signal that we have left the regime in which (VI.7.17) is a four-dimensional localized charge.

Localized versus fixed-line sectors

A twisted sector of $g \in \Gamma$ is *fully localized* (isolated, $\mathcal{N}$=1) when g has no eigenvalue 1 on $\mathbb{C}^3$, equivalently when every $2\sin\pi kv_a \neq 0$. These sectors carry the four-dimensional $SU(N_i)^3$ cubic anomaly. A sector whose g fixes a complex line ($kv_a \in \mathbb{Z}$, one sine factor zero) is $\mathcal{N}$=2-like and encodes logarithmic running, not a cubic anomaly. Cancelling the localized tadpoles is therefore dual to the full rank equation, with its small-rank qualifications; it is *not* the same as cancelling every tadpole. The vanishing sine factor is a sign that the sector is not a four-dimensional localized tadpole, not a sign that the sector is physically absent.

The two running examples make the difference concrete, and we set them side by side because the contrast is the lesson. The isolated quiver $dP_0 = \mathbb{C}^3/\mathbb{Z}_3$ has weights $(1,1,1)$ scaled by $1/3$; no nontrivial power of the generator has an integral weight, since $k/3 \notin \mathbb{Z}$ for $k = 1, 2$, so every sector is fully localized, every sine factor $2\sin(\pi k/3) = \sqrt{3} \neq 0$, the anomaly equations (VI.7.7) bite, and the regular direction is singled out. The non-isolated quiver $\mathbb{C}^3/(\mathbb{Z}_2 \times \mathbb{Z}_2)$ behaves oppositely. Its three



Figure VI.7.2: The geometric difference behind the two kinds of twisted sector. A group element with no eigenvalue 1 fixes only the apex (left): an isolated point, an $\mathcal{N}$=1 sector probing a four-dimensional cubic anomaly whose coefficient can vanish. An element with one eigenvalue 1 fixes a whole complex line (right): an $\mathcal{N}$=2-like locus of $\mathbb{C}^2/\mathbb{Z}_2$ singularities carrying logarithmic running. The cones are schematic; the apex is the orbifold tip.

nontrivial elements are $\mathrm{diag}(1,-1,-1)$ and its two partners; each has exactly one weight equal to zero, hence fixes a complex line of $\mathbb{C}^2/\mathbb{Z}_2$ singularities, the corresponding sine factor $2\sin(\pi\cdot 0)=0$ vanishes, and the defining **3** restricts to three real characters, so the adjacency is symmetric, $a=a^{\mathsf{T}}$. The cubic $SU(N_i)^3$ anomaly then vanishes for *any* ranks, by (VI.7.2) with $a-a^{\mathsf{T}}=0$; yet the three fixed-line sectors persist, and they still constrain the running and any eventual compact completion. The lesson is a slogan with teeth:

$$\text{(non-abelian) anomaly-free} \;\not\Rightarrow\; \text{tadpole-free (compact)}. \tag{VI.7.19}$$

Common misconception: every tadpole is a 4d anomaly

It is tempting to read "twisted tadpole" and "gauge anomaly" as synonyms. They coincide only for the fully localized sectors. A sector that fixes a complex line is $\mathcal{N}$=2-like; its tadpole is logarithmic-running data, not a four-dimensional cubic anomaly. So a quiver can be free of all $SU(N_i)^3$ anomalies, as $\mathbb{C}^3/(\mathbb{Z}_2\times\mathbb{Z}_2)$ is for every rank, and still carry fixed-line tadpoles that matter for the physics and for any compact embedding.

VI.7.6 The abelian sector: mixed anomalies, Stückelberg masses, FI terms

The construction outputs unitary gauge factors, and each $U(N_i)$ contains an abelian piece,

$$U(N_i) \;\simeq\; \frac{SU(N_i)\times U(1)_i}{\mathbb{Z}_{N_i}}. \tag{VI.7.20}$$

A general abelian gauge boson is a combination of the node charges,

$$Q_\lambda \;=\; \sum_i \lambda_i\, Q_i, \tag{VI.7.21}$$

and unlike the non-abelian factors its infrared fate is not visible on the diagram. This section computes the mixed anomaly carefully, because the naive guess for the anomaly-free condition is wrong away from equal ranks, and then assembles the Stückelberg mass and the Fayet–Iliopoulos partner that decide which abelian factors survive.

Charges of the bifundamentals

For distinct nodes $i \neq j$, fix the normalization so that the bifundamental X_{ij} carries charge $+1$ under $U(1)_i$ and -1 under $U(1)_j$, the natural sign for a field in $(\square_i, \overline{\square}_j)$,

$$Q_i(X_{ij}) = +1, \qquad Q_j(X_{ij}) = -1, \qquad Q_k(X_{ij}) = 0 \;(k \neq i, j). \tag{VI.7.22}$$

Under the combination Q_λ of (VI.7.21) the same field then has charge

$$Q_\lambda(X_{ij}) = \lambda_i - \lambda_j, \tag{VI.7.23}$$

the difference of the endpoint coefficients. One consequence is immediate, and worth stating now because it recurs. The diagonal combination $\lambda_i \propto 1$ assigns $Q_\lambda(X_{ij}) = 0$ to *every* bifundamental, so the diagonal $U(1)$ is charged on nothing. The reader can read this off (VI.7.23) directly: with all λ_i equal the difference is zero on every arrow. At the regular ranks this is the gauge-theory statement that the overall $U(1)$ is the decoupled centre of mass, to which we return. Being uncharged on the bifundamentals is, however, not the same as being free. The diagonal combination can still carry a twisted Stückelberg coupling $K_{\mathrm{diag},g} = \operatorname{Tr}\gamma_g$ (the Green–Schwarz coupling (VI.7.28) below, at $\lambda_i = 1$). This vanishes in the regular direction, by $\operatorname{Tr}\gamma_g = \sum_i N_i\chi_i(g) = N\chi_{\mathrm{reg}}(g) = N|\Gamma|\delta_{g,e}$, but it need not vanish at a fractional rank vector. Away from the regular direction the diagonal $U(1)$ stays uncharged on bifundamentals yet can couple to twisted axions through $\operatorname{Tr}\gamma_g$.

The mixed $U(1)_\lambda$–$SU(N_k)^2$ anomaly

The mixed anomaly of $U(1)_\lambda$ with a non-abelian factor $SU(N_k)^2$ is the sum over the matter charged under $SU(N_k)$ of its $U(1)_\lambda$ charge times its $SU(N_k)$ Dynkin index. The fields charged under $SU(N_k)$ are exactly the arrows touching node k. An outgoing arrow $k \to j$ is a_{kj} copies of $(\square_k, \overline{\square}_j)$: as $SU(N_k)$ matter it is N_j fundamentals, with index $\frac{1}{2}$ each, carrying $U(1)_\lambda$ charge $\lambda_k - \lambda_j$ by (VI.7.23). An incoming arrow $j \to k$ is a_{jk} copies of $(\square_j, \overline{\square}_k)$: N_j antifundamentals of $SU(N_k)$, also index $\frac{1}{2}$, carrying $U(1)_\lambda$ charge $\lambda_j - \lambda_k$. The antifundamental contributes to the mixed $U(1)$–$SU(N_k)^2$ anomaly with the same sign as the fundamental (the $SU(N_k)^2$ factor is real, insensitive to conjugation; the $U(1)$ charge enters linearly), so both terms add with their own $U(1)$ charge. Define A_k to be twice the standard triangle coefficient with $T(\square) = \frac{1}{2}$. With this convention the coefficient at node k is

$$A_k(\lambda) \;=\; \sum_j N_j \Big[\, a_{kj}\,(\lambda_k - \lambda_j) \;+\; a_{jk}\,(\lambda_j - \lambda_k) \,\Big]. \tag{VI.7.24}$$

This is the formula to derive and keep; the rest is algebra. Expand it by splitting the two brackets and collecting the λ_k terms and the λ_j terms,

$$\begin{aligned} A_k(\lambda) &= \lambda_k \sum_j N_j \,(a_{kj} - a_{jk}) \;-\; \sum_j N_j \,(a_{kj} - a_{jk})\,\lambda_j \\ &= \lambda_k \left[(a - a^{\mathsf{T}})\, N\right]_k \;-\; \left[(a - a^{\mathsf{T}})\,(N \circ \lambda)\right]_k, \end{aligned} \tag{VI.7.25}$$

where $(N \circ \lambda)_j = N_j \lambda_j$ is the componentwise (Hadamard) product. The first term is λ_k times the *non-abelian* anomaly vector $[(a - a^{\mathsf{T}})N]_k$ of (VI.7.1); the second is the antisymmetric adjacency acting on the rank-weighted charge vector $N \circ \lambda$. Now impose the non-abelian anomaly-free condition (VI.7.2), $(a - a^{\mathsf{T}})N = 0$, as an explicit hypothesis on the full rank vector. The first term drops, and the mixed anomaly reduces to

$$A_k(\lambda) \;=\; -\left[(a - a^{\mathsf{T}})\,(N \circ \lambda)\right]_k. \tag{VI.7.26}$$

For the full rank constraint and with $N_k \geq 2$ at every tested node, the combination Q_λ is free of mixed anomalies exactly when the *rank-weighted* charge vector lies in the kernel of the antisymmetric adjacency,

$$Q_\lambda \text{ mixed-anomaly-free} \quad\Longleftrightarrow\quad (a - a^{\mathsf{T}})\,(N \circ \lambda) = 0. \tag{VI.7.27}$$

The rank factor counts the multiplicity of charged fermions at the other end of each arrow. Consequently the condition is $(a - a^{\mathsf{T}})(N \circ \lambda) = 0$, the rank-weighted statement, *not* $(a - a^{\mathsf{T}})\lambda = 0$. The two reduce to the same equation when all ranks are equal, $N_i = N$, for then $N \circ \lambda = N\lambda$ and the common factor pulls out. At equal ranks, as in dP_0, the naive condition is correct and we lose nothing by it. But for a quiver whose nodes carry different ranks the dimension weights are essential, and the naive criterion misidentifies the anomalous combinations. The clean diagnostic is the diagonal $U(1)$ itself. We saw from (VI.7.23) that $\lambda = (1, \ldots, 1)$ is charged on nothing, so it must be anomaly-free; and indeed the rank-weighted condition certifies it, because $N \circ (1, \ldots, 1) = N = Nd$ at the regular ranks and $(a - a^{\mathsf{T}})d = 0$ by (VI.7.4). The naive condition, on the other hand, would test $(a - a^{\mathsf{T}})(1, \ldots, 1)$, which for a chiral quiver is the vector of out-degree minus in-degree and need not vanish at all. We make this failure explicit on $\Delta(27)$ in §VI.7.9, where the naive condition wrongly flags the harmless diagonal $U(1)$ as anomalous.

Warning: the mixed-anomaly condition is rank-weighted

Assuming $(a - a^{\mathsf{T}})N = 0$ and testing occupied $SU(N_k)$ factors with $N_k \geq 2$, the combination $Q_\lambda = \sum_i \lambda_i Q_i$ is mixed-anomaly-free when $(a - a^{\mathsf{T}})(N \circ \lambda) = 0$ with $(N \circ \lambda)_j = N_j \lambda_j$, *not* when $(a - a^{\mathsf{T}})\lambda = 0$. Equal ranks guarantee agreement. For regular ranks $N_j = N \dim R_j$ the dimension weights are decisive: the diagonal centre-of-mass $U(1)$ is always anomaly-free, but the unweighted criterion can fail on it for a chiral quiver. Always weight the charge vector by the ranks before testing the kernel.

The Green–Schwarz coupling and the Stückelberg mass

In the string construction, a $U(1)$ with a nonzero matter anomaly can be consistent because suitable axionic couplings cancel that anomaly by a generalized Green–Schwarz

mechanism, a coupling of the abelian gauge field to the twisted-sector Ramond–Ramond axions c_g that already appeared in the tadpole. The coupling is governed by a matrix that pairs the abelian directions λ with the group elements g,

$$K_{\lambda,g} \;=\; \sum_i N_i\,\lambda_i\,\chi_i(g), \tag{VI.7.28}$$

the rank-and-charge-weighted version of the Chan–Paton trace (VI.7.15): it is $\mathrm{Tr}(Q_\lambda\gamma_g)$, the trace of the abelian charge against the twisted group action. The two-derivative coupling and the resulting mass take the schematic form

$$S_{\mathrm{BF}} \;\sim\; \sum_g K_{\lambda,g}\int C_{2,g}\wedge F_\lambda, \qquad m^2_{\lambda\lambda'} \;\sim\; \sum_{A,B} q_{A\lambda}\,G_{AB}\,q_{B\lambda'}, \tag{VI.7.29}$$

where $C_{2,g}$ is a Ramond–Ramond two-form, dual in four dimensions to an axion. For the mass formula, $q_{A\lambda}$ denotes the coupling in a real basis of dynamical axions and G_{AB} their positive-definite kinetic metric; gauge-field normalizations are suppressed. Conjugate character sectors must be combined into real modes before this formula is used. The mass term follows from the axion kinetic expression

$$-\frac{1}{2}G_{AB}(dc_A + q_{A\lambda}A_\lambda)\wedge *(dc_B + q_{B\lambda'}A_{\lambda'}).$$

Under $A_\lambda \mapsto A_\lambda + d\epsilon_\lambda$ and $c_A \mapsto c_A - q_{A\lambda}\epsilon_\lambda$, the displayed covariant derivative is invariant. Interpreting these fields as the duals of the RR two-forms requires their kinetic terms. Cancellation of a matter anomaly additionally requires the axionic couplings to gauge-field densities with the matching coefficients. In unitary gauge the shifting axion supplies the longitudinal polarization of the massive vector. Its low-energy selection rule can survive perturbatively; this does not establish an exact continuous global symmetry against nonperturbative effects.

For any real vector u of abelian coefficients,

$$u^{\mathsf{T}}m^2u \;\sim\; (qu)^{\mathsf{T}}G(qu), \qquad \ker m^2 = \ker q \quad (G>0).$$

This is a conditional linear-algebra statement. The traces in (VI.7.28) fix Chan–Paton dependence, while the choice of normalizable modes, their kinetic terms, and possible untwisted couplings depend on the background. In particular, fixed-line fields need not be four-dimensional dynamical axions in a noncompact limit. Nonzero K alone is not a complete mass calculation there. At regular ranks the diagonal twisted overlap is $K_{\mathrm{diag},g} = N|\Gamma|\delta_{g,e}$. It vanishes for $g\neq e$; in the four-dimensional field-theory limit this is compatible with the free centre of mass.

The distinction between an anomaly and a mass is visible in the two matrices: (VI.7.28) can be nonzero even when the mixed anomaly (VI.7.26) vanishes. A non-anomalous combination can therefore still be lifted, by the analogous Bianchi/Stückelberg coupling to a Ramond–Ramond form with no anomaly to cancel; these are the "baryonic" abelian factors, massive but anomaly-free. For specified dynamical modes with positive kinetic metric, massless combinations must lie in $\ker q$ as well as satisfy the anomaly constraints. Counting them requires those closed-string

$U(1)$ type	anomaly $A_k(\lambda)$	real coupling $q\lambda$	infrared role
regular diagonal / centre	0	0	centre of mass
anomalous	$\neq 0$	$\neq 0$	massive; selection rule
non-anomalous massive	0	$\neq 0$	possible selection rule
truly massless	0	0	special; condition-dep.

Table VI.7.4: The four fates of an abelian gauge boson, keyed to the two computed quantities: the mixed anomaly $A_k(\lambda)$ of (VI.7.26) and the real dynamical coupling $q\lambda$ entering (VI.7.29). With finite positive kinetic metrics, $\lambda^{\mathsf{T}} m^2 \lambda = 0$ precisely when $q\lambda = 0$, in the stated gauge basis. The regular-diagonal row also assumes the D3 field-theory limit and decoupled bulk modes. This table describes a four-dimensional axion theory; it does not determine the normalizable spectrum of a noncompact fixed line.

data. Table VI.7.4 lays out the four fates after the derivation, so that each row now corresponds to a computed condition rather than a name.

Warning: anomaly-free is not massless

An anomaly-free $U(1)$ need not remain massless. A Stückelberg / Bianchi coupling to a dynamical Ramond–Ramond form, with real coupling obtained from $K_{\lambda,g}$, can lift a non-anomalous combination, leaving a massive "baryonic" gauge boson and potentially a perturbative global selection rule. The genuinely massless abelian factors are those that are anomaly-free *and* carry no such dynamical coupling, under the positive kinetic assumptions above. This can be a smaller set. "Anomaly-free" is a necessary, not a sufficient, condition for "massless".

Fayet–Iliopoulos terms as the NSNS partner

The abelian factors carry one more piece of data relevant to consistency. Each $U(1)_i$ admits a Fayet–Iliopoulos parameter ζ_i, and the D-term condition of the worldvolume theory is

$$\mu_i \;=\; \zeta_i, \tag{VI.7.30}$$

with μ_i the moment map of the i-th node. These parameters are not free decorations: in the string theory the ζ_i depend on twisted Neveu–Schwarz blow-up scalars. They are not identified here with arbitrary B-field periods; those also enter other closed-string couplings. Taking the trace of the node D-term equations gives $\sum_i N_i \zeta_i = 0$, since every bifundamental contributes opposite traces at its two endpoints. The pairing is the cleanest way to see that the abelian story has two halves of one set of twisted fields: the same twisted multiplet that supplies the Ramond–Ramond axion c_g eaten by an anomalous $U(1)$ in (VI.7.29) supplies its Neveu–Schwarz partner ζ_i, the Fayet–Iliopoulos coupling. An anomalous $U(1)$ and a Fayet–Iliopoulos term are thus two faces of one twisted closed-string mode, and a complete accounting of the abelian sector tracks both together. We are not, in this chapter, resolving the singularity or constructing the moduli space; that was the geometry of Chapter 4 in two complex dimensions and is identified for $\mathbb{C}^3/\Gamma$ in Chapter 6, with the toric and crepant-resolution machinery

routed to Volume VI. Here (VI.7.30) identifies the scalar partner of the axionic coupling and the constraint on its allowed node values.

Before running the worked examples, we collect the three quantities and the geometric input the analysis uses. The examples emphasize different parts of the calculation: the localized rank constraint, the fixed-line sector classification, and the effect of unequal ranks on mixed anomalies.

object	formula	what it determines
non-abelian coefficient	$(a - a^{\mathsf{T}})\,N$	cubic anomaly at occupied $SU(N_i \geq 3)$ nodes
sector geometry	$\ker(Q(g) - I)$	fixed locus of the specified sector
twisted source overlap	$\mathrm{Tr}\,\gamma_g = \sum_i N_i\,\chi_i(g)$	CP source coefficient in that sector
$U(1)$ coupling overlap	$K_{\lambda,g} = \sum_i N_i\,\lambda_i\,\chi_i(g)$	input to q; mass needs dynamical modes and $G > 0$

Table VI.7.5: Quiver coefficients and the geometric input that distinguishes twisted sectors. The trace does not determine the fixed locus. The abelian overlap is a coupling, with a mass consequence only after the real dynamical axions and their positive kinetic metric have been specified. Sections VI.7.7–VI.7.9 apply these quantities.

VI.7.7 Worked example I: dP_0 in full

We now run the entire apparatus on three groups, in order of increasing structure. The point is not new geometry but practice: the first example relates the rank kernel to the twisted traces; the second shows what the cubic anomaly misses; the third tests the rank weights in a nonabelian orbifold.

The chiral isolated case is $dP_0 = \mathbb{C}^3/\mathbb{Z}_3$, with the input data of Table VI.7.6. The generator θ acts as $\omega\mathbb{1}$ with $\omega = e^{2\pi i/3}$; the three irreducibles are one-dimensional, $\chi_k(\theta) = \omega^k$ for $k = 0, 1, 2$; and the adjacency is $a_{ij} = 3\delta_{j,i+1}$, the matrix (VI.7.5).

group	$\mathbb{Z}_3$, weights $(1,1,1)/3$ (order 3, isolated, chiral)
irreducibles	R_0, R_1, R_2, all $\dim 1$; $\chi_k(\theta^m) = \omega^{km}$
adjacency	$a_{ij} = 3\delta_{j,i+1}$, a triple-arrow 3-cycle
$a - a^{\mathsf{T}}$	$3(P - P^{\mathsf{T}})$, eq. (VI.7.5)
regular ranks	$d = (1,1,1)$, so $N_i = N$

Table VI.7.6: Input data for the dP_0 consistency check.

The quiver is three $U(N_i)$ nodes joined cyclically by a triple arrow on each edge (Figure VI.7.3). Before the consistency checks proper, it is worth running the first checklist item, the gauge invariance of the superpotential, since it is the cheapest condition and the only one that does not need the ranks. The cubic coupling inherited

from the $\mathcal{N}$=4 parent is the single ε-contracted triangle

$$W \;=\; \varepsilon_{abc}\,\mathrm{Tr}\big(X^{a}_{01}X^{b}_{12}X^{c}_{20}\big), \tag{VI.7.31}$$

with a, b, c the three transverse flavour indices and $X^{a}_{i,i+1}$ the three chiral fields on the edge $i \to i{+}1$. The word is gauge invariant because the gauge indices close: X_{01} runs from node 0 to node 1, X_{12} from 1 to 2, X_{20} from 2 back to 0, so the product is an oriented loop whose trace is a singlet of $\prod_i U(N_i)$. Any open string of arrows, or a loop traversed against an arrow, would fail to contract and is forbidden; the only cubic path shape, up to cyclic rotation, is $0 \to 1 \to 2 \to 0$. There are nevertheless 3^3 flavour-labelled cubic traces. The antisymmetric ε contraction is selected by the inherited interaction, not by gauge invariance alone. With step 1 passed, the rank-dependent checks follow.

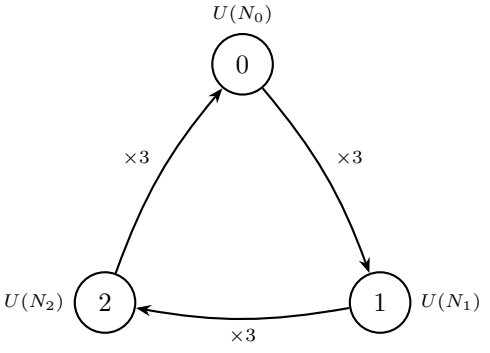


Figure VI.7.3: The $dP_0 = \mathbb{C}^3/\mathbb{Z}_3$ quiver: three $U(N_i)$ nodes joined cyclically $0 \to 1 \to 2 \to 0$ by a triple bifundamental arrow on each edge ($\times 3$ denotes three chiral fields, $a_{ij} = 3\delta_{j,i+1}$). No reverse arrows: the theory is chiral, and the only closed cubic path shape is the triangle. Its flavour-labelled traces allow many cubic invariants; the inherited superpotential (VI.7.31) selects their ε contraction.

Table VI.7.7 lays out the matter at node 0 as the anomaly count of §VI.7.2, so the cancellation can be read directly off the arrows.

arrow at node 0	rep of $SU(N_0)$	multiplicity	anomaly
$0 \to 1$ (three flavours)	fundamental $\square_0$	$a_{01}N_1 = 3N_1$	$+3N_1$
$2 \to 0$ (three flavours)	antifundamental $\overline{\square}_0$	$a_{20}N_2 = 3N_2$	$-3N_2$
net $\mathcal{A}_0 = 3N_1 - 3N_2$			$= 0$ iff $N_1 = N_2$

Table VI.7.7: The anomaly count at the dP_0 node 0. The triple arrow $0 \to 1$ brings three fundamentals (sign $+$), the triple arrow $2 \to 0$ brings three antifundamentals (sign $-$); the net vanishes when $N_1 = N_2$, and the three nodes together force $N_0 = N_1 = N_2$. There are no arrows $1 \to 0$ or $0 \to 2$, so no further contributions.

Anomaly vector and kernel. The anomaly vector is (VI.7.6), $\mathcal{A} = 3(N_1 - N_2, N_2 - N_0, N_0 - N_1)$, and $\mathcal{A} = 0$ forces $N_0 = N_1 = N_2$. The integer kernel of $a - a^{\mathsf{T}}$ is therefore one-dimensional. We can confirm its rank from the Smith normal form: row- and column-reducing (VI.7.5) over $\mathbb{Z}$ gives invariant factors $(3, 3, 0)$, so the kernel has rank one and is generated by $(1, 1, 1)$, the regular direction. There is no additional direction solving the full rank equation; its nonnegative solutions are exactly the nonnegative multiples of the regular brane.

Twisted Chan–Paton traces. The two nontrivial sectors are $k = 1, 2$. Both generators act as $\omega^k \mathbb{1}$ with no eigenvalue 1, so both are fully localized, every sine factor $2\sin(\pi k/3) = \sqrt{3} \neq 0$, and both tadpoles are of the four-dimensional type. The Chan–Paton trace in the sector θ^k is, by (VI.7.15) with $\chi_k(\theta) = \omega^k$,

$$\operatorname{Tr} \gamma_{\theta^k} \;=\; \sum_{i=0}^{2} N_i\, \omega^{ik} \;=\; N_0 + \omega^k N_1 + \omega^{2k} N_2. \tag{VI.7.32}$$

This is the discrete Fourier transform of the rank vector, and it vanishes for both $k = 1$ and $k = 2$ exactly when $N_0 = N_1 = N_2$: setting the $k = 1$ trace $N_0 + \omega N_1 + \omega^2 N_2$ to zero, its real and imaginary parts give two independent linear relations that, with the reality of the N_i, force the three ranks equal. So

$$\operatorname{Tr} \gamma_\theta = \operatorname{Tr} \gamma_{\theta^2} = 0 \quad \Longleftrightarrow \quad N_0 = N_1 = N_2, \tag{VI.7.33}$$

and the twisted tadpole cancellation reproduces the anomaly condition (VI.7.7), exactly as the localized-tadpole/anomaly duality predicts. At the regular ranks $N_i = N$ this is the special case of (VI.7.16): $\sum_i N\omega^{ik} = N(1 + \omega^k + \omega^{2k}) = 0$ for $k \neq 0$. A fractional brane breaks it: one brane on node 0 alone, $N = (1, 0, 0)$, gives $\operatorname{Tr} \gamma_\theta = 1 \neq 0$, so it sources twisted flux and carries a localized twisted charge. This example has no non-abelian gauge factor, so the nonzero trace is not evidence of a cubic gauge anomaly.

Abelian fates. The ranks are equal, so the rank-weighted and naive conditions coincide here and we may use the simpler one. With $a - a^{\mathsf{T}} = 3(P - P^{\mathsf{T}})$, the criterion (VI.7.27) separates the diagonal from the relative combinations,

$$(a - a^{\mathsf{T}})\,(1, 1, 1)^{\mathsf{T}} = 0, \qquad (a - a^{\mathsf{T}})\,(1, -1, 0)^{\mathsf{T}} = 3\,(-1, -1, 2)^{\mathsf{T}} \neq 0. \tag{VI.7.34}$$

For $N \geq 2$, the diagonal $U(1)$ is the free centre of mass in the field-theory limit; the relative combination $(1, -1, 0)$ has a nonzero mixed anomaly and is lifted by a Green–Schwarz coupling and massive, leaving a global selection rule. We can confirm the diagonal's masslessness from the Stückelberg overlap (VI.7.28): $K_{\mathrm{diag},\theta^k} = \sum_i N\omega^{ik} = 0$ for $k = 1, 2$, so it couples to no twisted axion. The relative combination's overlap is nonzero, consistent with its being eaten. With the localized twisted modes retained and the four-dimensional field-theory limit understood, the abelian analysis gives one massless $U(1)$, the centre of mass, and two relative factors lifted, so the interacting gauge group at the singularity is $\prod_i SU(N)$ with a single decoupled abelian centre, matching the count Chapter 2 anticipated.

VI.7.8 Worked example II: $\mathbb{C}^3/(\mathbb{Z}_2 \times \mathbb{Z}_2)$ in full

The non-chiral non-isolated case is $\mathbb{C}^3/(\mathbb{Z}_2 \times \mathbb{Z}_2)$, with the input data of Table VI.7.8. The group is generated by the three diagonal sign matrices, has four one-dimensional real characters, and its McKay adjacency is the doubled K_4, $a = J - \mathbb{1}_4$.

group	$\mathbb{Z}_2 \times \mathbb{Z}_2$, gens $\mathrm{diag}(1,-1,-1)$, etc. (order 4, non-isolated, non-chiral)
irreducibles	four dim 1, real characters $\chi_{(s,t)}$
adjacency	$a = J - \mathbb{1}_4$ (doubled K_4), symmetric
$a - a^{\mathsf{T}}$	0
fixed loci	three lines of $\mathbb{C}^2/\mathbb{Z}_2$, one per generator

Table VI.7.8: Input data for the $\mathbb{C}^3/(\mathbb{Z}_2 \times \mathbb{Z}_2)$ consistency check.

Anomaly vector and kernel. Because the three transverse characters are real, $a = a^{\mathsf{T}}$, so the antisymmetric part vanishes identically and

$$\mathcal{A} = (a - a^{\mathsf{T}})\, N = 0 \quad \text{for every } N. \tag{VI.7.35}$$

Every rank vector passes this perturbative cubic test; and the integer kernel of $a - a^{\mathsf{T}}$ is all of $\mathbb{Z}^4$. The reader can confirm the symmetry directly from $a = J - \mathbb{1}$: the all-ones matrix J is symmetric, so $a - a^{\mathsf{T}} = 0$ with no computation, and every node has three arrows in and three out, so even the per-node count of Table VI.7.2 balances trivially.

Fixed-line classification. The cubic anomaly being empty, the content is in the twisted sectors, and these are the fixed-line sectors that (VI.7.35) cannot see. There are three nontrivial elements, and we classify each by its weights. The generator $g_1 = \mathrm{diag}(1,-1,-1)$ has weights $v = (0, \frac{1}{2}, \frac{1}{2})$: the first weight is integral, so g_1 fixes the z_1-line, the first sine factor $2\sin(\pi \cdot 0) = 0$ vanishes, and along that line g_1 acts as $\mathrm{diag}(-1,-1)$ on (z_2, z_3), an $\mathbb{C}^2/\mathbb{Z}_2$ surface singularity. The partners $g_2 = \mathrm{diag}(-1,1,-1)$ and $g_3 = \mathrm{diag}(-1,-1,1)$ fix the z_2- and z_3-lines the same way. So all three nontrivial sectors are $\mathcal{N}$=2-like fixed-line sectors,

$$m_1(g_1) = m_1(g_2) = m_1(g_3) = 1, \tag{VI.7.36}$$

none of them isolated, in flat contradiction to the heuristic that an abelian orbifold should be a point singularity. The reader can verify directly that no nontrivial element acts freely: each has eigenvalue $+1$ on one axis. Table VI.7.9 classifies all three nontrivial elements at once, and Figure VI.7.4 draws the three lines meeting at the origin.

Twisted traces and the running. Order the character labels as $(0,0)$, $(1,0)$, $(0,1)$, $(1,1)$, with $\chi_{(s,t)}(g_1^a g_2^b) = (-1)^{sa+tb}$. Then the three traces are

$$\big(\mathrm{Tr}\,\gamma_{g_1}, \mathrm{Tr}\,\gamma_{g_2}, \mathrm{Tr}\,\gamma_{g_3}\big) = (N_0 - N_1 + N_2 - N_3,\ N_0 + N_1 - N_2 - N_3,\ N_0 - N_1 - N_2 + N_3). \tag{VI.7.37}$$

element	weights v	fixed locus	sine factor	sector type
$g_1 = \mathrm{diag}(1,-1,-1)$	$(0,\frac{1}{2},\frac{1}{2})$	z_1-line	0	$\mathcal{N}$=2-like
$g_2 = \mathrm{diag}(-1,1,-1)$	$(\frac{1}{2},0,\frac{1}{2})$	z_2-line	0	$\mathcal{N}$=2-like
$g_3 = \mathrm{diag}(-1,-1,1)$	$(\frac{1}{2},\frac{1}{2},0)$	z_3-line	0	$\mathcal{N}$=2-like

Table VI.7.9: The three nontrivial twisted sectors of $\mathbb{C}^3/(\mathbb{Z}_2\times\mathbb{Z}_2)$. Each element has one integral weight, fixes a complex line of $\mathbb{C}^2/\mathbb{Z}_2$ singularities, has a vanishing sine factor, and is $\mathcal{N}$=2-like. None is fully localized, so none contributes to the four-dimensional cubic anomaly, consistent with $a = a^{\mathsf{T}}$.

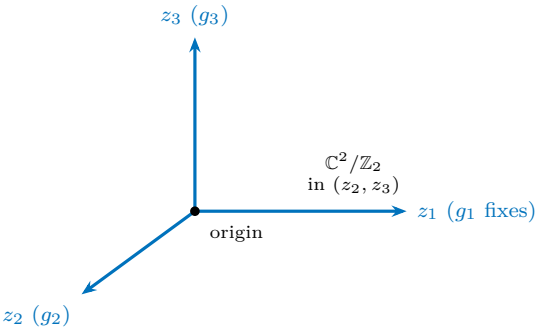


Figure VI.7.4: The non-isolated singular locus of $\mathbb{C}^3/(\mathbb{Z}_2 \times \mathbb{Z}_2)$: three complex lines of $\mathbb{C}^2/\mathbb{Z}_2$ singularities meeting at the origin, one fixed by each nontrivial generator. Each line is a fixed-line ($\mathcal{N}$=2-like) sector with a vanishing sine factor. (Schematic: the three complex lines are drawn as real axes.)

For example, ranks $(3,4,5,6)$ give $(-2,-4,0)$ despite the vanishing cubic vector. This explicitly separates the trace condition from the cubic test.

The Chan–Paton traces are still given by (VI.7.15), now with the real characters of $\mathbb{Z}_2 \times \mathbb{Z}_2$. At the regular ranks $N_i = N$ they vanish off the identity by (VI.7.16), so a regular brane sources no twisted field as always. But because the sine factors vanish, even a nonzero trace in one of these sectors is multiplied by zero in the schematic localized tadpole (VI.7.17): that is not the statement that the sector is absent, only that its data are not a four-dimensional localized tadpole. What the three sectors carry instead is the logarithmic running of three $\mathcal{N}$=2-like $\mathbb{C}^2/\mathbb{Z}_2$ subsectors, beta-function data for the gauge couplings rather than a cubic anomaly. This is the example that forces the slogan (VI.7.19): the quiver is anomaly-free for *all* ranks, the cubic count is empty at every rank, and yet it is far from a complete compact model, because the three fixed-line sectors still constrain any embedding. The abelian sector adds nothing chiral here: with $a - a^{\mathsf{T}} = 0$ every Q_λ is mixed-anomaly-free by (VI.7.27), so a possible axionic mass would be independent of this mixed-anomaly test. Its presence depends on which fixed-line modes become dynamical.

For a bounded illustration of the mass question, take regular ranks $N_i = 3$ and *suppose* that three real axions with kinetic metric $G = \mathbb{1}_3$ are dynamical, with the

character couplings just computed. In the node basis their charge matrix is

$$q = 3\begin{pmatrix} 1 & -1 & 1 & -1 \\ 1 & 1 & -1 & -1 \\ 1 & -1 & -1 & 1 \end{pmatrix}, \qquad q^{\mathsf{T}} q = 9(4\mathbb{1}_4 - J), \qquad \ker q = \mathbb{R}(1,1,1,1). \tag{VI.7.38}$$

The rows of $q/3$ are orthogonal to the constant vector and span its three-dimensional complement. Thus the diagonal is the only massless direction in this stipulated kinetic model, even though every direction passes the mixed-anomaly test. This calculation does not assert that the three axions are normalizable in the noncompact orbifold. It isolates the extra physical assumption needed to turn the traces into masses.

VI.7.9 Worked example III: $\Delta(27)$ regular ranks

The non-abelian case is the trihedral group $\Delta(27)$, which we use to show that the rank weights of §VI.7.6 are not optional. The input data are in Table VI.7.10: nine one-dimensional irreducibles $\mathbf{1}_{r,s}$ ($r, s \in \mathbb{Z}_3$) and a complex-conjugate pair $\mathbf{3}, \overline{\mathbf{3}}$, with the directed arrows $\mathbf{1}_{r,s} \to \mathbf{3} \to \overline{\mathbf{3}} \to \mathbf{1}_{r,s}$ and a triple arrow $\mathbf{3} \to \overline{\mathbf{3}}$.

group	$\Delta(27) = (\mathbb{Z}_3 \times \mathbb{Z}_3) \rtimes \mathbb{Z}_3$ (order 27, chiral)
irreducibles	nine $\mathbf{1}_{r,s}$ ($\dim 1$), $\mathbf{3}$, $\overline{\mathbf{3}}$ ($\dim 3$)
arrows	$\mathbf{1}_{r,s} \to \mathbf{3}$, $\mathbf{3} \xrightarrow{\times 3} \overline{\mathbf{3}}$, $\overline{\mathbf{3}} \to \mathbf{1}_{r,s}$
regular ranks	$N_{\mathbf{1}_{r,s}} = N$, $N_{\mathbf{3}} = N_{\overline{\mathbf{3}}} = 3N$

Table VI.7.10: Input data for the $\Delta(27)$ regular-rank check. The dimension vector is $d = (1, \dots, 1, 3, 3)$ over the eleven nodes.

The arrows close into one directed cycle through three layers, drawn schematically in Figure VI.7.5: the nine $\mathbf{1}_{r,s}$ each emit one arrow to $\mathbf{3}$, the $\mathbf{3}$ emits a triple arrow to $\overline{\mathbf{3}}$, and $\overline{\mathbf{3}}$ emits one arrow back to each $\mathbf{1}_{r,s}$. The asymmetry of the layers is the chirality, and it is also what makes the unweighted and rank-weighted $U(1)$ criteria disagree below.

Regular-rank anomaly. The regular ranks are $N_i = N \dim R_i$, so

$$N_{\mathbf{1}_{r,s}} = N, \qquad N_{\mathbf{3}} = N_{\overline{\mathbf{3}}} = 3N, \tag{VI.7.39}$$

and $\sum_i N_i \dim R_i = N \sum_i (\dim R_i)^2 = N(9 \cdot 1 + 9 + 9) = 27N = N|\Gamma|$, the size of the regular representation, a first arithmetic check that no irreducible was dropped. The chiral arrows make the quiver directed, but at the regular ranks the rank-weighted incoming and outgoing indices agree node by node, by (VI.7.3), so $(a - a^{\mathsf{T}})N = 0$ holds automatically. The reader can check the two most informative nodes by hand. At the $\mathbf{3}$ node the only outgoing arrows are the triple arrow to $\overline{\mathbf{3}}$, contributing $a_{\mathbf{3},\overline{\mathbf{3}}} N_{\overline{\mathbf{3}}} = 3 \cdot 3N = 9N$ fundamentals, while the incoming arrows are the nine from the $\mathbf{1}_{r,s}$, contributing $\sum_{r,s} a_{\mathbf{1}_{r,s},\mathbf{3}} N_{\mathbf{1}_{r,s}} = 9 \cdot 1 \cdot N = 9N$ antifundamentals: equal, so the node is anomaly-free. At a $\mathbf{1}_{r,s}$ node the single outgoing arrow to $\mathbf{3}$ gives $1 \cdot N_{\mathbf{3}} = 3N$ and the single incoming

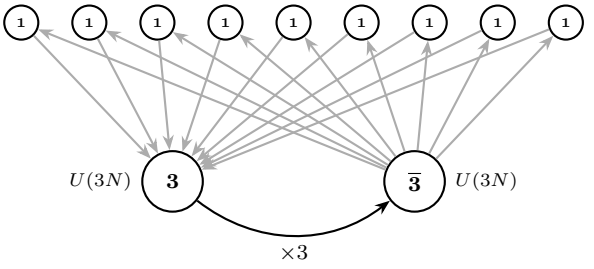


Figure VI.7.5: The $\Delta(27)$ quiver (schematic). Nine one-dimensional nodes (top, each a $U(N)$ factor) send one arrow each to the $\mathbf{3}$; the $\mathbf{3}$ sends a triple arrow to $\overline{\mathbf{3}}$; and $\overline{\mathbf{3}}$ sends one arrow back to each $\mathbf{1}_{r,s}$. The two lower nodes carry $U(3N)$ at regular ranks. The directed cycle $\{\mathbf{1}\} \to \mathbf{3} \to \overline{\mathbf{3}} \to \{\mathbf{1}\}$ is chiral.

arrow from $\overline{\mathbf{3}}$ gives $1 \cdot N_{\overline{\mathbf{3}}} = 3N$: equal again. Thus the regular brane passes the cubic test.

The rank weights are decisive. Now the point of the example. Consider the diagonal centre-of-mass $U(1)$, $\lambda = (1, \ldots, 1)$. By (VI.7.23) it is charged on no bifundamental, so it is manifestly mixed-anomaly-free, and the direct count (VI.7.24) gives $A_k = 0$ at every node. The rank-weighted criterion (VI.7.27) agrees: $N \circ \lambda = N = Nd$, and $(a - a^{\mathsf{T}})d = 0$ certifies it. But the *naive* criterion fails here. Test $(a - a^{\mathsf{T}})\lambda$ with $\lambda = (1, \ldots, 1)$: this is the vector of out-degree minus in-degree at each node, and the quiver is chiral, so it does not vanish. At the $\mathbf{3}$ node, for instance, the out-degree is $a_{\mathbf{3},\overline{\mathbf{3}}} = 3$ (the triple arrow) while the in-degree is $\sum_{r,s} a_{\mathbf{1}_{r,s},\mathbf{3}} = 9$ (nine incoming arrows), so

$$\left[(a - a^{\mathsf{T}})\,(1, \ldots, 1)\right]_{\mathbf{3}} = 3 - 9 = -6 \;\neq\; 0. \tag{VI.7.40}$$

The naive condition would therefore brand the harmless diagonal $U(1)$ as anomalous, which is wrong; the rank-weighted condition, which restores the factor $N_{\overline{\mathbf{3}}} = 3N$ on the outgoing arrow and $N_{\mathbf{1}_{r,s}} = N$ on the incoming ones, gives $3 \cdot 3N - 9 \cdot 1 \cdot N = 0$ correctly. This is exactly the failure mode the warning box named: at unequal ranks the dimension weights matter, and $\Delta(27)$, with its mix of $\dim 1$ and $\dim 3$ nodes, is the smallest place in the chapter where one sees it. We are *not* classifying all anomaly-free fractional ranks of $\Delta(27)$ here; this example exists only to expose the rank-weighting that is invisible in the equal-rank abelian quivers. Solving the full anomaly-free $U(1)$ lattice and the fractional-rank kernel is a larger exercise; the remaining kernel directions require a separate calculation. The rank weights already explain why the diagonal charge is harmless.

A non-diagonal charge tests more than the neutral diagonal does. Take three regular branes, so the nine singlet nodes have rank 3 and the last two nodes have rank 9. Set $\lambda_{\mathbf{1}_{0,0}} = 1$, the other eight singlet coefficients to zero, $\lambda_{\mathbf{3}} = 2$, and $\lambda_{\overline{\mathbf{3}}} = -1$. At any singlet node,

$$A_{\mathbf{1}} = 9(\lambda_{\mathbf{1}} - 2) + 9(-1 - \lambda_{\mathbf{1}}) = -27.$$

At the other two nodes the same arrow count gives

$$A_{\mathbf{3}} = 3 \cdot 9(2+1) + 3(1-2) + 8 \cdot 3(0-2) = 30, \qquad A_{\overline{\mathbf{3}}} = 51. \tag{VI.7.41}$$

These are the doubled coefficients A_k; with $T(\square) = 1/2$ the standard triangle coefficients are $-27/2$, 15, and $51/2$. Here all nodes carry a genuine cubic non-abelian factor, and the charge differences are nonzero, so neither small ranks nor neutrality can hide a sign or normalization error.

VI.7.10 What the consistency analysis gives

The directed matter spectrum determines a rank-weighted cubic coefficient. Solving its full rank equation gives a lattice, from which nonnegative ranks must be selected. The Chan–Paton traces express the same rank data in a basis adapted to twisted sectors. Their interpretation changes with the fixed locus. Finally, the mixed abelian anomaly and the axionic mass matrix answer different questions: one counts charged fermions, while the other needs dynamical closed-string modes and their kinetic terms.

These calculations impose necessary conditions on the local construction. They do not by themselves establish every gauge consistency condition or a complete string background. A compact embedding must cancel total Ramond–Ramond charge, including untwisted charge, over its cycles and all its sources. Global anomalies and discrete charge constraints also require their own tests. The next chapter introduces orientifold contributions; a complete embedding additionally specifies the other branes, fluxes, and global geometry.

Consistency checklist

Given an adjacency a_{ij}, ranks N_i, and the cubic W:

1. check that W is gauge invariant (closed oriented loops, ε-contracted);
2. form $(a - a^{\mathsf{T}})N$; interpret cubic coefficients at $N_i \geq 3$, check $SU(2)$ parity separately, and state when the full rank equation is imposed;
3. compute the integer kernel $\ker_{\mathbb{Z}}(a - a^{\mathsf{T}})$ (Smith normal form) for the fractional directions, then impose nonnegative total ranks;
4. compute the Chan–Paton traces $\operatorname{Tr}\gamma_g = \sum_i N_i \chi_i(g)$;
5. separate the fully localized sectors (no fixed line) from the fixed-line $\mathcal{N}$=2-like ones via the sine factors;
6. for each $U(1)$ direction λ, test the rank-weighted $(a - a^{\mathsf{T}})(N \circ \lambda) = 0$ and identify the dynamical axionic couplings needed for its mass;
7. state the local conditions tested and the additional data needed for compact completion.

Common misconception: local consistency is global consistency

Passing local anomaly and trace conditions does not arrange global charge neutrality. Anomaly cancellation also does not by itself make an abelian gauge boson massless. Each assertion requires the corresponding spectrum, couplings, and boundary conditions.

The annulus derivation of the localized tadpole relation and the closed-string kinetic normalizations have been used as physical inputs. The chapter derives their quiver arithmetic, not the full worldsheet amplitude. It classifies fixed sectors but does not compute their exact running. Those dynamics and compact completion require the additional constructions and background data described above.

Status and sources

This section is for source tracking and internal consistency, not part of the first reading. The evidence-code tags ([WS] a physical-worldsheet derivation in the untwisted string, [MATH] a mathematical theorem with stated hypotheses and proof status), the convention pointers, and the anchors are collected here, keyed by section. The chapter completes the $\mathbb{C}^3/\Gamma$ ($\mathcal{N}$=1) construction of Chapter 6 by its consistency conditions, after the quiver-from-projection of Douglas and Moore (1996), the chiral orbifold daughters of Lawrence et al. (1998), the orbifold tadpole/anomaly relation of Aldazabal, Font, et al. (1998), the bottom-up D-branes at singularities of Aldazabal, Ibanez, et al. (2000), and the anomalous-$U(1)$ Stückelberg mechanism of Ibanez et al. (1999). It reuses the McKay adjacency, the arrow orientation (fundamental-at-tail arrows), the gauge/rank data, the superpotential inheritance, and the Fayet–Iliopoulos / discrete-data conventions; the relative-$U(1)$ infrared fate that quiver gauge groups and ranks routed forward is analyzed subject to the closed-string kinetic premises. No new convention is introduced. Selected arithmetic follows from the stated dimension and charge conventions.

§VI.7.1 Why a drawable quiver still needs consistency checks. Framing: the place in Volume VI, the three levels of consistency (Table VI.7.1), the regime of each, and the computational roadmap (the three objects: the anomaly vector, the twisted Chan–Paton traces, the $U(1)$ coupling matrix). The overview inherits the premises and limitations of the detailed claims; it supplies no additional physical evidence.

§VI.7.2 Non-abelian anomalies. The cubic $SU(N_i)^3$ anomaly as the antisymmetric adjacency acting on the ranks (VI.7.1) (with the matter-content Table VI.7.2), anomaly freedom (VI.7.2), the regular-rank identity (VI.7.3) and automatic cancellation, the $SU(2)$/Witten qualifier, and the dP_0 rank quantization (VI.7.7). have field-theory index premises and mathematical arithmetic, not a worldsheet proof from these checks. Primary physical classification remains unassigned (McKay multiplicities, fundamental-at-tail arrows, quiver gauge groups and ranks; Lawrence et al. (1998)). $\mathcal{A}$ two ways and the regular-rank vanishing; the dP_0 kernel = the line $N_0 = N_1 = N_2$.

§VI.7.3 Fractional ranks and the integer kernel. The decomposition (VI.7.8), the reduced anomaly (VI.7.9), the integer kernel (VI.7.10) as a method (Smith normal form; nonnegativity), the three regimes (Table VI.7.3), and the circulant $\mathbb{C}^3/\mathbb{Z}_n$ drill (VI.7.12). is lattice algebra, derived under the full rank equation (McKay multiplicities, quiver gauge groups and ranks). the rational nullity and a generator for dP_0 (dimension one) and $\mathbb{C}^3/(\mathbb{Z}_2 \times \mathbb{Z}_2)$ (full), while a rank vector outside the kernel gives a nonzero anomaly.

§VI.7.4 Twisted RR tadpoles from the annulus. The cylinder in the closed channel, the Chan–Paton trace (VI.7.15), the regular-representation vanishing (VI.7.16), and the kinematic sine factors / twisted tadpole (VI.7.17). uses a sourced physical-worldsheet amplitude; the character identity is separate algebra (orbifold action; Douglas and Moore (1996), Douglas, Greene, et al. (1997), Aldazabal, Ibanez, et al. (2000)). Foundations for the orbifold cylinder/boundary-state amplitudes are finite-group character theory and the new anomaly inflow and the Green–Schwarz mechanism (anomaly inflow and the tadpole/anomaly dictionary, with the Green–Schwarz/Stückelberg mass; developed further in the treatment of orientifold anomalies and in the planned anomaly volume). $\mathrm{Tr}\,\gamma_g = \sum_i N_i \chi_i(g)$ from the character tables, the regular-rep vanishing off e, while a fractional-brane character can be nonzero.

§VI.7.5 Localized versus fixed-line sectors. The fully localized ($\mathcal{N}$=1) versus fixed-line ($\mathcal{N}$=2-like) split via the sine factors / eigenvalue 1 (VI.7.18), the duality of the localized tadpoles with the cubic anomaly, the "vanishing sine factor is not absence" warning, and the slogan (VI.7.19). uses the sourced localized-tadpole relation; fixed-locus arithmetic alone does not derive it (Lawrence et al. (1998), Aldazabal, Font, et al. (1998); anomaly inflow and the Green–Schwarz mechanism). This files (only

fully localized twisted tadpoles are four-dimensional cubic anomalies; fixed-line sectors are $\mathcal{N}$=2-like running). the per-element fixed-line classification for dP_0 (all isolated) and $\mathbb{C}^3/(\mathbb{Z}_2 \times \mathbb{Z}_2)$ (three fixed lines), tied to the vanishing sine factor.

§VI.7.6 The abelian sector. The decomposition (VI.7.20), the bifundamental charges (VI.7.23), the *full mixed-anomaly derivation* (VI.7.24)–(VI.7.26) with the **rank-weighted** anomaly-free condition (VI.7.27) (the correction: the naive $(a - a^{\mathsf{T}})\lambda = 0$ is a uniform simplification at equal ranks), the Green–Schwarz coupling matrix (VI.7.28), the Stückelberg mass (VI.7.29), the four fates keyed to the two computed quantities (Table VI.7.4), and the Fayet–Iliopoulos D-term $\mu_i = \zeta_i$ (VI.7.30) as the twisted-NSNS partner of the RR axion. use sourced RR and NSNS couplings; the mass-kernel result is conditional on dynamical real axions and a positive kinetic metric (quiver gauge groups and ranks, resolution and discrete data; Ibanez et al. (1999), Douglas, Greene, et al. (1997); anomaly inflow and the Green–Schwarz mechanism). This files (anomaly-free does not imply massless; local does not imply compact). the mixed anomaly two ways (bifundamental count vs the closed form), the diagonal COM anomaly-free, and the *rank-weighted* criterion versus the failing naive one on $\Delta(27)$.

§VI.7.7–VI.7.9 Worked examples. dP_0 in full (anomaly vector and one-dimensional kernel, the twisted CP traces $\mathrm{Tr}\,\gamma_{\theta^k} = N_0 + \omega^k N_1 + \omega^{2k} N_2$ (VI.7.32) vanishing iff equal ranks, the diagonal-vs-relative $U(1)$ fates); $\mathbb{C}^3/(\mathbb{Z}_2 \times \mathbb{Z}_2)$ in full ($a = a^{\mathsf{T}}$, anomaly-free for all ranks (VI.7.35), the three fixed-line sectors classified (VI.7.36), the running); and $\Delta(27)$ (regular ranks (VI.7.39), the per-node regular-rank check, and the explicit failure of the naive $U(1)$ criterion (VI.7.40) that the rank weights repair). worked.

§VI.7.10 What the consistency analysis gives. The summary of the anomaly and trace calculations and conditional mass criterion, the local/compact boundary, the consistency checklist, and what is deferred: anomaly inflow and the Green–Schwarz mass (cited, anomaly inflow and the Green–Schwarz mechanism), the fixed-line running (Part III), and the compact completions and orientifold charges (Chapter 8 and beyond). states the local/compact boundary; primary classification is left unassigned. No worldsheet derivation of a compact completion is supplied. This files (local consistency ≠ compact consistency). **Further sources and calculation scope.** For the weighted tadpole constraint use

Aldazabal, Ibanez, et al. (2000), §2.2, equations (2.14)–(2.18); the absent-factor qualification and the mixed anomaly normalization appear in §2.3, before (2.19). The two-form coupling and its NSNS partner are respectively (2.2) and (5.1) of Ibanez et al. (1999). The symbol $\mathcal{T}_k$ is a weighted cancellation condition, not a normalized emission amplitude. The exact examples establish the identities and Smith nullity for the stated lattices. A general saturated-basis construction requires a separate argument. The detailed Witten-anomaly derivation locator and a general nonabelian fixed-line amplitude derivation remain outstanding. For the abelian fixed-line amplitude and running relation, see Leigh and Rozali (1999), §4, (21) and (28), printed pp. 10–11. This is the brane-box/orbifold route, not a general nonabelian amplitude theorem. For volume-dependent axion masses and four-dimensional anomaly-free massive factors, see Antoniadis et al. (2002), §1, points 2–3, and §5, printed pp. 24–25. Those orientifold examples do not supply a normalizable mode spectrum for the noncompact example here. The doublet-parity obstruction is stated in the primary abstract of Witten (1982), p. 324; its detailed derivation and general-representation extension have not been checked here. The BF source coupling has worldsheet support; the kinetic identification, dual axion shift, and anomaly-canceling coefficients are separate physical inputs. The Gram-kernel equality is only linear algebra once the real charge matrix and positive metric are given. No arithmetic check proves a compact completion.

References

Aldazabal, G., A. Font, et al. (1998). "D = 4, N=1, type IIB orientifolds". In: *Nucl. Phys. B* 536, pp. 29–68. DOI: 10.1016/S0550-3213(98)00666-X. arXiv: hep-th/9804026.

Aldazabal, G., L. E. Ibanez, et al. (2000). "D-branes at singularities: A Bottom up approach to the string embedding of the standard model". In: *JHEP* 08, p. 002. DOI: 10.1088/1126-6708/2000/08/002. arXiv: hep-th/0005067.

Antoniadis, I., E. Kiritsis, and J. Rizos (2002). "Anomalous U(1)s in type 1 superstring vacua". In: *Nucl. Phys. B* 637, pp. 92–118. DOI: 10.1016/S0550-3213(02)00458-3. arXiv: hep-th/0204153.

Douglas, M. R., B. R. Greene, and D. R. Morrison (1997). "Orbifold resolution by D-branes". In: *Nucl. Phys. B* 506, pp. 84–106. DOI: 10.1016/S0550-3213(97)00517-8. arXiv: hep-th/9704151.

Douglas, M. R. and G. W. Moore (1996). "D-branes, quivers, and ALE instantons". In: arXiv preprint; not published in a journal. arXiv: hep-th/9603167.

Ibanez, L. E., R. Rabadan, and A. M. Uranga (1999). "Anomalous U(1)'s in type I and type IIB D = 4, N=1 string vacua". In: *Nucl. Phys. B* 542, pp. 112–138. DOI: 10.1016/S0550-3213(98)00791-3. arXiv: hep-th/9808139.

Johnson, C. V. (2003). *D-Branes*. Cambridge Monographs on Mathematical Physics. Cambridge University Press. DOI: 10.1017/CBO9780511606540.

Lawrence, A. E., N. Nekrasov, and C. Vafa (1998). "On conformal field theories in four-dimensions". In: *Nucl. Phys. B* 533, pp. 199–209. DOI: 10.1016/S0550-3213(98)00495-7. arXiv: hep-th/9803015.

Leigh, R. G. and M. Rozali (1999). "Brane boxes, anomalies, bending and tadpoles". In: *Phys. Rev. D* 59, p. 026004. DOI: 10.1103/PhysRevD.59.026004. arXiv: hep-th/9807082.

Witten, E. (1982). "An SU(2) Anomaly". In: *Phys. Lett. B* 117. Ed. by M. A. Shifman, pp. 324–328. DOI: 10.1016/0370-2693(82)90728-6.

Chapter VI.8

Orientifolded probes: SO/Sp quivers

VI.8.1 Orientifolds of the probe quiver

An orientifold changes which open strings describe independent fields. Worldsheet parity reverses the two endpoints, while a geometric involution maps each brane to its image. Strings related by this operation describe one surviving field. On a fixed brane stack, the same identification constrains the gauge boson matrix and gives an orthogonal or symplectic gauge algebra. On a pair of distinct stacks, it identifies their unitary groups.

This operation gives access to matter that the oriented orbifold quiver did not contain. An arrow connecting a node to its image can become a two-index tensor of the surviving unitary group. Its anomaly differs from that of a bifundamental. For the chiral dP_0 example, three such tensors and three surviving bifundamentals give $N_0 = N_u - 4$ for antisymmetric tensors, or $N_0 = N_u + 4$ for symmetric tensors. The shift follows from the tensor anomaly coefficient $N_u \mp 4$.

To obtain this theory we must project the interactions as well as the spectrum. The geometric involution, the parity of each open-string state, and the symmetry of the Chan–Paton projection matrix enter different parts of that calculation. We keep them separate until the superpotential relates them. The orientifold plane also carries Ramond–Ramond charge. Its cancellation is a further string condition, whose sector-dependent coefficients cannot be inferred from a drawing of the folded quiver.

Take-home message of this chapter

An orientifold gauges worldsheet parity Ω together with a geometric involution σ that normalizes Γ. On the quiver this is an *involution*, and it does four things. It folds the nodes, $i \leftrightarrow \sigma(i)$: a node paired with a distinct mirror keeps one $U(N_i)$, while a node fixed by σ is projected to $SO(N_i)$ or $USp(N_i)$. It folds the arrows by the orientation reversal $X_{ij} \mapsto X_{\sigma(j)\sigma(i)}$, identifying image pairs and projecting fixed loops into symmetric, antisymmetric, or adjoint matter. It must *preserve* the cubic superpotential. And it adds the crosscap charge q_O to the tadpole, giving a brane-plus-crosscap charge condition. The affine expression $(a - a^{\mathsf{T}})N + q_O = 0$ is used below only as a schematic model of that shift. *Orientifolding is a fold of the whole theory, not a relabeling of its gauge groups.*

Common misconception: an orientifold is just $U(N) \to SO/Sp$

The gauge-group replacement is the visible tip of a much larger operation, which acts on every layer of the construction at once. On the geometry it is the involution σ on $\mathbb{C}^3$. On the Chan–Paton factors it is the projection that selects SO or USp. On the arrows it identifies image pairs and projects fixed loops to symmetric/antisymmetric/adjoint matter. It must preserve the superpotential, and it adds the crosscap charge q_O to the Ramond–Ramond tadpoles. A relabeling that touches only the gauge group is not an orientifold. It will in general fail to preserve W and will miscount the matter. The correct statement is that the quiver is folded by an involution, and the gauge group is read off the fixed points of the fold.

Three calculations organize the examples: the *symmetry of the projection matrix* γ_Ω (which fixes SO versus USp), the *cubic anomaly index* of two-index matter (which is $N \pm 4$ and not the adjoint), and the *covering-space tadpole charge* q_O (which shifts the rank condition). We first determine the projected fields, then their interactions and consistency conditions. Section VI.8.2 sets up the orientifold data $O = \Omega(-1)^{F_L}\sigma$ for the holomorphic D3/O3/O7 probe class and classifies the nodes into paired and fixed. Section VI.8.3 carries out the Chan–Paton projection explicitly, with a worked $N = 4$ matrix example, and reads SO versus USp off the symmetry of γ_Ω. Section VI.8.4 folds the nodes, the arrows, and the superpotential in one boxed procedure, the place where an arbitrary involution fails to be an orientifold. Section VI.8.5 separates the two conditions that the schematic equation $(a - a^{\mathsf{T}})N + q_O = 0$ confuses: the covering-space crosscap tadpole and the genuine folded gauge anomaly, computed from the folded matter. Sections VI.8.6–VI.8.8 work three examples in increasing order of structure: flat $\mathbb{C}^3$ with an O3-plane, the $\mathbb{C}^2/\mathbb{Z}_2$ quiver with two conditional graph folds, and the dP_0 orientifold in full. Section VI.8.9 states plainly what orientifolds add and what they do not solve.

VI.8.2 The orientifold data

We work with one orientifold class throughout, the one relevant to a D3-brane probe sitting at an O3/O7 singularity. The orientifold operation is

$$O \;=\; \Omega\,(-1)^{F_L}\,\sigma, \tag{VI.8.1}$$

where Ω is worldsheet parity (the reversal of the open-string orientation), $(-1)^{F_L}$ is the left-moving spacetime fermion number, present in the standard O3/O7 form of the operation, and σ is a geometric involution acting on the transverse $\mathbb{C}^3$. We gauge O: the physical theory keeps only states invariant under it. The combination $\Omega(-1)^{F_L}$ is the worldsheet operation and is common to every example below; σ is the geometric choice that we make case by case. We are not deriving the form (VI.8.1) from the unoriented-string worldsheet here; that derivation, the crosscap states, the Klein-bottle and Möbius-strip amplitudes, and the full O3/O5/O7/O9 catalogue, are foundations cited and routed forward, and only the projection they imply is used.

The involution is holomorphic. For the D3/O3/O7 class of Type IIB probes the geometric involution σ is *holomorphic*: it acts on the complex coordinates z_a of $\mathbb{C}^3$ by a linear holomorphic map and acts on the holomorphic three-form by $\sigma^*\Omega_3 = -\Omega_3$, with $\Omega_3 = dz_1 \wedge dz_2 \wedge dz_3$. We make this the main line throughout, because it is the involution compatible with the $\mathcal{N}$=1 holomorphic data of the probe (the superpotential, the chiral arrows, the holomorphic Chan–Paton projection). Antiholomorphic involutions $z_a \mapsto \bar{z}_a$ also exist and define orientifolds. They belong to a different setting, the Type IIA O6 class. There the fixed loci are special Lagrangian rather than holomorphic, and the probe is a D6-brane, not a D3. We note that class once and then leave it: everything below is holomorphic σ.

For the orientifold to coexist with the orbifold, σ must be compatible with Γ. Concretely σ is a holomorphic isometric involution of $\mathbb{C}^3$ that normalizes the orbifold group,

$$\sigma\,\Gamma\,\sigma^{-1} \;=\; \Gamma, \qquad \sigma^2 = \mathbb{1}, \tag{VI.8.2}$$

so that $\alpha(g) = \sigma g \sigma^{-1}$ is an automorphism of Γ. There are two maps to distinguish. Geometry supplies α; orientation reversal dualizes the Chan–Paton representation. For an ordinary, untwisted lift their combined action on the irreducible representations is

$$R_i \longmapsto R_{\sigma(i)} \simeq (R_i \circ \alpha^{-1})^*, \qquad \sigma^2(i) = i. \tag{VI.8.3}$$

We continue to write $\sigma(i)$ for this combined node map, not for the geometric pullback alone. At the level of characters it reads

$$\chi_{\sigma(i)}(g) = \overline{\chi_i(\sigma^{-1} g \sigma)}. \tag{VI.8.4}$$

For example, the scalar $\mathbb{Z}_3$ action commutes with $\sigma = -\mathbb{1}$, yet dualization sends R_i to R_{-i}. A phase in the Chan–Paton lift can modify this rule; such a lift must be specified separately rather than attributed to geometry.

The involution (VI.8.3) sorts the nodes into two classes, and the entire fold follows from this classification:

$$\begin{aligned} &i \neq \sigma(i) \;:\; i \text{ is } \textit{paired} \text{ with its image } \sigma(i); \\ &i = \sigma(i) \;:\; i \text{ is } \textit{fixed} \text{ by the involution.} \end{aligned} \tag{VI.8.5}$$

A paired node and its distinct image are identified by the projection into a single unitary factor; a fixed node is projected to an orthogonal or symplectic factor. There is an

immediate consequence for the ranks: the involution forces the two members of a paired pair to carry the same Chan–Paton dimension, because the orientifold maps the brane block of i isomorphically onto that of $\sigma(i)$,

$$N_{\sigma(i)} \;=\; N_i, \tag{VI.8.6}$$

so a paired pair is described by one integer, not two, while a fixed node keeps its own N_i, subject also to parity, anomaly, and string consistency conditions. The folded rank vector therefore lives on the sublattice fixed by σ,

$$\Lambda^{\sigma} \;=\; \{\, N \in \mathbb{Z}^{r+1} : N_{\sigma(i)} = N_i \;\forall i \,\}, \tag{VI.8.7}$$

a sublattice of the unfolded one; positivity and even symplectic dimension impose further restrictions. If the involution has f fixed nodes and p image-pairs, the original $r+1 = f+2p$ independent ranks collapse to

$$\dim \Lambda^{\sigma} \;=\; f + p \;=\; (r+1) - p, \tag{VI.8.8}$$

one integer per fixed node and one per pair.

Fixed loci of σ on $\mathbb{C}^3$. The geometric content of the involution is where it fixes points. A linear holomorphic involution of $\mathbb{C}^3$ is diagonalizable with eigenvalues ± 1 on the three coordinates, and its fixed locus is the eigenspace with eigenvalue $+1$. Table VI.8.1 lists the three patterns and the O-plane each one carries for a D3 probe. A sign assignment with all three coordinates odd fixes only the origin, an O3-plane; one coordinate odd and two even fixes a complex plane, an O7-plane wrapping a divisor; the all-even sign fails $\sigma^*\Omega_3 = -\Omega_3$ and is outside this O3/O7 class. The pattern that survives the orbifold compatibility (VI.8.2) is the one whose sign assignment normalizes Γ, and that is the geometric choice each example below specifies.

local σ on (z_1, z_2, z_3)	fixed locus	O-plane in the D3 probe
$(z_1, z_2, z_3) \mapsto (-z_1, -z_2, -z_3)$	the origin (a point)	O3
$(z_1, z_2, z_3) \mapsto (-z_1, z_2, z_3)$	a complex plane (a divisor)	O7
$(z_1, z_2, z_3) \mapsto (z_1, z_2, z_3)$	all of $\mathbb{C}^3$	excluded in this class

Table VI.8.1: Fixed loci of a holomorphic involution σ of $\mathbb{C}^3$ for the Type IIB D3-probe class. The fixed locus is the $+1$ eigenspace; its (complex) codimension fixes the O-plane type, O3 for a point and O7 for a divisor. The involution must normalize Γ (VI.8.2), which is what ties the sign assignment to the orbifold.

The arrows fold by the same involution, with an orientation reversal that we develop in §VI.8.4. Before that we make the node-level statement precise: it is the Chan–Paton projection that turns a fixed node into SO or USp, and the choice between the two is not free.

node class	condition	projected gauge factor
paired	$i \neq \sigma(i)$	one $U(N_i)$ (the pair identified)
fixed, γ_Ω symmetric	$i = \sigma(i)$	$SO(N_i)$
fixed, γ_Ω antisymmetric	$i = \sigma(i)$	$USp(N_i)$

Table VI.8.2: The orientifold sorts each node by the involution (VI.8.3). A paired node contributes a single unitary factor; a fixed node contributes an orthogonal or symplectic factor according to the symmetry of the projection matrix γ_Ω (§VI.8.3). Ranks are quoted in Chan–Paton (covering) units.

VI.8.3 The Chan–Paton projection: SO versus USp

Gauging O acts on the open-string Chan–Paton matrices. A massless state with Chan–Paton matrix λ is kept when it is invariant under the orientifold, and worldsheet parity acts on λ by transposition dressed with a fixed unitary γ_Ω that represents Ω on the Chan–Paton indices. For the gauge field the parity of Ω on the vector gives a relative minus sign, so the surviving gauge field obeys

$$A_\mu \;=\; -\,\gamma_\Omega\, A_\mu^{\mathsf{T}}\, \gamma_\Omega^{-1}. \tag{VI.8.9}$$

This single equation determines the gauge group. Applying the projection (VI.8.9) twice returns the state to itself, $\Omega^2 = \mathbb{1}$ on the open string, and tracking the transposes gives

$$A_\mu \;=\; \gamma_\Omega \left(\gamma_\Omega A_\mu^{\mathsf{T}} \gamma_\Omega^{-1}\right)^{\mathsf{T}} \gamma_\Omega^{-1} \;=\; \left(\gamma_\Omega^{\mathsf{T}} \gamma_\Omega^{-1}\right)^{-1} A_\mu \left(\gamma_\Omega^{\mathsf{T}} \gamma_\Omega^{-1}\right), \tag{VI.8.10}$$

which holds for all A_μ only if $\gamma_\Omega^{\mathsf{T}}\gamma_\Omega^{-1}$ is a multiple of the identity. Transposing $\gamma_\Omega^{\mathsf{T}} = c\gamma_\Omega$ again gives $c^2 = 1$, hence

$$\gamma_\Omega^{\mathsf{T}} \;=\; \pm\,\gamma_\Omega, \qquad \gamma_\Omega^{\mathsf{T}}\gamma_\Omega^{-1} = \pm\mathbb{1}, \tag{VI.8.11}$$

that is γ_Ω is either symmetric or antisymmetric, and the two signs are the two orientifold projections:

$$\gamma_\Omega^{\mathsf{T}}\,\gamma_\Omega^{-1} = +\mathbb{1} \;\;(\gamma_\Omega = \mathbb{1}) \;\Longrightarrow\; SO(N), \qquad \gamma_\Omega^{\mathsf{T}}\,\gamma_\Omega^{-1} = -\mathbb{1} \;\;(\gamma_\Omega = J) \;\Longrightarrow\; USp(N), \tag{VI.8.12}$$

with $J = \left(\begin{smallmatrix} 0 & \mathbb{1} \\ -\mathbb{1} & 0 \end{smallmatrix}\right)$ the antisymmetric symplectic form, $J^{\mathsf{T}} = -J$, $J^2 = -\mathbb{1}$. The mechanism is visible by solving (VI.8.9) directly. With $\gamma_\Omega = \mathbb{1}$ the condition reads

$$A_\mu \;=\; -\,A_\mu^{\mathsf{T}}, \tag{VI.8.13}$$

the antisymmetric matrices in the complexified orthogonal algebra. The compact gauge algebra also obeys the usual anti-Hermiticity condition. With $\gamma_\Omega = J$ the condition reads $A_\mu = -JA_\mu^{\mathsf{T}}J^{-1}$, equivalently in terms of $M = JA_\mu$ the symmetric condition $M = M^{\mathsf{T}}$, which selects $usp(N)$. Counting complex parameters before imposing the compact reality condition, an antisymmetric $N \times N$ matrix has its N diagonal entries fixed to zero and its off-diagonal entries paired, while a symmetric one keeps the diagonal,

$$\dim so(N) = \tfrac{1}{2}N(N-1), \qquad \dim usp(N) = \tfrac{1}{2}N(N+1). \tag{VI.8.14}$$

The two dimensions add to the parent,

$$\dim so(N) + \dim usp(N) \;=\; \tfrac{1}{2}N(N-1) + \tfrac{1}{2}N(N+1) \;=\; N^2 \;=\; \dim u(N), \tag{VI.8.15}$$

For even N this is an identity between the dimensions of two different projections. Their invariant subspaces, defined using different γ_Ω, need not be complementary subspaces of one fixed $u(N)$. The actual projector is $(1+\mathcal{P})/2$, where $\mathcal{P}(A) = -\gamma_\Omega A^{\mathsf{T}} \gamma_\Omega^{-1}$ is an involution. Neither invariant dimension is exactly $N^2/2$.

A worked $N = 4$ projection. It is worth solving (VI.8.9) once with explicit matrices, because the abstract sign chain becomes a counting exercise. Take $N = 4$. With $\gamma_\Omega = \mathbb{1}$ the surviving A_μ are the 4×4 antisymmetric matrices,

$$A \;=\; \begin{pmatrix} 0 & a_{12} & a_{13} & a_{14} \\ -a_{12} & 0 & a_{23} & a_{24} \\ -a_{13} & -a_{23} & 0 & a_{34} \\ -a_{14} & -a_{24} & -a_{34} & 0 \end{pmatrix}, \tag{VI.8.16}$$

whose six free entries $a_{12}, \ldots, a_{34}$ count $\dim so(4) = \frac{1}{2} \cdot 4 \cdot 3 = 6$. The diagonal is forced to zero and the lower triangle is minus the upper, so the projection has cut the sixteen real parameters of $u(4)$ down to six. With $\gamma_\Omega = J$, written in the basis where $J = \left(\begin{smallmatrix} 0 & \mathbb{1}_2 \\ -\mathbb{1}_2 & 0 \end{smallmatrix}\right)$, the surviving A satisfy $A = -JA^{\mathsf{T}}J^{-1}$, which in 2×2 blocks $A = \left(\begin{smallmatrix} P & Q \\ R & S \end{smallmatrix}\right)$ reads

$$S = -P^{\mathsf{T}}, \qquad Q = Q^{\mathsf{T}}, \qquad R = R^{\mathsf{T}}, \tag{VI.8.17}$$

Over $\mathbb{C}$, P is arbitrary (4 parameters) and Q, R are symmetric (3 each), giving complex dimension 10. For the compact real form, $P^\dagger = -P$ and $R = -Q^\dagger$, leaving $4 + 6 = 10$ real parameters and $\dim usp(4) = 10$. The two counts 6 and 10 add to $16 = \dim u(4)$, the split (VI.8.15) in numbers. The reader can read off from (VI.8.17) why $USp(N)$ *requires even* N: the symplectic form J pairs the Chan–Paton indices two by two, and an odd-dimensional antisymmetric J is degenerate, with no inverse to write γ_Ω^{-1}. There is no USp projection on an odd Chan–Paton block; the SO projection, by contrast, exists for every N.

On the orbifold the Chan–Paton index runs over the nodes, and the projection matrix γ_Ω acts block by block. The Chan–Paton space decomposes as $\bigoplus_i \mathbb{C}^{N_i} \otimes R_i$, and the orientifold pairs the block of node i with the block of its image $\sigma(i)$, so that γ_Ω is block off-diagonal between a paired pair and block diagonal on a fixed node,

$$(\gamma_\Omega)_{i,\sigma(i)} \;\neq\; 0, \qquad \gamma_\Omega^{\mathsf{T}} \gamma_\Omega^{-1} = \pm\mathbb{1} \text{ on each fixed block.} \tag{VI.8.18}$$

On a paired pair the off-diagonal block carries no sign choice of its own: it simply identifies the two unitary factors, $U(N_i) \times U(N_{\sigma(i)}) \to U(N_i)$ with $N_{\sigma(i)} = N_i$ forced by the involution. On a fixed block the sign in (VI.8.18) is the one that (VI.8.12) reads as SO or USp, and it is determined by the geometry of σ and the worldsheet data, not chosen freely. This is the precise sense in which the gauge group is read off the fixed points of the fold.

The matter projects by the same rule with a possibly different sign. A holomorphic bifundamental X obeys

$$X \;=\; \pm\,\gamma_\Omega\, X^{\mathsf{T}}\, \gamma_\Omega^{-1} \tag{VI.8.19}$$

at a fixed node. For $\gamma_\Omega = J$, raising or lowering an index with J changes how the transpose sign is read as tensor symmetry; the sign alone does not identify the representation. With $\gamma_\Omega = \mathbb{1}$ this is the symmetric/antisymmetric split of the tensor square of the fundamental,

$$\square \otimes \square \;=\; \underbrace{\tfrac{1}{2}(X + X^{\mathsf{T}})}_{\text{sym, }+} \;\oplus\; \underbrace{\tfrac{1}{2}(X - X^{\mathsf{T}})}_{\text{antisym, }-}, \tag{VI.8.20}$$

the orientifold keeping one summand. In the orbifold-compatible form the projection ties together the node and its image,

$$X_{ij} \;=\; \eta\, C_i\, X^{\mathsf{T}}_{\sigma(j)\sigma(i)}\, C_j^{-1}, \tag{VI.8.21}$$

Here C_i identifies the dual image block with block i; with equal image dimensions the product has size $N_i \times N_j$. The factor $\eta = \pm 1$ is a sector-dependent sign. The sign η is not an independent decoration: it is fixed once the worldsheet parity action on the relevant ground state and the signs in γ_Ω are fixed, and it must also obey the orientifold group relations and preserve the action. Geometry, sector parity, and the Chan–Paton sign are distinct inputs. The arrow content of the folded quiver is the content of (VI.8.21), and we unpack it in the next section.

Convention: $USp(2k)$ is Witten's $Sp(k)$

We write the symplectic gauge factor as $USp(N)$ with N even, the compact form of $sp(N/2)$, using Chan–Paton dimensions for all gauge factors. In particular $USp(2k)$ denotes the rank-k symplectic group, which some references (Witten among them) write as $Sp(k)$: the two are the same group, and the symbol Sp when it appears in the literature anchors below is read as USp. Ranks here, for SO, USp, and U alike, are quoted in Chan–Paton (covering) units, so the node label is the dimension of the Chan–Paton block; the physical brane count is half, and the physical-unit translation is stated once in the apparatus.

VI.8.4 Folding the nodes, arrows, and superpotential

Folding the quiver is one procedure applied to three kinds of data: the nodes (done in §VI.8.2), the arrows, and the superpotential. We do the arrows and the superpotential here, and collect the whole procedure as a boxed recipe at the end of the section.

Folding the arrows. The arrows fold because Ω reverses the orientation of an open string. An oriented string stretched from a brane of type i to a brane of type j, carrying the field X_{ij}, is sent by Ω to the string of opposite orientation, from j to i; composing with the geometric involution σ that relabels the nodes, the image of the arrow $i \to j$ is the arrow

$$X_{ij} \;\longmapsto\; X_{\sigma(j)\,\sigma(i)}, \tag{VI.8.22}$$

from $\sigma(j)$ to $\sigma(i)$. The orientation reversal is the swap of the two indices *before* the relabeling, the two candidate maps being

$$\begin{aligned} \text{(orientation kept)} \quad & i \to j \;\longmapsto\; \sigma(i) \to \sigma(j), \\ \text{(orientation reversed)} \quad & i \to j \;\longmapsto\; \sigma(j) \to \sigma(i), \end{aligned} \tag{VI.8.23}$$

and Ω enforces the second. This distinction is the whole arithmetic of the fold, and getting it backwards produces a quiver that is not the orientifold of anything. On the adjacency the map (VI.8.22) reads

$$(a^\sigma)_{kl} \;=\; a_{\sigma(l)\,\sigma(k)} \;=\; (P a^{\mathsf{T}} P)_{kl}, \tag{VI.8.24}$$

with P the permutation matrix of σ, $P_{ki} = \delta_{k,\sigma(i)}$; the transpose is the orientation reversal and the conjugation by P is the relabeling. An orientifold of the given quiver exists only when the quiver is invariant under the fold,

$$a^\sigma \;=\; a \qquad\Longleftrightarrow\qquad P\,a^{\mathsf{T}}\,P \;=\; a, \tag{VI.8.25}$$

so that the involution is a symmetry of the directed graph.

When that holds, the surviving arrows sort into three classes according to how (VI.8.22) acts on their endpoints. The classification is the heart of the chapter, so we go through it slowly, naming the surviving representation in each case.

1. *Both endpoints paired, with distinct images.* The arrow $i \to j$ and its image $\sigma(j) \to \sigma(i)$ are two distinct arrows of the unfolded quiver. The projection identifies them into a single field, a bifundamental of the two identified unitary factors. The folded quiver keeps one of each image pair.

2. *A self-image arrow.* This means $i = \sigma(j)$ and $j = \sigma(i)$. When $i \neq j$, its endpoints form an image pair and its matrix transforms as $T \mapsto gTg^{\mathsf{T}}$ after the fold, giving symmetric or antisymmetric matter of the surviving unitary group. A loop at a fixed node instead uses that node's invariant form to identify its dual. An arrow joining two distinct fixed nodes is not a self-image arrow and is not a two-index tensor of either node.

3. *One endpoint a fixed node, one a paired node.* An arrow between a fixed node and one of a paired pair folds together with its image into a single bifundamental connecting the SO/USp factor to the surviving unitary factor.

Collecting the three cases, the fold sends the arrow content to

$$\begin{aligned} \text{(paired, paired)}\ X_{ij}\oplus X_{\sigma(j)\sigma(i)} \;&\longmapsto\; \text{one bifundamental of } U\times U, \\ \text{(self-folded loop on one node)}\ X_{ij} \;&\longmapsto\; \text{sym / antisym / adjoint of that node}, \\ \text{(fixed, paired)}\ X_{ij}\oplus X_{\sigma(j)\,i} \;&\longmapsto\; \text{one bifundamental of } (SO/USp)\times U, \end{aligned} \tag{VI.8.26}$$

the sign in the middle line set by (VI.8.21). The crucial subtlety, the one the worked dP_0 example below turns on, is in the middle line: the tensor matter lives on the node

to which the *folded* arrow returns, which need not be the geometrically fixed node. The matter of the orientifolded theory is therefore richer than that of the parent: alongside the bifundamentals it now contains two-index tensors, symmetric and antisymmetric, of the surviving factors, and these are exactly the representations whose anomaly indices we will need in §VI.8.5.

Folding the superpotential. A fold of the nodes and arrows is not yet an orientifold. The cubic superpotential is part of the data of the $\mathcal{N}$=1 theory, the projected image of the unique cubic invariant of $SU(3)$, and the orientifold must *preserve* it. Writing W as a sum of gauge-invariant oriented cubic words, the involution acts on each word by relabeling its nodes and reversing the order of its arrows,

$$W \;=\; \sum_{T} c_T\, T, \qquad \sigma:\; T \;\longmapsto\; \sigma(T), \tag{VI.8.27}$$

and the requirement is that W map to itself, $W \mapsto W$, up to the sign that the superspace measure absorbs. The terms then sort into three kinds according to the orbit of T and a sign $s(T) = \pm 1$ that the projection assigns along its arrows,

$$\begin{aligned} \sigma(T) \neq T \;&:\quad T + \sigma(T) \text{ kept with a common coefficient (paired)},\\ \sigma(T) = T,\; s(T) = +1 \;&:\quad T \text{ kept (fixed, survives)},\\ \sigma(T) = T,\; s(T) = -1 \;&:\quad T \text{ removed (fixed, projected out)}. \end{aligned} \tag{VI.8.28}$$

The constraint is therefore a sign condition, one per orbit of words, and a fold that fails it is simply not an orientifold of this theory.

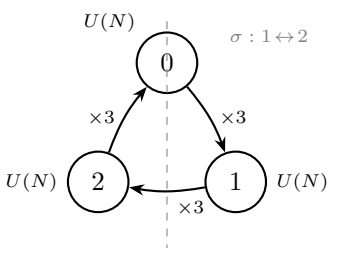
The folding procedure

Given an oriented $\mathbb{C}^3/\Gamma$ quiver, its adjacency a, its cubic W, and a candidate involution σ with $\sigma\Gamma\sigma^{-1} = \Gamma$:

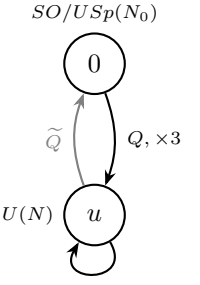
1. *Node involution.* Read $\sigma(i)$ off the character table (VI.8.4); classify each node as paired ($i \neq \sigma(i)$) or fixed ($i = \sigma(i)$).
2. *Graph symmetry.* Check $Pa^{\mathsf{T}}P = a$ (VI.8.25). If it fails, σ is not an orientifold; stop.
3. *Arrow orbits.* For each arrow $i \to j$ compute the image $\sigma(j) \to \sigma(i)$. Group the arrows into orbits and tabulate, for each orbit, the parent arrow, its image, and the folded representation, by (VI.8.26).
4. *Gauge group.* Assign $SO(N_i)$ or $USp(N_i)$ to each fixed node by the symmetry of γ_Ω, one $U(N_i)$ to each paired pair.
5. *Superpotential.* Apply σ to each cubic word; verify $W \mapsto W$ (VI.8.28). If a surviving term maps to a forbidden one, σ is not an orientifold.
6. *Consistency.* Impose the covering-space tadpole and recompute the folded gauge anomaly from the folded matter (§VI.8.5).

Warning: a quiver involution is not enough; it must preserve W

It is tempting to choose any node involution σ with $\sigma\Gamma\sigma^{-1} = \Gamma$, fold the quiver, and declare the result an orientifold. The missing condition is that the superpotential be preserved. The inherited cubic signs are fixed by the parent projection, not free choices; the orientifold adds one further sign per word-orbit, and a σ that maps a surviving term to a forbidden one, or that fails to close the cubic words back onto themselves, does not define an orientifold. Always check $W \mapsto W$ after folding the quiver; the gauge content alone never settles it.



unfolded dP_0



folded orientifold quiver

Figure VI.8.1: Folding the dP_0 triangle by the conjugation involution $\sigma : i \mapsto -i \bmod 3$, which fixes node 0 and swaps nodes 1 and 2. Left: the unfolded directed triangle with the fold axis through node 0. Right: node 0 becomes an SO or USp factor, nodes 1 and 2 are identified into one $U(N)$ (labelled u), and the three arrows $0 \to 1/2 \to 0$ fold to a *single* bifundamental Q between them (drawn with its orientifold image $\widetilde{Q}$ in grey, which is not an independent field). The self-image arrow $1 \to 2$ becomes a loop *on the* U_u *node* and projects to a two-index (symmetric or antisymmetric) tensor of $U(N)$, not of node 0, correcting the naive assignment. The SO/USp choice and the precise tensor are fixed by the projection signs.

The fold of the dP_0 triangle. We run steps 1–3 once now, on the chiral $dP_0 = \mathbb{C}^3/\mathbb{Z}_3$ triangle, both to illustrate the procedure and to fix the arrow-orbit table that the full worked example in §VI.8.8 computes against. The adjacency is $a_{ij} = 3\delta_{j,i+1 \bmod 3}$, a single directed triangle $0 \to 1 \to 2 \to 0$ with three flavour copies on each edge, and the conjugation involution $\sigma : i \mapsto -i \bmod 3$ fixes node 0 and swaps nodes 1 and 2. Step 2 holds: the conjugation reverses the 3-cycle, which the orientation reversal flips back, so $Pa^{\mathsf{T}}P = a$. Step 3 is the arrow-orbit table. We label the surviving identified U node u (the merger of nodes 1 and 2), and node 0 stays the fixed SO/USp node.

The table makes the subtlety concrete and corrects the naive reading. The self-image arrow is $1 \to 2$, because $\sigma(2) \to \sigma(1) = 1 \to 2$ returns it to itself; once nodes 1 and 2 are merged into the single unitary node u, this arrow becomes a loop $u \to u$ and projects to a two-index tensor (symmetric or antisymmetric) *of the* U_u *node.* The fixed node 0,

parent arrow	image $\sigma(j) \to \sigma(i)$	after 1=2=u	folded representation
$0 \to 1$	$2 \to 0$	$0 \to u$	bifund. $(SO/USp)_0$–U_u
$2 \to 0$	$0 \to 1$	$u \to 0$	(the same bifund., paired)
$1 \to 2$	$1 \to 2$	$u \to u$	two-index tensor of U_u

Table VI.8.3: Arrow orbits of the dP_0 triangle under $\sigma : 1 \leftrightarrow 2$. The arrow $0 \to 1$ and its image $2 \to 0$ identify into a single bifundamental between the fixed node 0 and the merged U node u. The arrow $1 \to 2$ is its *own* image ($\sigma(2) \to \sigma(1) = 1 \to 2$); after identifying $1 = 2 = u$ it becomes a loop $u \to u$, hence a two-index tensor of the surviving U_u node, *not* of the fixed node 0. Each edge carries the threefold flavour multiplicity of the **3**.

by contrast, never sees a self-image loop: its three outgoing arrows $0 \to 1$ pair with the three incoming $2 \to 0$ to make bifundamentals, and node 0 carries *no* two-index tensor. Writing the tensor on node 0 would put it on the wrong node, miscount the $SU(N_u)$ anomaly, and break the very consistency the orientifold is supposed to deliver. We will use Table VI.8.3 verbatim in §VI.8.8.

The cubic interaction tests more than the directed graph. Write the parent fields as $A^\alpha = X_{01}^\alpha$, $B^\beta = X_{12}^\beta$, and $C^\gamma = X_{20}^\gamma$. Their sizes are $N_0 \times N_u$, $N_u \times N_u$, and $N_u \times N_0$, respectively. The inherited interaction is

$$W \sim \varepsilon^{\alpha\beta\gamma} \operatorname{Tr}(X_{01}^\alpha X_{12}^\beta X_{20}^\gamma). \tag{VI.8.29}$$

Choose a fixed-node form G with $G^{\mathsf{T}} = sG$, $s = \pm 1$. A consistent candidate field action with a flavour-independent tensor sign t is

$$A^\alpha \mapsto G(C^\alpha)^{\mathsf{T}}, \quad B^\beta \mapsto t(B^\beta)^{\mathsf{T}}, \quad C^\gamma \mapsto s(A^\gamma)^{\mathsf{T}} G^{-1}. \tag{VI.8.30}$$

The matrix products have the right sizes. Since $G^{\mathsf{T}} = sG$, this action squares to the identity on all three fields. The extra s on C is necessary for this statement on the symplectic branch. The transpose reverses the matrix order, while exchanging α and γ reverses the flavour epsilon. Together they give

$$W \mapsto st\varepsilon^{\alpha\beta\gamma} \operatorname{Tr}[(A^\gamma B^\beta C^\alpha)^{\mathsf{T}}] = -stW. \tag{VI.8.31}$$

Thus the action preserves this parent cubic when $st = -1$. Its lift to a supersymmetric orientifold still requires the superspace measure and geometric flavour action. For the surviving interaction the direct contraction in Section VI.8.8 will instead fix the correlation of the fixed-node and tensor symmetries without an ambiguous reversed word.

VI.8.5 Ramond–Ramond charges and folded gauge anomalies

The consistency of the orientifolded theory is governed by two distinct equations that look deceptively similar, and confusing them is the most common error in the subject.

The first is a *covering-space tadpole*, a Ramond–Ramond charge-neutrality condition written upstairs, before the fold. The second is the genuine *gauge anomaly* of the folded theory, written downstairs, after the gauge groups and matter have changed. We treat them in turn and then state exactly how they differ.

The covering-space crosscap tadpole

In the oriented theory the twisted Ramond–Ramond charge of a brane configuration was the Chan–Paton trace, and the localized tadpole cancellation was dual to the four-dimensional anomaly $(a - a^{\mathsf{T}})N = 0$. The orientifold plane is an additional source of twisted charge: read in the closed-string channel, the Möbius strip and Klein bottle add a crosscap contribution q_O to the same twisted fields the branes emit. After choosing an appropriate charge basis, one sometimes represents this shift schematically by

$$(a - a^{\mathsf{T}})\, N \;+\; q_O \;=\; 0, \tag{VI.8.32}$$

an affine equation in the covering ranks rather than the linear one of the oriented case. We stress, because the next subsection turns on it, that (VI.8.32) is a statement about the *covering* quiver, the unfolded a and the unfolded N before identification: it models an affine shift. The actual sector charge map need not be $a - a^{\mathsf{T}}$, and no equality with a folded anomaly is assumed. The origin of q_O is the crosscap. In the oriented theory the twisted charge came from the cylinder, which in the closed channel is the brane emitting and reabsorbing a twisted closed string; its tadpole was the square of the Chan–Paton trace in the sector g,

$$\mathcal{T}_g^{\mathrm{cyl}} \;\sim\; |c_g \,\mathrm{Tr}\,\gamma_g|^2 \;=\; \left| c_g \sum_i N_i \chi_i(g) \right|^2 . \tag{VI.8.33}$$

The unoriented theory adds two worldsheets with crosscaps, the Möbius strip (one boundary, one crosscap) and the Klein bottle (two crosscaps), and in the closed channel these are the O-plane emitting the same twisted fields. The total twisted tadpole is therefore the square of a sum, the brane trace plus a crosscap term,

$$\mathcal{T}_g \;\sim\; \left| c_g \sum_i N_i \chi_i(g) + q_O(g) \right|^2 , \tag{VI.8.34}$$

Here c_g contains the sector normalization, and complex sectors pair with their conjugates. Cancellation sets the relevant brackets to zero. Relating them to (VI.8.32) requires the actual charge map, which is not computed here. We keep q_O schematic: it is the crosscap twisted charge, sign- and sector-dependent, and its precise normalization (the $O3^{\pm}$, $O7^{\pm}$ charges and their twisted-sector decomposition) is the business of the orientifold volume and is routed there. What matters here is the structure. Setting $q_O = 0$ recovers Chapter 7 exactly. With $q_O \neq 0$ the allowed covering ranks form an affine sublattice: if N and N' both solve (VI.8.32), their difference solves the homogeneous equation,

$$(a - a^{\mathsf{T}})\, N + q_O = 0 \text{ and } (a - a^{\mathsf{T}})\, N' + q_O = 0 \implies (a - a^{\mathsf{T}})(N - N') = 0, \tag{VI.8.35}$$

so $N - N' \in \ker(a - a^{\mathsf{T}})$, the same homogeneous kernel that classified the oriented anomaly-free deformations; the orientifold shifts the solution set without changing its translational structure. On the dP_0 adjacency $a - a^{\mathsf{T}}$ annihilates the regular direction, and a formal source chosen for any $N_\star$ makes both $N_\star$ and its regular translates solutions,

$$q_O \;=\; -(a - a^{\mathsf{T}})\, N_\star \;\Longrightarrow\; (a - a^{\mathsf{T}})\big(N_\star + k\,(1,1,1)\big) + q_O \;=\; 0 \quad \forall k \in \mathbb{Z}, \tag{VI.8.36}$$

This proves an affine-system identity, not the existence of an O-plane with that chosen charge.

Charge cancellation and gauge anomaly cancellation

The physical charge equation has the form $Q_D(N) + Q_O = 0$ in each relevant Ramond–Ramond sector. Equation (VI.8.32) illustrates its affine character, but the parent adjacency alone does not determine Q_D or Q_O after orientifolding. The folded gauge anomaly must be calculated from the surviving chiral representations. Even a vanishing perturbative anomaly does not settle global anomalies, K-theory charge, compact tadpoles, or supersymmetry of a proposed string configuration.

The folded gauge anomaly

The surviving orthogonal and symplectic fundamentals are real or pseudoreal. For these representations, and the tensor representations built here, conjugation pairs the cubic trace with its negative, so

$$d_R^{abc} = \mathrm{Tr}_R(T^a\{T^b, T^c\}) = 0 \quad \text{for the real or pseudoreal representations used here.} \tag{VI.8.37}$$

This is a statement about representations. It is not an unrestricted assertion about all orthogonal Lie algebras: $so(6) \simeq su(4)$ admits a cubic invariant in complex spinor representations, which are absent in these open-string spectra. We therefore compute the perturbative $SU(N_u)^3$ anomaly from the unitary-node matter. Abelian and mixed anomalies require separate treatment.

What does still discriminate is the anomaly index of the two-index matter that the fold produces, computed against the unitary factor. Embedding a traceless abelian generator

$$Q \;=\; \mathrm{diag}(N-1,\, -1, \ldots, -1), \qquad \mathrm{Tr}\, Q = 0, \tag{VI.8.38}$$

in $SU(N)$ and summing the cube of the charge over the states of a representation gives the cubic index $A(R) = \sum_{\text{states}} q^3$, normalized to $A(\square)$. The fundamental has one state of charge $N-1$ and $N-1$ states of charge -1, fixing the normalization,

$$A_{\text{raw}}(\square) \;=\; (N-1)^3 + (N-1)(-1)^3 \;=\; N(N-1)(N-2), \qquad A(\square) = \frac{A_{\text{raw}}(\square)}{A_{\text{raw}}(\square)} = 1. \tag{VI.8.39}$$

For $N \geq 3$, the denominator is nonzero. The two-index tensors carry the pairwise charge sums $q_a + q_b$ over ordered index pairs ($a \leq b$ symmetric, $a < b$ antisymmetric);

dividing each raw sum by $A_{\rm raw}(\square)$ gives

$$\begin{aligned} A(\text{antisym}) &= \frac{\sum_{a<b}(q_a+q_b)^3}{N(N-1)(N-2)} = N-4, \\ A(\text{sym}) &= \frac{\sum_{a\le b}(q_a+q_b)^3}{N(N-1)(N-2)} = N+4, \end{aligned} \tag{VI.8.40}$$

in units of $A(\square)$, computed directly from the charge cubes, so that

$$A(\square)=1, \qquad A(\text{antisym})=N-4, \qquad A(\text{sym})=N+4. \tag{VI.8.41}$$

Their sum and difference are clean,

$$A(\text{sym})+A(\text{antisym}) = 2N = A(\square\otimes\square), \qquad A(\text{sym})-A(\text{antisym}) = 8. \tag{VI.8.42}$$

The first identity is worth stating carefully, because it is a frequent trap. The sum $2N$ is the index of the *product* representation $\square\otimes\square = \text{sym}\oplus\text{antisym}$, not the index of the adjoint. The $SU(N)$ adjoint is a *real* representation, and a real representation has vanishing cubic anomaly,

$$A(\text{adjoint}) = \sum_{\text{roots}} (q_i-q_j)^3 = 0. \tag{VI.8.43}$$

So $A(\text{sym})+A(\text{antisym})=2N$ is correctly read as the product-rep index; writing it as "$A(\text{adjoint})=2N$" is wrong on both counts. Two special cases anchor the formula (VI.8.41),

$$\begin{aligned} A(\text{antisym})\big|_{N=4} &= N-4 = 0 \qquad (\text{the real } \mathbf{6}), \\ A(\text{antisym})\big|_{N=3} &= N-4 = -1 = -A(\square), \end{aligned} \tag{VI.8.44}$$

the first because the antisymmetric of $SU(4)$ is the real $\mathbf{6}$, the second because the antisymmetric of $SU(3)$ is the conjugate fundamental $\overline{\mathbf{3}}$, whose index is minus that of the fundamental, as it must be.

Warning: a vanishing cubic trace does not remove global anomalies

The vanishing of d_R^{abc} for the representations above removes the *local perturbative* cubic gauge anomaly. It does *not* remove every anomaly. Symplectic groups in particular carry a mod-2 *global* (Witten) anomaly: a $USp(2k)$ gauge theory (and in particular $SU(2)\cong USp(2)$) with an *odd* number of left-handed fundamental Weyl fermions (or fundamental half-hypermultiplets in $\mathcal{N}=2$ language) has an inconsistent path integral, because $\pi_4(USp(2k))=\mathbb{Z}_2$ obstructs a globally well-defined fermion measure. This is a separate parity constraint, not visible in the cubic trace calculation, and an orientifolded USp node must satisfy it independently. A spectrum can pass the local cubic anomaly (trivially, for the representations just discussed) and still fail the global mod-2 test. We flag it here and route the systematic treatment to the anomaly-inflow foundations.

representation of $SU(N)$	cubic index $A(R)/A(\square)$	note
fundamental $\square$	1	normalization
antisymmetric	$N-4$	$\to 0$ at $N=4$ (the real **6**)
symmetric	$N+4$	
$\square\otimes\square=\text{sym}\oplus\text{antisym}$	$2N$	the *product* index
adjoint	0	real representation
SO/USp matter used here	0	real or pseudoreal

Table VI.8.4: Cubic anomaly indices, in units of the fundamental, for the matter the fold produces. The real or pseudoreal representations used at the orthogonal and symplectic nodes have vanishing cubic trace; the symmetric and antisymmetric tensors of a unitary factor carry $N+4$ and $N-4$. The sum $2N$ is the index of $\square\otimes\square$, not of the adjoint, which is real and contributes 0.

VI.8.6 Worked example I: flat $\mathbb{C}^3$ with an O3-plane

We run the projection on three configurations in order of increasing structure. The first has no orbifold at all and isolates the Chan–Paton projection; the second folds an $\mathcal{N}$=2 quiver the reader already knows, with two inequivalent involutions; the third folds the chiral dP_0 triangle and exercises every part of the chapter at once.

With Γ trivial there is a single node and no folding to do; the orientifold is the bare Chan–Paton projection on the $\mathcal{N}$=4 theory of N D3-branes at an O3-plane. The involution is the all-odd sign of Table VI.8.1, $z_a \mapsto -z_a$ on all three coordinates, whose fixed locus is the origin: an O3-plane. The parent gauge group $U(N)$, of dimension N^2, is projected by (VI.8.9) to one of the two factors according to the sign of $\gamma_\Omega^{\mathsf{T}}\gamma_\Omega^{-1}$,

$$U(N) \xrightarrow{\gamma_\Omega=\mathbb{1}} SO(N), \qquad U(N) \xrightarrow{\gamma_\Omega=J} USp(N), \tag{VI.8.45}$$

of dimension

$$N^2 \xrightarrow{SO} \tfrac{1}{2}N(N-1), \qquad N^2 \xrightarrow{USp} \tfrac{1}{2}N(N+1), \tag{VI.8.46}$$

the two dimensions adding back to N^2 by (VI.8.15).

The projection on the matter, sign by sign. It is worth tracking the six adjoint scalars and the fermions of $\mathcal{N}$=4 through the same projection, because the point of the example is that the full multiplet survives. The six real scalars ϕ^m ($m=1,\dots,6$, the transverse $\mathbb{R}^6=\mathbb{C}^3$) and the gauge field sit in the $\mathcal{N}$=4 vector. Under Ω dressed by σ the gauge field carries the worldsheet-parity sign, and the transverse scalars carry in addition the geometric reflection of the O3, which flips all six transverse coordinates; the two signs combine so that both obey the same condition,

$$A_\mu = -\gamma_\Omega A_\mu^{\mathsf{T}}\gamma_\Omega^{-1}, \qquad \phi^m = -\gamma_\Omega\,\phi^{m\,\mathsf{T}}\,\gamma_\Omega^{-1}, \tag{VI.8.47}$$

so that the scalars land in the *same* Lie algebra as the gauge field. With $\gamma_\Omega = \mathbb{1}$ both are antisymmetric, in the adjoint of $SO(N)$; the six scalars ϕ^m are then six adjoint scalars of $SO(N)$, exactly the $\mathcal{N}$=4 matter content. The fermions follow by supersymmetry. The surviving theory is therefore $\mathcal{N}$=4 super Yang–Mills with gauge group $SO(N)$ or $USp(N)$. An O3-plane produces precisely an orthogonal or symplectic gauge theory, with the full multiplet in the adjoint and no extra matter.

$O3^-$ versus $O3^+$. The ordinary $O3^-$ and $O3^+$ choices give SO and USp, respectively. Their physical D3 charges are $-1/4$ and $+1/4$, twice these values in the covering units used for Chan–Paton multiplicities. Thus $2n$ covering D3 indices give $SO(2n)$ or $USp(2n)$, with symplectic rank n.

The four variants are distinguished by NS–NS and RR discrete torsion. Nontrivial NS–NS torsion distinguishes the symplectic choices from the ordinary orthogonal one. The stuck half-D3 description belongs to $\widetilde{O3}^-$, which gives $SO(2n+1)$, not to $O3^+$. The two symplectic variants differ in discrete information rather than in their Lie algebra dimension. Table VI.8.5 records this distinction without using it to fix twisted charges at a singularity.

O3 type	γ_Ω	gauge group ($2n$ on cover)	charge (D3 units)
$O3^-$	symmetric ($\mathbb{1}$)	$SO(2n)$	$-\frac{1}{4}$
$O3^+$	antisymmetric (J)	$USp(2n)$	$+\frac{1}{4}$
$\widetilde{O3}^-$	symmetric, torsion	$SO(2n+1)$	$+\frac{1}{4}$
$\widetilde{O3}^+$	antisym., torsion	$USp(2n)$ (RR torsion)	$+\frac{1}{4}$

Table VI.8.5: The O3-plane variants and their gauge groups, for $2n$ D3-branes on the covering space. The main line uses $O3^- \to SO$ and $O3^+ \to USp$; the two discrete-torsion variants $\widetilde{O3}^{\pm}$ are named and routed forward. Physical charges are quoted in units of the D3-brane tension; covering ranks are twice the physical brane count.

VI.8.7 Worked example II: the $\mathbb{C}^2/\mathbb{Z}_2$ orientifold, two ways

The $\mathcal{N} = 2$ affine $\widehat{A}_1$ quiver supplies a useful distinction between a graph fold and a complete orientifold. Its transverse two-coordinate matter has adjacency

$$a = \begin{pmatrix} 0 & 2 \\ 2 & 0 \end{pmatrix}, \qquad a = a^{\mathsf{T}}. \tag{VI.8.48}$$

There are two opposite-arrow pairs, hence two parent bifundamental hypermultiplets. The spectator coordinate also supplies an adjoint chiral field at each node, which is not included in this 2×2 matter adjacency. Those adjoints enter $W = \sum_a \mathrm{Tr}(\Phi_0 X_a Y_a - \Phi_1 Y_a X_a)$. Symmetry of a establishes nonchirality of the parent; it does not establish nonchirality or supersymmetry of every proposed projection.

Involution A: the node-swap

The graph map $\sigma_A(0) = 1$, $\sigma_A(1) = 0$ obeys $Pa^{\mathsf{T}}P = a$. It requires $N_0 = N_1 = N$ and identifies the gauge factors,

$$U(N_0) \times U(N_1) \longrightarrow U(N), \qquad N_0 = N_1 = N. \tag{VI.8.49}$$

But an arrow $0 \to 1$ maps to $\sigma_A(1) \to \sigma_A(0) = 0 \to 1$. It is self-image, not paired with $1 \to 0$. After identification, $g_1 = g_0^*$, so $X \mapsto g_0 X g_0^{\mathsf{T}}$. The resulting representation is a two-index tensor, not the adjoint transformation $X \mapsto g_0 X g_0^{-1}$. The opposite arrows give conjugate tensors. If the lift acts diagonally on the two arrow flavours, each sign selects a symmetric or antisymmetric tensor. A lift mixing flavours must first be diagonalized on that flavour space.

For $\mathbb{Z}_2$ both irreducible characters are real and its group automorphism is trivial. Consequently this node-swap does not follow from the untwisted rule (VI.8.4). It requires extra Chan–Paton lift data. The graph computation above is conditional on that choice; it has not constructed a supersymmetric string background or determined the tensor multiplicities after all projections.

Involution B: the node-fix

The graph map fixing both nodes instead sends $0 \to 1$ to $1 \to 0$. Fixed Chan–Paton blocks give

$$U(N_0) \times U(N_1) \longrightarrow (SO \text{ or } USp)(N_0) \times (SO \text{ or } USp)(N_1). \tag{VI.8.50}$$

The two fixed nodes are distinct, so the surviving cross-node fields are bifundamentals, not tensors at one node. An image pair leaves one independent chiral field per surviving flavour orbit. Whether these assemble into full or half hypermultiplets depends on the invariant forms, flavour action, and projection of Φ_0, Φ_1. It cannot be read from a alone.

fold	node action	gauge factors	cross-node matter type
A	$0 \leftrightarrow 1$	$U(N)$	two-index tensors
B	both fixed	$(SO/USp)_0 \times (SO/USp)_1$	bifundamentals

Table VI.8.6: Two graph folds of the $\widehat{A}_1$ matter adjacency. The gauge factors and representation types follow conditionally from the displayed Chan–Paton action. A complete orientifold additionally requires a lift on the arrow flavours and spectator adjoints, preservation of W, and string consistency conditions.

These folds teach a practical order of calculation. First identify the image of each arrow before interpreting the apparent loops in the folded drawing. Then substitute the projected fields into the parent superpotential and test the surviving symmetry. Only that fuller calculation can justify an $\mathcal{N} = 2$ spectrum. The chiral example that follows supplies explicit fields and a cubic contraction, so that its tensor sign and anomaly can be calculated directly.

VI.8.8 Worked example III: the dP_0 orientifold in full

This is the same $dP_0 = \mathbb{C}^3/\mathbb{Z}_3$ triangle as in Chapters 6 and 7, with a different spectrum: there we built the chiral quiver and checked its anomaly; here we fold it under an orientifold and recompute the gauge group, matter, superpotential, and anomaly downstairs. The chiral dP_0 triangle is the example that uses everything: the node fold, the arrow orbits with a self-image loop, the projected superpotential with field labels, the folded gauge anomaly, and the covering-space tadpole. We assemble it step by step, using the procedure box of §VI.8.4 and the arrow-orbit Table VI.8.3.

Step 1–2: nodes and graph symmetry. The adjacency is $a_{ij} = 3\delta_{j,i+1}$ on three nodes, a single directed triangle traversed three times, with antisymmetric part

$$a \;=\; \begin{pmatrix} 0 & 3 & 0 \\ 0 & 0 & 3 \\ 3 & 0 & 0 \end{pmatrix}, \qquad a - a^{\mathsf{T}} \;=\; \begin{pmatrix} 0 & 3 & -3 \\ -3 & 0 & 3 \\ 3 & -3 & 0 \end{pmatrix}, \tag{VI.8.51}$$

and the conjugation involution

$$\sigma : \; i \;\longmapsto\; -i \bmod 3, \qquad \sigma(0) = 0, \;\; \sigma(1) = 2, \;\; \sigma(2) = 1, \tag{VI.8.52}$$

fixes node 0 and swaps nodes 1 and 2. Folding the adjacency by (VI.8.24) with σ returns it unchanged,

$$(a^{\sigma})_{kl} \;=\; a_{\sigma(l)\sigma(k)} \;=\; a_{kl}, \tag{VI.8.53}$$

so σ is a symmetry of the chiral quiver and a candidate orientifold.

Step 3–4: arrow orbits and gauge group. The node classification reads off Table VI.8.2: node 0 is fixed and becomes an SO or USp factor, while nodes 1 and 2 are paired and identify into a single $U(N)$, which we call U_u. The folded gauge group is

$$U(N_0) \times U(N_1) \times U(N_2) \;\longrightarrow\; \big(SO \text{ or } USp\big)(N_0) \;\times\; U(N), \qquad N_1 = N_2 = N. \tag{VI.8.54}$$

The arrow orbits are Table VI.8.3, and we apply the fold rule (VI.8.26) to the letter, because miscounting the surviving fields is the example's subtlest trap. The orbit $\{0 \to 1,\, 2 \to 0\}$ is the *(fixed, paired)* case: the arrow $0 \to 1$ and its image $2 \to 0$ are *exchanged* by $\Omega\sigma$, so the projection keeps *one* field of the pair, not both. They identify into a *single* bifundamental Q of $(SO/USp)_0 \times U_u$; the second member is the orientifold image $\widetilde{Q} = sQ^{\mathsf{T}}G^{-1}$ (VI.8.21), fixed by Q and *not* an independent chiral multiplet. The three self-image arrows $1 \to 2$ are the *(self-folded loop)* case: after $1 = 2 = u$ each becomes a loop on U_u, projecting to a two-index tensor T of $U(N)$. With the threefold flavour the surviving independent matter is

$$\begin{aligned} \text{bifundamentals:} \quad & 3 \times Q^{\alpha} \text{ in } (\square_0,\, r_u) \text{ of } (SO/USp)(N_0) \times U(N), \\ \text{tensor:} \quad & 3 \times T^{\alpha} \text{ in the sym or antisym of } U(N), \end{aligned} \tag{VI.8.55}$$

We take $r_u = \overline{\square}$ and T in two fundamentals of U_u, as required by the arrow convention and the cubic contraction. Conjugating all unitary representations reverses every cubic

index without changing its zero. There are *three* bifundamentals, one per flavour, not three plus three conjugates: writing the orbit $\{0 \to 1,\, 2 \to 0\}$ as two independent fields would un-fold the orientifold, double the matter, and spuriously cancel the $SU(N_u)^3$ anomaly between a field and its own image. Two features follow from Table VI.8.3 and the fold rule (VI.8.26): the tensor sits on the U_u node and not on the fixed SO/USp node (the self-image arrow is $1 \to 2$, a loop on the *unitary* node after $1 = 2 = u$), and the fixed–paired orbit leaves a *single* bifundamental, its conjugate being the projection image rather than a new field.

Step 5: the projected superpotential. We now evaluate the interaction on the surviving fields, keeping the fixed-node form explicit. After the identification $1 = 2 = u$ the parent fields project to

$$X^{\alpha}_{01} \to Q^{\alpha} \;\; \text{(surviving bifund 0–}u\text{)}, \qquad X^{\alpha}_{12} \to T^{\alpha} \;\; \text{(tensor on } u\text{)}, \tag{VI.8.56}$$

while the third parent field projects to the orientifold image of Q^{α}, fixed by it and not a new field,

$$X^{\alpha}_{20} \to \widetilde{Q}^{\alpha} = s(Q^{\alpha})^{\mathsf{T}} G^{-1}, \qquad G^{\mathsf{T}} = sG. \tag{VI.8.57}$$

The projected superpotential is the surviving cubic word in the independent fields $\{Q^{\alpha}, T^{\alpha}\}$,

$$W_{\text{orient}} \;\sim\; \varepsilon_{\alpha\beta\gamma}\, \mathrm{Tr}\big(Q^{\alpha}\, T^{\beta}\, \widetilde{Q}^{\gamma}\big), \tag{VI.8.58}$$

or, with indices made explicit (I, J the $SO/USp(N_0)$ indices contracted by its invariant tensor Ω^{IJ}, and a, b the $U(N_u)$ indices),

$$W_{\text{orient}} \;\sim\; \varepsilon_{\alpha\beta\gamma}\, Q^{\alpha}_{Ia}\, T^{\beta\, ab}\, Q^{\gamma}_{Jb}\, \Omega^{IJ}, \qquad \Omega^{IJ} = s(G^{-1})^{JI}, \tag{VI.8.59}$$

which makes visible that a *single* field Q enters: the image $\widetilde{Q} = sQ^{\mathsf{T}}G^{-1}$ of (VI.8.57) is just the Ω-contraction of Q, drawn in Figure VI.8.1 but not an independent field and not a second anomaly contribution. This is a gauge invariant of $(SO/USp)(N_0) \times U(N)$: the two node-0 indices are contracted through Ω^{IJ}, and the two U_u indices of the tensor T are saturated by the U_u ends. The cubic is the orientifold image of the parent $\varepsilon^{\alpha\beta\gamma}\,\mathrm{Tr}(X^{\alpha}_{01} X^{\beta}_{12} X^{\gamma}_{20})$, with the flavour ε intact; that the tensor T^{β} sits in the middle slot is the same statement as "the self-image arrow is $1 \to 2$," and the compatibility of the symmetry of T with the SO versus USp choice on node 0 is exactly what keeps (VI.8.58) nonzero. To derive that correlation, let $(T^{\beta})^{\mathsf{T}} = tT^{\beta}$. Exchange (α, I, a) with (γ, J, b) in the contraction. The flavour epsilon contributes -1, the invariant form contributes s, and the tensor contributes t. Since the chiral superfields commute, the same polynomial equals $-st$ times itself. A nonzero cubic therefore requires

$$st = -1: \qquad SO\,(s = +1) \;\Rightarrow\; T \text{ antisymmetric}, \qquad USp\,(s = -1) \;\Rightarrow\; T \text{ symmetric}. \tag{VI.8.60}$$

For the opposite tensor sign the epsilon contraction vanishes identically. This is the interaction-level reason the two signs are correlated. The full string lift remains a physical premise, but its surviving cubic can be tested explicitly.

Step 6a: the folded gauge anomaly. The orthogonal or symplectic node 0 carries no cubic anomaly by (VI.8.37), so the only cubic gauge anomaly to cancel is that of the single surviving $U(N)$ factor, $SU(N_u)^3$, fed by the folded matter of (VI.8.55) with the indices of Table VI.8.4. We compute it. The U_u node sees three bifundamentals Q^α, each in a fixed representation $r_u = \overline{\square}$ of $SU(N_u)$ with the $SO/USp(N_0)$ index a flavour multiplicity of N_0, and three tensors T^α in the symmetric or antisymmetric. There is *no* separate conjugate bifundamental to add: $\widetilde{Q}$ is the projection image of Q, already accounted for, not a second field. The $SU(N_u)^3$ anomaly is therefore

$$\mathcal{A}\big(SU(N_u)^3\big) \;=\; 3\,s_Q\,N_0\,A(\square) \;+\; 3\,A(\text{tensor}), \qquad s_Q = -1, \tag{VI.8.61}$$

with $s_Q = -1$ for our displayed antifundamental Q. A simultaneous conjugation changes both the bifundamental and tensor signs. This does *not* cancel by itself; with the antisymmetric tensor it reads

$$\mathcal{A}\big(SU(N_u)^3\big) \;=\; 3\,s_Q\,N_0 \;+\; 3(N_u - 4), \tag{VI.8.62}$$

and with the symmetric tensor $3\,s_Q N_0 + 3(N_u + 4)$. Setting it to zero is a *rank relation* between the two surviving gauge factors,

$$N_0 \;=\; N_u \pm 4, \tag{VI.8.63}$$

the $+4$ for the symmetric tensor and the -4 for the antisymmetric tensor, with $s_Q = -1$ in our convention. Equation (VI.8.60) then gives $USp(N_u + 4) \times U(N_u)$ or $SO(N_u - 4) \times U(N_u)$. Here $N_u \geq 3$ for the cubic-index calculation, the Chan–Paton dimensions must be nonnegative, and the symplectic dimension must be even. At small ranks where a factor disappears, the spectrum must be reconsidered. Conjugating the entire spectrum reverses the anomaly, so it leaves these rank relations unchanged. The shift replaces the equal-rank solution of the oriented triangle.

Off this relation the spectrum is anomalous; one possible completion adds fundamental flavour branes on U_u (each adding its own signed fundamental index); the crosscap, by contrast, is a covering-space Ramond–Ramond charge and does *not* enter this field-theory triangle, a separation we make precise in Step 6b. Thus the folded anomaly is computed downstairs from (VI.8.55) and Table VI.8.4, it *closes* on the rank relation (VI.8.63), and it is *not* the covering-space tadpole.

We tabulate the two representative branches explicitly, so the sign calculation is concrete rather than verbal.

Step 6b: the covering-space tadpole. Upstairs, a schematic model of the consistency condition is the shifted tadpole (VI.8.32). Without the O-plane the oriented anomaly $(a - a^{\mathsf{T}})N = 0$ forced the regular direction: from (VI.8.51)

$$(a - a^{\mathsf{T}})\,N \;=\; 0 \;\Longrightarrow\; N_0 = N_1 = N_2, \tag{VI.8.64}$$

the kernel spanned by $(1, 1, 1)$. In the schematic affine description a source instead gives

$$(a - a^{\mathsf{T}})\,N + q_O \;=\; 0, \tag{VI.8.65}$$

branch	T	Q	s_Q	$\mathcal{A}(SU(N_u)^3)=0$	rank relation
A	sym	$\overline{\square}$	-1	$-3N_0+3(N_u+4)=0$	$N_0=N_u+4$
B	antisym	$\overline{\square}$	-1	$-3N_0+3(N_u-4)=0$	$N_0=N_u-4$

Table VI.8.7: Representative sign branches of the dP_0 orientifold, not a complete catalogue. We do *not* identify branch A or B with a named O-plane charge in this chapter; the point is the field-theory anomaly calculation once a projection sign is chosen, with branch A symplectic and branch B orthogonal by (VI.8.60). This does not assign a twisted crosscap charge.

field	rep. of $SU(N_u)$	multiplicity	cubic index
Q (bifund.)	$\overline{\square}$	$3N_0$	$3\,s_Q N_0$
T (tensor)	sym or antisym	3	$3(N_u\pm 4)$
total			$3s_Q N_0+3(N_u\pm 4)\overset{!}{=}0$

Table VI.8.8: The $SU(N_u)^3$ anomaly sum of the dP_0 orientifold. The bifundamental Q enters once per flavour with the $SO/USp(N_0)$ index a flavour multiplicity N_0 and sign $s_Q=-1$ (antifundamental in the displayed convention); its conjugate is the orientifold image $\widetilde{Q}$, not an independent contribution. The tensor T enters with index $N_u\pm 4$ (symmetric $+$, antisymmetric $-$). Vanishing of the total is the rank relation (VI.8.63), $N_0=N_u\pm 4$.

and the allowed covering ranks shift by an amount set by q_O, the regular ranks solving it only when q_O vanishes in the relevant sectors. We emphasize the separation: (VI.8.65) models a source shift among the *covering* ranks, while (VI.8.62) and its rank relation (VI.8.63) are the downstairs gauge anomaly of the folded theory. They are different equations, computed on different sides of the fold, and they constrain different data: the covering tadpole fixes the crosscap-shifted covering ranks N, the folded anomaly fixes the downstairs relation $N_0=N_u\pm 4$ between the surviving factors. A comparison requires a specified crosscap charge and sector map; it is not supplied by the rank calculation. The orientifold has, in short, traded the three-node chiral triangle for a two-node theory. The two surviving gauge factors are one unitary and one real. The matter content is different: one bifundamental and a tensor on the U node, not a bifundamental–conjugate pair. The cubic is the projected (VI.8.58), the $SU(N_u)^3$ anomaly closes on the rank relation (VI.8.63), and the covering tadpole is affine rather than linear. The fold has changed every line of the Chapter 6 output, which is the lesson the misconception box warned of.

VI.8.9 What orientifolds add, and what they do not solve

The chapter has added one operation to the construction and traced its consequences. An orientifold gauges $\Omega(-1)^{F_L}\sigma$ on the probe, with a holomorphic involution σ. It folds the quiver by the induced node involution. It projects fixed nodes to SO or USp and identifies paired nodes into single unitary factors. It glues image-paired arrows and projects self-image loops into symmetric, antisymmetric, or adjoint matter. It demands that the cubic superpotential survive the fold, and it adds the crosscap charge q_O to the covering-space tadpole. The new ingredients are orthogonal and symplectic groups and two-index tensors. These tensors arise because image identification relates a representation to its dual; their real or pseudoreal node representations have vanishing local cubic traces; they shift the covering tadpole by a crosscap charge, so the allowed brane configurations can change along with the projected spectrum; and they retain only invariant deformations; the number removed need not be half.

Several things are deliberately not done, and the honest boundary is the same one Chapter 7 drew, now with the orientifold added. The chapter performs the *local* projection: the gauge groups, the matter, the projected superpotential, the folded gauge anomaly, and the structure of local crosscap-shifted tadpoles. It does not build a *compact* orientifold model, in which the total Ramond–Ramond charge, branes, crosscaps, fluxes, and the global involution together, must cancel over a compact geometry; that global cancellation is the boundary of the local description, as it was for the oriented quiver. The crosscap charge q_O is kept schematic: the precise normalization, the $O3^{\pm}/O7^{\pm}$ charges and their twisted-sector decomposition, the general crosscap-charge formula across the O-plane types, are routed to the orientifold volume. The global mod-2 Witten anomaly of USp nodes is named as a separate parity constraint and routed to the anomaly foundations. The O7/F-theory back-reaction and the Sen limit, which turn the local O7 into a global elliptic fibration, are not here either. The orientifold of the brane tiling, the toric realization of the SO/USp catalogue on the dimer, is named and routed to the tiling volume. And the leading classical statements carry the probe's α'/g_s caveats throughout, as every probe statement in this volume does. A given quiver may admit several inequivalent involutions; we have worked one or two per example, and the systematic catalogue of orientifolds per Γ belongs to the later catalogue.

Orientifold checklist

Given an oriented $\mathbb{C}^3/\Gamma$ quiver and a candidate holomorphic involution σ with $\sigma\Gamma\sigma^{-1} = \Gamma$:

1. check that σ is a symmetry of the directed quiver, $a^\sigma = a$ with $(a^\sigma)_{kl} = a_{\sigma(l)\sigma(k)}$ (orientation reversal);
2. classify the nodes: $i \neq \sigma(i)$ paired into one $U(N_i)$ ($N_{\sigma(i)} = N_i$), $i = \sigma(i)$ fixed and projected to $SO(N_i)$ or $USp(N_i)$ by the symmetry of γ_Ω;
3. fold the arrows: image pairs to bifundamentals, self-image loops to symmetric / antisymmetric / adjoint matter *of the node the folded loop returns to*;
4. verify the cubic superpotential is preserved, $W \mapsto W$ (a quiver involution is not enough);
5. compute the folded gauge anomaly downstairs from the surviving matter (the real or pseudoreal representations here carry no cubic anomaly; the unitary factor sees the bifundamentals and the two-index tensor with index $N \pm 4$), and separately impose the actual sector charge conditions, of which $(a - a^{\mathsf{T}})N + q_O = 0$ is only a schematic model;
6. check the global mod-2 Witten anomaly on any USp node, and state that the result is a *local* orientifolded theory, not a compact model.

What remains is a local description for the orientifolded probe: which nodes become orthogonal, symplectic, or unitary, which arrows fold to bifundamentals and which loops to symmetric or antisymmetric tensors (and on which node), which superpotential survives, which folded gauge anomaly the unitary factor carries, and which covering ranks the crosscap-shifted tadpole allows. Orientifolds enlarge the construction; they do not, by themselves, complete it into a compact string model, and saying so plainly is the boundary of the chapter.

Status and sources

This section is for source tracking and internal consistency, not part of the first reading. The evidence-code tags ([WS] physical worldsheet evidence, [MATH] a mathematical theorem with stated hypotheses and proof status), the convention pointers, and the anchors are collected here, keyed by section. The chapter adds the orientifold to the $\mathbb{C}^3/\Gamma$ probe of Chapters 6 and 7, after the orientifold consistency conditions of Gimon and Polchinski (1996), the SO/Sp-from-O-plane mechanism of Witten (1998), the quiver projection of Douglas and Moore (1996), the chiral orbifold daughters of Lawrence et al. (1998), and the orientifolded singularity probes of Aldazabal et al. (2000), with the textbook treatment of unoriented strings in Johnson (2003). It reuses the orientifold projection and the SO/USp assignment, the rank vectors extended to the $U/SO/USp$ schema, the superpotential inheritance and its W-compatibility constraint, the McKay adjacency and arrow orientation folded under σ (McKay multiplicities, fundamental-at-tail arrows), and the geometric orbifold action that σ normalizes; orientifold projection's first load-bearing use is this chapter, which activates it. No new convention is introduced. The finite projection and index calculations use the stated folded representations. The body quotes covering/Chan–Paton units (node = Chan–Paton dimension), and the physical-unit translation (so that the covering charge is twice the physical brane count, e.g. an $O3^-$ at $-\frac{1}{4}$ in D3 units) is stated once, and the gauge-group and torsion assignment is anchored to Witten (1998), Section 3.2; the physical O3 charges and the stuck half-D3 interpretation follow Bergman et al. (2001), Table 1 and Section 2.2. Those O3 charges do not determine the twisted-sector charge vector q_O of the dP_0 probe.

§VI.8.1 Orientifolds of the probe quiver. Framing: the place in Volume VI (orientifolds modify the Chapter 7 tadpole and anomaly equations), the real-structure view, the one move (the quiver is folded,

not relabeled), and the calculation-chapter roadmap (the symmetry of γ_Ω, the index $N \pm 4$, the charge q_O). This files (orientifolding is not $U(N) \to SO/Sp$; it folds the geometry, the Chan–Paton factors, the arrows, the superpotential, and the tadpoles). No new claim-atom.

§VI.8.2 The orientifold data. The operation $O = \Omega(-1)^{F_L}\sigma$ (VI.8.1) with a *holomorphic* σ (the IIB D3/O3/O7 class; the antiholomorphic IIA O6 class noted and set aside), the normalizing involution $\sigma\Gamma\sigma^{-1} = \Gamma$ (VI.8.2), the induced node involution $R_i \mapsto R_{\sigma(i)}$ (VI.8.3), the paired/fixed classification (VI.8.5) (Table VI.8.2), and the fixed-loci table (Table VI.8.1, O3 from a fixed point, O7 from a fixed divisor). (physical projection sourced; algebra separate) (orientifold projection, orbifold action; Gimon and Polchinski (1996)). New orientifold and crosscap amplitudes (orientifolds and unoriented strings as foundations: worldsheet parity, crosscap states, O-plane tension and Ramond–Ramond charge, the Klein-bottle/Möbius amplitudes, the O3/O7 holomorphic vs O6 antiholomorphic distinction; home the orientifold volume), reusing finite-group character theory (character theory) for the action of σ on the irreps.

§VI.8.3 The Chan–Paton projection. The gauge-field projection $A_\mu = -\gamma_\Omega A_\mu^{\mathsf{T}}\gamma_\Omega^{-1}$ (VI.8.9), the iff-chain $\gamma_\Omega^{\mathsf{T}}\gamma_\Omega^{-1} = \pm\mathbb{1} \Leftrightarrow SO/USp$ (VI.8.12), the projected dimensions $\dim so(N) = N(N-1)/2$, $\dim usp(N) = N(N+1)/2$ (VI.8.14), the worked $N = 4$ matrix projection (VI.8.16)–(VI.8.17) (with the USp-needs-even-N observation), and the matter projection (VI.8.21); the $USp(2k) = Sp(k)$ recall. (physical projection sourced; algebra separate) (orientifold projection; Gimon and Polchinski (1996), Witten (1998)). the projected algebra dimension computed live from $A = -\gamma_\Omega A^{\mathsf{T}}\gamma_\Omega^{-1}$ ($n(n-1)/2$ for $\gamma_\Omega = \mathbb{1}$, $n(n+1)/2$ for $\gamma_\Omega = J$), with a wrong-sign control assigning SO's dimension to the antisymmetric case; the finite nullspaces at $N = 2, 4, 6$ illustrate the general dimension identities.

§VI.8.4 Folding the nodes, arrows, and superpotential. The orientation reversal $X_{ij} \mapsto X_{\sigma(j)\sigma(i)}$ (VI.8.22), the folded adjacency (VI.8.24), the three arrow classes (paired bifundamentals; self-image loops to symmetric/antisymmetric/adjoint matter *of the node the folded loop returns to*; fixed-to-paired bifundamentals), the boxed folding procedure, the dP_0 arrow-orbit table (Table VI.8.3, the self-image arrow $1 \to 2$ landing the tensor on the U node), the folded figure (Figure VI.8.1), and the requirement $W \mapsto W$ (VI.8.27) with the explicit dP_0 check (VI.8.30)–(VI.8.31). (worldsheet endpoint reversal sourced; projected algebra derived) (orientifold projection, fundamental-at-tail arrows, McKay multiplicities, superpotential normalization). the fold of the $\widehat{A}_1$ and dP_0 adjacencies under σ, the paired/fixed split, the node-0-fixed / nodes-1, 2-paired classification, a control dropping the orientation reversal; the finite calculation tests defining-representation cubic traces, not W. The tensor-on-the-U-node assignment (Table VI.8.3, Figure VI.8.1, (VI.8.55)) follows from the self-image arrow, and the fixed–paired orbit $\{0 \to 1, 2 \to 0\}$ leaves a *single* bifundamental Q (its conjugate the projection image $\widetilde{Q}$), not an independent pair, so the $SU(N_u)^3$ anomaly closes on the rank relation $N_0 = N_u \pm 4$ (VI.8.63) (Table VI.8.8) rather than cancelling a field against its own image.

§VI.8.5 Two calculations: covering tadpoles and folded anomalies. The two distinct equations: the formal covering-space affine model $(a - a^{\mathsf{T}})N + q_O = 0$ (VI.8.32) (an illustration of how a sector-dependent Ramond–Ramond charge balance could be represented once an actual brane/crosscap charge map is supplied; the perfect-square structure (VI.8.34), the affine shift (VI.8.35), with the explicit warning box that it is *not* the folded anomaly), and the folded gauge anomaly downstairs: the vanishing symmetric cubic trace for the real or pseudoreal representations used here (without excluding, for example, the complex chiral spinor of Spin(6)) (VI.8.37), the symmetric/antisymmetric anomaly indices $N \pm 4$ (VI.8.41), the product-rep sum $2N$ versus the vanishing adjoint anomaly (VI.8.42)–(VI.8.43) (Table VI.8.4), and the global mod-2 Witten-anomaly caveat for USp (the warning box). (charge-sector source premise and separate algebraic anomaly calculation) (orientifold projection, quiver gauge groups and ranks; Gimon and Polchinski (1996); anomaly inflow anomaly inflow and the Green–Schwarz mechanism, orientifold and crosscap amplitudes). The crosscap normalization of q_O is schematic, routed to the orientifold volume / orientifold and crosscap amplitudes; the global USp anomaly is routed to anomaly inflow and the Green–Schwarz mechanism. $d_R^{abc} = 0$ in the defining representations of $so(N)$, $usp(N)$ and nonzero for $su(3)$; the indices $N - 4$, $N + 4$ computed from charge cubes with $A(\text{sym}) + A(\text{antisym}) = 2N = A(\square \otimes \square)$ and $A(\text{adjoint}) = 0$ verified separately; the affine q_O-shift of the rank solution set.

§VI.8.6 Worked example I: flat $\mathbb{C}^3 + O3$. The $\mathcal{N}$=4 $U(N) \to SO(N)/USp(N)$ projection (VI.8.45) (the clean orbifold-trivial case), the matter projection sign by sign (VI.8.47) (the full $\mathcal{N}$=4 multiplet

survives), and the $O3^-$ vs $O3^+$ table (Table VI.8.5, with the $\widetilde{O3}^{\pm}$ variants named and routed). (string spectrum sourced; dimensions checked separately) (orientifold projection; Witten (1998)).

§VI.8.7 Worked example II: the $\mathbb{C}^2/\mathbb{Z}_2$ orientifold, two ways. The $\widehat{A}_1$ quiver (VI.8.48) folded two inequivalent ways: the node-swap A ($U(N)$ with conditional tensor matter, (VI.8.49)) and the node-fix B ($(SO/USp) \times (SO/USp)$ with bifundamental matter, (VI.8.50)), side by side in Table VI.8.6; the parent adjacency does not settle the projected supersymmetry or anomaly. (conditional graph calculation; physical lift unresolved) (orientifold projection; VI.3 recall). the $\widehat{A}_1$ fold under the node-swap, the paired-node classification.

§VI.8.8 Worked example III: the dP_0 orientifold in full. The conjugation involution (VI.8.52), the folded gauge group $(SO/USp)(N_0) \times U(N)$ (VI.8.54), the surviving matter (VI.8.55) (one bifundamental Q per flavour, its conjugate the orientifold image $\widetilde{Q}$ and not independent, plus the two-index tensor *on the U node*), the projected superpotential (VI.8.58) with field labels, the folded $SU(N_u)^3$ anomaly $3s_Q N_0 + 3(N_u \pm 4)$ (VI.8.62), which closes on the rank relation $N_0 = N_u \pm 4$ (VI.8.63) (Table VI.8.8), not by a bifundamental cancelling against its own image, and the q_O-shifted covering tadpole (VI.8.65). (matter projection sourced; anomaly and cubic calculations conditional) (orientifold projection, superpotential normalization, McKay multiplicities, quiver gauge groups and ranks; Lawrence et al. (1998), Aldazabal et al. (2000); VI.3 recall). The examples give the fold of the dP_0 adjacency, the charge-cube anomaly indices, the one-bifundamental-per-orbit count, and the rank relation that closes the $SU(N_u)^3$ anomaly, plus the q_O-shifted condition. The single-Q anomaly sum, the projected cubic, and the tensor node assignment follow under the stated local projection.

§VI.8.9 What orientifolds add. What the fold buys (SO/USp groups, two-index matter, vanishing cubic traces for the stated node representations, the crosscap tadpole shift, reduced moduli) and what it does not solve (the compact model, the precise q_O catalogue, the global USp mod-2 anomaly, O7/F-theory back-reaction and the Sen limit, the dimer realization, chirality), with the probe α'/g_s caveats, the orientifold checklist, and the per-Γ catalogue routed to the later catalogue. (scope statement), stated as the honest boundary. The orientifolded $\mathbb{C}^3/\Gamma$ probe: a folded $SO/Sp/U$ quiver with symmetric/antisymmetric/bifundamental matter, a preserved cubic W, the folded U-node anomaly, and the covering-space crosscap-shifted tadpole $(a - a^{\mathsf{T}})N + q_O = 0$.

Calculation scope and further sources. Gimon and Polchinski (1996), equations (2.1)–(2.8), support endpoint transposition and the symmetric/antisymmetric Chan–Paton forms; its Section 3 supplies the worldsheet charge-factorization mechanism. Aldazabal et al. (2000), Section 3.6.4 and equation (3.27), specify the odd-cyclic node pairing and SO/antisymmetric versus USp/symmetric matter; equation (4.14) illustrates why the charge coefficients require sector data. For $\sigma^*\Omega_3 = -\Omega_3$ in the O3/O7 class see Grimm and Louis (2004), Section 3.1, equation (3.2). The $\widehat{A}_1$ section determines conditional graph and representation types, while its flavour action, superpotential projection, and string lift remain open. The displayed charge-sum calculation derives the $N \pm 4$ identities under the specified open-string action, chirality, and local probe assumptions. The recorded checks cover these algebraic statements; they do not determine the RR-sector coefficients, K-theory conditions, or supersymmetry of the conditional $\widehat{A}_1$ folds.

References

Aldazabal, G. et al. (2000). "D-branes at singularities: A Bottom up approach to the string embedding of the standard model". In: *JHEP* 08, p. 002. DOI: 10.1088/1126-6708/2000/08/002. arXiv: hep-th/0005067.

Bergman, O., E. G. Gimon, and S. Sugimoto (2001). "Orientifolds, RR torsion, and K theory". In: *JHEP* 05, p. 047. DOI: 10.1088/1126-6708/2001/05/047. arXiv: hep-th/0103183.

Douglas, M. R. and G. W. Moore (1996). "D-branes, quivers, and ALE instantons". In: arXiv preprint; not published in a journal. arXiv: hep-th/9603167.

Gimon, E. G. and J. Polchinski (1996). "Consistency conditions for orientifolds and D-manifolds". In: *Phys. Rev. D* 54, pp. 1667–1676. DOI: 10.1103/PhysRevD.54.1667. arXiv: hep-th/9601038.

Grimm, T. W. and J. Louis (2004). "The Effective action of N = 1 Calabi-Yau orientifolds". In: *Nucl. Phys. B* 699, pp. 387–426. DOI: 10.1016/j.nuclphysb.2004.08.005. arXiv: hep-th/0403067.

Johnson, C. V. (2003). *D-Branes*. Cambridge Monographs on Mathematical Physics. Cambridge University Press. DOI: 10.1017/CBO9780511606540.

Lawrence, A. E., N. Nekrasov, and C. Vafa (1998). "On conformal field theories in four-dimensions". In: *Nucl. Phys. B* 533, pp. 199–209. DOI: 10.1016/S0550-3213(98)00495-7. arXiv: hep-th/9803015.

Witten, E. (1998). "Baryons and branes in anti-de Sitter space". In: *JHEP* 07, p. 006. DOI: 10.1088/1126-6708/1998/07/006. arXiv: hep-th/9805112.

Chapter VI.9

Discrete torsion probes

VI.9.1 Discrete torsion as a choice of orbifold CFT

The quotient $\mathbb{C}^3/\Gamma$ tells a D-brane where it can move, but it does not by itself specify every orbifold string theory on that space. In the torus partition function, closed strings can wind with commuting group twists around the two cycles. Their sectors may carry relative phases even though the action of $\Gamma \subset SU(3)$ on the three coordinates is unchanged. The discrete choice is a class

$$[\alpha] \;\in\; H^2(\Gamma, U(1)), \tag{VI.9.1}$$

in the second group cohomology with phase coefficients. It is called *discrete torsion*. For a brane probe, the question is concrete: how can a phase invisible in the quotient change the quiver and its superpotential? It enters the closed-string sector weights and the multiplication of open-string Chan–Paton representatives. The coordinate representation $Q = \mathbf{3}$ stays the honest one used in Chapter 6, while those Chan–Paton representatives become projective. This differs from the orientifold operation of Chapter 8, which adds an Ω real structure and changes the gauge-group type. Here the gauge factors remain unitary.

The torus partition function shows where the phase first appears. An orbifold partition function on the torus is a sum over twisted sectors labelled by commuting pairs $(g, h) \in \Gamma \times \Gamma$, the holonomies around the two cycles. Discrete torsion multiplies each such sector by a phase $\epsilon(g, h)$ before summing,

$$Z \;=\; \frac{1}{|\Gamma|} \sum_{gh=hg} \epsilon(g,h)\, Z\begin{bmatrix} g \\ h \end{bmatrix}, \qquad \epsilon(g,h) \;=\; \frac{\alpha(g,h)}{\alpha(h,g)}, \tag{VI.9.2}$$

and in the abelian cases studied here the consistent phase is the alternating bicharacter obtained from a two-cocycle. Its cohomology class is a finite choice for these finite abelian groups. In the worldsheet orbifold construction these phases distinguish CFTs on the same quotient. The finite-group calculation below identifies their possible values. For a D-brane, the same commutator phase controls the projective Chan–Paton multiplication; Section VI.9.2 derives that algebraic relation.

Which groups admit it. Before any computation, it pays to know for which Γ the choice (VI.9.1) is nontrivial, because that single question already explains why the chapter rests on $\mathbb{Z}_2 \times \mathbb{Z}_2$ rather than on $dP_0 = \mathbb{C}^3/\mathbb{Z}_3$. The Schur multiplier of a cyclic group is trivial, $H^2(\mathbb{Z}_n, U(1)) = 0$, so a cyclic orbifold has no discrete torsion at all: dP_0, the chiral workhorse of Chapter 6, simply has no torsion variant. The smallest group with a nontrivial multiplier is the product of two cyclics, and there the multiplier is again cyclic,

$$H^2(\mathbb{Z}_m \times \mathbb{Z}_n,\, U(1)) \;=\; \mathbb{Z}_{\gcd(m,n)}, \tag{VI.9.3}$$

so $\mathbb{Z}_m \times \mathbb{Z}_n$ carries torsion precisely when $\gcd(m,n) > 1$. The diagonal case is the one we use,

$$H^2(\mathbb{Z}_n \times \mathbb{Z}_n,\, U(1)) \;=\; \mathbb{Z}_n, \tag{VI.9.4}$$

with one nontrivial class for $\mathbb{Z}_2 \times \mathbb{Z}_2$ and two for $\mathbb{Z}_3 \times \mathbb{Z}_3$. Table VI.9.1 collects the small cases that orient the rest of the chapter.

Γ	$H^2(\Gamma, U(1))$	discrete torsion?
$\mathbb{Z}_n$	0	none (cyclic: dP_0 has no variant)
$\mathbb{Z}_m \times \mathbb{Z}_n$	$\mathbb{Z}_{\gcd(m,n)}$	yes if $\gcd(m,n) > 1$
$\mathbb{Z}_2 \times \mathbb{Z}_2$	$\mathbb{Z}_2$	one nontrivial class
$\mathbb{Z}_3 \times \mathbb{Z}_3$	$\mathbb{Z}_3$	two nontrivial classes

Table VI.9.1: Discrete torsion exists exactly when the Schur multiplier $H^2(\Gamma, U(1))$ is nontrivial. A single cyclic factor never admits it; a product of two cyclics admits the gcd, so the smallest example is $\mathbb{Z}_2 \times \mathbb{Z}_2$ with one class. The order n of the cohomology equals the order of the commutator pairing β for the chosen primitive class of §VI.9.2, which is why (VI.9.4) is the count that the projective quiver feels.

It is worth saying at once what discrete torsion is *not*, because the most common errors read it as a continuous deformation. The cohomology group (VI.9.1) is finite, by (VI.9.4) cyclic in our cases, so the choices form a discrete set rather than a continuous modulus. A torsion class cannot be varied gradually and is not a Fayet–Iliopoulos parameter and not a blow-up mode. The Fayet–Iliopoulos terms of Chapter 7 were the twisted Neveu–Schwarz moduli, continuous knobs that resolve the singularity; discrete torsion is an orthogonal, discrete choice that does not resolve anything. These are different kinds of input to an orbifold theory. The torsion choice can also change which continuous closed-string moduli survive, so their independent definitions do not imply that every background admits both.

Discrete torsion is not an FI parameter and not a blow-up mode

A discrete-torsion class $[\alpha] \in H^2(\Gamma, U(1))$ is a *discrete* choice in the orbifold conformal field theory. It does not vary continuously; it does not resolve or deform the singularity; it is not a Fayet–Iliopoulos parameter and not a blow-up mode. The Fayet–Iliopoulos / Neveu–Schwarz blow-up data of Chapters 4 and 7 and the torsion class are *orthogonal*: one is a continuous modulus of the geometry, the other a discrete label of the string theory built on it. Whether an FI or blow-up modulus survives in a torsion background is a separate closed-string spectrum question; no simultaneous availability is assumed here.

Take-home message of this chapter

Discrete torsion does not change how Γ acts on the coordinates; it changes how the Chan–Paton factors multiply. Ordinary representations are replaced by *projective* representations, $\rho(g)\rho(h) = \alpha(g,h)\,\rho(gh)$, so the McKay construction of Chapter 6 runs in the projective category. The projective irreducibles are fewer and larger, so the quiver *collapses*; the superpotential picks up cocycle phases and turns commutators into q-commutators; and the worldvolume algebra becomes *noncommutative*, with the ordinary quotient geometry surviving only as its centre. The whole chapter is the working out of these four clauses on the single example $\mathbb{C}^3/(\mathbb{Z}_2 \times \mathbb{Z}_2)$.

VI.9.2 Cocycles and projective representations

To make (VI.9.1) concrete we need a representative phase. A two-cocycle is a function $\alpha : \Gamma \times \Gamma \to U(1)$ obeying the associativity condition

$$\alpha(g,h)\,\alpha(gh,k) \;=\; \alpha(h,k)\,\alpha(g,hk), \tag{VI.9.5}$$

for all $g, h, k \in \Gamma$. This is exactly the condition that makes the multiplication law

$$\rho(g)\,\rho(h) \;=\; \alpha(g,h)\,\rho(gh) \tag{VI.9.6}$$

associative on triple products: associating $\big(\rho(g)\rho(h)\big)\rho(k)$ two ways gives

$$\alpha(g,h)\,\alpha(gh,k)\,\rho(ghk) \;=\; \alpha(h,k)\,\alpha(g,hk)\,\rho(ghk), \tag{VI.9.7}$$

which is (VI.9.5) after cancelling $\rho(ghk)$. Two cocycles that differ by a *coboundary*,

$$\alpha'(g,h) \;=\; \alpha(g,h)\,\frac{\lambda(g)\,\lambda(h)}{\lambda(gh)}, \tag{VI.9.8}$$

for some one-cochain $\lambda : \Gamma \to U(1)$, are physically equivalent: the coboundary is absorbed into a redefinition of the representatives,

$$\rho(g) \;\longrightarrow\; \lambda(g)\,\rho(g), \tag{VI.9.9}$$

which changes no physics. The torsion class (VI.9.1) is the cocycle modulo coboundaries, and only this class is meaningful. We fix a representative once and declare the coboundary freedom; the representative of choice is the bilinear form, which for $\Gamma = \mathbb{Z}_n \times \mathbb{Z}_n$ with elements written additively as $g = (a_1, a_2)$ is

$$\alpha\big((a_1,a_2),(b_1,b_2)\big) \;=\; \omega^{\,a_1 b_2}, \qquad \omega = e^{2\pi i/n}. \tag{VI.9.10}$$

One checks directly that (VI.9.10) satisfies (VI.9.5): both sides reduce to $\omega^{\,a_1b_2+(a_1+b_1)c_2}$ and $\omega^{\,b_1c_2+a_1(b_2+c_2)}$, equal because

$$a_1 b_2 + (a_1+b_1)c_2 \;=\; b_1 c_2 + a_1(b_2+c_2), \tag{VI.9.11}$$

For $n > 1$ its commutator pairing on the two generators is nontrivial, whereas every abelian-group coboundary has trivial commutator pairing. This shows that this representative is not a coboundary. The full classification (VI.9.4) remains an imported mathematical result.

The coboundary ambiguity is the reason the cocycle itself is not the natural invariant. The clean invariant is the *commutator phase*, the ratio of the two orders of multiplication,

$$\beta(g,h) \;=\; \frac{\alpha(g,h)}{\alpha(h,g)}, \tag{VI.9.12}$$

which is coboundary-independent. This is worth seeing in one line rather than asserting, because it is the reason every later statement can be phrased through β alone. Replace α by a coboundary-shifted cocycle α' as in (VI.9.8) and form the ratio: the symmetric factor $\lambda(g)\lambda(h)/\lambda(gh)$ appears in both $\alpha'(g,h)$ and $\alpha'(h,g)$ with the *same* value, since $\lambda(g)\lambda(h) = \lambda(h)\lambda(g)$ and $\lambda(gh) = \lambda(hg)$, so it cancels in the quotient,

$$\frac{\alpha'(g,h)}{\alpha'(h,g)} \;=\; \frac{\alpha(g,h)}{\alpha(h,g)} \cdot \frac{\lambda(g)\lambda(h)/\lambda(gh)}{\lambda(h)\lambda(g)/\lambda(hg)} \;=\; \frac{\alpha(g,h)}{\alpha(h,g)}. \tag{VI.9.13}$$

Two cocycles in the same class give the same β; for finite abelian Γ, the classification of cocycles by alternating pairings also says that $\beta \equiv 1$ represents the trivial class. That converse uses the standard group-cohomology classification rather than the cancellation alone. The pairing β is antisymmetric, $\beta(g,h)\beta(h,g) = 1$, and bilinear in each slot for abelian Γ; it measures by how much $\rho(g)$ and $\rho(h)$ fail to commute,

$$\rho(g)\,\rho(h) \;=\; \beta(g,h)\,\rho(h)\,\rho(g). \tag{VI.9.14}$$

For the representative (VI.9.10) the pairing reads off directly from (VI.9.12),

$$\beta\big((a_1,a_2),(b_1,b_2)\big) \;=\; \frac{\omega^{\,a_1 b_2}}{\omega^{\,b_1 a_2}} \;=\; \omega^{\,a_1 b_2 - a_2 b_1}, \tag{VI.9.15}$$

manifestly antisymmetric under $(a) \leftrightarrow (b)$, and its order is exactly n since the generator pairing $\beta\big((1,0),(0,1)\big) = \omega$ has order n. This is the invariant the convention dictionary stores; the representative cocycle is fixed once and the coboundary freedom is declared, so that all later statements depend on β and not on the gauge choice α. The reader can check from (VI.9.13) that the symmetric representative $\alpha_{\mathrm{sym}}\big((a_1,a_2),(b_1,b_2)\big) = \omega^{a_1 b_1}$ gives $\beta \equiv 1$ and hence trivial torsion, a coboundary masquerading as a nontrivial phase; only the *antisymmetric* part of the exponent survives in β.

A second, often more comfortable, way to picture a projective representation removes the cocycle from sight entirely.

A projective representation is an honest representation of a central extension

A projective representation of Γ with cocycle α is the same data as an ordinary representation of a larger group $\widetilde{\Gamma}$, the *central extension* of Γ by the phases that α generates,

$$1 \longrightarrow A \longrightarrow \widetilde{\Gamma} \longrightarrow \Gamma \longrightarrow 1, \qquad A \subset U(1) \text{ central},$$

in which chosen lifts $\widetilde{g}$ of $g \in \Gamma$ multiply in the extension as $\widetilde{g}\widetilde{h} = \alpha(g,h)\,\widetilde{gh}$, with the phase $\alpha(g,h)$ now a genuine central group element rather than a cocycle. For $\mathbb{Z}_n \times \mathbb{Z}_n$ with the maximal class the extension is the *discrete Heisenberg group*: two generators P, S with a central commutator $PSP^{-1}S^{-1} = \omega$. A projective irreducible of Γ is then literally an ordinary irreducible of $\widetilde{\Gamma}$ on which the centre acts by the chosen phase, and the whole projective representation theory of this chapter is ordinary representation theory of $\widetilde{\Gamma}$ read one level down.

VI.9.3 Twisted group algebras and projective characters

A projective representation ρ obeying $\rho(g)\rho(h) = \alpha(g,h)\rho(gh)$ is precisely a genuine representation of the *twisted group algebra* $\mathbb{C}_\alpha[\Gamma]$, the algebra spanned by symbols $\{e_g\}_{g\in\Gamma}$ with the twisted product

$$e_g\, e_h \;=\; \alpha(g,h)\, e_{gh}. \tag{VI.9.16}$$

Ordinary representation theory is the case $\alpha \equiv 1$, where $\mathbb{C}_\alpha[\Gamma] = \mathbb{C}[\Gamma]$ and the irreducibles are the ordinary irreps R_i. When α is a nontrivial cocycle the algebra is different, and so is its list of irreducibles. The whole of this chapter is the statement that the brane probe of Chapter 6 runs verbatim with $\mathbb{C}[\Gamma]$ replaced by $\mathbb{C}_\alpha[\Gamma]$ and the ordinary irreps replaced by the α-projective ones.

The single fact about $\mathbb{C}_\alpha[\Gamma]$ that drives everything is how its irreducibles are sized. As with any semisimple algebra the squared dimensions of the irreducibles sum to the dimension of the algebra,

$$\sum_i (\dim R_i^\alpha)^2 \;=\; |\Gamma|, \tag{VI.9.17}$$

but the multiset of dimensions depends on α. When the commutator pairing β is *non-degenerate* (when no nontrivial g has $\beta(g,h) = 1$ for all h) the twisted group algebra of an abelian group of order $|\Gamma| = n^2$ is the full matrix algebra,

$$\mathbb{C}_\alpha[\mathbb{Z}_n \times \mathbb{Z}_n] \;\cong\; M_n(\mathbb{C}), \tag{VI.9.18}$$

which has a *single* irreducible, of dimension n, and indeed $n^2 = |\Gamma|$ as (VI.9.17) demands. Where the ordinary group algebra of an abelian group splits into $|\Gamma|$ one-dimensional characters, the maximally twisted algebra is irreducible as a matrix algebra. That collapse, from n^2 one-dimensional pieces to one n-dimensional piece, is the mechanism behind every quiver in the chapter. One sees at once that a one-dimensional projective irreducible is impossible for nontrivial torsion: a one-dimensional ρ takes values in

numbers, which commute, so $\beta(g,h) = \rho(g)\rho(h)/\rho(h)\rho(g) \equiv 1$, the trivial class. The reader can take this as exercise zero of the chapter, and the clock–shift construction of §VI.9.7 will exhibit the forced n-dimensional irreducible explicitly.

Projective character orthogonality gives a second way to determine the irreducible dimension. For the abelian groups used here, a projective character $\chi^\alpha(g) = \operatorname{Tr}\rho^\alpha(g)$ can be nonzero only at α-*regular* elements, those for which $\beta(g,h) = 1$ for every h; on the others it vanishes identically. The reason it vanishes is worth one line: if g commutes with h in Γ but $\beta(g,h) \neq 1$, then conjugating $\rho^\alpha(g)$ by $\rho^\alpha(h)$ multiplies it by $\beta(g,h)^{-1}$, so its trace obeys $\chi^\alpha(g) = \beta(g,h)^{-1}\,\chi^\alpha(g)$ and must be zero. For an abelian Γ with non-degenerate β the only α-regular element is the identity, so a projective character is supported at $g = e$ alone, and the orthogonality relation

$$\frac{1}{|\Gamma|}\sum_{g} \chi_i^\alpha(g)\,\overline{\chi_j^\alpha(g)} \;=\; \delta_{ij} \tag{VI.9.19}$$

collapses to its $g = e$ term alone,

$$\frac{1}{|\Gamma|}\,\chi^\alpha(e)\,\overline{\chi^\alpha(e)} \;=\; \frac{1}{n^2}\,(\dim R^\alpha)^2 \;=\; 1, \tag{VI.9.20}$$

so $(\dim R^\alpha)^2 = n^2$ and $\dim R^\alpha = n$, reproducing (VI.9.17) with one irreducible of dimension n. The point of (VI.9.19) is that it is the same orthogonality that diagonalized the ordinary McKay problem, now run with projective characters; the projective McKay adjacency of the next section is computed by exactly this inner product.

VI.9.4 The projective McKay quiver

The brane probe of Chapter 6 assigned a node to each irreducible R_i of Γ, an arrow $i \to j$ for each copy of R_j in $Q \otimes R_i$, and a gauge factor $U(N_i)$ to each node. Discrete torsion changes the list of irreducibles, and nothing else in the recipe. Replace each R_i by an α-projective irreducible R_i^α, a representation of $\mathbb{C}_\alpha[\Gamma]$. The defining representation $Q = \mathbf{3}$ stays honest, because Γ acts on the coordinates by ordinary matrices with no torsion phase; so the tensor product $Q \otimes R_i^\alpha$ is again α-projective (an honest factor times an α-projective factor carries the same cocycle), and decomposes back into the same projective irreducibles,

$$Q \otimes R_i^\alpha \;=\; \bigoplus_j a_{ij}^{(\alpha)}\, R_j^\alpha, \qquad a_{ij}^{(\alpha)} \;=\; \dim \operatorname{Hom}_\Gamma^{(\alpha)}\!\big(R_j^\alpha,\, Q \otimes R_i^\alpha\big). \tag{VI.9.21}$$

The adjacency $a_{ij}^{(\alpha)}$ is the projective McKay matrix, computed by exactly the Chapter 6 inner product but in the twisted (projective) class functions. The construction is formally identical; only the category in which it is run has changed.

The consequence is that the quiver *collapses*. Because the projective irreducibles are fewer and larger, the projective McKay quiver has fewer nodes than the ordinary one for the same group. Take the two abelian examples that will carry the rest of the chapter. For $\Gamma = \mathbb{Z}_2 \times \mathbb{Z}_2$ the ordinary quiver of Chapter 6 had four one-dimensional

nodes (the doubled K_4); with the nontrivial class $[\alpha] \in H^2 = \mathbb{Z}_2$ the twisted algebra is $M_2(\mathbb{C})$, a single two-dimensional projective node, and the four nodes collapse to one,

$$4 \;\longrightarrow\; 1, \qquad \dim R^\alpha = 2, \qquad 2^2 = 4 = |\Gamma|. \tag{VI.9.22}$$

For $\Gamma = \mathbb{Z}_3 \times \mathbb{Z}_3$ the nine ordinary one-dimensional nodes collapse to a single three-dimensional projective node,

$$9 \;\longrightarrow\; 1, \qquad \dim R^\alpha = 3, \qquad 3^2 = 9 = |\Gamma|. \tag{VI.9.23}$$

It is worth pausing on (VI.9.23), because the natural wrong guess is to keep nine nodes, or to imagine three three-dimensional irreducibles. Either fails (VI.9.17): three copies of a three-dimensional irreducible would give

$$3 \cdot 3^2 \;=\; 27 \;\neq\; 9 \;=\; |\Gamma|, \tag{VI.9.24}$$

while the single three-dimensional irreducible gives $3^2 = 9 = |\Gamma|$ as required. The maximally twisted $\mathbb{Z}_3 \times \mathbb{Z}_3$ has exactly one projective irreducible, of dimension three, and the quiver is a single node.

What does that single node carry? With only one projective irreducible R^α, the decomposition (VI.9.21) must read

$$Q \otimes R^\alpha \;=\; a\, R^\alpha \tag{VI.9.25}$$

for one integer a, and counting dimensions fixes it:

$$\dim(Q \otimes R^\alpha) \;=\; (\dim Q)(\dim R^\alpha) \;=\; 3\, \dim R^\alpha \;=\; a\, \dim R^\alpha, \tag{VI.9.26}$$

so $a = 3$. The collapsed quiver is one node with three self-arrows,

$$Q \otimes R^\alpha \;=\; 3\, R^\alpha, \tag{VI.9.27}$$

the three coordinates z_1, z_2, z_3 surviving as three adjoint chiral fields Φ_1, Φ_2, Φ_3 of a single $U(m)$, where m is the multiplicity of the unique projective irreducible, i.e. the rank of the collapsed node (we fix its normalization against the bulk-probe count in the box below). The ordinary $\mathbb{Z}_2 \times \mathbb{Z}_2$ or $\mathbb{Z}_3 \times \mathbb{Z}_3$ gauge theory with its many nodes and bifundamentals has become a single-node theory with three adjoints, exactly the field content of $\mathcal{N}$=4 super Yang–Mills, but, as the next section shows, with a different superpotential.

The dimension count (VI.9.26) is decisive, but it is more instructive to see where the three self-arrows come from at the level of the tensor decomposition, because that exhibits the mechanism that the count summarizes. Take $\Gamma = \mathbb{Z}_2 \times \mathbb{Z}_2$. The defining representation Q is honest and decomposes, exactly as in Chapter 6, into the three *nontrivial* one-dimensional characters of the group,

$$Q \;=\; \chi_1 \oplus \chi_2 \oplus \chi_3, \tag{VI.9.28}$$

one for each transverse coordinate z_a. Now tensor each honest character into the single two-dimensional projective irreducible R^α. Tensoring a one-dimensional honest

character χ into a projective irreducible does not change its cocycle (an honest factor carries no phase), so $\chi \otimes R^\alpha$ is again α-projective and two-dimensional; since there is only one projective irreducible of that dimension, it must be R^α itself,

$$\chi_a \otimes R^\alpha \;\cong\; R^\alpha \qquad (a = 1, 2, 3). \tag{VI.9.29}$$

The isomorphism is concrete on the Pauli realization of the next section: tensoring by the sign character χ_a changes the signs of the appropriate two Pauli lifts by conjugation with a Pauli matrix, returning an equivalent projective representation. The group elements themselves are not permuted. Summing (VI.9.29) over the three characters of (VI.9.28) reproduces (VI.9.27) term by term,

$$Q \otimes R^\alpha \;=\; (\chi_1 \oplus \chi_2 \oplus \chi_3) \otimes R^\alpha \;=\; R^\alpha \oplus R^\alpha \oplus R^\alpha \;=\; 3\, R^\alpha, \tag{VI.9.30}$$

so the adjacency matrix is the 1×1 entry

$$a^{(\alpha)} \;=\; \dim \mathrm{Hom}_\Gamma^{(\alpha)}\big(R^\alpha,\, Q \otimes R^\alpha\big) \;=\; 3, \tag{VI.9.31}$$

three arrows from the one node to itself, one of each transverse colour. This is the honest content of the collapse: the three bifundamental colours of the parent did not disappear, they became three *adjoint* colours of the surviving single node. The reader can run the same decomposition for $\mathbb{Z}_3 \times \mathbb{Z}_3$, where Q is a sum of three nontrivial characters of the dual $\mathbb{Z}_3 \times \mathbb{Z}_3$ and each tensors the single three-dimensional R^α back to itself, again giving $Q \otimes R^\alpha = 3R^\alpha$ and a single node with three self-arrows.

Rank convention: projective multiplicity m versus bulk-probe number N

Discrete torsion forces a choice of unit, and Chapters 9 and 10 make opposite ones, so we fix both here. Write m for the *multiplicity* of the unique projective irreducible R^α, which is the rank of the single collapsed node: its gauge group is $U(m)$. The twisted regular module has dimension $|\Gamma|$ and decomposes as $\bigoplus_i (\dim R_i^\alpha) R_i^\alpha$. If N counts regular bulk probes in the Chapter 6 normalization, the Chan–Paton space has dimension $N|\Gamma|$, and the $(\dim R^\alpha)$-dimensional projective irreducible appears with multiplicity

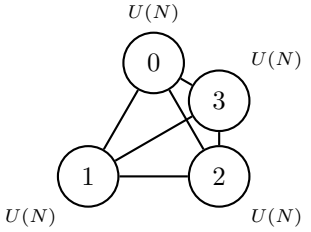
$$m \;=\; \frac{N\,|\Gamma|}{\dim R^\alpha} \;=\; n\,N \qquad \text{for maximal } \mathbb{Z}_n \times \mathbb{Z}_n \text{ torsion}, \tag{VI.9.32}$$

since there $|\Gamma| = n^2$ and $\dim R^\alpha = n$. For $\mathbb{Z}_2 \times \mathbb{Z}_2$ this is $m = 2N$: the maximally torsioned daughter is a single $U(m) = U(2N)$ node, one node of rank *twice* the per-node rank $U(N)$ of the untorsioned $U(N)^4$ theory. Chapter 10 writes the same theory as "a single $U(2N)$" in its bulk-probe normalization; this chapter writes $U(m)$ in the multiplicity normalization, and (VI.9.32) is the dictionary between them.

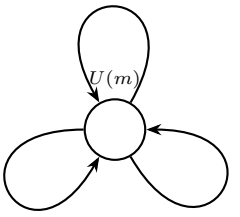
VI.9.5 Torsion phases in W and q-commutator F-terms

The cubic superpotential of Chapter 6 inherits cocycle phases. In the ordinary $\mathcal{N}{=}4$ parent the three adjoints Φ_1, Φ_2, Φ_3 enter through the commutator superpotential

$$W_0 \;=\; \mathrm{Tr}\big(\Phi_1[\Phi_2, \Phi_3]\big) \;=\; \mathrm{Tr}\big(\Phi_1\Phi_2\Phi_3 - \Phi_1\Phi_3\Phi_2\big), \tag{VI.9.33}$$



ordinary: four nodes



torsion: one node, ×3

Figure VI.9.1: Discrete torsion collapses the $\mathbb{C}^3/(\mathbb{Z}_2 \times \mathbb{Z}_2)$ quiver. Left: the ordinary doubled-K_4 on four one-dimensional nodes (the conjugate bifundamentals drawn undirected). Right: with the nontrivial $[\alpha] \in H^2 = \mathbb{Z}_2$ the four nodes become a single two-dimensional projective node carrying three adjoint self-arrows, by (VI.9.22)–(VI.9.27).

whose F-term equations $\partial_{\Phi_i} W_0 = 0$ are the commutativity conditions $[\Phi_i, \Phi_j] = 0$: the three adjoints of $\mathcal{N}$=4 commute on the moduli space, and a common eigenbasis assigns each brane a point of $\mathbb{C}^3$. Turning on discrete torsion changes the relative coefficient of the two cubic orderings. Fix the projected Chan–Paton factors in the order $A_1 = P$, $A_2 = S$, $A_3 = (PS)^{-1}$, with $PS = \omega SP$. Their products obey $\mathrm{Tr}(A_1A_2A_3) = n$ and $\mathrm{Tr}(A_1A_3A_2) = n\omega^{-1}$. Thus the coefficient of the second ordering, in this field orientation, is

$$q \;=\; \beta(g_2, g_3)^{-1} \;=\; \omega^{-1}, \tag{VI.9.34}$$

where g_2, g_3 label the ordered projective factors A_2, A_3. For $n = 2$, inverse and direct phases coincide at -1; for $n > 2$ the orientation matters. The relation between the two orders of the matrices is

$$\Phi_1\Phi_2\Phi_3 \;\longleftrightarrow\; A_1A_2A_3, \qquad A_2A_3 \;=\; \beta(g_2, g_3)\, A_3A_2, \tag{VI.9.35}$$

so the relative trace multiplying the reverse ordering is $\beta(g_2, g_3)^{-1}$. This is a consequence of the projective Chan–Paton projection with the stated matrix orientation, not a freely chosen coupling. The torsioned cubic is

$$W_q \;=\; \mathrm{Tr}\big(\Phi_1\Phi_2\Phi_3 - q\,\Phi_1\Phi_3\Phi_2\big), \tag{VI.9.36}$$

which reduces to the commutator form (VI.9.33) at $q = 1$. The clean way to read off what (VI.9.36) imposes is not to manipulate the trace but to differentiate it, exactly as for any superpotential. Using cyclicity of the trace to bring Φ_1 to the front of each monomial, the F-term in Φ_1 is

$$\partial_{\Phi_1} W_q \;=\; \Phi_2\Phi_3 - q\,\Phi_3\Phi_2 \;=\; 0, \tag{VI.9.37}$$

and the same computation on the other two fields, cyclically, gives

$$\partial_{\Phi_2} W_q \;=\; \Phi_3\Phi_1 - q\,\Phi_1\Phi_3 \;=\; 0, \qquad \partial_{\Phi_3} W_q \;=\; \Phi_1\Phi_2 - q\,\Phi_2\Phi_1 \;=\; 0. \tag{VI.9.38}$$

Each F-term relates one oriented pair. The three relations in (VI.9.37)–(VI.9.38) are

$$\Phi_2\Phi_3 = q\Phi_3\Phi_2, \qquad \Phi_3\Phi_1 = q\Phi_1\Phi_3, \qquad \Phi_1\Phi_2 = q\Phi_2\Phi_1. \tag{VI.9.39}$$

Reversing any pair gives q^{-1}, not another q unless $q^2 = 1$. The torsion has not relabelled the arrows; it has changed the algebra they obey. At $q = 1$ these are the ordinary commutators $[\Phi_i, \Phi_j] = 0$ of $\mathcal{N}$=4, and the moduli space is $\mathbb{C}^3$ as before. At the maximal $\mathbb{Z}_2 \times \mathbb{Z}_2$ torsion the pairing is $q = \beta = -1$, by (VI.9.15), and the F-terms (VI.9.39) become *anticommutators*,

$$\{\Phi_i, \Phi_j\} \;=\; \Phi_i\Phi_j + \Phi_j\Phi_i \;=\; 0 \qquad (i \neq j), \tag{VI.9.40}$$

which are the F-terms of the anticommutator cubic

$$W_- \;=\; \mathrm{Tr}\big(\Phi_1\{\Phi_2, \Phi_3\}\big) \;=\; \mathrm{Tr}\big(\Phi_1\Phi_2\Phi_3 + \Phi_1\Phi_3\Phi_2\big). \tag{VI.9.41}$$

For $n = 2$ this is the full cubic contrast, and it is best stated as a contrast between two genuinely different algebras rather than as any single numerical factor: the commutator cubic (VI.9.33) of $\mathcal{N}$=4 and the anticommutator cubic (VI.9.41) of the torsioned theory impose, through (VI.9.37)–(VI.9.38), commuting versus anticommuting adjoints. The two are not proportional and do not reduce to one another. On the Pauli realization of the next section the witness is sharp: the anticommutator cubic (VI.9.41) vanishes identically (because $\{\sigma_y, \sigma_z\} = 0$, distinct Pauli matrices anticommuting) while the commutator cubic does not ($\mathrm{Tr}\,\sigma_x[\sigma_y, \sigma_z] = 2i\,\mathrm{Tr}\,\sigma_x^2 = 4i$), so the same field content (Φ_1, Φ_2, Φ_3) obeys a strictly different cubic constraint depending on the torsion class. Discrete torsion is exactly this change of the algebra the adjoints satisfy, q-commuting rather than commuting.

VI.9.6 Worked example: $\mathbb{C}^3/(\mathbb{Z}_2 \times \mathbb{Z}_2)$ with Pauli matrices

This is the same $\mathbb{C}^3/(\mathbb{Z}_2 \times \mathbb{Z}_2)$ as in Chapters 6 and 7, but the description is different: there it was an ordinary four-node toric quiver, here we switch on the nontrivial discrete-torsion class and watch the four nodes collapse to one with anticommuting adjoints. It is the example that makes every clause of the chapter concrete, and we work it in full. The group is $\Gamma = \mathbb{Z}_2 \times \mathbb{Z}_2$, generated by the diagonal sign matrices

$$g_1 = \mathrm{diag}(1, -1, -1), \quad g_2 = \mathrm{diag}(-1, 1, -1), \quad g_3 = g_1g_2 = \mathrm{diag}(-1, -1, 1) \tag{VI.9.42}$$

inside $SU(3)$, the same group and the same action on $\mathbb{C}^3$ as in Chapter 6; the quotient $\mathbb{C}^3/(\mathbb{Z}_2 \times \mathbb{Z}_2)$ is unchanged, three lines of $\mathbb{C}^2/\mathbb{Z}_2$ singularities meeting at the origin. The Schur multiplier is $H^2 = \mathbb{Z}_2$ by Table VI.9.1, so there is exactly one nontrivial torsion class to turn on, and we turn it on. Everything that changes is in the Chan–Paton sector.

Ordinary versus torsioned quiver. It is worth seeing the two theories side by side before computing, because the contrast is the content. Without torsion (Chapter 6) the four one-dimensional irreducibles give four nodes, each $U(N)$, joined by the symmetric "doubled K_4" adjacency $a = J - \mathbb{1}_4$: twelve bifundamental chiral multiplets, vectorlike in the full arrow set, with the toric cubic superpotential. With the nontrivial class the four nodes collapse to one, by (VI.9.22), carrying a single $U(m)$ and three *adjoint* fields, the three self-arrows of (VI.9.31). Table VI.9.2 records the comparison and Figure VI.9.1 (above) draws it. The ordinary quotient coordinate ring is commutative, but its quiver path algebra is noncommutative even before torsion. The torsioned F-term algebra is noncommutative while its centre recovers that same coordinate ring.

	ordinary ($[\alpha] = 0$)	torsioned ($[\alpha] \neq 0$)
irreducibles	four 1-dimensional χ_i	one 2-dimensional R^α
nodes	4	1
gauge group	$U(N)^4$	$U(m)$, $m = 2N$
matter	12 bifundamentals, $a = J - \mathbb{1}_4$	3 adjoints Φ_1, Φ_2, Φ_3
F-terms	toric (path relations)	$\{\Phi_i, \Phi_j\} = 0$
algebra	invariant ring commutative	F-term algebra noncommutative
$\sum(\dim)^2$	$4 \cdot 1^2 = 4$	$1 \cdot 2^2 = 4$

Table VI.9.2: The $\mathbb{C}^3/(\mathbb{Z}_2 \times \mathbb{Z}_2)$ quiver without and with discrete torsion. The same geometry (VI.9.42) supports both. Turning on the class collapses the four-node doubled-K_4 theory to a single $U(m)$ with three adjoints, and replaces the toric F-terms by anticommutators. The squared dimensions sum to $|\Gamma| = 4$ either way. Here N counts bulk regular probes and $m = 2N$ is the projective multiplicity (VI.9.32): the torsioned node has twice the per-node rank of the untorsioned $U(N)^4$.

The Pauli representation and its multiplication. The two-dimensional projective irreducible is realized by the Pauli matrices: assign to the three nontrivial elements

$$\rho(g_1) = \sigma_x, \qquad \rho(g_2) = \sigma_y, \qquad \rho(g_3) = \sigma_z, \qquad \rho(e) = \mathbb{1}_2. \tag{VI.9.43}$$

That this is a genuine *projective* representation of $\mathbb{Z}_2 \times \mathbb{Z}_2$, and not an ordinary one, is the whole point, and it is worth verifying the multiplication law (VI.9.6) directly rather than quoting it. These Pauli lifts are gauge equivalent to $\rho(a, b) = S^b P^a$ at $n = 2$; in particular their cocycle values $\pm i$ need not equal the ± 1 values of (VI.9.10), while their commutator pairing agrees. The Pauli matrices square to the identity and multiply into one another with the Levi-Civita sign,

$$\sigma_a^2 = \mathbb{1}_2, \qquad \sigma_a \sigma_b \;=\; \delta_{ab}\, \mathbb{1}_2 + i\, \epsilon_{abc}\, \sigma_c. \tag{VI.9.44}$$

Take $g_1 g_2 = g_3$ in the group; the representatives multiply as $\rho(g_1)\rho(g_2) = \sigma_x \sigma_y = i\sigma_z = i\,\rho(g_3)$, so the cocycle value is $\alpha(g_1, g_2) = i$, while in the opposite order $\rho(g_2)\rho(g_1) =$

$\sigma_y\sigma_x = -i\sigma_z = -i\,\rho(g_3)$, so $\alpha(g_2, g_1) = -i$. The representatives are honest matrices but they do *not* compose like the group: their product carries the phase α. The commutator phase is the invariant,

$$\rho(g_i)\,\rho(g_j) \;=\; \beta(g_i, g_j)\,\rho(g_j)\,\rho(g_i), \qquad \beta(g_i, g_j) \;=\; \frac{\alpha(g_i, g_j)}{\alpha(g_j, g_i)} \;=\; -1 \quad (i \neq j), \tag{VI.9.45}$$

the value -1 demanded by (VI.9.15) for the nontrivial $\mathbb{Z}_2$ class, and realized here because distinct Pauli matrices anticommute, $\sigma_a\sigma_b = -\sigma_b\sigma_a$ for $a \neq b$. There is exactly one such irreducible, of dimension two, with $2^2 = 4 = |\Gamma|$, and no one-dimensional projective irreducible can exist because numbers commute and would force $\beta \equiv 1$.

The projective character table is short, and reading it against the ordinary one shows the collapse directly. The ordinary $\mathbb{Z}_2 \times \mathbb{Z}_2$ has four one-dimensional characters, each a row of signs; the maximally twisted algebra has the single two-dimensional projective character, which is traceless away from the identity because each of $\sigma_x, \sigma_y, \sigma_z$ has trace zero. Table VI.9.3 sets them side by side.

	e	g_1	g_2	g_3
ordinary χ_0	1	1	1	1
ordinary χ_1	1	1	-1	-1
ordinary χ_2	1	-1	1	-1
ordinary χ_3	1	-1	-1	1
projective χ^α	2	0	0	0

Table VI.9.3: Characters of $\mathbb{Z}_2 \times \mathbb{Z}_2$ without and with discrete torsion. The four ordinary one-dimensional characters (four nodes) are replaced by the single two-dimensional projective character (one node), which is supported only at the identity, the projective orthogonality (VI.9.19) reading $\frac{1}{4} \cdot 2^2 = 1$. The reader can verify the single nonzero entry $\chi^\alpha(e) = \operatorname{Tr} \mathbb{1}_2 = 2$ and that $\operatorname{Tr} \sigma_a = 0$ for each Pauli matrix gives the three zeros.

The anticommutator gauge theory. The regular projective brane is built on this single node, and the three transverse coordinates descend to three adjoint chiral fields Φ_1, Φ_2, Φ_3 realized along the Pauli directions. Substituting $q = \beta = -1$ into the F-terms (VI.9.39) gives the anticommutator equations

$$\{\Phi_i, \Phi_j\} \;=\; 0 \qquad (i \neq j), \tag{VI.9.46}$$

the gauge theory of a single $U(m)$ with three adjoints anticommuting pairwise rather than commuting. This is the noncommutative deformation promised in the introduction, and it is a genuinely different field theory from the commuting $\mathcal{N}$=4 parent.

The centre and the relation $u^2 = xyz$. The moduli space is read from the centre of the algebra generated by the Φ_i subject to (VI.9.46). With the Φ_i anticommuting, the gauge-invariant combinations that commute through everything are the squares

and the triple product,

$$x = \Phi_1^2, \qquad y = \Phi_2^2, \qquad z = \Phi_3^2, \qquad u = \Phi_1\Phi_2\Phi_3. \tag{VI.9.47}$$

That each of these is central is a short parity count, worth doing once. The square Φ_i^2 commutes with Φ_i trivially and with $\Phi_{j\neq i}$ by two sign flips, pushing Φ_j left through the two factors of Φ_i,

$$\Phi_i^2\,\Phi_j \;=\; \Phi_i\,(\Phi_i\Phi_j) \;=\; -\,\Phi_i\,\Phi_j\,\Phi_i \;=\; (-1)^2\,\Phi_j\,\Phi_i^2 \;=\; \Phi_j\,\Phi_i^2 \qquad (i\neq j), \tag{VI.9.48}$$

so x, y, z are central; and $u = \Phi_1\Phi_2\Phi_3$ commutes with each Φ_k because moving Φ_k through the three factors costs (-1) from each of the two factors $\Phi_{j\neq k}$ and nothing from the matching factor, an even number of sign flips. So all four generators of (VI.9.47) are central. They are not independent. Forming u^2 and sorting the second copy of $\Phi_1\Phi_2\Phi_3$ to the left past the first, using (VI.9.46),

$$u^2 \;=\; \Phi_1\Phi_2\Phi_3\,\Phi_1\Phi_2\Phi_3 \;=\; (-1)^3\,\Phi_1^2\Phi_2^2\Phi_3^2 \;=\; -\,x\,y\,z, \tag{VI.9.49}$$

the three sign flips being the three transpositions needed to march the second Φ_1 left past $\Phi_3\Phi_2$ and then sort the rest. The raw central relation is therefore $u^2 = -xyz$. On the Pauli realization this is immediate and pins the sign: $u = \sigma_x\sigma_y\sigma_z = i\,\mathbb{1}_2$, so $u^2 = -\mathbb{1}_2$ while $xyz = \mathbb{1}_2$, giving $u^2 = -xyz$ exactly. The minus sign follows from the chosen ordering of three anticommuting generators. Rescale the central coordinate $u \to iu$ to obtain the isomorphic hypersurface

$$u^2 \;=\; x\,y\,z, \tag{VI.9.50}$$

the standard hypersurface. Either sign cuts out the *same* variety up to the linear change $u \to iu$; (VI.9.50) is the form in which the geometry is recognizable. That hypersurface in $\mathbb{C}^4_{(x,y,z,u)}$ is exactly the ordinary commutative quotient $\mathbb{C}^3/(\mathbb{Z}_2\times\mathbb{Z}_2)$, whose coordinate ring is generated by the three $\mathbb{Z}_2\times\mathbb{Z}_2$-invariant squares z_a^2 and the invariant product $z_1z_2z_3$ with precisely the relation $(z_1z_2z_3)^2 = z_1^2z_2^2z_3^2$. To see that these four elements generate the whole centre, move every word into the ordered form $x^a y^b z^c \Phi_1^{e_1}\Phi_2^{e_2}\Phi_3^{e_3}$ with $e_i \in \{0,1\}$. Commuting such a word with each Φ_i forces the three parities to agree, so only $(e_1,e_2,e_3) = (0,0,0)$ and $(1,1,1)$ survive. Their coefficients are polynomials in x, y, z, giving precisely the two sectors $f(x,y,z) + u\,g(x,y,z)$ subject to $u^2 = -xyz$. This also proves that the displayed hypersurface is the full centre, rather than just a central subring. The torsion has changed the full open-string algebra while its commutative centre remains the quotient.

The geometry is the centre, not the whole algebra

For $\mathbb{C}^3/(\mathbb{Z}_2\times\mathbb{Z}_2)$ with torsion the worldvolume algebra of the Φ_i is noncommutative ($\{\Phi_i,\Phi_j\} = 0$). Its *centre* is the commutative ring generated by $x = \Phi_1^2$, $y = \Phi_2^2$, $z = \Phi_3^2$, $u = \Phi_1\Phi_2\Phi_3$ with the single relation $u^2 = xyz$ (up to an absorbable sign; the raw computation gives $u^2 = -xyz$), and that ring is the coordinate ring of the ordinary quotient $\mathbb{C}^3/(\mathbb{Z}_2\times\mathbb{Z}_2)$. The ordinary quotient geometry is therefore the centre of the open-string algebra, not the whole algebra. This is the precise sense in which discrete torsion makes the moduli problem noncommutative.

Three things one must not confuse. At this point a careful reader needs three phrases kept apart, because they are routinely run together and the moduli-space picture depends on the distinction. They are:

(i) *one projective irreducible block* R^{α}, the two-dimensional representation (VI.9.43) of the twisted group algebra. This is a property of $(\Gamma, [\alpha])$ alone, fixed once and for all, and is the analogue of "one node";

(ii) *one bulk brane*, a finite-dimensional representation of the noncommutative world-volume algebra generated by the Φ_i obeying (VI.9.46). This is a choice of where the brane sits, and as we are about to see the smallest such representation away from the singularity is again two-dimensional, but it is a representation of a *different* algebra (the F-term algebra, not the group algebra);

(iii) a *rank-m node* with $N = m/n$ regular bulk probes, whose projected quiver gauge space is $\mathbb{C}^m$ and whose original Chan–Paton space is $R^{\alpha} \otimes \mathbb{C}^m$. For N regular bulk probes, $m = nN$ by (VI.9.32); their generic F-term matrices decompose into N blocks of size n.

A "single projective fractional brane," a "regular projective brane," and a "single bulk probe" are therefore not interchangeable. The first is the fractional constituent that cannot leave the singularity; the regular projective module has dimension $|\Gamma| = n^2$ and consists of n simple projective constituents, each of dimension n; the bulk probe is a representation of the F-term algebra at a generic point. The next paragraph makes the bulk probe explicit and shows why "geometry is the centre" is a statement about finite-dimensional irreducibles.

A point of the geometry is a finite-dimensional irreducible. Take one regular bulk probe, which has $m = 2$ for this $n = 2$ torsion class, and ask what representation of the F-term algebra (VI.9.46) sits over a chosen point of the moduli space. Over a *smooth* point of the centre, where at least two of x, y, z are nonzero, the smallest representation of three anticommuting operators with prescribed squares is two-dimensional, and it is again given by the Pauli matrices rescaled,

$$\Phi_1 = x_1\,\sigma_x, \qquad \Phi_2 = x_2\,\sigma_y, \qquad \Phi_3 = x_3\,\sigma_z, \tag{VI.9.51}$$

up to scaling and signs. One checks at once that this realizes the anticommutators (VI.9.46), $\{\Phi_i, \Phi_j\} = x_i x_j \{\sigma_i, \sigma_j\} = 0$, and reads off the central coordinates as the squared scales,

$$x = \Phi_1^2 = x_1^2\,\mathbb{1}_2, \qquad y = \Phi_2^2 = x_2^2\,\mathbb{1}_2, \qquad z = \Phi_3^2 = x_3^2\,\mathbb{1}_2, \tag{VI.9.52}$$

with the triple product $u = \Phi_1\Phi_2\Phi_3 = i\,x_1x_2x_3\,\mathbb{1}_2$, so $u^2 = -x_1^2x_2^2x_3^2 = -xyz$, the raw relation again. The three numbers (x_1, x_2, x_3) lift the central point to $\mathbb{C}^3$, and their gauge-invariant squares $(x, y, z) = (x_1^2, x_2^2, x_3^2)$ together with $u \propto x_1x_2x_3$ are exactly the central coordinates that coordinatize the quotient. This is the concrete meaning of "geometry is the centre": a generic point of $\mathbb{C}^3/(\mathbb{Z}_2 \times \mathbb{Z}_2)$ at a smooth point selects a two-dimensional irreducible representation of the noncommutative F-term algebra,

labelled by the eigenvalues that the central elements take on it; the quotient invariant $z_a \mapsto z_a^2$ (and the sign identifications it implies) is built in because the Pauli realization (VI.9.51) only ever sees the squares. The Clifford flavour of (VI.9.51) is not an accident: three anticommuting operators are exactly the complex Clifford algebra at a fixed generic central character. Its two-dimensional irreducible is selected by the value of the central triple product u; the opposite sign of that product lies over the other point of the double cover of (x, y, z).

What happens at the singular centre. The Pauli block remains irreducible if one scale vanishes and the other two do not: two nonzero anticommuting Pauli matrices still generate $M_2(\mathbb{C})$. Reducibility first appears when at most one scale is nonzero. For example, if $x_1 \neq 0$ and $x_2 = x_3 = 0$, only $\Phi_1 = x_1\sigma_x$ remains; it diagonalizes into two one-dimensional F-term modules with opposite eigenvalues. The corresponding centre has $y = z = u = 0$, one of the three singular lines of $u^2 = -xyz$. At the origin all three fields vanish, and the same two-dimensional module decomposes into two copies of the one-dimensional zero-field module. These are statements about modules of the F-term algebra. The unique projective irreducible of the twisted group algebra remains two-dimensional throughout; it must not be identified with either one-dimensional F-term constituent. The three singular axes of the centre, where two of x, y, z vanish, reproduce the fixed-line structure of the quotient.

Counting, and the multi-brane branch. The dimension count confirms that the centre is the right three-dimensional space. The four generators x, y, z, u of (VI.9.47) satisfy the single relation (VI.9.50), so the centre is a hypersurface of complex dimension three in $\mathbb{C}^4$, matching the transverse $\mathbb{C}^3$ that a brane probes. The generic probe branch thus reconstructs $\mathbb{C}^3/(\mathbb{Z}_2 \times \mathbb{Z}_2)$ as before, and the torsion is invisible to the commutative moduli space alone, the entire imprint of $[\alpha]$ being in the noncommutativity of the open-string algebra over that space. For $m = 2N$ the projected gauge matrices admit N generic two-dimensional F-term blocks. The resulting bulk branch is expected to contain Sym^N of the centre; what the torsion changes is the algebra at each point of that branch, not its coarse geometry. (This chapter pins the single projective brane, the anticommuting algebra, its centre, and the bulk irreducible over a generic point; the multi-brane branch is the expected extension, not a separate check.)

VI.9.7 General $\mathbb{Z}_n \times \mathbb{Z}_n$: clock and shift

The Pauli realization (VI.9.43) is the $n = 2$ case of a uniform construction for every $\mathbb{Z}_n \times \mathbb{Z}_n$. The two generators of the maximally twisted algebra are realized by the clock and shift matrices P, S of size n,

$$P \;=\; \mathrm{diag}(1, \omega, \omega^2, \ldots, \omega^{n-1}), \qquad S \;=\; \sum_k |k+1\rangle\langle k|, \qquad \omega = e^{2\pi i/n}, \quad \text{(VI.9.53)}$$

the diagonal phase P and the cyclic shift S, indices read mod n. Acting on a basis vector $|k\rangle$, the two orders differ by one power of ω,

$$P\,S\,|k\rangle \;=\; \omega^{\,k+1}\,|k+1\rangle, \qquad S\,P\,|k\rangle \;=\; \omega^{\,k}\,|k+1\rangle, \qquad \text{(VI.9.54)}$$

so they obey the ω-commutation relation

$$P\,S \;=\; \omega\,S\,P, \tag{VI.9.55}$$

which is exactly the projective relation (VI.9.14) with commutator phase $\beta = \omega$ of order n. In the convention (VI.9.10), the explicit representatives are $\rho(a,b) = S^b P^a$: multiplying them gives $\rho(a,b)\rho(c,d) = \omega^{ad}\rho(a+c, b+d)$. The alternative ordering $P^a S^b$ is gauge equivalent but realizes a different cocycle representative. The pair (P, S) generates the full matrix algebra $M_n(\mathbb{C})$ of (VI.9.18), so it is the single n-dimensional projective irreducible, and the quiver of $\mathbb{Z}_n \times \mathbb{Z}_n$ with maximal torsion collapses to one node with three self-arrows just as in (VI.9.27). For $n = 2$ one may take $P = \sigma_z$ and $S = \sigma_x$, with $\omega = -1$, recovering the anticommuting Pauli pair of the previous section: $\sigma_z\sigma_x = -\sigma_x\sigma_z$ is (VI.9.55) at $\omega = -1$. By the impossibility of a one-dimensional projective irreducible established in §VI.9.3, the collapse to a single n-dimensional node is forced, not merely available.

The smallest nontrivial step up: $\mathbb{Z}_3 \times \mathbb{Z}_3$. It is worth writing the $n = 3$ representatives once, both to see that the Pauli case was not special and to have a non-Pauli instance in hand. With $\omega = e^{2\pi i/3}$,

$$P = \begin{pmatrix} 1 & 0 & 0 \\ 0 & \omega & 0 \\ 0 & 0 & \omega^2 \end{pmatrix}, \qquad S = \begin{pmatrix} 0 & 0 & 1 \\ 1 & 0 & 0 \\ 0 & 1 & 0 \end{pmatrix}, \qquad PS = \omega\,SP, \tag{VI.9.56}$$

a single three-dimensional irreducible, $3^2 = 9 = |\Gamma|$, so the nine ordinary one-dimensional nodes collapse to one three-dimensional node with three self-arrows by (VI.9.23). The reader can verify $\operatorname{Tr} P^a S^b = 3\,\delta_{a,0}\delta_{b,0}$ directly: S^b has no diagonal entry unless $b \equiv 0$, and for $b \equiv 0$ the trace is the geometric sum $\sum_k \omega^{ak} = 3\delta_{a,0}$. The projective character is again supported at the identity, the n-dimensional counterpart of Table VI.9.3, and the F-term cubic is now a genuine q-commutator with $q = \omega^{-1}$ a primitive cube root, not a sign: the three adjoints obey the cyclically oriented relations (VI.9.39) with $q = \omega^{-1}$ (the reverse order has q^{-1}), a noncommutative cubic algebra rather than the $\mathbb{Z}_2$ Clifford one.

When the pairing is degenerate. The collapse to a *single* node used the nondegeneracy of β: every nontrivial element pairs nontrivially with something, so the only α-regular class is the identity and there is one irreducible. This is the maximal class. For a non-maximal class, or for $\mathbb{Z}_m \times \mathbb{Z}_n$ with $m \neq n$, the pairing β can have a *radical*: a subgroup $\Gamma_0 \subset \Gamma$ of elements that pair trivially with all of Γ. On the radical the torsion is invisible, and the twisted group algebra is no longer a single full matrix algebra but a sum of blocks,

$$\mathbb{C}_\alpha[\Gamma] \;\cong\; \mathbb{C}[\Gamma_0] \otimes M_d(\mathbb{C}) \;\cong\; \bigoplus_{\chi \in \widehat{\Gamma_0}} M_d(\mathbb{C}), \qquad d^2 = |\Gamma/\Gamma_0| = \frac{|\Gamma|}{|\Gamma_0|}, \tag{VI.9.57}$$

one block for each character of the radical, each of dimension $d = \sqrt{|\Gamma|/|\Gamma_0|}$ fixed by the nondegenerate quotient Γ/Γ_0. The number of *nodes* of the projective quiver is the

number of these blocks, $|\Gamma_0|$, and the dimension of each projective irreducible is set by the nondegenerate quotient. The maximal $\mathbb{Z}_n \times \mathbb{Z}_n$ class is the extreme $\Gamma_0 = \{e\}$, one block of dimension n; the trivial class is the other extreme $\Gamma_0 = \Gamma$, $|\Gamma|$ blocks of dimension one, the ordinary quiver. The general class interpolates, with a partly collapsed quiver.

Discrete torsion does not always collapse to one node

The single-node collapse is the *maximal*, non-degenerate case. In general the commutator pairing β has a radical Γ_0 (the elements pairing trivially with everything), the twisted group algebra splits into one matrix block per character of Γ_0, and the projective quiver has $|\Gamma_0|$ nodes, each of dimension set by the nondegenerate quotient Γ/Γ_0. "Torsion collapses the quiver to one node" is true only when the class is non-degenerate (for instance the maximal class of $\mathbb{Z}_n \times \mathbb{Z}_n$). A degenerate class collapses it only partway.

We do not catalogue the general $\mathbb{Z}_n \times \mathbb{Z}_n$ quivers, the non-maximal (degenerate) classes, or the non-abelian Schur multipliers here; those are tabulated with the atlas and the toric machinery of Volume VI. The clock–shift pair is recorded as the universal generator of abelian discrete torsion, of which the Pauli example is the smallest instance.

VI.9.8 Charges, tadpoles, and projective traces

Two pieces of Chapter 5 and Chapter 7 calculation must be redone once the representations turn projective: the fractional-brane charges and the twisted-sector tadpoles. We treat them together, because both are read from the same projective characters, and both illustrate the chapter's discipline that a check imported verbatim from the untorsioned orbifold is wrong.

Projective labels of fractional branes. In the ordinary orbifold a fractional brane carried one ordinary irrep R_i, pinned to the singularity by a nonzero twisted charge, and $\mathbb{Z}_2 \times \mathbb{Z}_2$ had four of them, one per node, the four basis vectors of a rank-four charge lattice. With torsion the fractional branes carry the *projective* irreducibles R_i^α instead, and there are correspondingly fewer: the four ordinary representation labels are replaced by one projective representation label, of dimension two. The twisted regular module contains that label twice. This representation count does not by itself determine a physical charge lattice or prove that a projective node is pinned at the origin: the exceptional-cycle reading of Chapter 5, in which a fractional brane wrapped a vanishing cycle of a geometric resolution, need not survive, because with torsion the relevant choice is a class of the B-field rather than a homology cycle, and the charge classification is expected to require twisted K-theoretic data. We do not develop that classification; the derived-category and twisted-K-theory description of fractional branes is the subject of the later worldsheet volume, and the conclusion established here is the change of representation labels and regular-module multiplicity.

Projective tadpole traces. The consistency analysis of Chapter 7 must likewise be redone, not copied, because the calculation that fed it has changed. There the

twisted Ramond–Ramond tadpole of a configuration was the Chan–Paton trace $\operatorname{Tr}\gamma_g = \sum_i N_i\chi_i(g)$ weighted by the ordinary characters χ_i. With torsion the relevant characters are the *projective* ones, the traces of the projective representatives,

$$\operatorname{Tr}\gamma_g \;=\; \sum_i N_i\,\chi_i^{\alpha}(g), \qquad \chi_i^{\alpha}(g) \;=\; \operatorname{Tr}\rho_i^{\alpha}(g), \tag{VI.9.58}$$

and these are not the ordinary characters. For the maximally twisted $\mathbb{Z}_n \times \mathbb{Z}_n$ there is one projective irreducible, and its projective character is supported only at the identity,

$$\chi^{\alpha}(g) \;=\; \begin{cases} n, & g = e, \\ 0, & g \neq e, \end{cases} \tag{VI.9.59}$$

because the clock–shift representatives (VI.9.53) are traceless away from the identity: a nontrivial element is a monomial P^aS^b with $(a,b) \neq (0,0)$, and

$$\operatorname{Tr}\big(P^aS^b\big) \;=\; \begin{cases} \displaystyle\sum_{k=0}^{n-1}\omega^{\,ak} \;=\; n\,\delta_{a,0}, & b \equiv 0, \\ 0, & b \not\equiv 0, \end{cases} \tag{VI.9.60}$$

since S^b has no diagonal entry when $b \neq 0$ and the geometric sum of ω^{ak} vanishes for $a \neq 0$. For the maximal $\mathbb{Z}_2 \times \mathbb{Z}_2$ this is the Pauli realization (VI.9.43): a stack of m projective branes has $\gamma_e = \mathbb{1}_2 \otimes \mathbb{1}_m$ and $\gamma_{g_i} = \sigma_i \otimes \mathbb{1}_m$, so the Chan–Paton traces are

$$\operatorname{Tr}\gamma_e \;=\; 2m, \qquad \operatorname{Tr}\gamma_{g_i} \;=\; m\operatorname{Tr}\sigma_i \;=\; 0 \quad (i = 1,2,3), \tag{VI.9.61}$$

the tracelessness of the Pauli matrices doing for $\mathbb{Z}_2 \times \mathbb{Z}_2$ what (VI.9.60) does for the clock–shift: the projective Chan–Paton traces vanish for the three nonidentity elements. A physical twisted-sector coupling also depends on the worldsheet sector and its discrete-torsion projection; the trace alone does not determine a tadpole or anomaly. The untorsioned regular representation also has zero trace away from the identity, but it gets there by summing four different one-dimensional characters. The projective node instead has the character $(2,0,0,0)$. These per-node traces cannot be copied from the ordinary quiver; which physical twisted sectors couple requires the corresponding worldsheet projection.

The structural lessons of Chapter 7 carry over once the projective characters are in place, but their content is recomputed. The fully localized versus fixed-line distinction still sorts the twisted sectors by whether the group element fixes a complex line, and the regular projective module has zero nonidentity Chan–Paton traces by (VI.9.59). Which projected twisted states couple, and the resulting tadpole or anomaly conditions, require the corresponding worldsheet and spectrum calculation. The non-abelian anomaly, the abelian fates, and the localized-versus-fixed-line split must each be re-evaluated against the projective spectrum; the collapse of the quiver changes the rank data that enters them. The discipline is the one the box states.

Redo, do not copy: torsion changes the twisted-sector calculation

Discrete torsion changes which representations carry the Chan–Paton labels and therefore which characters weight the twisted-sector traces. The Chan–Paton part of a sector calculation uses $\sum_i N_i \chi_i^\alpha(g)$. The physical tadpole also needs the sector projection, and an anomaly needs the chiral spectrum and a count. Those conditions must be recomputed with the projective representations; the trace calculation here does not establish either one.

VI.9.9 What discrete torsion does and does not do

We have run the brane probe of Chapter 6 once more, with the single change that the Chan–Paton factors carry a discrete-torsion class $[\alpha] \in H^2(\Gamma, U(1))$. The geometry of the quotient is untouched and the defining representation $Q = \mathbf{3}$ stays honest; what changes is the multiplication law. Ordinary representations are replaced by projective ones, the McKay quiver runs in the projective category and collapses (four nodes to one for $\mathbb{Z}_2 \times \mathbb{Z}_2$, nine to one for $\mathbb{Z}_3 \times \mathbb{Z}_3$, a single n-dimensional node carrying three self-arrows in general), the superpotential turns commutators into q-commutators, and the worldvolume algebra becomes noncommutative with the ordinary quotient recovered only as its centre, $u^2 = xyz$ for the Pauli example. It is worth being blunt about what this is and is not, because every clause of it has a tempting wrong reading.

Common misconception: what discrete torsion is

Discrete torsion is *not* a Fayet–Iliopoulos parameter, *not* a blow-up mode, *not* a mere relabelling of arrows, and it does *not* resolve the singularity or preserve the ordinary representation category. It *is* a discrete class $[\alpha] \in H^2(\Gamma, U(1))$ in the orbifold conformal field theory. It does not vary continuously, does not deform the geometry, replaces honest representations by *projective* ones (a different category), modifies the superpotential by cocycle phases, and produces a *noncommutative* moduli algebra whose centre is the ordinary commutative quotient. The continuous Fayet–Iliopoulos / blow-up data and the discrete torsion class are distinct kinds of data. Their simultaneous availability depends on the closed-string spectrum.

Several things are deliberately not done. The classification of $H^2(\Gamma, U(1))$, the Schur multiplier and the theory of projective representations and twisted group algebras, is cited and used for the small cases, not proved; it belongs to the foundations volume. The twisted K-theory and derived-category description of fractional branes with torsion, and the precise torsion charge lattice, are stated qualitatively and routed to the later worldsheet volume; the exceptional-cycle reading of Chapter 5 is flagged as needing the torsion B-field, not retained verbatim. The full per-group torsion catalogues, the non-maximal classes, the non-abelian Schur multipliers, and the brane-tiling realizations are the atlas and Volume VI. The infrared dynamics of the noncommutative-moduli field theory is superconformal-dynamics data, routed to Part III. What remains here is the precise statement of the move: the same quotient, a different discrete string theory, a collapsed projective quiver, a phased superpotential, and a noncommutative algebra whose commutative centre is the geometry one already knew.

Status and sources

This section is for source tracking and internal consistency, not part of the first reading. The evidence-code tags ([WS] physical worldsheet or worldvolume evidence, [MATH] a mathematical theorem with stated hypotheses and proof status), the convention pointers, and the anchors are collected here, keyed by section. The chapter turns on a discrete-torsion class on the $\mathbb{C}^3/\Gamma$ ($\mathcal{N}$=1) probe of Chapter 6, after the discrete-torsion modular invariant of Vafa (1986) and the orbifold geometry of Vafa and Witten (1995), the projective Chan–Paton / clock–shift picture of Douglas (1998), the worked $\mathbb{C}^3/(\mathbb{Z}_2 \times \mathbb{Z}_2)$ quiver and $u^2 = xyz$ of Douglas and Fiol (2005), the noncommutative-algebra / geometry-as-centre reading of Berenstein and Leigh (2000), and the reconciliation of the cocycle conventions of Aspinwall (2000); the textbook treatment is Johnson (2003). It is parallel to Chapter 8 (the orientifold modification of the projection): a *different* mechanism, an H^2 phase rather than an Ω real structure, and the two are not merged. The chapter reuses the discrete-data / projective Chan–Paton master convention (resolution and discrete data, whose discrete-torsion half is activated here, orthogonal to its Fayet–Iliopoulos half), the McKay adjacency in the projective category, and the phased superpotential; the rank/gauge data is quiver gauge groups and ranks. No new convention is introduced. The finite calculations use the stated projective representations.

The sector phase is in Vafa and Witten (1995), §2, Eqs. (2.1)–(2.4); the projective lift and $\mathbb{Z}_2^2$ chiral matter are in Douglas (1998), §§2–3, Eqs. (2.3)–(2.4) and (3.1)–(3.6). The regular multiplicity, oriented cubic, invariant relation, and fixed-line branches are in Douglas and Fiol (2005), §3.1, Eq. (3.5) and following paragraph, §3.2, Eqs. (3.6)–(3.10), and §5.1, Eq. (5.1), respectively. The projective-simple and phased-cubic comparison is in Berenstein and Leigh (2000), §3, Eqs. (3.1)–(3.5). The cocycle and torus-phase conventions are compared with Aspinwall (2000), §1, Eqs. (6)–(9), and §2, Eqs. (11)–(14). These sources supply physical premises and located examples, not proofs of the general mathematical classifications listed below.

§VI.9.1 Discrete torsion as a choice of orbifold CFT. Framing: the place in Volume VI parallel to Chapter 8, the discrete-torsion class $[\alpha] \in H^2(\Gamma, U(1))$ (VI.9.1), the orientation table $H^2(\mathbb{Z}_m \times \mathbb{Z}_n) = \mathbb{Z}_{\gcd(m,n)}$ (VI.9.3) and the diagonal $\mathbb{Z}_n$ (VI.9.4) (Table VI.9.1, with $H^2(\mathbb{Z}_n) = 0$ so dP_0 has no variant), and the required distinction from Fayet–Iliopoulos / blow-up data. The cohomology table has no assigned evidence class pending a checked theorem source or proof; the discrete choice in the worldsheet orbifold is the physical [WS] (resolution and discrete data; Vafa (1986), Vafa and Witten (1995)). the representative pairing order and the cocycle identity.

§VI.9.2 Cocycles, coboundaries, and projective representations. The displayed local finite-group identities below are [MATH] under the stated abelian-group hypotheses and shown calculations; their use in an orbifold CFT retains the physical [WS] premise. The two-cocycle condition (VI.9.5), coboundary equivalence (VI.9.8), the bilinear representative (VI.9.10), the commutator pairing β (VI.9.12) with its explicit coboundary-invariance (VI.9.13) and order n, and the central-extension viewpoint (the discrete Heisenberg group; resolution and discrete data). The general classification of extensions retains unassigned evidence class pending a checked theorem source or proof. The group-cohomology / projective-representation / twisted-group-algebra mathematics is the new Schur multipliers and discrete torsion (the group cohomology $H^2(\Gamma, U(1))$, projective characters, and $\mathbb{C}_\alpha[\Gamma]$; home Vol. IV), cited not proved, extending the character theory of finite-group character theory. the Vafa–Witten cocycle satisfies (VI.9.5) exhaustively, β antisymmetric and of order n, a symmetric phase flagged as a coboundary.

§VI.9.3 Twisted group algebras and projective characters. The twisted group algebra $\mathbb{C}_\alpha[\Gamma]$ (VI.9.16), the squared-dimension sum (VI.9.17), the matrix-algebra collapse (VI.9.18), the impossibility of a one-dimensional projective irreducible, and the projective orthogonality (VI.9.19) collapsing to its $g = e$ term (VI.9.20). The displayed matrix-algebra example and one-dimensional obstruction are local [MATH] statements. The general semisimple dimension sum and projective orthogonality remain without assigned evidence class until their theorem sources or proofs are pinned in Schur multipliers and discrete torsion; the brane interpretation uses resolution and discrete data. In these finite examples, the relations are $\sum(\dim R^\alpha)^2 = |\Gamma|$, the single n-dimensional piece, and the twisted orthogonality $(1/|G|)\sum|\chi^\alpha|^2 = 1$. These examples do not prove the imported theorems.

§VI.9.4 The projective McKay quiver. The projective adjacency (VI.9.21) with Q honest, the collapses (VI.9.22)–(VI.9.23), the explicit tensor decomposition $Q \otimes R^\alpha = (\chi_1 \oplus \chi_2 \oplus \chi_3) \otimes R^\alpha = 3R^\alpha$

(VI.9.28)–(VI.9.31), and the single node with three self-arrows (VI.9.27) (Figure VI.9.1). [WS] (McKay multiplicities, resolution and discrete data; Douglas (1998)). The tensor decomposition and counts are [MATH] under the projective Chan–Paton premise; identifying the arrows as open-string fields is the [WS] step. the projective irreducibles ($\sum(\dim R^\alpha)^2 = |\Gamma|$, one n-dimensional piece), the projective McKay adjacency two ways, and $Q \otimes R^\alpha = 3R^\alpha$; a "three n-dimensional irreducibles" would violate the dimension formula ($3n^2 \neq n^2 = |\Gamma|$).

§VI.9.5 Torsion phases in W and q-commutator F-terms. The commutator parent (VI.9.33), the oriented torsion phase $q = \beta(g_2, g_3)^{-1}$ (VI.9.34), the F-terms by direct differentiation $\partial_{\Phi_1} W_q = \Phi_2\Phi_3 - q\Phi_3\Phi_2$ (VI.9.37)–(VI.9.38) yielding the oriented q-commutators (VI.9.39), and the commutator-versus-anticommutator contrast (VI.9.41)–(VI.9.40). (The faithful statement is the comm/anticomm split, derived from ∂W_q, not the $(1-q^2)$ single-relation reduction.) The projected cubic is the physical [WS] input (superpotential normalization, resolution and discrete data; Douglas and Fiol (2005), Eq. (3.5)–(3.7)); its cyclic derivatives are [MATH]. An explicit matrix calculation checks the inverse phase for the stated clock–shift orientation by reading the labelled q and W_q displays and comparing phase and cyclic derivatives. Reversing the generic-q relation would give a different $(1-q^2)$ reduction, which does not apply to the displayed F-terms. on the Pauli rep the $q = -1$ cubic is the anticommutator form and vanishes while the $q = +1$ commutator cubic does not, so the two give distinct cyclic derivatives.

§VI.9.6 Worked example: $\mathbb{C}^3/(\mathbb{Z}_2 \times \mathbb{Z}_2)$ with Pauli matrices. The ordinary-versus-torsion comparison (Table VI.9.2), the Pauli realization (VI.9.43) with its verified projective multiplication (VI.9.44)–(VI.9.45), the anticommutator F-terms (VI.9.46), the central generators (VI.9.47) with the parity proof of centrality (VI.9.48), the raw $u^2 = -xyz$ (VI.9.49) absorbable to $u^2 = xyz$ (VI.9.50), the three-things distinction (projective simple / bulk probe / node multiplicity), the Pauli point $\Phi_a = x_a\sigma_a$ (VI.9.51)–(VI.9.52) realizing a smooth central point with at least two nonzero scales as a 2-dimensional Clifford irreducible, and F-term-module reducibility on the singular axes; this does not classify physical fractional-brane charges. The centre and its raw sign are [MATH]; identifying the F-term algebra as the probe theory is the source-based [WS] (resolution and discrete data; Douglas and Fiol (2005), Berenstein and Leigh (2000)). This files (discrete torsion is not FI / not blow-up / not a relabelling; it does not resolve the singularity and does not preserve the ordinary representation category). $(\sigma_x, \sigma_y, 0)$ generates $M_2(\mathbb{C})$ at a smooth central point while $(\sigma_x, 0, 0)$ reduces on a singular axis; $\sigma_x\sigma_y\sigma_z = i\mathbb{1}$, $\{\sigma_i, \sigma_j\} = 0$, x, y, z, u central, raw $u^2 = -xyz$ and $(iu)^2 = +xyz$ exactly, where the anticommutation relations are essential.

§VI.9.7 General $\mathbb{Z}_n \times \mathbb{Z}_n$: clock and shift. The clock–shift pair (VI.9.53), $PS = \omega SP$ (VI.9.55), the single n-dimensional projective irreducible, $n = 2$ as the Pauli case, the explicit $\mathbb{Z}_3 \times \mathbb{Z}_3$ representatives (VI.9.56), and the degenerate-pairing (radical) case (VI.9.57) with $|\Gamma_0|$ nodes (the box: torsion does not always collapse to one node). The clock–shift algebra is [MATH]; the general radical classification retains unassigned evidence class pending a checked theorem source or proof. Its use as a projective Chan–Paton block has a [WS] source premise (resolution and discrete data; Douglas (1998)). $PS = \omega SP$ for $n = 2, 3$; the explicit representative S^bP^a realizes (VI.9.10), while P^aS^b has the same pairing but another cocycle; $n = 2$ reproduces the Pauli pair, and a one-dimensional projective representation is impossible because $\beta \equiv 1$ would follow. Full $\mathbb{Z}_n \times \mathbb{Z}_n$ catalogues, non-maximal classes, and non-abelian Schur multipliers → atlas / Vol. VI.

§VI.9.8 Charges, tadpoles, and projective traces. The representation labels change from four ordinary irreducibles to one projective irreducible for $\mathbb{Z}_2 \times \mathbb{Z}_2$; this does not establish the physical fractional-brane charge lattice. The charge interpretation is source-based (Douglas and Fiol (2005), Sec. 6); twisted-K-theory and derived-category classification remain at Vol. V.6, the surface derived McKay correspondence/the threefold derived McKay correspondence. The projective trace (VI.9.58) and identity-supported character (VI.9.59)–(VI.9.60) are [MATH] calculations under resolution and discrete data. The physical sector couplings, tadpole conditions, and anomaly count remain uncomputed here. χ^α is recomputed from the clock–shift matrices and differs per node from the honest one-dimensional character; the regular honest character also vanishes away from e.

§VI.9.9 What discrete torsion does and does not do. The summary, the misconception box, and what is deferred: the full H^2 classification (cited, Schur multipliers and discrete torsion), the twisted-K-theory fractional branes (Vol. V.6), the per-group catalogues (atlas / Vol. VII), and the noncommutative-moduli infrared (Part III). [WS], stated as the boundary.

References

Aspinwall, P. S. (2000). "A Note on the equivalence of Vafa's and Douglas's picture of discrete torsion". In: *JHEP* 12, p. 029. DOI: 10.1088/1126-6708/2000/12/029. arXiv: hep-th/0009045.

Berenstein, D. and R. G. Leigh (2000). "Discrete torsion, AdS / CFT and duality". In: *JHEP* 01, p. 038. DOI: 10.1088/1126-6708/2000/01/038. arXiv: hep-th/0001055.

Douglas, M. R. (1998). "D-branes and discrete torsion". In: arXiv: hep-th/9807235.

Douglas, M. R. and B. Fiol (2005). "D-branes and discrete torsion. 2." In: *JHEP* 09, p. 053. DOI: 10.1088/1126-6708/2005/09/053. arXiv: hep-th/9903031.

Johnson, C. V. (2003). *D-Branes*. Cambridge Monographs on Mathematical Physics. Cambridge University Press. DOI: 10.1017/CBO9780511606540.

Vafa, C. (1986). "Modular Invariance and Discrete Torsion on Orbifolds". In: *Nucl. Phys. B* 273, pp. 592–606. DOI: 10.1016/0550-3213(86)90379-2.

Vafa, C. and E. Witten (1995). "On orbifolds with discrete torsion". In: *J. Geom. Phys.* 15, pp. 189–214. DOI: 10.1016/0393-0440(94)00048-9. arXiv: hep-th/9409188.

Chapter VI.10

Large-N inheritance from $\mathcal{N}$=4 SYM

VI.10.1 Orbifold daughters of $\mathcal{N}$=4: statement and scope

The quivers built in this volume retain only fields invariant under a finite group Γ. At regular D3-brane ranks, the same projection acts directly on $\mathcal{N}$=4 super Yang–Mills. It gives a comparison between daughter ribbon diagrams and diagrams of a parent with a known planar expansion. The comparison concerns connected, properly normalized neutral single-trace observables at matched couplings. It does not determine every operator or vacuum.

The rank vector and action normalization come first. We then follow group labels through ribbon diagrams and work out the degree count and leading gauge beta coefficient for three quivers. A sphere diagram admits the planar comparison; a handle can carry group holonomy that obstructs the same simple comparison. The diagrammatic result is perturbative. Its extension to nonperturbative large-N equivalence requires the relevant projection and daughter symmetries to remain unbroken.

Take-home message of this chapter

An orbifold quiver gauge theory is a daughter of $\mathcal{N}$=4 $U(K)$ theory with $K = N|\Gamma|$. At regular ranks $N_i = N \dim R_i$ and matched couplings, corresponding connected planar diagrams of neutral single-trace operators agree after the operator normalization below. Handles give relative $O(1/N^2)$ terms in the normalized connected expansion. A statement about the full large-N vacuum also needs unbroken projection symmetries.

The road is short to state. We compute three things and learn how they fit. These are the projected action and its matched 't Hooft coupling (§VI.10.2–VI.10.2); the double-line argument that the daughter's planar neutral diagrams are the parent's (§VI.10.3–VI.10.3); and the consequences, the $1/|\Gamma|$ degree count and the vanishing one-loop gauge coefficient (§VI.10.4–VI.10.4), tested on dP_0, $\mathbb{C}^3/(\mathbb{Z}_2 \times \mathbb{Z}_2)$, and $\Delta(27)$

(§VI.10.5–VI.10.6). The geometry of the same parentage, the holographic bridge, and the honest gap close the volume (§VI.10.7–VI.10.7).

VI.10.2 Projection and coupling matching

The construction is Chapter 6's; we recall only what the inheritance argument needs, in the field-theory language that the rest of the chapter speaks. Place K D3-branes in flat space and take the decoupling limit. The worldvolume theory is $\mathcal{N}$=4 super Yang–Mills with gauge group $U(K)$. In $\mathcal{N}$=1 language its matter is three adjoint chiral multiplets Φ^1, Φ^2, Φ^3, rotated into one another by an $SU(3) \subset SU(4)_R$ flavour symmetry, with the cubic superpotential

$$W_{\text{parent}} \;=\; \sqrt{2}\, g_p \;\operatorname{Tr} \Phi^1[\Phi^2, \Phi^3] \;=\; \tfrac{\sqrt{2} g_p}{3}\, \varepsilon_{abc} \operatorname{Tr}\big(\Phi^a \Phi^b \Phi^c\big), \tag{VI.10.1}$$

in canonical chiral-field normalization. The kinetic action below uses fields with the coupling extracted; a field rescaling relates the two conventions. The two cubic forms agree because $\varepsilon_{abc} \operatorname{Tr}(\Phi^a \Phi^b \Phi^c) = 3 \operatorname{Tr} \Phi^1[\Phi^2, \Phi^3]$ by the cyclicity of the trace. This is the most symmetric four-dimensional gauge theory, exactly conformal, with a known planar expansion.

Now orbifold. Let $\Gamma \subset SU(3)$ act on the three transverse complex planes through the defining representation Q, and embed Γ in the gauge group by the Chan–Paton representation γ_g. The orbifold projection keeps the fields invariant under the combined action of Γ on the spacetime (flavour) index and on the Chan–Paton indices. Concretely, a field Φ transforming in a representation $\rho_{\text{flavour}}(g)$ of the $SU(3)$ flavour and as $\gamma_g \Phi \gamma_g^{-1}$ on the matrix indices survives if and only if

$$\Phi \;=\; \rho_{\text{flavour}}(g)\, \gamma_g\, \Phi\, \gamma_g^{-1} \qquad \text{for all } g \in \Gamma. \tag{VI.10.2}$$

The gauge field is a flavour singlet, $\rho_{\text{flavour}} = 1$, so it survives where $A_\mu = \gamma_g A_\mu \gamma_g^{-1}$, the commutant of Γ. The three Φ^a are the flavour $\mathbf{3} = Q$, so they survive where $\Phi^a = Q(g)^a{}_b\, \gamma_g \Phi^b \gamma_g^{-1}$, the McKay condition. For the regular embedding the Chan–Paton space decomposes as

$$\begin{aligned} V \;&=\; \bigoplus_i \mathbb{C}^{N_i} \otimes R_i, \qquad N_i = N \dim R_i, \\ K \;&=\; \sum_i N_i \dim R_i \;=\; N \sum_i (\dim R_i)^2 \;=\; N|\Gamma|, \end{aligned} \tag{VI.10.3}$$

where R_i runs over the irreducibles of Γ and the last equality is the order formula

$$|\Gamma| \;=\; \sum_i (\dim R_i)^2. \tag{VI.10.4}$$

To see the order formula directly, the character of the regular action on $\mathbb{C}[\Gamma]$ is m at the identity and zero elsewhere. Its inner product with χ_i is therefore d_i. The regular representation contains d_i copies of R_i, and its dimension is $\sum_i d_i^2 = m$. Solving

(VI.10.2) on this decomposition gives the surviving gauge group as the commutant of Γ in $U(K)$,

$$G \;=\; \prod_i U(N_i) \;=\; \prod_i U(N \dim R_i), \tag{VI.10.5}$$

one unitary factor per node, and the surviving matter from projecting the three adjoints. An adjoint of $U(K)$ is $V \otimes V^*$, which decomposes under Γ as $\bigoplus_{i,j} (\mathbb{C}^{N_i} \otimes \mathbb{C}^{N_j\,*}) \otimes (R_i \otimes R_j^*)$; tensoring in the flavour Q and keeping the trivial Γ-summand leaves a chiral bifundamental for each McKay arrow, with multiplicity

$$Q \otimes R_i \;=\; \bigoplus_j a_{ij}\, R_j, \qquad a_{ij} \;=\; \dim \mathrm{Hom}_\Gamma\big(R_j,\, Q \otimes R_i\big), \tag{VI.10.6}$$

the McKay adjacency of Chapter 6. The arrow $i \to j$ carries $X_{ij} \in (\Box_i, \overline{\Box}_j)$, fundamental of $U(N_i)$ and antifundamental of $U(N_j)$. The daughter is therefore exactly the quiver we have been drawing all along, with gauge group (VI.10.5), a chiral bifundamental for each arrow, and (as §VI.10.5 derives) a cubic superpotential descended from (VI.10.1). The new content of the chapter is the *reading*. The same quiver is the orbifold daughter of a known parent, and the rest of the chapter exploits that parentage diagram by diagram.

Matching the coupling

Inheritance is a statement about diagrams that carry the same weight in the parent and the daughter, and weight in a large-N expansion is fixed by the action. Before the diagrammatics we must say which daughter action the projection produces and how its coupling relates to the parent's, because the orbifold-equivalence literature is sensitive to exactly this point. A careless identification $g_i = g$ can hide factors of $|\Gamma|$. We derive the matching from the action rather than assert it.

Write the parent gauge kinetic term with its coupling out front,

$$S_{\text{parent}} \;=\; \frac{1}{g_p^2} \int d^4x \;\; \mathrm{Tr}_K\big(F_{\mu\nu} F^{\mu\nu}\big) + \cdots\,, \tag{VI.10.7}$$

the trace running over the full $K \times K$ Chan–Paton space and the dots standing for the matter and Yukawa terms that descend the same way. The orbifold projection sets the off-commutant components of F to zero and block-diagonalizes the survivor. Under (VI.10.5) the field strength splits into one block F_i per node,

$$\mathrm{Tr}_K\big(F^2\big) \;\longrightarrow\; \sum_i (\dim R_i)\, \mathrm{Tr}_{N_i}\big(F_i^2\big), \tag{VI.10.8}$$

because the full trace over $V = \bigoplus_i \mathbb{C}^{N_i} \otimes R_i$ restricts, on a gauge field that acts only on the $\mathbb{C}^{N_i}$ multiplicity factors and as the identity on R_i, to $\sum_i (\dim R_i)\, \mathrm{Tr}_{N_i}(F_i^2)$, the $\dim R_i$ counting the identical R_i-copies of each block. Put $m = |\Gamma|$ and $d_i = \dim R_i$. There are two distinct actions. The bare restriction $S_{\text{bare}} = S_{\text{parent}}|_{\text{inv}}$ has $g^2_{i,\text{bare}} =$

g_p^2/d_i, hence $g_{i,\text{bare}}^2 N_i = \lambda/m$. To compare with the original parent at $\lambda = g_p^2 K$, divide the entire restricted action by m,

$$S_{\text{daughter}} = \frac{1}{m} S_{\text{parent}}|_{\text{inv}} = \sum_i \frac{d_i}{m g_p^2} \int d^4x \ \text{Tr}_{N_i}(F_i^2) + \cdots . \tag{VI.10.9}$$

This changes the physical coupling. The same factor multiplies the matter and interaction terms in the convention with the coupling extracted. Keeping fundamental traces at every node gives

$$\frac{1}{g_i^2} = \frac{d_i}{m g_p^2}, \qquad g_i^2 = \frac{m g_p^2}{d_i}. \tag{VI.10.10}$$

The node 't Hooft coupling is

$$\lambda_i = g_i^2 N_i, \tag{VI.10.11}$$

and the regular ranks give

$$\lambda_i = \frac{m g_p^2}{d_i}(N d_i) = m g_p^2 N. \tag{VI.10.12}$$

Thus the expansion parameter agrees with the parent's at every node,

$$\lambda_i = \lambda = g_p^2 K, \qquad K = mN. \tag{VI.10.13}$$

For $\mathbb{Z}_3$ this means $g_i^2 = 3g_p^2$; for $\mathbb{Z}_2 \times \mathbb{Z}_2$, $g_i^2 = 4g_p^2$. For $\Delta(27)$ the singlet nodes have $g_i^2 = 27 g_p^2$ and the triplet nodes have $g_i^2 = 9g_p^2$, while both have $\lambda_i = 27 N g_p^2$. A change of trace convention cannot turn the bare restriction into this matched theory without changing the complete action coefficient.

Matching the daughter couplings

The comparison in this chapter uses $S_D = S_P|_{\text{inv}}/m$, $g_i^2 = m g_p^2/d_i$, and $\lambda_i = \lambda_P$. The bare restriction $S_P|_{\text{inv}}$ instead has $\lambda_i = \lambda_P/m$. For an abelian daughter, the first gauge contraction in a normalized neutral Wilson loop has weight $g_i^2 N$; the parent's is $g_p^2 mN$. Their ratio is 1 for the matched action and $1/m$ for the bare restriction. At fixed $m > 1$ and fixed λ_P, the latter discrepancy persists as $N \to \infty$. It disappears only in the trivial projection $m = 1$.

The regular ranks are not an optional decoration. The cancellations that make inheritance work, and the one-loop fixed-point condition of §VI.10.4, both rely on the regular relation $N_i = N \dim R_i$ and on the representation identities of Chapter 6 that it activates. A general (fractional) rank assignment is a different theory, possibly anomalous (Chapter 7) and certainly not in the regular-brane inheritance class; we return to that point when we state what inheritance does not do.

VI.10.3 Planar inheritance and the neutral sector

The central statement is combinatorial, and the right language for it is 't Hooft's double-line (ribbon) notation. In a $U(K)$ theory every adjoint field carries a pair of

indices, one fundamental and one antifundamental, so its propagator is drawn as two oriented lines running in opposite directions. A connected vacuum diagram is then a ribbon graph. Gluing the lines at the vertices turns it into a closed oriented surface, and the powers of K and the coupling are read off from that surface. Writing V for the number of vertices, E for propagators, and F for closed index loops (faces), a connected ribbon diagram of the parent carries the weight

$$g_p^{2(E-V)}\, K^{F} \;=\; \lambda^{E-V}\, K^{V-E+F} \;=\; \lambda^{E-V}\, K^{2-2h}, \tag{VI.10.14}$$

where each vertex brings a factor g_p^{-2}, each propagator a g_p^2, each index loop a factor K from the free sum over the index circulating in it, and the Euler relation $V - E + F = 2 - 2h$ identifies h as the number of handles of the surface. Planar diagrams ($h = 0$) scale as K^2; each handle costs $1/K^2$. This is the parent's genus expansion.

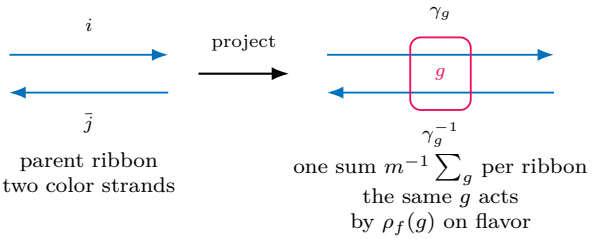


Figure VI.10.1: One projector acts on the whole propagator. The two color strands carry γ_g and γ_g^{-1}, and its flavor carries $\rho_f(g)$, all with the same group element. Independent strand averages would remove allowed diagonal blocks of a $\mathbb{Z}_3$ gauge field. The matched action supplies an additional factor m to each projected propagator and $1/m$ to each interaction vertex.

The projector acts on an entire matrix field, including its flavor index,

$$(P\Phi)^{a}{}_{i}{}^{j} = \frac{1}{m}\sum_{g\in\Gamma} \rho_f(g)^{a}{}_{b}(\gamma_g)_{i}{}^{k}\Phi^{b}{}_{k}{}^{\ell}(\gamma_g^{-1})_{\ell}{}^{j}. \tag{VI.10.15}$$

There is one group variable per propagator. Interaction vertices are already invariant under the simultaneous color and flavor action. For a gauge field in the $\mathbb{Z}_3$ example, the block (r, s) receives $3^{-1}\sum_{t=0}^{2}\omega^{t(r-s)} = \delta_{rs}$, retaining all three diagonal blocks. Averaging the two strands independently would instead give $\delta_{r0}\delta_{s0}$ and discard two gauge factors.

Around a closed color face the edge matrices multiply in their oriented order. For the regular embedding their trace is

$$\mathrm{Tr}_V\, \gamma_H = K\delta_{H,e}, \qquad H = \overrightarrow{\prod_{e\in\partial f}} g_e^{\sigma_{fe}}, \quad \sigma_{fe} = \pm 1. \tag{VI.10.16}$$

Thus the nonzero terms have identity holonomy around every face. The elementary regular-character average is

$$\frac{1}{m}\sum_{g} \mathrm{Tr}_V\, \gamma_g = N, \qquad \mathrm{Tr}_V\, \gamma_g = mN\delta_{g,e}. \tag{VI.10.17}$$

The face constraints couple adjacent edge variables. Counting them together is the step that fixes the coupling comparison.

Consider the planar theta graph, two cubic vertices joined by three edges with the sphere cyclic ordering. It has $V = 2$, $E = 3$, $F = 3$. Orient the edges from the first vertex to the second. The face holonomies can be taken as $g_1 g_2^{-1}$, $g_2 g_3^{-1}$, and $g_3 g_1^{-1}$. All three traces are nonzero exactly when $g_1 = g_2 = g_3$. There are m allowed edge assignments, for an arbitrary finite group, and the three projectors contribute m^{-3}. At the bare restricted coupling the group factor relative to the parent is consequently

$$\frac{1}{m^3} \sum_{g_1,g_2,g_3} \delta_{g_1 g_2^{-1},e} \delta_{g_2 g_3^{-1},e} \delta_{g_3 g_1^{-1},e} = \frac{1}{m^2}. \tag{VI.10.18}$$

For gauge edges the flavor factor is unity. For matter edges the same flat assignment can be removed at the vertices by the flavor symmetry of the parent interaction. The matched propagators multiply this result by m^3 and the two vertices by m^{-2}, leaving $1/m$. The parent graph weighs $g_p^2 K^3 = \lambda K^2$, so the daughter weighs $\lambda K^2/m$. The ratio is precisely the ratio of gauge degrees of freedom.

The general sphere count follows by fixing a reference vertex and transporting labels to the other $V - 1$ vertices along a spanning tree. Every flat edge assignment has the form $g_{uv} = h_u^{-1} h_v$. The m^V vertex assignments have one common left multiplication redundancy, leaving m^{V-1} distinct flat connections. Hence the projector sum contributes m^{V-1-E}. Euler's relation gives $V - E + F = 2$, so this is also m^{1-F}. The matched action multiplies it by m^{E-V},

$$\frac{A_{D,\mathrm{bare}}}{A_P} = m^{V-1-E}, \qquad \frac{A_D}{A_P} = m^{V-1-E} m^{E-V} = \frac{1}{m}. \tag{VI.10.19}$$

For an abelian gauge graph this can also be read directly as $mN^F/(mN)^F = m^{1-F}$ before coupling matching. After removing the degree ratio $1/m$, the bare answer retains $m^{-(E-V)}$. It changes with perturbative order and cannot be repaired by a fixed operator factor. At fixed $m > 1$ it stays different in the large-N limit. On a handle, flat connections can retain noncontractible holonomies; the sphere reduction then no longer determines the coefficient.

Now mark k vertices as neutral trace insertions, and write V for the remaining interaction vertices. There are m^{V+k-1} flat assignments, but only the V interaction vertices carry action factors. For the same normalization $K^{-1}\,\mathrm{Tr}$ on both sides, the ratio of the connected planar correlators is therefore m^{k-1}, since $m^{V+k-1-E} m^{E-V} = m^{k-1}$. For abelian Γ, the daughter trace is $O_D = m^{-1} \sum_i N^{-1}\,\mathrm{Tr}_N(\mathrm{loop}_i)$. The coefficient comparison is explicitly

$$\begin{gathered} \mathcal{C}_{k,P} = (K^2)^{k-1} \langle O_P \cdots O_P \rangle_{\mathrm{conn}}, \qquad \mathcal{C}_{k,D} = (K^2/m)^{k-1} \langle O_D \cdots O_D \rangle_{\mathrm{conn}}, \\ \mathcal{C}_{k,D}^{(h=0)} = \mathcal{C}_{k,P}^{(h=0)}, \qquad \mathcal{C}_{k,D} = \mathcal{C}_{k,P} + O(N^{-2}). \end{gathered} \tag{VI.10.20}$$

For $k = 1$ the normalized expectation values already match; for $k = 2$ the daughter's raw connected correlator is m times the parent's. For nonabelian groups the same perturbative count uses the weighted restricted trace below. It does not assert a nonperturbative nonabelian equivalence. These statements hold order by order at fixed

finite m, fixed k and fixed λ in the symmetric perturbative vacuum. Neutral insertions allow the vertex flavor transformations used above. Charged insertions, independent double-trace interactions and symmetry-breaking vacua require a different argument.



planar ($h = 0$)
contractible face constraints

nonplanar (h=1)
noncontractible holonomy

Figure VI.10.2: Topology in the double-line expansion. On the sphere the projector constraints reduce to contractible face conditions, allowing planar neutral matching. A handle admits noncontractible group holonomies. The usual oriented ribbon-graph weight suppresses genus one by N^{-2} at fixed Γ; topology alone does not determine its coefficient.

The genus estimate in (VI.10.14) supplies the power of the first possible oriented correction. It does not compute that correction. For a connected graph with trace insertions, the corresponding boundary factors must be removed before comparing coefficients; this is the normalization built into $\mathcal{C}_k$ in (VI.10.20). The next question is which insertions are neutral.

Neutral versus twisted operators

Inheritance is selective. It applies to the neutral sector, and the selection rule is the orbifold *quantum symmetry*. We treat the abelian case first, where it is a group of phases, then say carefully what replaces it for non-abelian Γ.

Abelian Γ. For an abelian $\mathbb{Z}_n$ daughter the irreducibles are the n characters and the nodes are labelled by $i \in \mathbb{Z}_n$. The quantum symmetry is the dual group $\widehat{\mathbb{Z}_n} \cong \mathbb{Z}_n$, generated by the cyclic shift of nodes $i \mapsto i+1$. A gauge-invariant single-trace operator built at node i, say a product of bifundamentals closing into a loop at i, can be combined across nodes in two ways. The *neutral* (untwisted) combination is the uniform sum

$$O_{\text{neutral}} \;=\; \sum_i \operatorname{Tr}\bigl(\text{loop}_i\bigr), \tag{VI.10.21}$$

invariant under $i \mapsto i+1$. The *twisted* combinations carry a nontrivial dual phase,

$$O_{\text{tw},\,q} \;=\; \sum_i \omega^{\,qi}\, \operatorname{Tr}\bigl(\text{loop}_i\bigr), \qquad \omega = e^{2\pi i/n}, \quad q = 1, \dots, n-1. \tag{VI.10.22}$$

Acting with the generator $g : i \mapsto i+1$ of the quantum $\mathbb{Z}_n$ multiplies each by a definite phase,

$$g \cdot O_{\text{neutral}} \;=\; O_{\text{neutral}}, \qquad g \cdot O_{\text{tw},\,q} \;=\; \omega^{-q}\, O_{\text{tw},\,q}, \tag{VI.10.23}$$

so O_{neutral} has quantum charge 0 and $O_{\text{tw},\,q}$ has charge q. (The reader can check (VI.10.23) directly. Shifting $i \to i+1$ inside (VI.10.22) relabels the sum and pulls out ω^{-q}.) Inheritance is the charge-zero statement. The neutral operators (VI.10.21) are exactly the ones whose face phases cancel in (VI.10.16), and they descend from the parent single traces $\mathrm{Tr}(\Phi^a \cdots)$; equation (VI.10.20) applies cleanly to them. The twisted operators (VI.10.22) have no parent single-trace ancestor of the same form. Their face phases do *not* cancel, the g-sums in (VI.10.16) no longer collapse to $g = e$, and their correlators are a separate problem. They are precisely the operators that distinguish the daughter from the parent, the field-theory image of the orbifold's twisted sectors.

Operator normalization

The statement "the daughter correlator equals the projected parent correlator" (VI.10.20) is normalization-sensitive, so we fix the convention once. Neutral daughter operators are restrictions of the normalized parent trace,

$$O_D \;=\; \frac{1}{|\Gamma|}\sum_i O_i, \tag{VI.10.24}$$

where $O_i = N^{-1}\,\mathrm{Tr}_{N_i}(\mathrm{loop}_i)$ uses the same rank unit N at every node. It follows from the normalized parent trace $K^{-1}\,\mathrm{Tr}_K$ for a projected parent word. Equation (VI.10.24) is the abelian, unit-dimension form; for non-abelian Γ the node sum carries the $\dim R_i$ weights of (VI.10.26) (made explicit for $\Delta(27)$ in (VI.10.52)). For connected correlators, the leading large-N power is also removed as in $\mathcal{C}_k$. The connected factors in (VI.10.20) are part of the comparison, in addition to these single-operator normalizations.

Non-abelian Γ. Here the simple "replace phases by characters" shortcut is too quick, and we state the correct structure. For a non-abelian Γ there is in general *no* ordinary dual group of one-dimensional characters indexing the operators; the quantum symmetry is not $\mathbb{Z}_n$ and the twisted sectors are not labelled by a phase ω^{qi}. What survives is the decomposition of the group algebra $\mathbb{C}[\Gamma]$, and it is cleanest stated through its central idempotents. The center of $\mathbb{C}[\Gamma]$ is spanned by the projectors onto the isotypic components,

$$e_i \;=\; \frac{\dim R_i}{|\Gamma|}\sum_{g\in\Gamma}\overline{\chi_i(g)}\,g, \qquad e_i e_j = \delta_{ij}\,e_i, \qquad \sum_i e_i = 1, \tag{VI.10.25}$$

The coefficients are class functions, so e_i is central. By Schur's lemma it acts as a scalar on each R_j. Taking that trace and using character orthogonality gives $\mathrm{Tr}_{R_j} e_i = d_i\delta_{ij}$, so the scalar is δ_{ij}. This proves orthogonality and completeness on every irreducible and hence on the faithful regular representation. The neutral combination is always the one weighted by the parent-trace weights, namely the node sum weighted by $\dim R_i$,

$$O_{\text{neutral}} \;=\; \sum_i \dim R_i\;\mathrm{Tr}\big(\mathrm{loop}_i\big), \tag{VI.10.26}$$

which follows by restricting a parent trace on $V = \bigoplus_i \mathbb{C}^{N_i}\otimes R_i$. It is the identity-sector combination because the regular character annihilates nonidentity group elements. The

e_i in (VI.10.25) instead project onto irreducible representation blocks. Their Fourier transform relates representation labels to conjugacy-class sums, but an individual nontrivial e_i is not itself a twisted sector. Closed-string twisted sectors for a non-abelian orbifold are indexed by nonidentity conjugacy classes, with centralizer conditions on states. This distinction matters when the gauge-theory operator basis is related to the closed-string sector basis.

Warning: "quantum symmetry" is not always a dual group

For an abelian $\mathbb{Z}_n$ orbifold the node-shift symmetry gives characters ω^{qi}. For non-abelian Γ, ordinary one-dimensional characters do not furnish a dual group labelling every twisted sector. The central idempotents (VI.10.25) are an irreducible-block basis of the group-algebra center, while twisted closed-string sectors are organized by conjugacy classes. The neutral trace (VI.10.26) is the identity-sector combination used here.

VI.10.4 Two consequences, the degree count and the vanishing one-loop gauge coefficient

The projected gauge and chiral-field component counts are each $1/|\Gamma|$ of the parent counts at regular ranks. We verify both halves, gauge and matter. The parent has K^2 gauge generators and, with its three adjoints, $3K^2$ matter components. At the regular ranks the daughter gauge count is

$$\sum_i N_i^2 \;=\; \sum_i (N \dim R_i)^2 \;=\; N^2 \sum_i (\dim R_i)^2 \;=\; N^2|\Gamma|, \tag{VI.10.27}$$

using the order formula (VI.10.4), and the rank-weighted matter count is

$$\sum_{i,j} a_{ij}\, N_i N_j \;=\; N^2 \sum_i \dim R_i \sum_j a_{ij} \dim R_j \;=\; N^2 \sum_i \dim R_i \,(3 \dim R_i) \;=\; 3N^2|\Gamma|, \tag{VI.10.28}$$

where the regular-rank McKay identity $\sum_j a_{ij} \dim R_j = 3 \dim R_i$ of Chapter 6 collapses the inner sum. Writing both as fractions of the parent counts $K^2 = N^2|\Gamma|^2$,

$$\sum_i N_i^2 \;=\; \frac{K^2}{|\Gamma|}, \qquad \sum_{i,j} a_{ij}\, N_i N_j \;=\; \frac{3K^2}{|\Gamma|}, \tag{VI.10.29}$$

the daughter gauge and matter degrees of freedom are each exactly $1/|\Gamma|$ of the parent's. These counts are necessary checks on the projection. They do not by themselves establish equality of planar amplitudes; that comparison also uses the action and group constraints above. One consequence will reappear at the holographic bridge: a daughter free-energy density (or central charge) of order $\sum_i N_i^2 = N^2|\Gamma| = K^2/|\Gamma|$, the parent's K^2 divided by $|\Gamma|$.

One-loop beta functions at regular ranks

Inheritance has an immediate dynamical corollary: the coefficient of the one-loop non-abelian gauge beta function vanishes at regular ranks. For an $\mathcal{N}$=1 gauge factor $U(N_i)$

with chiral matter, the one-loop beta-function coefficient is the gauge contribution minus the matter contribution. Throughout, b_i is the coefficient of the interacting non-abelian $SU(N_i)$ factor; the fate of the abelian $U(1) \subset U(N_i)$ pieces (anomalous, massive, or decoupled) is the subject of Chapter 7 and is not part of the planar-inheritance statement. With the bifundamentals counted by the adjacency, the coefficient at node i is

$$b_i \;=\; 3\,N_i \;-\; \tfrac{1}{2}\sum_j \big(a_{ij} + a_{ji}\big)\,N_j, \tag{VI.10.30}$$

the factor 3 from $3T(\mathrm{adj}) = 3N_i$ of the $U(N_i)$ vector multiplet, and the factor $\frac{1}{2}$ from the index $T(\mathrm{fund}) = \frac{1}{2}$ of each chiral bifundamental, summed over the arrows in and out of node i. The symmetrized adjacency $a + a^{\mathsf{T}}$ appears because both orientations of an arrow contribute matter charged under $U(N_i)$: an outgoing arrow $i \to j$ gives $a_{ij}N_j$ fundamentals and an incoming arrow $j \to i$ gives $a_{ji}N_j$ antifundamentals, each with index $\frac{1}{2}$. (The factor $\frac{1}{2}$ is the index normalization that makes $b_i = 3N_i - \sum_{\text{chirals}} T_r N_r$ with $T_{\text{fund}} = \frac{1}{2}$. The reader can confirm it reproduces the familiar $b = 3N - N_f$ for $SU(N)$ with N_f fundamental *flavours*, each flavour a fundamental plus an antifundamental, $2 \cdot \frac{1}{2} \cdot N_f$.) Now evaluate at the regular ranks $N_j = N \dim R_j$. The two rank-weighted row sums of Chapter 6 are

$$\sum_j a_{ij}\,\dim R_j \;=\; 3\dim R_i, \qquad \sum_j a_{ji}\,\dim R_j \;=\; 3\dim R_i, \tag{VI.10.31}$$

the first from tensoring R_i with the three-dimensional Q (the outgoing arrows), the second from the regular-representation identity $Q \otimes \mathbb{C}[\Gamma] = \mathbb{C}[\Gamma]^{\oplus 3}$ (the incoming arrows). Their sum is

$$\sum_j \big(a_{ij} + a_{ji}\big)\dim R_j \;=\; 3\dim R_i + 3\dim R_i \;=\; 6\dim R_i. \tag{VI.10.32}$$

Substituting (VI.10.32) into (VI.10.30) at $N_j = N \dim R_j$,

$$b_i \;=\; 3\,N\dim R_i \;-\; \tfrac{1}{2}\,N\,(6\dim R_i) \;=\; 3N\dim R_i - 3N\dim R_i \;=\; 0, \tag{VI.10.33}$$

for every node. The leading beta function vanishes: the one-loop gauge coefficient vanishes at regular ranks. This cancellation is consistent with the parent projection but is not, by itself, an infrared fixed-point calculation. The vanishing is sharp in the ranks. The reader can check that a *fractional* rank changes this coefficient: for a formal dP_0 rank test $(N, N, 2N)$, equation (VI.10.30) gives at node 0, with the symmetric adjacency row sum, a nonzero b_0, because (VI.10.32) used the regular relation $N_j = N \dim R_j$ that the deformation breaks. This rank test is only a diagnostic of the coefficient; the altered chiral quiver may fail anomaly cancellation and need not define a consistent theory. The vanishing coefficient follows specifically in the regular direction.

It is, however, only the one-loop statement. The exact superconformal R-symmetry, the anomalous dimensions, and the precise location of the fixed point under the exact (NSVZ) beta function are dynamical questions reserved for Part III: one-loop vanishing follows from the representation identities (VI.10.31), but an exact fixed point needs the anomalous dimensions and R-charges that a-maximization fixes. Table VI.10.1 records what the leading large-N analysis controls and what it does not.

observable	inherited at leading large N?
planar neutral single-trace correlators	yes (Eq. VI.10.20)
one-loop beta functions at regular ranks	yes ($b_i = 0$, Eq. VI.10.33)
charged traces / double-trace couplings	no (separate analysis)
$U(1)$ factor fates (decouple / massive)	no (Chapter 7)
finite-N corrections	no (not controlled by inheritance)
nonsupersymmetric daughter stability	no (may be unstable)

Table VI.10.1: What basic planar inheritance does and does not control. The top two rows are the content of this chapter; the lower rows are explicitly outside it and routed to Chapter 7 and Part III.

VI.10.5 Worked abelian examples: dP_0 and $\mathbb{C}^3/(\mathbb{Z}_2 \times \mathbb{Z}_2)$

The two abelian daughters make the inheritance concrete from opposite ends: $dP_0 = \mathbb{C}^3/\mathbb{Z}_3$ is chiral and isolated, $\mathbb{C}^3/(\mathbb{Z}_2 \times \mathbb{Z}_2)$ non-chiral and non-isolated, and both inherit the planar neutral sector of $\mathcal{N}$=4 at their regular ranks.

dP_0 from block matrices

This is the same $dP_0 = \mathbb{C}^3/\mathbb{Z}_3$ of Chapters 7 and 8, but the physical question differs. There we tested its anomaly and folded it under an orientifold; here we read it as a large-N orbifold daughter and watch the planar neutral sector descend from the parent. It is the cleanest illustration of the chiral isolated case, and it is worth doing in full, from the parent block matrices to the daughter superpotential, because it is where the projection is most transparent and where a careless reading produces a superpotential with arrows that do not exist.

Parent and projection. The parent is $\mathcal{N}$=4 with gauge group $U(3N)$, since $|\Gamma| = 3$ and the three one-dimensional irreducibles each carry $N_i = N$, so $K = 3N$. Write the $3N \times 3N$ matrices in 3×3 blocks of $N \times N$, labelled by the nodes $0, 1, 2$. The generator embeds as $\gamma_\theta = \mathrm{diag}(\mathbb{1}_N, \omega\mathbb{1}_N, \omega^2\mathbb{1}_N)$, $\omega = e^{2\pi i/3}$, so a block $(\Phi)_{rs}$ $(r, s \in \{0, 1, 2\})$ picks up $\gamma_\theta \Phi \gamma_\theta^{-1} = \omega^{r-s}(\Phi)_{rs}$. The three transverse adjoints Φ^a carry flavour weight ω each (the **3** of the $\mathbb{Z}_3$ acts as $\omega\mathbb{1}$), so the projection condition (VI.10.2) reads

$$(\Phi^a)_{rs} \;=\; \omega \cdot \omega^{\,r-s}\,(\Phi^a)_{rs} \qquad \Longrightarrow \qquad r - s \equiv -1 \pmod 3, \tag{VI.10.34}$$

that is $s = r + 1$. The surviving block of each Φ^a is the single super-diagonal $(\Phi^a)_{r,\,r+1}$, which we call $X^a_{r,\,r+1}$, an $N \times N$ matrix from node r to node $r + 1$. The gauge field, flavour-neutral, survives where $r = s$, the diagonal blocks, giving

$$G \;=\; U(N)_0 \times U(N)_1 \times U(N)_2, \tag{VI.10.35}$$

and three flavours of bifundamental on each of the three super-diagonal arrows. With weights $(1,1,1)$ the adjacency is

$$a_{ij} \;=\; 3\,\delta_{j,\,i+1}, \tag{VI.10.36}$$

a single directed triangle $0\to1\to2\to0$, each edge traversed three times (once per flavour a). The surviving block pattern is exactly this triangle, and the reader should note what is *absent*. There is no $X_{r,\,r-1}$ block, because (VI.10.34) forces $s=r+1$, not $s=r-1$. The quiver has arrows $0\to1$, $1\to2$, $2\to0$ and *no* reverse arrows $0\to2$, $2\to1$, $1\to0$.

The superpotential as a single triangle, no reverse arrows. The parent cubic (VI.10.1) projects onto the gauge-invariant cubic words, the oriented three-cycles of the triangle. Restricting each Φ^a in

$$W_{\text{parent}} \;\propto\; \varepsilon_{abc}\,\mathrm{Tr}\big(\Phi^a\Phi^b\Phi^c\big) \tag{VI.10.37}$$

to its surviving block $X^a_{r,r+1}$ and contracting the gauge indices around the only closed length-three path leaves the dP_0 superpotential

$$W_{dP_0} \;=\; \varepsilon_{abc}\;\mathrm{Tr}\big(X^a_{01}\,X^b_{12}\,X^c_{20}\big), \tag{VI.10.38}$$

in the holomorphic toric normalization. To track the physical coupling separately, use coupling-extracted parent fields $\Phi=g_pX_P$ and invariant blocks $\Phi_{r,r+1}=g_DX^{\text{can}}_{r,r+1}$ with $g_D^2=3g_p^2$. The parent's cubic coefficient in those extracted fields is $\sqrt{2}/g_p^2$ multiplying $\mathrm{Tr}\,\Phi^1[\Phi^2,\Phi^3]$. Division of the restricted action by 3 gives the canonical daughter coefficient $\sqrt{2}g_D$ multiplying the epsilon triangle. Equation (VI.10.38) absorbs that coefficient into the holomorphic convention; it does not set $g_D=g_p$. The single ε-antisymmetrized triangle descends from (VI.10.37) and is identical to the form fixed in Chapter 6. Its multiple terms come from the *flavour* antisymmetrization over (a,b,c), not from any reverse quiver arrow. Expanding the ε, with the path order $0\to1\to2\to0$ held *fixed* and the antisymmetrization carried in the flavour labels, gives the six sign-weighted words

$$\begin{aligned} W_{dP_0} \;=\;& \mathrm{Tr}\;X^1_{01}\big(X^2_{12}X^3_{20}-X^3_{12}X^2_{20}\big)+\mathrm{Tr}\;X^2_{01}\big(X^3_{12}X^1_{20}-X^1_{12}X^3_{20}\big)\\ &+\mathrm{Tr}\;X^3_{01}\big(X^1_{12}X^2_{20}-X^2_{12}X^1_{20}\big), \end{aligned} \tag{VI.10.39}$$

each product is a composable $0\to1\to2\to0$ path: the antisymmetrization is in flavour, never a matrix commutator of fields on different edges. Each of the nine fields $X^a_{r,r+1}$ then appears in exactly two terms with opposite sign, the toric "two-terms-per-field" structure of Chapter 6. A word such as $\mathrm{Tr}(X_{02}X_{21}X_{10})$ *cannot* occur, for the simple reason that the fields X_{02},X_{21},X_{10} do not exist. There are no arrows $0\to2$, $2\to1$, $1\to0$. The F-terms are read off by differentiating (VI.10.38) as in Chapter 6, $\partial W/\partial X^a_{01}=\varepsilon_{abc}X^b_{12}X^c_{20}$ and cyclically, the relations that reconstruct the $\mathbb{C}^3/\mathbb{Z}_3$ geometry.

Counts and operators. The beta-function check is immediate. Each node has three incoming and three outgoing bifundamentals, so

$$\tfrac{1}{2}\sum_j \big(a_{ij}+a_{ji}\big)N_j \;=\; \tfrac{1}{2}(3+3)N \;=\; 3N, \qquad b_i \;=\; 3N-3N \;=\; 0. \tag{VI.10.40}$$

The inheritance count (VI.10.29) reads

$$\sum_i N_i^2 \;=\; 3N^2 \;=\; \frac{K^2}{3}, \qquad \sum_{i,j} a_{ij}N_iN_j \;=\; 9N^2 \;=\; \frac{3K^2}{3}, \tag{VI.10.41}$$

the $U(N)^3$ daughter being a clean one-third slice of the $U(3N)$ parent. Finally the two sectors. A neutral operator is the symmetric node sum, for instance a projected mesonic single trace

$$O_{\text{neutral}} \;=\; \sum_{i=0}^{2} \mathrm{Tr}\big(X^a_{i,i+1}X^b_{i+1,i+2}X^c_{i+2,i}\big), \tag{VI.10.42}$$

which descends from the parent single trace $\mathrm{Tr}(\Phi^a\Phi^b\Phi^c)$ and inherits its planar correlators; the twisted partners

$$O_{\mathrm{tw},\,q} \;=\; \sum_{i=0}^{2} \omega^{\,qi}\; \mathrm{Tr}\big(X^a_{i,i+1}X^b_{i+1,i+2}X^c_{i+2,i}\big), \qquad q=1,2, \tag{VI.10.43}$$

carry quantum $\mathbb{Z}_3$ charge q and are the operators that see the orbifold. The reader can check that the quantum $\mathbb{Z}_3$ generator $i\mapsto i+1$ fixes (VI.10.42) and rotates (VI.10.43) by ω^{-q}, exactly the charges (VI.10.23).

The non-chiral $\mathbb{C}^3/(\mathbb{Z}_2\times\mathbb{Z}_2)$ daughter

The same $\mathbb{C}^3/(\mathbb{Z}_2\times\mathbb{Z}_2)$ ran through Chapters 7 and 9 (fixed-line tadpoles, then discrete torsion); here the question is its large-N inheritance, and the non-chiral non-isolated case is the instructive contrast, showing that "orbifold daughter" does not mean "chiral". Here $\Gamma=\mathbb{Z}_2\times\mathbb{Z}_2$ has four one-dimensional irreducibles, so the parent is $U(4N)$, $K=4N$, and the daughter is

$$G \;=\; U(N)^4, \tag{VI.10.44}$$

one node per irreducible. The three nontrivial elements are $\mathrm{diag}(1,-1,-1)$ and its two partners; the defining **3** restricts to three real characters, so each character equals its conjugate and the adjacency is symmetric,

$$a \;=\; a^{\mathsf{T}} \;=\; J-\mathbb{1} \quad \text{on four nodes}, \tag{VI.10.45}$$

the doubled complete graph K_4 (J the all-ones matrix), the same adjacency built in Chapters 6 and 7. The matter is therefore non-chiral, every arrow paired with its reverse, because the defining Q is real (self-conjugate) here so $a_{ij}=a_{ji}$; the daughter is

no less an orbifold daughter for being non-chiral. The inheritance count (VI.10.29) still holds,

$$\sum_i N_i^2 \;=\; 4N^2 \;=\; \frac{K^2}{4}, \qquad \sum_{i,j} a_{ij} N_i N_j \;=\; 12N^2 \;=\; \frac{3K^2}{4}, \tag{VI.10.46}$$

and the one-loop coefficient still vanishes: each node connects to the other three with one arrow in and one out, so

$$\tfrac{1}{2}\sum_j \big(a_{ij}+a_{ji}\big)N_j \;=\; \tfrac{1}{2}\cdot 2\cdot 3N \;=\; 3N, \qquad b_i \;=\; 3N-3N \;=\; 0. \tag{VI.10.47}$$

The difference from dP_0 is entirely in the chirality of the matter and the fixed-line structure of the geometry (Chapter 7), not in the large-N parentage: the planar neutral correlators of the $U(N)^4$ theory obey the same perturbative planar neutral comparison with the $U(4N)$ parent. The representation trace of each face thinned by $|\Gamma| = 4$. The neutral sector is again the uniform node sum, and because Γ is abelian the three twisted sectors are labelled by the nontrivial characters of $\mathbb{Z}_2 \times \mathbb{Z}_2$, the dual group.

VI.10.6 Worked non-abelian example: $\Delta(27)$

The same $\Delta(27)$ whose rank-weighted anomaly we computed in Chapter 7 returns here for a different representation structure for the non-abelian inheritance check. The abelian examples might suggest that the node labels must be group elements. They need not be. For a non-abelian Γ the nodes are the irreducible representations, and the inheritance rank arithmetic is identical with $\dim R_i$ in place of the unit cyclic weights. Take the trihedral $\Delta(27)$, with nine one-dimensional irreducibles $1_{r,s}$ and a conjugate pair $\mathbf{3}, \overline{\mathbf{3}}$. The regular ranks are

$$N_{1_{r,s}} = N, \qquad N_{\mathbf{3}} = N_{\overline{\mathbf{3}}} = 3N, \tag{VI.10.48}$$

so the parent size is

$$K \;=\; \sum_i N_i \dim R_i \;=\; 9\,(N)(1) + (3N)(3) + (3N)(3) \;=\; 27N \;=\; N|\Gamma|, \tag{VI.10.49}$$

matching $|\Gamma| = \sum_i (\dim R_i)^2 = 9\cdot 1 + 2\cdot 9 = 27$. The parent is $\mathcal{N}{=}4$ $U(27N)$, and the daughter is the product

$$G \;=\; \Big(\prod_{r,s} U(N)_{1_{r,s}}\Big) \times U(3N)_{\mathbf{3}} \times U(3N)_{\overline{\mathbf{3}}}, \tag{VI.10.50}$$

nine $U(N)$ factors and two $U(3N)$ factors. The McKay arrows $1_{r,s} \to \mathbf{3} \to \overline{\mathbf{3}} \to 1_{r,s}$ make the quiver chiral, and the cubic superpotential descends from the parent exactly as for dP_0, now with the ε-contraction labelled by the Γ-intertwiners rather than a single triangle. The inheritance arithmetic is unchanged. The gauge count is

$$\sum_i N_i^2 \;=\; 9\,(N)^2 + (3N)^2 + (3N)^2 \;=\; 27N^2 \;=\; \frac{K^2}{27}, \tag{VI.10.51}$$

one twenty-seventh of the parent, and the one-loop coefficient vanishes node by node because the regular-rank row sum (VI.10.32) holds for every irreducible, $b_i = 3N_i - \frac{1}{2}N(6\dim R_i) = 0$. The non-abelian feature shows up exactly where §VI.10.3 said it would. There is no quantum $\mathbb{Z}_n$ phase here, so the neutral operator is the $\dim R_i$-weighted node sum (VI.10.26), which for $\Delta(27)$ reads explicitly, the nine singlets weighted by 1 and the two triplets by their dimension 3,

$$O_{\text{neutral}} \;=\; \sum_{r,s} \mathrm{Tr}\big(\mathrm{loop}_{1_{r,s}}\big) \;+\; 3\,\mathrm{Tr}\big(\mathrm{loop}_{\mathbf{3}}\big) \;+\; 3\,\mathrm{Tr}\big(\mathrm{loop}_{\overline{\mathbf{3}}}\big), \tag{VI.10.52}$$

the $\dim R_i$ weighting following from the regular trace; the twisted closed-string sectors are indexed by nonidentity conjugacy classes, related by a finite character transform to the central idempotents (VI.10.25) of $\mathbb{C}[\Delta(27)]$ rather than by a character ω^{qi}. The lesson is that the parentage is a property of the orbifold projection, not of the abelian-ness of Γ. An ordinary regular-rank $\mathbb{C}^3/\Gamma$ quiver, abelian or not, has the perturbative planar neutral comparison with its $\mathcal{N}$=4 parent under the stated conditions. Table VI.10.2 collects the three.

Γ	$\lvert\Gamma\rvert$	parent	daughter G	chiral?
$\mathbb{Z}_3$ (dP_0)	3	$U(3N)$	$U(N)^3$	yes
$\mathbb{Z}_2 \times \mathbb{Z}_2$	4	$U(4N)$	$U(N)^4$	no
$\Delta(27)$	27	$U(27N)$	$U(N)^9 \times U(3N)^2$	yes

Table VI.10.2: The three worked daughters. Each has $K = N\lvert\Gamma\rvert$, gauge count $\sum_i N_i^2 = K^2/\lvert\Gamma\rvert$, matter count $3K^2/\lvert\Gamma\rvert$, and $b_i = 0$ at the regular ranks; the abelian cases have dual quantum groups $\widehat{\mathbb{Z}_3} = \mathbb{Z}_3$ and $\widehat{\mathbb{Z}_2 \times \mathbb{Z}_2} = \mathbb{Z}_2 \times \mathbb{Z}_2$, respectively. The latter is noncyclic. The nonabelian twisted sectors are indexed by conjugacy classes.

VI.10.7 Boundaries and bridges

Orientifolds and discrete torsion

The order of this block was $7 \to 8 \to 9 \to 10$, and a reader who has come through the orientifold and discrete-torsion chapters should ask whether their modified daughters inherit too. The honest answer is that the ordinary perturbative inheritance described above is the *reference case*, and each modification requires its own projection and its own equivalence statement; we state the boundary, not a theorem.

For an *orientifold* daughter (Chapter 8) the parent is still $\mathcal{N}$=4 $U(K)$, but the surviving theory is now the simultaneous projection by Γ *and* the orientifold Ω, folding $U(K)$ to an SO or USp factor and the bifundamentals to the folded matter content. Large-N equivalence in this case is a separate result. It requires an orientifold projection compatible with the planar limit and a restriction to the *neutral, orientifold-even* sector, because a crosscap gives a nonorientable contribution. The closed ribbon surface has Euler characteristic $\chi = 2 - 2h - c$ with c crosscaps, so one crosscap has relative

order $1/N$, while one oriented handle has relative order $1/N^2$ at fixed couplings. The projection and parity conditions must be treated separately. The possible orientifold equivalence concerns suitable even-sector planar correlators, subject to its own symmetry assumptions; the odd sector, and the global anomalies that Chapter 8 flagged for SO/USp, are genuinely new data not fixed by the oriented parent.

For a *discrete-torsion* daughter (Chapter 9) the quotient is still $\mathbb{C}^3/\Gamma$, so one still has an orbifold daughter, but the parent projection now carries *projective* Chan–Paton phases. The embedding γ_g is a projective representation with cocycle $\alpha \in H^2(\Gamma, U(1))$, and the superpotential is the q-deformed cubic of Chapter 9. The node content, the McKay adjacency, and the superpotential are all the torsion-twisted data, not the ordinary ones, so the inheritance count and the one-loop check must be run with the *projective* irreducibles and the q-deformed vertices. The single projective irreducible of $\mathbb{Z}_2 \times \mathbb{Z}_2$ with its nontrivial class, for instance, has dimension 2, so the torsion daughter is a single $U(2N)$ factor rather than $U(N)^4$, an entirely different large-N theory from the untorsioned one. Here N counts bulk regular probes, the unit of this chapter, so the single projective node has rank $2N$; Chapter 9 writes the same node $U(m)$ in its multiplicity normalization, with $m = 2N$ the multiplicity of the projective irreducible (its rank convention box). A diagrammatic comparison would require the projective action and its vertex phases to be treated explicitly; the ordinary count above does not establish it.

Inheritance with the modifications of Chapters 8 and 9

Ordinary oriented $\mathbb{C}^3/\Gamma$ daughters inherit the parent's planar neutral sector, as described above. This is the reference case. *Orientifold* daughters need their own orientifold large-N equivalence and a restriction to the parity-even neutral sector; the crosscap and the SO/USp global anomalies are new data. *Discrete-torsion* daughters are still orbifold daughters, but with projective Chan–Paton phases and a q-deformed superpotential; the inheritance count must use the projective irreducibles (e.g. $\mathbb{Z}_2 \times \mathbb{Z}_2$ with torsion gives a single $U(2N)$ for N bulk probes, not $U(N)^4$; Chapter 9 calls the same node $U(m)$, $m = 2N$). Combining *both* modifications at once, an orientifold of a discrete-torsion daughter, requires compatible real and projective Chan–Paton data simultaneously and is beyond this volume. The projector structure changes with the projective representation and must be checked in that theory.

The holographic bridge

There is a second, geometric statement of the same parentage, and it is the natural exit toward the later volumes. A stack of N regular D3-branes at the tip of $\mathbb{C}^3/\Gamma$ has a near-horizon geometry that is, schematically, $AdS_5 \times S^5/\Gamma$, the parent's $AdS_5 \times S^5$ with the five-sphere quotiented by the same $\Gamma \subset SU(3) \subset SO(6)$. The untwisted supergravity modes descend from the parent S^5 harmonics and give the neutral operators their holographic duals. For a nonfree action, twisted sectors can be localized at fixed loci on S^5. The $\mathbb{Z}_3$ action $(z_1, z_2, z_3) \mapsto \omega(z_1, z_2, z_3)$ is free on S^5, since a fixed vector would obey $z = 0$. Its twisted strings instead wind noncontractible cycles of $S^5/\mathbb{Z}_3$; they are not fixed-locus supergravity modes. The central charge scales as the parent's divided

by $|\Gamma|$. The parent $\mathcal{N}$=4 $U(K)$ has $c \sim K^2$, and the daughter inherits

$$c_{\text{daughter}} \sim \frac{K^2}{|\Gamma|} = N^2|\Gamma|, \tag{VI.10.53}$$

exactly the $1/|\Gamma|$ slice of the degree count (VI.10.29), now read holographically as the ratio of the S^5/Γ volume to the S^5 volume. The preserved supersymmetry is fixed by where Γ sits, $\mathcal{N}$=1 for $\Gamma \subset SU(3)$ and $\mathcal{N}$=2 for the surface case $\Gamma \subset SU(2)$. For a non-isolated quotient the twisted modes are supported on the fixed locus, a curve rather than a point, and their spectrum depends on that locus; this is the holographic face of the localized-versus-fixed-line distinction of Chapter 7. We state all of this as a bridge only. The holographic dictionary itself, the matching of Kaluza–Klein spectra to operators, the twisted-sector states, and the precise central-charge computations, belongs to Part III and Volume VI.

What inheritance does not prove

The chapter has established a perturbative planar comparison, and it is important to state precisely how far the claim reaches. Planar inheritance is the statement (VI.10.20): at large N, regular ranks, and matched couplings, the *planar* correlators of the *neutral* sector of an orbifold daughter equal the projected planar correlators of the $\mathcal{N}$=4 parent, up to $O(1/N^2)$. The full physical equivalence also depends on the realization of projection symmetries in the vacuum.

> **Common misconception: inheritance proves equivalence**
>
> Planar inheritance does *not* prove that the daughter equals the parent at finite N. It is leading order in $1/N^2$ and applies to the neutral sector only. It does not establish the stability of the twisted sector, the exact conformality of nonsupersymmetric daughters, a-maximization results, Seiberg or toric dualities, duality-cascade dynamics, or the cancellation of compact tadpoles. Those are separate statements with their own evidence; some are true, some fail, and inheritance decides none of them.

Spelling out the boundary: finite-N corrections are not controlled, because the lift of §VI.10.3 breaks at the first handle (Figure VI.10.2). The twisted operators of §VI.10.3 are a separate sector with no neutral parent ancestor; their dynamics, including the possibility of twisted-sector tachyons in nonsupersymmetric quotients, must be analyzed on their own. The $U(1)$ factors of each $U(N_i)$ have the fates worked out in Chapter 7, decoupling or becoming massive by Green–Schwarz couplings; they are not captured by the simplest planar inheritance. And the exact infrared dynamics are the business of Part III and Volume VII: the superconformal R-charges that a-maximization fixes, the network of Seiberg and toric dualities, the duality cascades that relate different ranks, and the conformal manifold of marginal couplings. A nonperturbative equivalence requires unbroken projection symmetry in the parent and the relevant daughter symmetry in the selected vacuum. If either is spontaneously broken, the perturbative graph map does not establish equality of physical observables. The general field-theory result is routed forward as a foundation stub. What this chapter gives is its diagrammatic core for the neutral sector, and the honest fence around how

much that control buys. With it, Volume VI closes, having built the theories, tested them, and named the structure that makes their large-N dynamics tractable. The dynamics themselves begin in the volumes that follow.

Status and sources

This section is for source tracking and internal consistency, not part of the first reading. The evidence-code tags ([WS] physical-worldsheet derivation in the untwisted string, [MATH] a mathematical theorem with stated hypotheses and proof status), the convention pointers, and the anchors are collected here, keyed by section. This chapter is a teaching chapter on planar inheritance closing Volume V. It reads the $\mathbb{C}^3/\Gamma$ quiver of Chapter 6 as the orbifold daughter of $\mathcal{N}$=4, explains the perturbative planar inheritance of its neutral sector by a double-line argument, and routes the dynamics forward, after the orbifold conformal field theories of Kachru and Silverstein (1998), the chiral orbifold daughters of Lawrence et al. (1998), and the large-N inheritance argument of Bershadsky and Johansen (1998) and Bershadsky, Kakushadze, et al. (1998); the holographic bridge is the near-horizon of Maldacena (1998). The nonperturbative symmetry condition is stated in Kovtun, Unsal and Yaffe, hep-th/0411177, v1, §4.2, pp. 12–13, (4.18)–(4.20), and §5.3, pp. 18–19, (5.18); the warning about leading double-trace running in nonsupersymmetric orbifolds is supported by Dymarsky, Klebanov and Roiban, hep-th/0505099v2, §2, pp. 2–3, (1)–(5). For the non-abelian worldsheet orbifold-sector distinction, see Ginsparg, hep-th/9108028, v1, §8, pp. 119–120, (8.17), where twisted sectors are indexed by conjugacy classes and projected by centralizers. Bershadsky–Johansen, hep-th/9803249v2, pp. 2–6, (2), (7), (10)–(15) and the paragraph after (15), provides the common-element propagator projector and the residual loop-dependent group factor. The theta and spanning-tree calculations above make the matched rescaling explicit. The finite graph and coefficient identities are [MATH] only conditional on the stated ribbon rules and matter indices. The planar physical interpretation, symmetry realization, conformality and holographic bridge retain unassigned primary classification. The imported physical-worldsheet sector statement from Ginsparg is [WS]; it is not a topological twist. The representation order and idempotent identities are proved by the regular representation and character orthogonality. The orientifold and torsion paragraphs are boundary statements, with setup-specific equivalence sources still deferred; they do not assert those equivalences. No numerical check supplies the missing physical premises.

It reuses the gauge/rank data, the McKay adjacency and arrow orientation (McKay multiplicities, fundamental-at-tail arrows) as the projected matter, the superpotential inheritance from the parent cubic (superpotential normalization), the supercharge count set by Γ, and the orbifold/quantum-symmetry action (orbifold action) that labels twisted versus untwisted operators. No new convention is introduced; the coupling matching is a tagged prose claim derived from the projected action, not a convention entry. Finite group calculations use the character tables of Chapter 6.

§VI.10.1 Orbifold daughters, statement and scope. Framing. The place of the chapter in Volume VI, the parentage idea, the road map, and the explicit scope guard that the dynamics (no a-maximization, Seiberg/toric duality, cascades, nonsupersymmetric stability, or detailed holographic spectra) are Part III / Volume VII.

§VI.10.2 Projection and coupling matching. The parent $\mathcal{N}$=4 $U(K)$ with $K = N|\Gamma|$ (VI.10.3), the projection condition (VI.10.2), the daughter gauge group (VI.10.5), and the projected matter $Q \otimes R_i = \bigoplus_j a_{ij} R_j$ (VI.10.6), a one-page recap of Chapter 6 in the field-theory language. The trace restriction (VI.10.8) is an algebraic identity. The matched action is $S_D = S_P|_{\text{inv}}/m$, so $g_i^2 = m g_p^2/d_i$ and $\lambda_i = \lambda_P$. Lawrence–Nekrasov–Vafa, hep-th/9803015v2, §2, pp. 3–6, (2.1)–(2.2), gives $\tau_i = d_i\tau/m$ immediately before (2.2); (2.7) supplies the inherited cubic via intertwiners (Lawrence et al. (1998)). The brane premise also uses Kachru and Silverstein (1998). The conditional rank identity is [MATH]; the field-theory and decoupling interpretations retain unassigned primary classification here. The bare and matched couplings are explicit in the cyclic and nonabelian examples.

§VI.10.3 Planar inheritance and the neutral sector. The ribbon weight (VI.10.14), the orbifold projector on a double line (Figure VI.10.1, (VI.10.15)), the regular-character trace identity (VI.10.16)–(VI.10.17), with edge constraints retained, the planar neutral comparison giving the inheritance

statement (VI.10.20), and the handle obstruction (Figure VI.10.2); then (§VI.10.3) the neutral sum (VI.10.21) versus the twisted combinations (VI.10.22) for abelian $\mathbb{Z}_n$, the quantum charges (VI.10.23), and for non-abelian Γ the central-idempotent formulation (VI.10.25)–(VI.10.26) with the explicit warning that there is no dual group of characters, plus the operator-normalization convention. are field-theory planar and representation-theoretic statements, not worldsheet derivations (orbifold action; Bershadsky and Johansen (1998), Bershadsky, Kakushadze, et al. (1998), Lawrence et al. (1998)). This files the new orientifold large-N equivalence (the conditional nonperturbative large-N orbifold/orientifold equivalence as a field-theory theorem; home Part III / the large-N volume; VI.10 explains its perturbative diagrammatic core for the neutral sector and routes the general proof). the $1/|\Gamma|$ projection of the gauge and matter degrees of freedom at regular ranks, and that the uniform $\mathbb{Z}_n$ sum is quantum-invariant while the ω^{qi}-weighted sum is charged, for the stated representations. The finite identities are separate from the projector sums and planar amplitude argument. The new `planar-theta` and `connected-k3` tasks evaluate (VI.10.18) and the factors in (VI.10.20), respectively; the general graph argument is the derivation in the body.

§VI.10.4 Two consequences, the degree count and the vanishing one-loop gauge coefficient. The gauge count (VI.10.27), the matter count (VI.10.28), and the $1/|\Gamma|$ slice (VI.10.29); then (§VI.10.4) the one-loop coefficient (VI.10.30) with the $\frac{1}{2}$ index normalization (the $3N - N_f$ cross-check), the regular-rank row sum (VI.10.32), and the vanishing $b_i = 0$ (VI.10.33) (Table VI.10.1), with the fractional-rank departure noted and b_i taken for the non-abelian $SU(N_i)$ factor (U(1) fates → Chapter 7). use field-theory perturbation theory and the [MATH] McKay identity (McKay multiplicities; the Chapter 6 identities). The factor $\frac{1}{2}$ on the symmetrized adjacency is kept throughout. $\sum_i N_i^2 = K^2/|\Gamma|$, $\sum_{ij} a_{ij} N_i N_j = 3K^2/|\Gamma|$, and $b_i = 0$ at regular ranks for every fixture via $\sum_j (a_{ij} + a_{ji}) \dim R_j = 6 \dim R_i$, with a fractional rank giving $b_i \neq 0$; the dimensional-form checks are in the dimensional and consistency checks.

§VI.10.5–VI.10.6 Worked examples. dP_0 in full (parent $U(3N)$ as 3×3 blocks, the block-projection (VI.10.34) keeping only the super-diagonal $s = r + 1$, the daughter $U(N)^3$, the triple triangle, the parent cubic $\varepsilon_{abc} \operatorname{Tr}(\Phi^a \Phi^b \Phi^c)$ to the single ε-antisymmetrized dP_0 triangle (VI.10.38) with NO reverse-arrow term, the flavour-antisymmetrized expansion (VI.10.39), $b_i = 0$, the neutral/twisted operators (VI.10.42)–(VI.10.43)); $\mathbb{C}^3/(\mathbb{Z}_2 \times \mathbb{Z}_2)$ (parent $U(4N)$, daughter $U(N)^4$, doubled K_4, non-chiral with the real-Q symmetry $a = a^{\mathsf{T}}$); and $\Delta(27)$ (regular ranks (VI.10.48), $K = 27N$ (VI.10.49), daughter (VI.10.50), the non-abelian inheritance with conjugacy-class twisted sectors). use projected field content and finite representation calculations (superpotential normalization, quiver gauge groups and ranks; Lawrence et al. (1998)). The dP_0 superpotential matches the Chapter 6 convention (superpotential normalization, McKay multiplicities) exactly, the single triangle, multiple terms from flavour antisymmetrization, no nonexistent reverse arrows. the parent-cubic to dP_0-triangle projection ($K = 3N$), the $U(N)^4$ count ($K = 4N$), and the $\Delta(27)$ count ($K = 27N$, $\sum(\dim R_i)^2 = 27$), from the stated representations. Expanding the parent commutator into projected paths gives the six signed words in (VI.10.39) with their matrix order preserved.

§VI.10.7 Boundaries and bridges. Three boundary statements collected into one closing section. *Orientifolds and discrete torsion.* The orientifold daughter needs its own orientifold large-N equivalence and a parity-even neutral restriction (the crosscap and SO/USp global anomalies are new data); the discrete-torsion daughter is still an orbifold daughter but with projective Chan–Paton phases and a q-deformed superpotential (the $\mathbb{Z}_2 \times \mathbb{Z}_2$ torsion daughter has a single $U(2N)$ node in the stated multiplicity convention, unlike the untwisted $U(N)^4$), Q9 is a scoped physical boundary, routing to Chapters 8/9 and orientifold large-N equivalence. *The holographic bridge* (§VI.10.7). The near-horizon $AdS_5 \times S^5/\Gamma$, untwisted from S^5 modes, twisted at fixed loci only for nonfree actions and winding sectors for the free $\mathbb{Z}_3$ action, the central charge $c \sim K^2/|\Gamma| = N^2|\Gamma|$ (VI.10.53), the supersymmetry set by $\Gamma \subset SU(3)/SU(2)$, Q8 is a source-based brane/holographic bridge (spinor and supersymmetry counting; Maldacena (1998); Kachru and Silverstein (1998)), reusing the finite-subgroup classification for $SU(3)$/the threefold derived McKay correspondence for the geometry. *What inheritance does not prove* (§VI.10.7). The precise reach of (VI.10.20) is a normalized connected perturbative planar neutral comparison with relative $O(1/N^2)$ corrections; the honest fence around finite-N equivalence, twisted-sector stability, nonsupersymmetric conformality, a-maximization, Seiberg/toric duality, cascades, and compact tadpoles, Q9 is a scoped physical boundary. This files (large-N inheritance proves neither finite-N equivalence nor exact conformality nor stability; it is planar and neutral-sector only).

References

Bershadsky, M. and A. Johansen (1998). "Large N limit of orbifold field theories". In: *Nucl. Phys. B* 536, pp. 141–148. DOI: 10.1016/S0550-3213(98)00526-4. arXiv: hep-th/9803249.

Bershadsky, M., Z. Kakushadze, and C. Vafa (1998). "String expansion as large N expansion of gauge theories". In: *Nucl. Phys. B* 523, pp. 59–72. DOI: 10.1016/S0550-3213(98)00272-7. arXiv: hep-th/9803076.

Johnson, C. V. (2003). *D-Branes*. Cambridge Monographs on Mathematical Physics. Cambridge University Press. DOI: 10.1017/CBO9780511606540.

Kachru, S. and E. Silverstein (1998). "4-D conformal theories and strings on orbifolds". In: *Phys. Rev. Lett.* 80, pp. 4855–4858. DOI: 10.1103/PhysRevLett.80.4855. arXiv: hep-th/9802183.

Lawrence, A. E., N. Nekrasov, and C. Vafa (1998). "On conformal field theories in four-dimensions". In: *Nucl. Phys. B* 533, pp. 199–209. DOI: 10.1016/S0550-3213(98)00495-7. arXiv: hep-th/9803015.

Maldacena, J. M. (1998). "The Large N limit of superconformal field theories and supergravity". In: *Adv. Theor. Math. Phys.* 2, pp. 231–252. DOI: 10.4310/ATMP.1998.v2.n2.a1. arXiv: hep-th/9711200.

Chapter VI.11

Atlas: a low-rank orbifold catalog with calculation checks

VI.11.1 What this atlas is, and how to read it

A D3-brane at an orbifold singularity turns a finite-group action into a gauge theory. The Chan–Paton representation determines the gauge factors; tensoring its irreducibles with the coordinate representation determines the matter. The inherited parent interaction then connects the arrows into a superpotential. The same group can act in different ways, so the starting point is an embedding $\Gamma \subset SU(n)$, not an abstract group name alone.

This atlas brings the constructions of Chapters 2–10 together. It gives the reader a route from a singularity to its quiver, and from a quiver to the calculations and physical assumptions that define it. The dP_0 example below shows that route explicitly. The tables then separate ADE families, selected $SU(3)$ embeddings, conditional orientifold projections, and discrete torsion. A catalogued example need not be an independently constructed string background. In particular, anomaly cancellation and an admissible graph involution do not supply the missing orientifold lift or a compact completion.

The four axes. The catalog is the product of two classifications and two refinements.

- **Axis 1**, $\mathbb{C}^2/\Gamma$ with $\Gamma \subset SU(2)$ (Table VI.11.1) gives the $\mathcal{N}$=2 ADE quivers. Here the McKay graph is an affine Dynkin diagram and the list is the complete ADE list.
- **Axis 2**, $\mathbb{C}^3/\Gamma$ with $\Gamma \subset SU(3)$ (Table VI.11.2) gives the quivers written in $\mathcal{N}$=1 language. There is no ADE miracle here; the quiver is read off the character table. We tabulate six cyclic embeddings, five product embeddings, and the indicated non-abelian Δ/Σ examples with $|\Gamma| \leq 60$.
- **Axis 3**, orientifold fixtures and checks (Table VI.11.3) contains representative SO/USp projections, arrow folds, and local anomaly equations with their lift

assumptions. This is not a full orientifold classification.

- **Axis 4**, discrete torsion (Table VI.11.4) gives, for those entries with a nontrivial Schur multiplier, the projective quiver.

Axes 3 and 4 are not new groups; they hang off the groups of axes 1 and 2.

The range of the tables. The ADE table lists the complete families of nontrivial finite subgroups of $SU(2)$, using their defining representation. The $SU(3)$ table has a narrower purpose. Its abelian rows are the displayed cyclic groups $\mathbb{Z}_2, \ldots, \mathbb{Z}_7$ and five displayed products, with one weight assignment per row. They do not enumerate all abelian groups of order at most 60, or all their embeddings. The non-abelian rows follow the stated Δ/Σ selection through order 60 and retain $\Sigma(168)$ as one larger example. Other families, including the order-21 Frobenius group, are deferred. These boundaries let the reader use a row without mistaking absence from the table for a nonexistence result.

The recipe in one box. For an ordinary orbifold, the following procedure reconstructs its quiver. Orientifolds and discrete torsion require additional input at the last step.

From a finite subgroup to its catalog row.

1. Realize $\Gamma \subset SU(n)$ as explicit matrices; record the defining representation Q (the **2** for $SU(2)$, the **3** for $SU(3)$).
2. Build the character table; read the irreducible representations R_i (the nodes) and their dimensions d_i.
3. Compute the McKay adjacency $a_{ij} = \dim \mathrm{Hom}_\Gamma(R_j, Q \otimes R_i)$ (the arrows). Symmetric for $SU(2)$, generically directed for $SU(3)$.
4. Read off the gauge group $\prod_i U(Nd_i)$. Project the parent cubic using explicit arrow intertwiners to determine its coefficients.
5. Check the consistency conditions, including the formal rank equation $(a - a^{\mathsf{T}})N = 0$ at regular ranks; optionally fold by an orientifold involution (axis 3) or twist by a discrete-torsion cocycle (axis 4).

The next section walks one example, $dP_0 = \mathbb{C}^3/\mathbb{Z}_3$, through all five steps and the two refinements; the catalog tables then record where the procedure lands for every entry. For the $SU(3)$ embeddings, symmetry of the adjacency tests whether Q is self-dual, while eigenvalue 1 of a nonidentity element detects a fixed line. These two tests answer different questions about matter and geometry.

VI.11.2 The recipe applied to $dP_0 = \mathbb{C}^3/\mathbb{Z}_3$

We take the smallest isolated chiral example, the one that has appeared in the most chapters, and run it end to end. Let $\Gamma = \mathbb{Z}_3$ act on $\mathbb{C}^3$ with weights $(1, 1, 1)$, that is by

$g = \omega\,\mathbb{1}_3$ with $\omega = e^{2\pi i/3}$. The generator has determinant $\omega^3 = 1$, so $\Gamma \subset SU(3)$ and the quotient is Calabi–Yau.

Steps 1–2. representations. $\mathbb{Z}_3$ is abelian; its three irreducible representations are the characters $R_k : g \mapsto \omega^k$, $k = 0, 1, 2$, each one-dimensional. The defining $Q = \mathbf{3}$ acts by $\omega\,\mathbb{1}_3$, so as a representation $Q = R_1 \oplus R_1 \oplus R_1$, with character

$$\chi_Q(g^m) = \mathrm{Tr}\,(\omega^m \mathbb{1}_3) = 3\,\omega^m, \qquad m = 0, 1, 2. \tag{VI.11.1}$$

Because χ_Q is not real, Q is complex, $\mathbf{3} \ncong \bar{\mathbf{3}}$, and, anticipating the next step, the quiver will be chiral.

Step 3. the quiver. The McKay rule $a_{ij} = \dim \mathrm{Hom}_\Gamma(R_j, Q \otimes R_i)$ reads, for the cyclic group,

$$a_{ij} = \frac{1}{3}\sum_{m=0}^{2} \chi_Q(g^m)\,\omega^{mi}\,\omega^{-mj} = \frac{1}{3}\sum_{m=0}^{2} 3\,\omega^{m(1+i-j)} = 3\,\delta_{j,\,i+1}, \tag{VI.11.2}$$

so each node i sends three arrows to node $i + 1 \bmod 3$, giving a directed triangle with all multiplicities 3. The adjacency is not symmetric, $a_{ij} \neq a_{ji}$; the quiver is chiral, exactly because Q is complex.

Step 4. gauge theory. At the regular ranks $N_i = N \dim R_i = N$ the gauge group is $U(N)^3$, with three bifundamentals $X^a_{i,i+1}$ $(a = 1, 2, 3)$ on each edge. The superpotential is the ϵ-antisymmetrized cubic

$$W = \epsilon_{abc}\,\mathrm{Tr}\big(X^a_{01}\,X^b_{12}\,X^c_{20}\big)\,, \tag{VI.11.3}$$

inherited from the parent $\mathcal{N}$=4 cubic by the $\mathbb{Z}_3$ projection (Chapter 6), with one contribution per closed length-three path, antisymmetrized in the three flavours.

Step 5. consistency. The signed rank vector at regular ranks is

$$A_i = \sum_j (a_{ij} - a_{ji})\,N_j = \big[(a - a^{\mathsf{T}})N\big]_i, \qquad N_j = N \dim R_j = N. \tag{VI.11.4}$$

With the triangle (VI.11.2) each node receives three incoming and emits three outgoing arrows, so $A_i = 3N - 3N = 0$. For $N \geq 3$ this cancels the perturbative cubic $SU(N)^3$ anomaly. At $N = 2$ the cubic invariant is absent and the global doublet-parity condition is separate; at $N \leq 1$ there is no nonabelian factor. To test isolation, the only group element with an eigenvalue 1 on Q is the identity, so $\mathbb{C}^3/\mathbb{Z}_3$ is an isolated singularity. Also $a_{ii} = 0$ at every node of the McKay triangle. Under the D3 orbifold projection, this absence of self-arrows means that the quiver has no spectator adjoint.

Axis 3, orientifold. Folding the dP_0 quiver by the involution $\sigma : i \mapsto -i \bmod 3$ (Chapter 8) pairs nodes 1 and 2 and fixes node 0. The surviving matter is one bifundamental per fixed-paired arrow orbit plus a two-index tensor on the surviving unitary node. The folded $SU(N_u)^3$ anomaly no longer cancels on its own; with one surviving bifundamental of sign s_Q and a tensor of anomaly index $A(T) = N_u \mp 4$ it instead closes on a rank relation,

$$3\, s_Q\, N_0 + 3\, A(T) = 0 \xrightarrow{\text{antisym, } s_Q=-1} N_0 = N_u - 4, \tag{VI.11.5}$$

Here $s_Q = -1$ means that the surviving bifundamentals are antifundamentals of $U(N_u)$; it is not a freely adjustable orientifold sign. The inherited cubic correlates the orthogonal projection with an antisymmetric tensor and the symplectic projection with a symmetric tensor. The latter gives $N_0 = N_u + 4$. These are local anomaly equations for the stated matter. Physical RR charges must still be computed sector by sector. We return to this distinction in Section VI.11.5.

Axis 4, discrete torsion. $\mathbb{Z}_3$ is cyclic, so its Schur multiplier $H^2(\mathbb{Z}_3, U(1))$ is trivial, so dP_0 has *no* discrete-torsion variant. To exercise axis 4 we will instead carry $\mathbb{C}^3/(\mathbb{Z}_2 \times \mathbb{Z}_2)$ as the secondary example, since $\mathbb{Z}_2 \times \mathbb{Z}_2$ has $H^2 = \mathbb{Z}_2$ and a single nontrivial cocycle that collapses its four ordinary one-dimensional representations to one two-dimensional projective irreducible (Section VI.11.6).

This is the whole procedure. The tables below retain this construction where it is available and state which additional choices a refinement needs.

VI.11.3 Axis 1: the ADE catalog ($\mathbb{C}^2/\Gamma$, $\mathcal{N}$=2)

For $\Gamma \subset SU(2)$ the defining **2** is pseudoreal, the McKay adjacency is symmetric, and the quiver is the affine Dynkin diagram of the corresponding ADE type, with the Dynkin marks equal to the irreducible dimensions. Two relations make the table self-checking. The McKay adjacency is the affine Cartan matrix $\widehat{C}$ subtracted from twice the identity, and the mark vector m (the node labels in the last column) is its null vector,

$$a = 2\,\delta - \widehat{C}, \qquad \widehat{C}\, m = 0 \iff \sum_j a_{ij}\, m_j = 2\, m_i, \qquad \sum_i m_i^2 = |\Gamma|. \tag{VI.11.6}$$

The marks are the irreducible dimensions, $m_i = d_i$, so the last identity is the familiar $\sum_i d_i^2 = |\Gamma|$.

This is the complete ADE list. The A series are the cyclic groups (Chapter 3), the D series the binary dihedral groups (the four-star $\widehat{D}_4 = Q_8$, at n=2, is the smallest non-abelian case), and the three exceptionals $\widehat{E}_6, \widehat{E}_7, \widehat{E}_8$ the binary tetrahedral, octahedral, and icosahedral groups. The reader can confirm any row by hand. Write the affine Dynkin graph, set $a = 2\delta - \widehat{C}$, and verify that the marks solve $\sum_j a_{ij} m_j = 2m_i$; for $\widehat{E}_8$ this reads, at the trivalent node of mark 6, $5 + 4 + 3 = 2 \cdot 6$.

Table VI.11.1: Axis 1: the complete $\mathbb{C}^2/\Gamma$ ADE catalog, as families. The McKay quiver is the affine Dynkin diagram; the marks are the irreducible dimensions and the null vector of the affine Cartan matrix, with $\sum_i m_i^2 = |\Gamma|$. The displayed families include the low-rank examples $\widehat{A}_{1\text{–}4}$, $\widehat{D}_{4\text{–}6}$ and the three exceptionals.

type	Γ	$\lvert\Gamma\rvert$	nodes	marks
$\widehat{A}_{n-1}$	$\mathbb{Z}_n$	n	n	$1^{\,n}$
$\widehat{D}_{n+2}$	$2D_n$	$4n$	$n{+}3$	$1,1,1,1,\ 2^{\,n-1}$
$\widehat{E}_6$	$2T$	24	7	$1,1,1,2,2,2,3$
$\widehat{E}_7$	$2O$	48	8	$1,2,3,4,3,2,1,2$
$\widehat{E}_8$	$2I$	120	9	$1,2,3,4,5,6,4,2,3$

VI.11.4 Axis 2: the $\mathbb{C}^3/\Gamma$ directed-quiver catalog ($\mathcal{N}\geq 1$)

For $\Gamma \subset SU(3)$ there is no ADE classification and no Cartan shortcut. The defining **3** is generically complex, the McKay quiver is directed, and the matter has net chirality precisely when Q is not self-dual. The supersymmetry count is $\mathcal{N} = 1 + \dim Q^\Gamma$ in the D3 setup. Thus the $\mathbb{Z}_2$ row with a spectator coordinate has $\mathcal{N} = 2$; the other displayed nontrivial embeddings have $\mathcal{N} = 1$. Table VI.11.2 catalogs the selected abelian embeddings and non-abelian Δ/Σ examples with $|\Gamma| \leq 60$, with $\Sigma(168)$ retained as a single beyond-cutoff exceptional sample. The column "Q" records whether the defining representation is real ($\mathbb{R}$, hence a non-chiral quiver) or complex ($\mathbb{C}$, chiral); "iso." records whether the singularity is isolated.

Table VI.11.2: Axis 2: the $\mathbb{C}^3/\Gamma$ catalog, $|\Gamma| \leq 60$ ($\Sigma(168)$ a beyond-cutoff sample). "dims" the irreducible dimensions (exponents = multiplicities); "weights/structure" the chosen $SU(3)$ embedding (cyclic groups have the weight triple (w_1, w_2, w_3); products have the two generator triples; non-abelian rows give the group structure); Q the reality of the defining **3**; "iso." whether the singularity is isolated. Abelian rows are reconstructible from the weights (box below); the non-abelian adjacency follows from the chosen defining character. The list is a selection of embeddings, not all groups below the cutoff.

Γ	$\lvert\Gamma\rvert$	dims	weights / structure	Q	iso.
abelian cyclic groups (nodes $i \in \mathbb{Z}_n$, arrows $i \to i + w_a$)					
$\mathbb{Z}_2$	2	1^2	$(1,1,0)$	$\mathbb{R}$	no
$\mathbb{Z}_3$	3	1^3	$(1,1,1)$	$\mathbb{C}$	yes
$\mathbb{Z}_4$	4	1^4	$(1,1,2)$	$\mathbb{C}$	no
$\mathbb{Z}_5$	5	1^5	$(1,2,2)$	$\mathbb{C}$	yes
$\mathbb{Z}_6$	6	1^6	$(1,2,3)$	$\mathbb{C}$	no
$\mathbb{Z}_7$	7	1^7	$(1,2,4)$	$\mathbb{C}$	yes
abelian products (representative embeddings)					
$\mathbb{Z}_2 \times \mathbb{Z}_2$	4	1^4	$(0,1,1),(1,0,1)$	$\mathbb{R}$	no
$\mathbb{Z}_3 \times \mathbb{Z}_3$	9	1^9	$(1,0,2),(0,1,2)$	$\mathbb{C}$	no
$\mathbb{Z}_2 \times \mathbb{Z}_4$	8	1^8	$(1,1,0),(0,1,3)$	$\mathbb{C}$	no
$\mathbb{Z}_2 \times \mathbb{Z}_6$	12	1^{12}	$(1,1,0),(0,1,5)$	$\mathbb{C}$	no
$\mathbb{Z}_4 \times \mathbb{Z}_4$	16	1^{16}	$(1,0,3),(0,1,3)$	$\mathbb{C}$	no
non-abelian groups, Δ/Σ main line					
$A_4 = \Delta(12)$	12	$1^3, 3$	$(\mathbb{Z}_2^2)\rtimes\mathbb{Z}_3$	$\mathbb{R}$	no
$S_4 = \Delta(24)$	24	$1^2, 2, 3^2$	$(\mathbb{Z}_2^2)\rtimes S_3$	$\mathbb{R}$	no
$\Delta(27)$	27	$1^9, 3, \bar{3}$	$(\mathbb{Z}_3^2)\rtimes\mathbb{Z}_3$	$\mathbb{C}$	no
$\Delta(48)$	48	$1^3, 3^5$	$(\mathbb{Z}_4^2)\rtimes\mathbb{Z}_3$	$\mathbb{C}$	no
$\Delta(54)$	54	$1^2, 2^4, 3^4$	$(\mathbb{Z}_3^2)\rtimes S_3$	$\mathbb{C}$	no
$A_5 = \Sigma(60)$	60	$1, 3, 3', 4, 5$	$A_5 \subset SO(3)$	$\mathbb{R}$	no
$\Sigma(168)$	168	$1, 3, \bar{3}, 6, 7, 8$	$PSL(2,7)$	$\mathbb{C}$	no

How to read a $\mathbb{C}^3/\Gamma$ atlas row. For an *abelian cyclic* row with weights (w_1, w_2, w_3) (with $w_1{+}w_2{+}w_3 \equiv 0 \bmod n$ so $\det = 1$), the nodes are the characters $i \in \mathbb{Z}_n$ and the arrows are $i \to i + w_a$ for $a = 1, 2, 3$; the regular ranks are $N_i = N$, the cubic W is the ϵ-contraction over closed oriented length-three paths, and the anomaly check is $(a - a^{\mathsf{T}})\, d = 0$. (Two weight triples related by a permutation and an overall unit of $\mathbb{Z}_n$ give the same quiver; these changes only relabel coordinates and characters.) For a *non-abelian* row the nodes are the irreducibles R_i and the directed McKay $a_{ij} = \dim \mathrm{Hom}_\Gamma(R_j, \mathbf{3} \otimes R_i)$ is generated from the character table; its identifying tensor products are

$$
\begin{aligned}
&A_4: \ \mathbf{3} \otimes \mathbf{3} = \mathbf{1}{+}\mathbf{1}'{+}\mathbf{1}''{+}2 \cdot \mathbf{3}; \qquad S_4: \ \mathbf{3} \otimes \mathbf{3} = \mathbf{1}{+}\mathbf{2}{+}\mathbf{3}{+}\mathbf{3}';\\
&\Delta(27): \ \mathbf{1}_{r,s} \to \mathbf{3} \to \bar{\mathbf{3}} \to \mathbf{1}_{r,s} \ \ (\mathbf{3} \otimes \mathbf{3} = 3 \cdot \bar{\mathbf{3}}, \ \ \mathbf{3} \otimes \bar{\mathbf{3}} = \textstyle\bigoplus_{r,s} \mathbf{1}_{r,s});\\
&\Delta(48): \ Q \otimes Q = 2\bar{Q} + R_{48}; \qquad \Delta(54): \ Q \otimes Q = \bar{Q} + 2R_{54};\\
&\Sigma(168): \ \mathbf{3} \otimes \mathbf{3} = \bar{\mathbf{3}}{+}\mathbf{6}.
\end{aligned}
$$

Here R_{48} and R_{54} are the three-dimensional representations on the diagonal symmetric tensors $e_i \otimes e_i$ for the defining matrices of these groups. The exterior square is $\bar{Q}$ because $\det Q = 1$. For $\Delta(48)$ the three off-diagonal symmetric tensors give another $\bar{Q}$, whereas for $\Delta(54)$ they give another R_{54}. This explains the multiplicity two. These products identify parts of an adjacency; the full tensor table is needed to reconstruct every row.

A few features of the table are worth naming, because they are the structural laws the volume established, now visible as columns.

The reality column is not correlated with abelian-ness. The cyclic $\mathbb{Z}_3$ is chiral; the product $\mathbb{Z}_2 \times \mathbb{Z}_2$ is non-chiral; the non-abelian $\Delta(27)$ is chiral while the non-abelian A_4 and S_4 are not. What governs chirality is whether Q is complex, full stop. The groups with a real $\mathbf{3}$ ($\mathbb{Z}_2$, $\mathbb{Z}_2 \times \mathbb{Z}_2$, A_4, S_4, A_5) sit inside $SO(3) \subset SU(3)$; their quivers are non-chiral. A non-abelian group therefore does *not* guarantee a chiral quiver, and an abelian group does not forbid one.

The isolation column is sparse. Only $\mathbb{Z}_3$, $\mathbb{Z}_5$, $\mathbb{Z}_7$ are isolated. A diagonal element with a zero weight fixes a coordinate line, so any group containing such an element gives a non-isolated quotient with a residual $\mathbb{C}^2/\Gamma' \times \mathbb{C}$ locus. The cyclic $\mathbb{Z}_n$ is isolated exactly when all three weights are coprime to n. A faithful action of a noncyclic abelian group cannot be isolated. Each coordinate is a character into $U(1)$; a noncyclic finite group cannot embed in $U(1)$, so each such character has a nontrivial kernel. An element in that kernel fixes its coordinate line. The noncyclic qualification matters because a product with $\gcd(n, m) = 1$ is itself cyclic.

The regular-rank equation also has a short derivation. Taking dimensions of $Q \otimes R_i$ gives $\sum_j a_{ij} d_j = 3d_i$; applying the same argument to the dual tensor product gives $\sum_j a_{ji} d_j = 3d_i$. Their difference annihilates the regular ranks $N_i = N d_i$. This is a formal representation identity, interpreted as cancellation of perturbative cubic anomalies at $SU(N_i)$ nodes with $N_i \geq 3$. It does not test the independent global conditions at small ranks. Nor does it cancel all RR sources on fixed lines or decide whether an anomaly-free $U(1)$ remains massless. Chapter 7 explains why those questions

require the sector charges and axion couplings.

The degenerate base case. One group in the $\Delta(6n^2)$ series is deliberately *not* a row of Table VI.11.2, the n=1 base $\Delta(6) = S_3$. Its irreducible dimensions are $1, 1, 2$, with no three-dimensional irreducible representation, so its "defining **3**" is reducible. For the determinant-one $SU(3)$ lift it is the sign character plus the doublet, $\mathbf{3} = \mathbf{1}' \oplus \mathbf{2}$ (the unit-determinant condition twists the trivial summand of the permutation representation to the sign $\mathbf{1}'$), and $\mathbb{C}^3/S_3$ is non-isolated and degenerate. We name it here as the base of the series (a parallel to $\Delta(3) = \mathbb{Z}_3$, the degenerate base of $\Delta(3n^2)$) with an important embedding distinction. The cyclic permutation at $n = 1$ has weights $(0, 1, 2)$, whereas the dP_0 row uses $(1, 1, 1)$. These are different actions of the same abstract group. We keep the non-abelian table to faithful, irreducible-**3** entries.

VI.11.5 Axis 3: orientifold fixtures and checks

An orientifold must act on fields and interactions, not just on the quiver vertices. In the D3/O3/O7 setting of Chapter 8 the geometric involution is holomorphic and the full operation includes worldsheet parity and the required fermion action. On a fixed Chan–Paton block, the vector constraint $A = -\gamma_\Omega A^{\mathsf{T}} \gamma_\Omega^{-1}$ yields $SO(n)$ for a symmetric form and $USp(n)$ for an antisymmetric form; the latter requires even n. Their dimensions are $n(n-1)/2$ and $n(n+1)/2$.

Table VI.11.3 separates these algebraic projections from their physical realization. For the A_1 examples, a supersymmetric lift with the complete flavour and Chan–Paton action remains additional input. The product orbifold row is a catalogued possibility with no specified lift or charge map here. Only the stated dP_0 matter supports the rank calculation below. The real or pseudoreal representations used on the fixed nodes have zero symmetric cubic trace. This is not a statement about every representation of an orthogonal algebra; complex spinors of $so(6) \simeq su(4)$ are a counterexample to that unrestricted assertion.

Table VI.11.3: Representative orientifold projections and their scope. The A_1 rows give conditional fixed-node algebras, not complete supersymmetric models. The dP_0 relation is a local cubic-anomaly condition for the specified tensors. No physical RR tadpole computation is supplied by this table.

parent	γ_Ω	gauge factor	condition
$\mathbb{C}^2/\mathbb{Z}_2$ (A_1)	symmetric	$SO(n)$	dim $= n(n-1)/2$, lift needed
$\mathbb{C}^2/\mathbb{Z}_2$ (A_1)	antisymmetric	$USp(n)$	dim $= n(n+1)/2$, lift needed
$\mathbb{C}^3/\mathbb{Z}_3$ (dP_0)	$O3$	$SO/USp \times U$	$N_0 = N_u \mp 4$
$\mathbb{C}^3/(\mathbb{Z}_2 \times \mathbb{Z}_2)$	O-plane	SO/USp candidate	lift unspecified

The dP_0 row is the representative worked case (Section VI.11.2). folding by $\sigma : i \mapsto -i$ leaves one bifundamental per fixed-paired arrow orbit and a two-index tensor on the surviving *unitary* node (not the fixed SO/USp node); the image bifundamental is not an independent field, and the un-folded double-count is not allowed. The sign of $N_0 = N_u \mp 4$ is the tensor branch.

tensor on U_u	$A(T)$	bifund. sign s_Q	rank relation
SO / antisymmetric	$N_u - 4$	-1	$N_0 = N_u - 4$
USp / symmetric	$N_u + 4$	-1	$N_0 = N_u + 4$

The correlation follows from the inherited cubic. If the fixed-node form has $G^{\mathsf{T}} = sG$ and the tensor has $T^{\mathsf{T}} = tT$, exchanging the two bifundamentals in the epsilon contraction multiplies the term by $-st$. A nonzero inherited interaction therefore requires $t = -s$. The bifundamental image is identified with the original field, so it must not be counted twice in the anomaly.

One can recover the tensor indices without a table. At $N_u = 8$, take the traceless fundamental charges $(7, -1, -1, -1, -1, -1, -1, -1)$. Their cubic sum is $7^3 - 7 = 336$. The antisymmetric pair charges have cubic sum $7 \cdot 6^3 + 21(-2)^3 = 1344$, giving index 4. Including the diagonal pairs adds $14^3 + 7(-2)^3 = 2688$, so the symmetric index is 12. The anomaly $-3N_0 + 3A(T)$ then selects $SO(4) \times U(8)$ or $USp(12) \times U(8)$ for these local spectra. Occupied ranks must be positive, the symplectic dimension even, and the unitary cubic-index argument uses $N_u \geq 3$.

These equations do not determine a crosscap charge. Physical tadpoles take the sector form $Q_D^{(k)} + Q_O^{(k)} = 0$, whose relation to rank variables needs a background-dependent RR map. Writing $(a - a^{\mathsf{T}})N + q_O = 0$ with an assigned constant vector gives an affine linear model; it does not construct that map. Small-rank global anomalies, discrete charges and compact completion remain separate requirements.

VI.11.6 Axis 4: discrete torsion

Discrete torsion exists only where the Schur multiplier $H^2(\Gamma, U(1))$ is nontrivial. For a product $\mathbb{Z}_n \times \mathbb{Z}_m$ the multiplier is $\mathbb{Z}_{\gcd(n,m)}$, so the membership rule on this axis is $\gcd(n, m) > 1$; a cyclic group, or a product with gcd $= 1$ (which is itself cyclic, $\mathbb{Z}_2 \times \mathbb{Z}_3 = \mathbb{Z}_6$), has no torsion row. For the standard generator of $H^2(\Gamma, U(1))$, the maximal alternating class used in this table, let $d = \gcd(n, m)$. The projective irreducibles have dimension d and occur in number nm/d^2. (When d is composite the multiplier has classes of smaller order whose projective dimension is below d; those are not part of this low-rank fixture table.) In the diagonal case $\mathbb{Z}_n \times \mathbb{Z}_n$ ($d = n$) this is especially simple. The clock-and-shift pair $PQ = \zeta QP$ generates a single irreducible n-dimensional projective representation, collapsing all n^2 ordinary one-dimensional nodes to one n-dimensional node. For a rectangular product the same construction on the $\mathbb{Z}_d \times \mathbb{Z}_d$ non-degenerate block gives nm/d^2 projective irreducibles, each of dimension d.

The secondary worked example $\mathbb{C}^3/(\mathbb{Z}_2 \times \mathbb{Z}_2)$ is the first row, and it is worth contrasting the two theories on the same group. The *ordinary* orbifold has the four one-dimensional nodes of Table VI.11.2 and gauge group $U(N)^4$ at regular ranks; the *torsion* orbifold collapses these, under the one nontrivial cocycle of $H^2 = \mathbb{Z}_2$, to a single two-dimensional projective node, $U(2N)$ in the bulk-probe normalization. The clock-and-shift construction explains irreducibility. The d^2 products $P^a Q^b$ are orthogonal under the matrix trace and span $M_d(\mathbb{C})$. Any invariant subspace would then be invariant

Table VI.11.4: Axis 4: discrete-torsion fixtures for product abelian groups. For $\Gamma = \mathbb{Z}_n \times \mathbb{Z}_m$ the Schur multiplier is $H^2(\Gamma, U(1)) = \mathbb{Z}_d$ with $d = \gcd(n, m)$, nontrivial iff $d > 1$. For the standard / maximal alternating class (the one tabulated), the projective irreducible dimension is d and the number of projective irreducibles is nm/d^2, so $\sum(\dim R_i^\alpha)^2 = (nm/d^2)\, d^2 = nm = |\Gamma|$. The last row is the coprime case ($d = 1$, no torsion).

Γ	$\lvert\Gamma\rvert$	H^2	torsion?	$d = \dim R^\alpha$	# proj. irr.
$\mathbb{Z}_2 \times \mathbb{Z}_2$	4	$\mathbb{Z}_2$	yes	2	1
$\mathbb{Z}_3 \times \mathbb{Z}_3$	9	$\mathbb{Z}_3$	yes	3	1
$\mathbb{Z}_4 \times \mathbb{Z}_4$	16	$\mathbb{Z}_4$	yes	4	1
$\mathbb{Z}_2 \times \mathbb{Z}_4$	8	$\mathbb{Z}_2$	yes	2	2
$\mathbb{Z}_2 \times \mathbb{Z}_6$	12	$\mathbb{Z}_2$	yes	2	3
$\mathbb{Z}_2 \times \mathbb{Z}_3 = \mathbb{Z}_6$	6	1	no	1	6

under every matrix, so it is zero or the whole space. The coprime example $\mathbb{Z}_2 \times \mathbb{Z}_3 = \mathbb{Z}_6$ confirms the rule. It is cyclic, has trivial multiplier, and carries no torsion row.

The dimension of a projective irreducible is not the gauge rank. In the twisted regular module each simple of dimension d appears d times. Hence N regular probes give multiplicity Nd and gauge factor $U(Nd)$ at each projective node. For maximal $\mathbb{Z}_n \times \mathbb{Z}_n$ torsion this is one $U(nN)$ node, not $U(N)$.

The rectangular case can be reconstructed from the commutator pairing

$$\beta((a, b), (c, e)) = \exp[2\pi i(ae - bc)/d]. \tag{VI.11.7}$$

An element is in its radical precisely when a and b are both divisible by d. There are $(n/d)(m/d)$ such elements, giving nm/d^2 blocks of dimension d. For $(n, m) = (2, 4)$, the radical is $\{(0, 0), (0, 2)\}$, so there are two two-dimensional simples. Each occurs twice in the twisted regular module, or $2N$ times in N copies. This calculation uses the maximal class; changing its order changes the radical. With the Chan–Paton centralizer interpretation, one regular D3 probe therefore gives $U(2) \times U(2)$.

The interaction retains a phase as well as the new ranks. With the Chapter 9 field matrices $P, S, (PS)^{-1}$ and $PS = \omega SP$, the ordered trace ratio in the daughter cubic is $q = \omega^{-1}$. Reversing the order inverts it. For $n = 2$ this distinction reduces to the sign $q = -1$; for $n = 3$ it matters. Finally, the fixed projective group irreducible and an irreducible block of the F-term algebra are different objects. In the Pauli example a generic size-two F-term block stays irreducible when two scales are nonzero, but splits on a singular axis when at most one remains. The projective group irrep remains two-dimensional throughout.

VI.11.7 Cross-catalog patterns and the large-N reading

Read across, the catalog makes the volume's structural laws legible as a small set of correlations.

- **Chirality ⇔ complex 3.** The Q column of Table VI.11.2 is the chirality column; nothing else (not abelian-ness, not the order, not the number of nodes) predicts it.
- **Isolation ⇔ no fixed line.** An entry is isolated iff no nontrivial element has eigenvalue 1 on Q; for cyclic groups this is the coprime-weight condition.
- **The $SU(2)$ miracle, and its absence for $SU(3)$.** Axis 1 is a complete classification with a Cartan shortcut; axis 2 is a catalog read off character tables, with no shortcut and no finite list.
- **Torsion needs a Schur multiplier.** Axis 4 hangs only off the groups with a nontrivial Schur multiplier $H^2(\Gamma, U(1))$ (for the abelian products this is $\gcd(n,m) > 1$), a strict subset of axis 2.

Chapter 10 gives the ordinary, untwisted $\mathbb{C}^3/\Gamma$ rows a second reading. For irreducible dimensions d_i, set $K = N|\Gamma|$. The regular-representation identity and the dimension-weighted McKay relation give $\sum_i (Nd_i)^2 = N^2|\Gamma| = K^2/|\Gamma|$ and $\sum_{ij} a_{ij}(Nd_i)(Nd_j) = 3K^2/|\Gamma|$. Under the D3 orbifold projection these are, respectively, the gauge-component and chiral-component counts at regular ranks $N_i = Nd_i$ in the daughter of a parent $U(K)$ theory. With that spectrum, the same relation gives the one-loop nonabelian coefficient $3Nd_i - \frac{1}{2}\sum_j (a_{ij} + a_{ji})Nd_j = 0$ in the convention $T(\square) = 1/2$. This counts the adjoint part of a self-arrow correctly; its gauge singlet does not contribute.

Planar comparison additionally needs the matched action. Put $m = |\Gamma|$. Restricting the parent trace gives $\sum_i d_i \operatorname{Tr}_{Nd_i}$, so the bare restricted action has $g^2_{\mathrm{bare},i} = g_p^2/d_i$. The matched action $S_D = S_P|_{\mathrm{inv}}/m$ instead gives $g_i^2 = m g_p^2/d_i$ and $g_i^2 N d_i = g_p^2 K$. Thus the 't Hooft couplings agree only after the action matching.

For a neutral trace the corresponding daughter operator is $O_D = K^{-1}\sum_i d_i \operatorname{Tr}(\mathrm{loop}_i)$. The connected k-point functions are compared after multiplying by $(K^2/m)^{k-1}$ on the daughter side and $(K^2)^{k-1}$ on the parent side. Their perturbative planar coefficients agree at fixed finite m, fixed k and matched 't Hooft coupling in the symmetric vacuum; the oriented genus expansion allows relative $O(N^{-2})$ corrections. Extending this to nonperturbative equivalence requires unbroken parent projection and daughter symmetries. Twisted operators, independent double-trace couplings, abelian masses and strong-coupling vacua need separate analysis. The orientifold and torsion refinements do not inherit this conclusion without their own argument.

VI.11.8 How to extend the atlas, and what is not in it

The catalog is finite by choice, and the rule that bounds it is the honest content of the chapter. On the $SU(3)$ side we stopped at $|\Gamma| \le 60$ and the selected Δ/Σ families. Groups of type C have the structure $(\mathbb{Z}_m \times \mathbb{Z}_p) \rtimes \mathbb{Z}_3$, with p dividing m and the action fixed by their defining matrices. The case $p = m$ gives $\Delta(3m^2)$, whose selected rows are already included. Further C-type groups outside those rows are deferred, including the order-21 Frobenius group $\mathbb{Z}_7 \rtimes \mathbb{Z}_3$ in the cyclic-normal-subgroup branch $p = 1$.

The exceptional groups above the cutoff begin with $\Sigma(108) = \Sigma(36 \times 3)$, the faithful $SU(3)$ lift of the order-36 projective group (its appearance as "$\Sigma(36)$" in the literature is a $PSU(3)$-versus-$SU(3)$ naming hazard, recorded in the sources). To extend the atlas one runs the same recipe with the new generators; one must specify the defining representation, resolve tensor multiplicities and project the interactions. A group name or a dimension list alone does not complete those steps.

Three boundaries are firmly outside this volume. The toric and dimer combinatorics that organize the abelian $\mathbb{C}^3/\Gamma$ orbifolds are named here but developed in Volume VI. The classification theorems for the finite subgroups of $SU(2)$ and $SU(3)$ are cited, not proved (Volume IV). And the strong-coupling dynamics that make these catalogs interesting as physics, a-maximization, Seiberg duality, the cascades, the holographic spectra, belong to Part III. What this chapter delivers is the construction made into a reference, with the selected orbifolds of Volume VI, their quiver data, and a route back to the corresponding calculations.

Status and sources

This apparatus records the sources, conventions and limits of the catalog. The label [WS] denotes a physical-worldsheet derivation, never ordinary gauge-theory algebra. [MATH] requires stated mathematical hypotheses and a proof or a cited theorem; a successful numerical evaluation is not a proof of a family. The limits of the source support are stated with each construction. No anomaly-matching tag is assigned to a rank cancellation without an independent comparison.

The conventions used are the supersymmetry count, the orientifold Chan–Paton units and signs, arrow orientation, the projected cubic, orbifold actions, McKay multiplicities (McKay multiplicities), gauge ranks and discrete torsion, with the quiver node labels used in the preceding chapters. The direct computations give cyclic arrows, tensor indices and maximal-torsion radicals for the stated examples. A vanishing numerical entry in a cubic-Casimir column leaves the cubic trace to be derived from the representation. The worldsheet lift and compact completion require separate data.

§VI.11.1–VI.11.2 Framing and the recipe. The recipe is the volume's construction, restated and walked on dP_0. The two readings of completeness (relative to a stated rule; the theory fixed by Γ *plus* its embedding, not the abstract group) are the stated distinction. The physical projection and decoupling premises are inherited from VI.1–VI.2 and VI.6; their unresolved source or classification debts remain open.

§VI.11.3 Axis 1: the ADE catalog. The complete $\mathbb{C}^2/\Gamma$ list as families; $a = 2\delta - \widehat{C}$, marks = null vector of $\widehat{C}$, $\sum_i m_i^2 = |\Gamma|$. [MATH] the McKay correspondence (McKay 1980); the physical $\mathcal{N}$=2 quiver interpretation is imported from Chapter 3 and is separate from the theorem. The finite arithmetic illustrates the McKay correspondence in the low-rank examples.

§VI.11.4 Axis 2: the $\mathbb{C}^3/\Gamma$ directed quivers. The $|\Gamma| \leq 60$ Δ/Σ main line. The physical quiver interpretation is imported from Chapter 6; its classification debt is retained. The finite character calculations do not derive the open-string spectrum. Chirality $\Leftrightarrow$ complex **3** and abelian $\neq$ isolated are non-abelian $\neq$ irreducible **3** (the $\Delta(6) = S_3$ degenerate base) is the stated distinction. The abelian weights give the McKay spectra directly. The $\Delta(48)$, $S_4 = \Delta(24)$ and $\Delta(54)$ spectra are compared numerically with the corresponding representations. The $SU(3)$ finite-subgroup classification is cited to the finite-subgroup classification for $SU(3)$ (Grimus and Ludl (2010) and Ludl (2011); for type C, Ludl, arXiv:1101.2308v3, §3, equations (9), (10), (18) and the cases following (18); for the $\Sigma(36 \times 3)$ order and central quotient, Grimus–Ludl, arXiv:1006.0098v2, Table 1 and equation (7); the $\Delta(6n^2)$ series Escobar and Luhn (2009)); the non-abelian gauge theories to Hanany and He (1999).

§VI.11.5 Axis 3: orientifold fixtures. The algebraic fixed-node dimensions use VI.8 equations `eq:V8-dims` and `eq:V8-split`; the A_1 lift debt is VI.8 equations `eq:V8-A1gaugeA,B`. The dP_0 tensor correlation, charge-cube indices and conditional ranks are VI.8 equations `eq:V8-tensorcorrelation`,

eq:V8-Asymanti and eq:V8-dP0rank. The representation calculation leaves the physical RR map undetermined. The conditional A_1 and unspecified product-orbifold rows carry no [WS] classification here. Foundations are deferred to orientifold and crosscap amplitudes.

§VI.11.6 Axis 4: discrete torsion. Discrete torsion (Vafa and Witten 1995); membership $\gcd(n, m) > 1$ since $H^2(\mathbb{Z}_n \times \mathbb{Z}_m) = \mathbb{Z}_{\gcd}$ (the tabulated dimensions are the maximal alternating class); projective collapse by clock-and-shift. The worldsheet torsion choice is imported from Chapter 9, while the radical and representation dimensions are separate algebraic statements. The $U(Nd)$ multiplicity is VI.9 equation eq:V9-rankconv; the inverse phase is fixed by eq:V9-Wq and eq:V9-z3clockshift. The Schur-multiplier calculation uses the chosen maximal alternating class.

§VI.11.7–VI.11.8 Patterns, large-N, and boundaries. The planar / neutral-sector inheritance (Lawrence et al. 1998; Bershadsky and Johansen 1998) and its limits are Chapter 10 equations eq:V10-gconvention, eq:V10-inherit, eq:V10-neutralNA and eq:V10-fixed; the dynamics are routed to Part III, the toric/dimer machinery to Volume VII, and the classifications to Volume III. Further C-type groups outside the selected Δ rows are deferred. The $\Sigma(36)$-versus-$\Sigma(108)$ distinction is fixed by the central quotient specified above.

References

Bershadsky, M. and A. Johansen (1998). "Large N limit of orbifold field theories". In: *Nucl. Phys. B* 536, pp. 141–148. DOI: 10.1016/S0550-3213(98)00526-4. arXiv: hep-th/9803249.

Escobar, J. A. and C. Luhn (2009). "The Flavor Group Delta(6n**2)". In: *J. Math. Phys.* 50, p. 013524. DOI: 10.1063/1.3046563. arXiv: 0809.0639 [hep-th].

Grimus, W. and P. O. Ludl (2010). "Principal series of finite subgroups of SU(3)". In: *J. Phys. A* 43, p. 445209. DOI: 10.1088/1751-8113/43/44/445209. arXiv: 1006.0098 [hep-ph].

Hanany, A. and Y.-H. He (1999). "NonAbelian finite gauge theories". In: *JHEP* 02, p. 013. DOI: 10.1088/1126-6708/1999/02/013. arXiv: hep-th/9811183.

Lawrence, A. E., N. Nekrasov, and C. Vafa (1998). "On conformal field theories in four-dimensions". In: *Nucl. Phys. B* 533, pp. 199–209. DOI: 10.1016/S0550-3213(98)00495-7. arXiv: hep-th/9803015.

Ludl, P. O. (2011). "Comments on the classification of the finite subgroups of SU(3)". In: *J. Phys. A* 44. [Erratum: J.Phys.A 45, 069502 (2012)], p. 255204. DOI: 10.1088/1751-8113/44/25/255204. arXiv: 1101.2308 [math-ph].

McKay, J. (1980). "Graphs, singularities, and finite groups". In: *Proc. Symp. Pure Math.* 37. American Mathematical Society, pp. 183–186.

Vafa, C. and E. Witten (1995). "On orbifolds with discrete torsion". In: *J. Geom. Phys.* 15, pp. 189–214. DOI: 10.1016/0393-0440(94)00048-9. arXiv: hep-th/9409188.